

Molecular Modulators of Bacterial Functional Amyloid Assembly

by

Margery Lee Evans

A dissertation submitted in partial fulfillment
of the requirements for the degree of
Doctor of Philosophy
(Molecular, Cellular and Developmental Biology)
in the University of Michigan
2015

Doctoral Committee:

Associate Professor Matthew R. Chapman, Chair
Professor Janine R. Maddock
Associate Professor Mary X. D. O'Riordan
Associate Professor Lyle A. Simmons

To my family.

Acknowledgements

My decision to pursue biology and research came naturally. My decision to join Matt Chapman's lab for my thesis work came even more easily. Never have I met someone with such a genuine zeal for what he does. Matt has been an extraordinary mentor to me both in science and in life. Matt follows all of his passions with pure excitement and joy, a characteristic that he cultivates in his lab. I cannot imagine, nor do I want to imagine, a life without the curiosity and enthusiasm for science that I have been so fortunate to be immersed in.

I couldn't have asked for better lab mates during this journey. I was immediately welcomed into the Chapman lab. When I first joined the lab Dan Smith was my student mentor, I was blown away by the tremendous amount of knowledge and ideas he had and was so excited to share. I still look back at my notes from our first conversation with awe and, admittedly, some confusion, which only means that there are still so many interesting and unanswered questions. I only overlapped with Neal Hammer and Ryan Frisch for a short period of time but enjoyed working with them immensely and still look forward to seeing them at conferences and Chapman lab events. Fei Li initiated the project that ultimately grew into my thesis. I am so grateful for all of her help launching this exciting work.

The people I spent the most time with in the lab were Yizhou Zhou, Will DePas, David Hufnagel and Adnan Syed. Neha Jain integrated into the lab seamlessly last winter. I will miss sharing a bay with her and going to yoga together so much. Yizhou, Will, Dave, Neha and Adnan have been outstanding colleagues and even better friends. Without them I would not be able to say that graduate school has been some of the best years of my life. The bonds I have formed with during graduate school will last a lifetime. Saying goodbye to lab members and colleagues throughout the years has been so bittersweet. I will miss them all dearly and I cannot wait to see what amazing things they do with their lives and careers.

I have also been fortunate enough to share a lab space with three other amazing labs. Bob Bender will always have a presence in the Chapman lab. Over the years I have received invaluable feedback from Bob. Joint lab meetings with the Boles lab and Supergroup meetings with the Maddock and Simmons labs were always fun and stimulating. I am sure that these meetings will continue to serve as creative and useful venues with the addition of Kimberley Seeds lab. Additionally, the Jakob and Bardwell labs have been hugely supportive and helpful, especially Claudia Cremers. Her expertise and patience were essential for much of my training. Jon Taylor and Steve Matthews at the Imperial College of London have been instrumental collaborators. Pernilla Wittung-Stefshede, Fredrik Almqvist and Erik Chorell have also been tremendous collaborators. Without their guidance and support the CsgC project would not be what it is.

My undergraduate and masters research assistants, Anisha Chadha, Sarah Kang, Phil Robinson and Kamirah Demouchet, have been excellent people to work with and train. Their excitement and curiosity for research was inspiring and rewarding.

I would also like to thank my thesis committee members for their incredible support and encouragement throughout the years. I always felt that I could approach any of them at any time with questions or ideas about my project and my career. I would also like to thank the MCDB staff, especially Mary Carr and Diane Durfy. They were always available to help me and happy to talk.

I would like to acknowledge and thank the Cellular Biotechnology Training Program for financial support and Joel Swanson for putting together such an excellent training program. I would also like to thank The Rackham Graduate School for the Predoctoral Fellowship.

Finally, I would like to thank my family, both logical and biological, for all of their unwavering support. They have always shown such great interest and enthusiasm for my work and wellbeing. I am so grateful for their encouragement to push harder when I needed to and to take breaks when I forgot to. Thank you all so much.

Table of Contents

Dedication	ii
Acknowledgements	iii
List of Figures	viii
List of Tables	x
List of Appendices	xi
Chapter 1: Introduction.....	1
Amyloids are Ubiquitous	1
Functional Amyloids in Biofilms and Floccs	2
Functional Amyloids as Adhesins	3
Functional Amyloids as Surface Property Modifiers	4
Functional Amyloids as Toxins	6
Functional Amyloids in Epigenetic Inheritance	7
Curli are Functional Amyloids	8
Amyloid assembly can be modulated and probed with antibodies, small molecules and protein folding factors	17
Dissertation Goals	19
Figures and Tables	21
References	29
Chapter 2: <i>Escherichia coli</i> Chaperones DnaK, Hsp33 and Spy Inhibit Bacterial Functional Amyloid Assembly	41
Abstract	41
Introduction	42
Results	45
Discussion	50
Materials and Methods	53

Figures	57
References	63
Chapter 3: The Bacterial Curli System Possesses a Potent and Selective Inhibitor of Amyloid Formation	69
Abstract	69
Introduction	69
Results	71
Discussion	78
Materials and Methods	83
Figures and Tables	88
References	106
Chapter 4: CsgE is Required for Efficient Translocation of Curli Subunits Across the Outer Membrane.....	111
Abstract	111
Introduction	112
Results	113
Discussion	117
Materials and Methods	119
Figures and Tables	123
References	130
Chapter 5: Discussion and Future Directions	133
Curli Biogenesis.....	133
General Protein Folding Factors Inhibit CsgA Amyloid Formation	135
Identification of CsgC as a Curli Amyloid Inhibitor.....	136
CsgC is a Potent and Selective Amyloid Inhibitor.....	137
A Putative Substrate Binding Domain in CsgC.....	139
CsgE is a Critical Curli Secretion Protein.....	140
Understanding CsgE Function <i>in vivo</i>	141
Amyloid Cytotoxicity and Designing Therapeutics.....	142
Concluding Remarks.....	142
Materials and Methods.....	143

Figures.....	144
References.....	147
Appendices.....	151

List of Figures

Figure 1.1 Curli production contributes to <i>E. coli</i> biofilm formation	21
Figure 1.2 Model of curli biogenesis	22
Figure 1.3 The curli biogenesis system possesses a unique outer membrane secretion apparatus.....	23
Figure 1.4 The molecular details of CsgA and CsgB.....	24
Figure 1.5 Schematic representation of amyloid polymerization.....	25
Figure 1.6 Interbacterial complementation.....	27
Figure 2.1 <i>In vitro</i> CsgA fiber formation in the presence of DnaK.....	57
Figure 2.2 <i>In vitro</i> CsgA fiber formation in the presence of Hsp33.....	58
Figure 2.3 Hsp33 _{ox} and DnaK significantly prolong the presence of a CsgA intermediate that is recognized by the A11 antibody.....	59
Figure 2.4 The addition of preformed fibers abolishes the inhibitory effects of Hsp33 _{ox} and DnaK on CsgA amyloid formation.....	60
Figure 2.5 <i>In vitro</i> CsgA fiber formation in the presence of Spy.....	61
Figure 2.6 Overexpression of Spy reduces curli secretion and assembly.....	62
Figure 3.1 Secretion deficient mutants induce an amyloid inhibitory activity in the periplasm.....	88
Figure 3.2 <i>csg</i> mutants exhibit varying degrees of amyloid inhibitory activity	89
Figure 3.3 Amyloid inhibition requires expression of <i>csgC</i>	90
Figure 3.4 Amyloid inhibitory activity is regulated by CsgD and requires expression of <i>csgC</i>	91
Figure 3.5 $\Delta csgG\Delta csgC$ mutants accumulate intracellular CsgA aggregates	92
Figure 3.6 $\Delta csgG\Delta csgC$ cells do not produce extracellular curli fibers but exhibit a decrease in cellular fitness	93
Figure 3.7 Purified CsgC inhibits CsgA amyloid formation at substoichiometric molar ratios	94

Figure 3.8 CsgA amyloid inhibition <i>in vitro</i>	96
Figure 3.9 Amyloid inhibition by CsgC is specific	98
Figure 3.10 CsgC inhibits CsgA repeating unit deletion mutants and synthetic peptides.....	99
Figure 3.11 Model of CsgC-mediated amyloid inhibition.....	100
Figure 4.1 CsgE interacts with CsgA and CsgB.....	123
Figure 4.2 <i>csgE</i> mutants exhibit different curli biogenesis phenotypes <i>in vivo</i>	124
Figure 4.3 <i>csgE</i> mutants exhibit differential CsgG gating phenotypes <i>in vivo</i>	125
Figure 4.4 Analysis of <i>yfgC</i> function <i>in vivo</i>	126
Figure 5.1 CsgC interacts directly with CsgA	144
Figure 5.2 Intramolecular disulfide bond formation and CsgC stability	145
Figure 5.3 CsgC contains a predicted aggregative domain	146
Figure A.1 Transcription analysis of curli operons	153
Figure B.1 Two-dimensional gel electrophoresis of periplasmic extracts	155
Figure C.1 Polyphosphate production curli biogenesis and curli-dependent biofilm formation <i>in vivo</i>	157
Figure C.2 Polyphosphate accelerates CsgA amyloid formation <i>in vitro</i>	158

List of Tables

Table 1.1 Direct Regulators of the Curli Operons.....	28
Table 3.1 Strains used in Chapter 3.....	101
Table 3.2 Plasmids used in Chapter 3.....	102
Table 3.3 Primers used in Chapter 3.....	104
Table 4.1 Strains used in Chapter 4	127
Table 4.2 Plasmids used in Chapter 4	128
Table 4.3 Primers used in Chapter 4	129

List of Appendices

Appendix A. Investigating Feedback Repression of the Curli Operons	152
Appendix B. One and Two Dimensional Gel Analysis of Periplasmic Extracts to Identify Amyloid Inhibitory Factors	154
Appendix C. The Effect of Polyphosphate on Curli <i>in vivo</i> and <i>in vitro</i>	156

Chapter 1

Introduction¹

Amyloids are ubiquitous

In 1894, Dr. Rudolf Virchow first used the word “amyloid” to describe aggregated material in brain tissue samples. Virchow noted that the observed aggregates stained with iodine, a characteristic of starch. Virchow named the aggregates “amyloid” for the Latin *amylum* and Greek *amylon* meaning starch. It was later demonstrated by Friedrich and Kekule that these iodine-staining aggregates were composed of protein, not starch (1). Amyloids have since been intensely studied for decades as they have been found to be hallmarks of many human illnesses including Alzheimer’s, Parkinson’s and Huntington’s diseases (2-5). More recently, a new class of amyloids—the so-called ‘functional’ amyloids—has been described, and new members of this class are rapidly being discovered (6, 7). Functional amyloids were first discovered in *Escherichia coli* as part of the extracellular matrix important to promote biofilm formation (8). Functional amyloids are now believed to be ubiquitous and they perform an enormous diversity of biological functions (8-12).

Microbial functional amyloids often mediate self and non-self interactions during biofilm formation. Loosely defined, biofilms are communities of bacteria encased in an extracellular matrix of proteins and polysaccharides (13). Amyloids are the major proteinaceous component in many biofilms (10). Amyloid fibers are well suited to serve as protein scaffolds in the biofilm matrix as they are remarkably strong can help aggregate individual cells together providing resistance to a variety of environmental

¹ Portions of this chapter were published in *Trends in Microbiology* (6) and *Biochemical Biophysical ACTA* (180). Luz Blanco and Matthew Badtke contributed to writing the sections on microbial amyloids. Will DePas supplied the image in Figure 1.1B and Dan Smith designed the model in Figures 1.2 and 1.5.

insults (14, 15). The assembly of amyloid fibers also does not require energy because amyloid proteins can 'seed' their own oligomerization (16).

Functional amyloids are not just involved in bacterial biofilm formation. Throughout this chapter I discuss the assembly of microbial amyloids and how these molecules participate in biofilm formation, persistence, and other cellular functions. I also illustrate, with an emphasis on curli, the many mechanisms that have evolved in functional amyloid systems that discourage potential amyloid-induced cytotoxicity.

Functional Amyloids in Biofilms and Floccs

A variety of microbes including bacteria and fungi are capable of biofilm formation. Gram-negative bacteria such as *Salmonella* and *E. coli* produce a complex extracellular matrix that contributes to the formation of biofilms (17, 18). This matrix includes cellulose, exopolysaccharides such as colonic acid, and curli (18, 19). Curli are critical determinants of biofilm formation as they can mediate initial surface attachment and also provide a scaffold that contributes to biofilm integrity (17, 20-23). Accordingly, curliated bacteria better colonize plant tissues, stainless steel and glass (23-26). Rationally designed, small, peptidomimetic molecules that are able to interfere with curli assembly also prevent biofilm formation, supporting a key role for curli in biofilm formation (27).

Amyloids have been identified in the natural environment in biofilms produced by *Proteobacteria*, *Bacteroidetes*, *Chloroflexi* and *Actinobacteria* (10). Amyloids have also been identified in organisms involved in water treatment processes, where the critical bioremediation step is mediated by biofilm-like structures called floccs: aggregative clusters of microbes in a network of polysaccharides and protein. Amyloids have been characterized in the matrix of activated sludge-derived floccs containing a broad variety of microbes (28). In this context, amyloids likely play diverse roles in adhesion and as a scaffold important for biofilm formation, integrity and persistence. However, amyloids may also help to act as physical barriers, scavengers of toxins, moisture regulators, or as toxins that kill other microbial species. Specific examples of these possible amyloid functions during biofilm development are discussed below.

Pseudomonas fluorescens and *Bacillus subtilis* produce identifiable functional amyloids in their biofilm matrix (20, 29, 30). FapC, originally characterized in *P. fluorescens*, is a highly conserved amyloid protein found in many *Pseudomonas* species. FapC has 3 repeat motifs and forms an extracellular amyloid matrix that contributes to the aggregative properties of *Pseudomonas* species (29). Biofilm integrity and persistence in *B. subtilis* are also influenced by the amyloid-forming protein TasA (11). TasA forms extracellular amyloid fibers that are anchored to the peptidoglycan layer of the cell wall by TapA (30). When biofilms age or D-amino acids are elevated, TapA is shed from the membrane releasing TasA fibers from the cell surface and allowing for dispersal from the biofilm (30). Although unrelated at the primary sequence level, TasA and FapC together with CsgA serve similar functions in biofilm formation demonstrating a common function for these amyloids in biofilms.

Functional Amyloids as Adhesins

Amyloids also function as adhesins, as is the case with *Mycobacterium tuberculosis* (31). Electron microscopic analysis of the *M. tuberculosis* pili (MTP) shows fibers that are strikingly similar to curli fibers. These fibers have also been reported in aged and carbon starved *M. tuberculosis* cultures (32, 33). Additionally, MTP are sodium dodecyl sulfate (SDS)-insoluble and bind Congo red (CR), suggesting that MTP are in fact amyloid fibers. MTP fibers have recently been shown to contain the protein product of the Rv3312a reading frame (31). The significance of MTP fibers for the pathogenesis of *M. tuberculosis* is unclear; however, MTP have been shown to bind laminin, a human extracellular matrix protein. MTP are conserved only in pathogenic mycobacterial species; a recent study showed that tuberculosis patients produce serum antibodies against to MTP (31). These data suggest that MTP are amyloid fibers that may be involved in *M. tuberculosis* cellular adherence and pathogenesis.

Amyloids produced by fungi also play a role in adhesion. *Candida albicans* produces Als adhesins, which are involved in host tissue adherence and self-aggregation (34-38). Als5p was shown to be important in surface changes that resulted in yeast aggregation when expressed heterologously in *Saccharomyces cerevisiae* or in *C. albicans* (39). Als5p was shown to undergo changes in protein secondary structure

and bind to CR. Short peptides from Als were also shown to form amyloids *in vitro*, demonstrated by CR binding, ThT fluorescence and electron microscopy (36). Intriguingly, oral infections in humans occur more prevalently with *C. albicans* when there is a higher amount of ferritin in the oral cavity. This observation led to the discovery that Als3 adhesin expression in the hyphae morphotype of *C. albicans* allows binding and utilization of iron sequestered in ferritin (40). Hence, in this yeast, expression of functional amyloid leads key events for fungal survival and virulence.

Functional Amyloids as Surface Property Modifiers

There are several examples of amyloids modifying the surface properties of microbes. One example, chaplins, are produced by the soil-derived bacteria *Streptomyces coelicolor*. *S. coelicolor* produce aerial hyphae in order to disperse spores. While underground, the hyphae are hydrophilic, whereas the aerial hyphae and spores are hydrophobic (41), and the formation of aerial hyphae requires a change in the surface hydrophobicity. This change in surface property is concomitant with the formation of an SDS-insoluble surface layer in the aerial hyphae and spores. The formation of this layer requires chaplin proteins, which are encoded by *chpA-H* (42). Chaplin proteins assemble into a network of amyloid fibers and cellulose on the surface of the aerial hyphae (43). The chaplins also self-assemble into β -sheet-rich fibers *in vitro* and bind CR and ThT (42). The amyloid properties of chaplins provide the dramatic hydrophobicity change to the surface layer that results in decreased surface tension at the air–water interface. The hyphae are then freed from the soil and continue to rise into the air (44).

The individual contributions of the eight chaplin proteins to the amyloid network are starting to be elucidated. Recently, five of them (ChpD-H) have been shown to form amyloid fibers *in vitro* (45). Remarkably, addition of crude cell extracts containing chaplins restores formation of aerial hyphae to mutant *S. coelicolor* lacking some of the *chp* genes. This observation is similar to the interbacterial complementation phenotype of *E. coli* *csgA* and *csgB* mutants where the individual strains are unable to produce curli, but when grown in close proximity to each other *csgA* and *csgB* mutants are able to make curli (42, 46). Further, there may be temporal regulation influencing the

expression of the chaplin genes suggesting that a coordinated biosynthesis pathway is at work in chaplin amyloid assembly (42). How chaplin assembly is controlled on the molecular level remains undefined. Several of the *chp* genes are not essential for fiber formation and could function as accessory factors for preventing inappropriate amyloidogenesis (45, 47). In addition, the importance of cellulose in chaplin formation could be another control mechanism, preventing chaplin fiber formation until the subunits contact cellulose on the cell surface (48).

Hydrophobins are another class of small, secreted proteins of about 100 amino acids that are produced by fungi. Hydrophobins play a similar role to that of chaplins in spore and fruiting body formation, but also play a role in attachment to host surfaces and protection against the host innate immune response during infection (49, 50). Hydrophobins can be divided into class I and II. The better-characterized class I hydrophobins are functionally related and can complement each other. Hydrophobins self-assemble at the hydrophilic-hydrophobic interface (reviewed in (49)). Strikingly, the hydrophobin polymerization process is most efficient over interfaces with high surface tension while agents that reduce this property slow down the rate of hydrophobin polymerization *in vitro* (51). The layer that forms from class I hydrophobins is SDS-insoluble, and can only be disassembled with formic acid (FA) treatment (52). Amino acid sequences among the hydrophobins are diverse, but they all have eight conserved cysteine residues. The SC3 hydrophobin is β -sheet rich and forms a helical intermediate at the hydrophilic-hydrophobic interface (53). This β -sheet rich structure forms stable 5-12 nm wide rodlets (rod-shaped structures) that fluoresce when mixed with ThT and can bind CR. Therefore, the rodlets appear to share many properties with amyloids.

Ustilago maydis is a fungal plant pathogen that produces proteins called repellents, which are involved in aerial hyphae formation and attachment to host cells. In *U. maydis*, these repellents perform a similar function to hydrophobins; however, these two classes of proteins are unrelated at the amino acid level. The *rep1* gene encodes a pre-pro-peptide that is processed into the 10 peptides that are collectively referred to as repellents. Teertstra and colleagues have shown that the peptide Rep1-1 is able to form filaments both *in vitro* and *in vivo* with amyloid characteristics (54). Microarray analysis conducted comparing a *rep1* mutant with a wild type strain found

induction of a small subset of genes encoding secreted cysteine rich proteins that are predicted to form amyloids (55, 56). Thus, these amyloids may be functionally redundant in order to ensure that proper fungal development occurs. This redundancy supports an essential role of functional amyloids in fungi.

Functional Amyloids as Toxins

One way many functional amyloids bypass the toxicity associated with amyloid formation is through separation of nucleator and major subunit functionalities. However, some functional amyloids capitalize on the inherent cytotoxicity of the amyloid fold. Microcin E492 is a bactericidal peptide produced by *Klebsiella pneumoniae* that assembles into oligomeric pores within the cytoplasmic membrane of neighboring bacteria, particularly Enterobacteriaceae species (57). Other microcins have also been described with similar antimicrobial functions (58). Microcin E492 is imported across the bacterial outer membrane in a receptor-mediated fashion (59), and has been shown to form voltage independent ion channels in planar lipid bilayers (57). The toxicity of the peptide changes during the growth cycle of the *K. pneumoniae*. The toxicity is greatest during exponential phase and lowest during stationary phase, and this change in microcin E492 toxicity is associated with the formation of mature amyloid fibers (60). The assembly of amyloid fibers can also be observed *in vitro*, and corresponds to a loss of toxicity (60). Therefore, the toxic pore forming microcin E492 is presumably a transient pre-amyloid oligomer intermediate. It has been speculated that the toxic microcin E492 species may have structural similarity with the transient oligomeric species formed by disease-associated amyloids. Microcin E492 has been shown to trigger apoptosis in some human cell lines, reminiscent of the toxic effect observed for disease-associated preamyloid oligomers (61). Microcin E492 is currently being explored as a method to eliminate malignant cells (62). The mechanisms for promoting oligomeric pore formation, but preventing aggregation into fibers, requires further study.

Harpins are proteins secreted by bacteria that elicit a hypersensitive immune response in plants, some of which might include the toxic aspect of amyloid formation intermediates. The hypersensitive response is characterized by localized cell death in plant tissue, which is a mechanism to prevent the spread of plant pathogens. Several

pathogens including *Xanthomonas*, *Erwinia* and *Pseudomonas* species secrete harpins as virulence factors to assist in movement through plant hosts (63, 64). Harpins from several bacterial species form amyloid-like fibers *in vitro* (65). The amyloid forming ability of HpaG, a harpin from *Xanthomonas*, directly correlates with hypersensitive response. A mutant form of HpaG that is unable to form amyloid also fails to elicit the hypersensitive response. Interestingly, size exclusion chromatography and visualization by electron microscopy suggests that a tetrameric oligomer is present when a hypersensitive response is observed (65). These results raise intriguing questions about how the bacteria avoid the toxicity associated with oligomer formation.

Functional Amyloids in Epigenetic Inheritance

Prions have been shown to cause many diseases, including transmissible spongiform encephalopathies (reviewed in (66)). The cause of the prion diseases is a normally soluble protein, PrP^c that misfolds and forms an amyloid aggregate, PrP^{sc}. The prion form can then convert other soluble PrP^c proteins into insoluble aggregates that propagate the misfolded protein conformation and cause cellular damage (67). However, several prions can be categorized as “functional” in yeast because a definable advantage is gained upon their formation (68). In addition, many of these proteins form a cytoplasmic amyloid that is passed on to progeny during cellular division. These prions are examples of an epigenetic, non-Mendelian type of inheritance. Sup35p is the best-studied example of how particular protein folds can impart heritable changes. Sup35 is a translation termination factor that prevents protein synthesis past stop codons in *S. cerevisiae*. This regulation is lost when Sup35p assembles into an amyloid in [PSI+] *S. cerevisiae* leading to C-terminal extensions on some proteins and therefore greater protein diversity (69). Similarly, through aggregation, Ure2p can regulate Gln3p activity. Gln3p is a transcription factor that regulates expression of *DAL5*, which encodes an ureidosuccinate and allantoate transporter. Aggregation of Ure2p in [URE3+] strains of yeast causes Gln3p to be constitutively active and *DAL5* expression is upregulated. This effectively eliminates nitrogen catabolite repression and enables yeast to utilize ureidosuccinate in the presence of ammonium (70). Rnq1p, a glutamine/asparagine rich protein with unknown function in *S. cerevisiae*, can also

polymerize into the prion form [PIN⁺] and has been shown to promote the formation of [PSI⁺], another prion phenotype (71, 72). Collectively, the transition to and from the amyloid form of these multi-domain proteins impacts cellular physiology.

Lastly, fungal hyphae from adjacent colonies can fuse to form heterokaryons, genetically different nuclei coexisting in a common cytoplasm, and this process is mediated by the specific interactions that occur between amyloidogenic proteins. A well-characterized protein named HET-s regulates heterokaryon formation in *Podospora anserina* by prion formation. The prion form of HET-s results in heterokaryon incompatibility of genetically similar fungi (73). This is a currently expanding field, with several new examples of functional yeast prions reported including Swi1p, a part of the SWI/SNF chromatin-remodeling complex that is involved in regulation of 6% of the genes in *S. cerevisiae*. Aggregation of Swi1p alters the regulation of the complex, and is transmitted to offspring by the cytoplasm (74, 75). Therefore amyloid aggregation can significantly impact fungal physiology, while also imparting inheritable changes.

Curli are Functional Amyloids

Curli, the first identified functional amyloid, are extracellular protein fibers produced by many enteric bacteria including *Escherichia coli* and *Salmonella* species (Fig. 1.1A) (18, 76-78). Curli are the major proteinaceous component of *E. coli* biofilms and are important for surface colonization and interacting with host factors and the host immune system (19, 77, 79-85). Curli production is easily scored in the lab by plating cells on agar plates containing Congo red (CR) (82, 86). Like all amyloids, the major curli subunit CsgA is capable of self-polymerizing *in vitro* into β -sheet-rich amyloid fibers that bind to the amyloid binding fluorescent dye Thioflavin T (ThT) and can be visualized using transmission electron microscopy (TEM) (8, 87, 88). *In vitro* assembled CsgA amyloid fibers are indistinguishable from fibers formed *in vivo* (88).

The ability of curli to act as a strong scaffolding agent in biofilm formation stems from properties inherent to all amyloids. Curli are highly stable 6-12 nm wide non-branching fibers (Fig. 1.1A) that are resistant to degradation by proteases and denaturation by detergents (8). Pretreatment with a strong denaturant such as formic acid (FA) or hexafluoroisopropanol (HFIP) is required to depolymerize curli fibers so that

monomers of the major subunit protein, CsgA, can be resolved on an SDS-PAGE gel (8). CsgA amyloids, like other amyloids, are β -sheet rich and assemble into a highly stable cross- β structure stabilized in large part by tight “steric zipper” interactions between side-chains on adjacent β -sheets (8, 89-91). The amyloid characteristics of curli fibers are clearly important for their biological function and afford many useful techniques for rapid *in vivo* and *in vitro* study of curli biogenesis, biofilm formation and integrity, and amyloid assembly (27, 92).

Curli expression is highly coordinated.

Curli gene expression is a highly regulated and coordinated event both on the cellular level and within a biofilm community. Curli are the major protein component of *E. coli* biofilms yet the production of curli within a biofilms is restricted to a distinct subpopulation (14, 19, 93-95). Expression is controlled by several environmental signals and chemical gradients including temperature, osmolarity and oxygen (96-98). Within a rugose, or rough, colony biofilm (Fig. 1.1B) curled cells localize to the air-colony interface (14, 95). This bimodal population development can be triggered by oxidative stress, and in turn, rugose biofilms are protected from oxidative damage resulting from exposure to hydrogen peroxide (14). Bacteria within *Salmonella enterica* curli- and cellulose-dependent rugose colonies are also protected from desiccation and are more resistant to sodium hypochlorite treatment (or bleach) when compared to non-curliated colonies or planktonic cells, respectively (15). Successful biofilm formation requires spatial and temporal regulation of curli assembly, which relies on elaborate coordination of gene expression and protein production (Table 1.1).

The curli specific genes (*csg*) are found in two divergently transcribed operons, the intergenic region of which is the 7th largest in *E. coli* and subject to extensive regulation (82, 99, 100). The *csgDEFG* promoter is recognized as one of the most complexly regulated promoters in *E. coli* (101). Curli are primarily expressed during stationary phase and at low temperature (below 30°C), although some clinical isolates can express curli at 37°C (18, 77, 97, 102). Both curli promoters are regulated by the stationary phase alternative sigma factor σ^S , which is assisted by the thermo-sensitive protein Crl (Table 1.1) (77, 102-104). Stationary phase expression of the *csgDEFG*

promoter is likewise positively regulated by the stationary phase transcription factor MlrA (Table 1.1) (105, 106). Curli expression is also internally regulated by the first gene product of the *csgDEFG* operon: CsgD (Table 1.1). CsgD is a member of the FixJ/LuxR family of transcriptional regulators that coordinates the expression of multiple biofilm components including curli and cellulose, while repressing expression of flagellar genes (82, 107-109). CsgD activity and stability is modulated by phosphorylation of an N-terminal aspartic acid residue (DNA binding is decreased by *in vitro* phosphorylation) (110). Several additional transcriptional regulators modulate expression of the *csgDEFG* promoter: the catabolite repressor/activator protein Cra, the cAMP receptor protein CRP, and the recently identified protein RcdA (Table 1.1) (105, 111-114). At least two known two-component systems negatively regulate the *csgDEFG* operon (CpxA/R and RcsA/B) and one positively (OmpR/EnvZ) (Table 1.1) (22, 115-119). The two global DNA organization protein complexes IHF and H-NS impact curli gene expression inversely: IHF contributes to promote curli gene expression while H-NS represses curli expression in *E. coli* (Table 1.1) (111, 120, 121). Both positive and negative regulation involves simultaneous binding of regulatory proteins as well as competitive binding between positive and negative regulators. For instance, H-NS and IHF act in competition for binding upstream of the *csgDEFG* promoter while CpxR and H-NS can bind simultaneously to negatively regulate the *csgDEFG* promoter and OmpR and RstA can bind simultaneously with IHF to positively regulate the *csgD* promoter (111). Finally, the *csgDEFG* transcript is also subject to negative post-transcriptional regulation by five small regulatory RNAs: OmrA, OmrB, McaS, GcvB and RprA (Table 1.1) (122-125). The small RNAs ArcZ and SdsR also positively regulate *csgD* in *S. enterica*, but whether this is a direct effect has yet to be determined (Table 1.1) (126). For a more comprehensive review of the role of small RNAs in regulating the transition between biofilm and sessile growth see Mika and Hengge, 2013 (127).

CsgA amyloid assembly by design

A striking aspect of curli biogenesis is that, despite the propensity of CsgA to aggregate, amyloid formation is so faithfully restricted to the cell surface. The major and minor curli subunits, CsgA and CsgB, respectively, are encoded by the *csgBAC* operon

(82, 99, 128). CsgA is secreted across the outer membrane as an unstructured soluble protein (Fig. 1.2 and Fig. 1.3) (129). Soluble CsgA is then templated into an amyloid on the cell surface by the nucleator and minor curli subunit CsgB (Fig. 1.2 and Fig. 1.3) (46, 130). This mechanism of secretion is termed nucleation-precipitation or Type VIII secretion (131). A third, and less well understood, gene *csgC* is located downstream of *csgA*. CsgC is a small periplasmic protein that is proposed to play a role in subunit secretion and is the focus of Chapter 3 (129, 132). CsgC is a β -sheet rich protein with an immunoglobulin-like fold and a conserved CxC motif that shares a high degree of structural similarity with the N-terminus of the redox-active DsbD (132). Whether the other curli proteins are redox substrates of CsgC still unclear; the curli pore protein CsgG, however, is an attractive substrate candidate as it is the only other curli protein that contains a solvent exposed cysteine residue (132). Additionally, the presence of CsgC renders the *csgBA* mutant more sensitive to bile salts compared to the *csgBAC* mutant suggesting that CsgC may keep the pore open or ungated (132). Furthermore, an *S. enteritidis* *csgC* mutant produces wider curli fibers (~20nm) suggesting that CsgC may also function in CsgA folding and curli fiber structure (129). The *csgE*, *csgF* and *csgG* genes encode the proteins that comprise the unique outer membrane curli secretion apparatus (Fig. 1.3). CsgG assembles into a pore-like structure in the outer membrane while CsgE and CsgF play chaperone-like functions assisting in secretion and cell surface attachment of the curli fibers (Fig. 1.3) (133-136). CsgD is a positive regulator that promotes biofilm formation by positively regulating curli and cellulose production (Table 1.1) (82, 107-109).

CsgA is the major subunit of the curli fiber and is secreted across the outer membrane as an unstructured and soluble peptide (Fig. 1.3) (8, 82, 129, 137, 138). The mature CsgA protein is comprised of an N-terminal 22 amino acids (N-term22) required for outer membrane secretion, and a C-terminal amyloid core domain (Fig. 1.4AB) (89, 91, 136). The amyloid core of CsgA is composed of five imperfect repeating units: R1 through R5 (Fig. 1.4AB) (88, 137). Each repeating unit contains a Ser-X₅-Gln-X-Gly-X-Gly-Asn-X-Ala-X₃-Gln motif and forms a β -sheet-turn- β -sheet secondary structure with an overall β -helical, cross- β structure (Fig. 1.4AB) (89, 91). The arrangement of the repeating units in the cross- β structure aligns the Gln and Asn residues in each

repeating unit in stacks that stabilize the amyloid fold (Fig. 1.4AB) (139). It is also worth noting that the placement and stacking of the Gly and Ala residues in the consensus sequence is highly conserved in Gammaproteobacteria and likely play an important role in amyloid assembly (76).

Purified CsgA self-assembles into amyloid fibers that bind ThT and can be visualized by TEM *in vitro* (Fig. 1.5A). CsgA polymerization *in vitro* is very robust: CsgA polymerizes into indistinguishable amyloid fibers over large pH (3.0-9.0) and ionic (0-500mM NaCl) ranges (87). CsgA polymerization is concentration dependent and can be divided into three phases: a lag phase, an elongation phase and a stationary phase (Fig. 1.5AB). At CsgA concentrations between 5 and 30 μ M, the lag phase is approximately 2 hours (87, 88). During the lag and elongation phases, a CsgA folding intermediate that is conserved in most amyloid-forming proteins can be detected with a conformation-specific antibody, A11 (88, 140). Although purified CsgA readily forms amyloid *in vitro*, CsgA amyloid formation *in vivo* requires the nucleator protein CsgB (46, 130). CsgB nucleated polymerization of CsgA can be recapitulated *in vitro* in a process called “seeding”. When added to soluble CsgA, preformed CsgB or CsgA fibers (also referred to as seeds) accelerate the polymerization of CsgA by eliminating the lag phase (139). Interestingly, curli subunits from closely related species exhibit a cross-seeding promiscuity. Curli subunits from *E. coli* and the closely related bacteria *Citrobacter koseri* and *Salmonella enterica* are capable of cross-seeding both *in vivo* and *in vitro* (141).

The molecular features of both CsgA and CsgB that contribute to amyloid formation and nucleation have been thoroughly dissected. The repeating units of CsgA have distinct characteristics that either promote or temper amyloid formation (Fig. 1.4AB) (139, 142). Repeating units R1, R3, and R5 are amyloidogenic, while R2 and R4 are non-amyloidogenic: synthetic peptides of R1, R3 and R5 rapidly assemble into amyloid fibers *in vitro* while R2 and R4 do not (88, 143). Furthermore, CsgA Δ R1 and Δ R5 do not assemble into curli fibers *in vivo* and cannot be seeded by either CsgA or CsgB *in vitro* (143). R1 and R5 are therefore not only important for amyloid assembly, but are also the domains that mediate CsgA-CsgA and CsgA-CsgB interactions. The Gln and Asn residues in R1 and R5 (at positions 49, 54, 139 and 144) are critical for

amyloid formation (Fig. 1.4A) (139). Mutation of the Gln and Asn in R1 and R5 results in a CsgA variant, aptly named CsgA_{slowgo}, that polymerizes with a significantly extended (~100x longer) lag phase compare to WT CsgA (88, 139). While R1, R3 and R5 synthetic peptides all polymerize into amyloids *in vitro*, R3 polymerizes more slowly (139). R1 and R5 are interchangeable with one another (R12341 and R52345 CsgA chimeras produce WT curli *in vivo*), while replacement of either R1 or R5 with R3 (R32345 or R12343) results in little to no curli (143).

Certain residues in the CsgA repeating units appear to temper or slow CsgA aggregation into amyloid (142). Asp residues at positions 91 and 104 within R3 have been identified as “gatekeeper” residues that reduce the amyloidogenicity of R3 (Fig. 1.4A) (142). Mutations to either of these Asp residues in such a way that the peptide more closely resembles R1 or R5 restore curli assembly of the R12343 chimera *in vivo* and polymerization *in vitro* (142). Conversely, substitution of Asn136 and His149 within R5 for Asp, thus rendering R5 more similar to R3, abolishes curli assembly *in vivo* (142). The non-amyloidogenic repeating units R2 and R4 also contain “gatekeeper” residues (Fig. 1.4A). Mutating Gly78/Asp80/Gly82 in R2 and Gly123/Asp127 in R4 to the corresponding amino acids in R1 and R5, respectively, restored curli assembly to the CsgA Δ R1 and Δ R5 truncations *in vivo* (142). Mutation of all of the “gatekeeper” residues in R2, R3 and R4 to the corresponding residues in R1 or R5 in full-length CsgA results in a variant (CsgA^{*}) that polymerizes without a lag phase *in vitro* (142). Furthermore, CsgA^{*} is capable of forming curli *in vivo* in a CsgB/CsgF-independent manner and exhibits a toxic effect when overexpressed (142). These “gatekeeper” residues enable a level of intramolecular control over CsgA amyloid assembly that is important in avoiding amyloid-associated cytotoxicity.

Amyloid assembly is nucleation-dependent in vivo

In addition to keeping CsgA polymerization in check with intramolecular “gatekeeping” residues, curli assembly is also controlled by dividing the tasks of nucleation and polymerization between two proteins, CsgB and CsgA, respectively. CsgB is dispensable for polymerization of CsgA *in vitro* but is required for curli assembly on the cell surface *in vivo* (8, 46, 88, 130, 139, 144). In the absence of the surface-

associated CsgB, CsgA is secreted away from the cell and remains SDS-soluble (130, 145, 146). However, soluble CsgA either supplemented exogenously or from a nearby *csgB* mutant donor cell can be engaged on the surface of cells presenting CsgB in a process referred to as interbacterial complementation (Fig. 1.6) (8, 130, 139). Donor and recipient strains streaked on an agar plate as far apart as three millimeters can still participate in interbacterial complementation, owing to the incredible efficiency of the nucleation-precipitation mechanism of curli (Fig. 1.6) (130).

Like CsgA, CsgB is a glutamine and asparagine-rich protein comprised of a Sec secretion signal sequence, an N-terminal domain and a core domain (Fig. 1.4C). CsgB shares 30% sequence identity with CsgA and has an amyloid-like core similar to CsgA (46, 147). Each of the first four repeating units of CsgB contains an Ala-X₃-Gln-X-Gly-X₂-Asn-X-Ala-X₃-Gln motif similar to the repeat motif of CsgA. Repeating unit 5, however, lacks several of these residues and instead contains four positively charged amino acids that are absent in the other CsgB repeating units: Lys133, Arg140, Arg147 and Arg151 (Fig. 1.4C). Deletion of repeating unit 5 results in a truncated version of CsgB (CsgB_{trunc}) that is no longer cell surface associated (144). Moreover, CsgB_{trunc} self-assembles into amyloid fibers *in vitro* and can seed the polymerization of CsgA consistent with the hypothesis that CsgB also assembles into an amyloid core (46). Repeating units 1-3 appear to be largely dispensable for *in vitro* polymerization and localization, leaving R4 and R5 of primary importance for localization and nucleation of CsgA (144). It is also possible, however, that some of the CsgB repeating units function redundantly. These observations suggest a model where CsgB associates with the cell membrane via the fifth repeating unit while R1-R4 assume an amyloid fold that can template soluble CsgA into amyloid fibers. How CsgB is associated with the outer membrane is still largely unknown. CsgB localization, however, requires at least one component of the curli secretion apparatus, CsgF (134).

Curli are secreted by a dedicated outer membrane secretion apparatus

The curli system possesses a unique outer membrane secretion apparatus comprised of at least three proteins: CsgG, CsgE and CsgF (Fig. 1.3) (8, 82, 133, 146). CsgG is a lipoprotein that spans the outer membrane and assembles into an oligomeric

annular-shaped structure with an inner diameter of approximately 2 nm (132, 136, 146). The crystal structure of CsgG has been solved and reveals the pore to be a nonameric β -barrel pore (133). CsgE interact with CsgG in the periplasm assembling into a cap like structure (133). Overexpression of CsgG results in increased sensitivity to the small antibiotic erythromycin (740 Da) but not the larger vancomycin (1440 Da) suggesting that CsgG has a pore-like activity (136). Overexpression of CsgE suppresses the erythromycin sensitivity phenotype of a CsgG overexpressing strains (93, 135). CsgE may therefore act, in part, by gating CsgG to prevent the influx of environmental chemicals and molecules through the pore.

The CsgG oligomers are not uniformly distributed around the cell but are instead spatially restricted to discrete regions of the cell that co-localize with what appears to be the primary curli fiber attachment site (93). The mechanism of CsgG localization, however, and how the curli secretion apparatus is spatially localized to discrete spots around the cell remains unknown. Because subcellular localization is important for many biological functions, including macromolecular organelle assembly in bacteria, it is not unreasonable to hypothesize that spatial restriction of the curli secretion apparatus is also important for curli assembly (148, 149). Diffusion of protein subunits into the environment is a significant challenge of the nucleation-precipitation/Type VIII secretion system (131, 150). Localized secretion of CsgA may lead to high local concentrations that promote efficient curli formation on the cell surface. Interestingly, CsgA and CsgB are both required for stable oligomerization of CsgG suggesting that either subunit secretion or active curli polymerization on the cell surface somehow facilitates stable pore assembly (93).

Stable oligomerization of CsgG is dependent on both of the major and minor curli subunits, CsgA and CsgB, as well as the accessory proteins CsgE and CsgF (93). Conversely, CsgG is required for the stability and secretion of CsgA, CsgB and CsgF across the outer membrane (134, 146). CsgG interacts with CsgE and CsgF as well as fusion proteins in which the N-term²² of CsgA has been fused to the N-terminus of a substrate protein (136). CsgF is extracellular and interacts with CsgG on the cell surface where it stabilizes and localizes CsgB to cell-surface (134). In the absence of CsgF, both CsgB and CsgA remain predominately SDS-soluble and are secreted away from

the cell (134). Overexpression of CsgB in a *csgF* mutant restores the cell-surface localization of CsgB but it does not restore WT cell-surface associated curli fibers (134). CsgF therefore may play a more important role in remodeling CsgB into an amyloid-templating conformation rather than actually anchoring CsgA fibers.

Ensuring that curli amyloid assembly occurs at the correct time and place is a feat that is at least in part achieved by molecular chaperones (135, 151). Nenninger *et al.* described CsgF as having chaperone-like activity: CsgF appears to assist in directing the assembly of CsgA into an amyloid on the cell surface (134). CsgE, on the other hand, functions earlier in the curli biogenesis pathway by inhibiting premature amyloid formation within the periplasm, but also by directing CsgA subunits to CsgG for secretion (135). CsgE inhibits CsgA amyloid formation and interacts with CsgA amyloid fibers *in vitro* (135, 152). Two lines of evidence using fusion protein constructs with the N-terminal domain of CsgA implicate the N-terminal 22 amino acids of CsgA as the interacting domain with both CsgE and CsgG (135, 136). First, the large periplasmic protein PhoA coimmunoprecipitated with CsgG when PhoA was fused to the N-terminal 42 amino acids of CsgA (including the Sec secretion signal sequence) (136). Second, expression of CsgE specifically permits the secretion of the second domain of PapD and CpxP only when C-terminally fused to the N-terminal 22 amino acids of CsgA (135). However, overexpression of CsgG results in unchecked secretion of CsgA indicating that secretion through CsgG doesn't necessarily require CsgE (135, 136). Together, these results suggest a coordinated chaperone/delivery and secretion mechanism. CsgE putatively has three functions: 1) bind to CsgG and gate the outer membrane secretion pore, 2) bind to and inhibit amyloid formation of curli subunits within the periplasm, and 3) deliver these subunits to CsgG for secretion.

The curli system can be exploited for studying other amyloids

Other bacteria may have also adapted the CsgG-like amyloid secretion pore. The *Caulobacter crescentus* holdfast protein HfaA shares the amyloid-like characteristics of being resistant to heat and SDS denaturation (153). Like CsgA, the secretion and stability of HfaA depends on an outer membrane lipoprotein, HfaB, which shares 31% identity and 42% similarity with CsgG (154). It is attractive to hypothesize that the curli

secretion mechanism is representative of a distinct class of apparatuses for secreting amyloid subunits across membranes.

The unique curli secretion apparatus may be ideally suited for transporting generic unfolded amyloid proteins across the outer membrane. Secreted CsgA is unstructured. The CsgG pore is only about 2 nm (or 20 Å) wide and not large enough to secrete CsgA in its folded conformation, suggesting that CsgA is maintained in an unstructured and soluble conformation prior to secretion (129, 136, 137). The N-terminal 22 amino acids of the mature CsgA not only direct its secretion across the outer membrane, but when fused to unrelated amyloid proteins, can also direct their secretion (92, 135, 136, 155). *E. coli* expressing fusions of unrelated amyloids with the N-terminal domain of CsgA produce Congo red binding colonies on agar plates and SDS-insoluble fibers (92, 155). Harnessing the curli secretion system to assemble heterologous amyloids on the bacterial cell surface may pave the way for new high throughput screening methods for modulators of amyloid assembly.

Amyloid assembly can be modulated and probed with antibodies, small molecules and protein folding factors

Folding intermediates can be probed using antibodies and small molecules

The discovery of conformation specific antibodies has contributed immensely to our understanding of amyloid assembly (140, 156, 157). We now have the tools to detect intermediate oligomeric and fibrillar species during the amyloid assembly process. The conformation-specific antibody A11 was raised against an oligomeric intermediate of A β , the amyloid protein associated with Alzheimer's disease, and reacts with the oligomeric intermediates of many other disease-associated amyloids (140). CsgA is also transiently recognized by A11 *in vitro* indicating that CsgA functional amyloid formation proceeds by the same mechanism of assembly as disease-associated amyloids *in vitro* (88). Antibodies have also been raised that specifically recognize the amyloid fiber conformation and also broadly react with unrelated amyloid fibers (156, 157). Conformation specific antibodies have motivated the development of a new class of antibodies, gammabodies (for grafted amyloid motif antibodies), which not only react specifically with the fiber conformation, but also have a high degree of

specificity for protein sequence (158, 159). Gammabodies have been demonstrated to act in distinct mechanisms, depending on the grafted sequence, to inhibit amyloid formation of several disease-associated amyloids (158). Gammabodies have been engineered against each repeating unit of CsgA and have been shown to exhibit the same sequence and conformation specificity as gammabodies designed to interact with disease-associated amyloids (152, 159). It has yet to be determined if similar inhibitory interactions are possible between gammabodies and functional amyloids.

Peptidomimetic compounds are also attractive candidates for modulating protein-protein interactions and amyloid formation. A screen of compounds originally designed to inhibit the elaboration of *E. coli* P pili yielded a set of small molecules capable of inhibiting amyloid formation of A β (160, 161). These compounds have since been subject to extensive chemical modification and assayed for biological activity against several amyloid substrates including curli (27, 152, 162). This extensive library of 2-pyridone compounds, or curlicides, exhibit varying degrees of CsgA amyloid inhibition and curli-dependent biofilm inhibition (27, 152, 162). Interestingly, the compound FN075 inhibits both A β and CsgA amyloid formation but accelerates amyloid formation of the Parkinson's Disease-associated protein α -synuclein (162). FN075 promotes the oligomerization of both CsgA and α -synuclein; however, the α -synuclein oligomers are competent for amyloid formation (on-pathway) while the CsgA oligomers are not (off-pathway) (162). These provocative results suggest that the 2-pyridone compounds may be used as tools for probing and distinguishing between on- and off-pathway protein folding intermediates. Andersson *et al.* have now identified other 2-pyridone compounds that are capable of accelerating CsgA polymerization (152). Further analysis of curli assembly in the presence of these curlicide and accelerator compounds may be instrumental in dissecting early stages of functional amyloid assembly.

Chaperones can modulate amyloid assembly

One major question that remains in the functional amyloid field is how organisms ensure that functional amyloids assemble only at the right time and in the right place so as to avoid the cytotoxic effects traditionally associated with amyloid assembly and amyloid intermediates. Proteostatic dysfunction is frequently, if not always, associated

with protein misfolding and amyloid-associated diseases (163). A class of molecular chaperones called small heat shock proteins (sHSP) has been found to be associated with many types of amyloid aggregates *in vivo*. The small heat shock proteins Hsp27 and α B-crystallin are induced in Alzheimer's disease and the heat shock response is induced in patients with Familial Amyloidotic Polyneuropathy resulting in increased expression of Hsp70 and Hsp27 (164-167). The chaperones Hsp20 and HspB2 colocalize with senile plaques in brain samples from patients with Alzheimer's disease and TorsinA (a homolog of the yeast Hsp104), Hsp70, Hsp27, Hsp40 and Hsp110 colocalize with α -synuclein in Lewy bodies in brain tissue samples from patients with Parkinson's disease (168-170).

Heat shock proteins have also been shown to inhibiting disease-associated amyloid assembly and amyloid-related cytotoxicity *in vitro* and *in vivo* (163). For instance, the heat shock protein Hsp70 inhibits amyloid assembly of the Alzheimer's Disease-associated protein A β and the Parkinson's Disease-associated protein α -synuclein *in vitro* (171-174). Overexpression of Hsp70 has also been found to reduce disease pathology in a murine model of Alzheimer's Disease (175). Similarly, overexpression of the small heat shock protein Hsp16.2 in a *Caenorhabditis elegans* model of Alzheimer's Diseases resulted in decreased amyloid deposits and toxicity (176). Modulating the protein folding environment as a means to ameliorate amyloid-associated diseases is an area of intense research focus (177-179).

Dissertation Goals

The amyloid field has undergone a sea change since curli were characterized as an amyloid and the functional amyloid field was born. Curli biology is ideal for studying protein secretion, folding and amyloid biology. The goal of this dissertation is to identify and characterize factors that are involved in the controlled secretion and assembly of curli amyloid fibers. In Chapter 2 (published in *Prion*) I describe the ability of known molecular chaperones from the *E. coli* cytoplasm and periplasm to inhibit CsgA amyloid assembly. In Chapter 3 (accepted for publication in *Molecular Cell*) I report the discovery that the curli gene *csgC* encodes an efficient and selective inhibitor of CsgA and α -synuclein amyloid assembly. Finally, in Chapter 4, I report molecular details of

CsgE function as a curli secretory protein. My findings contribute exciting new knowledge to the functional amyloid field by refining some of the elaborate mechanisms that are in place to ensure that curli are assembled only at the right time and in the right place.

Figures and Tables

Figure 1.1. Curli production contributes to *E. coli* biofilm formation. A. *E. coli* k-12 strain BW25113 grown on a low salt agar plate at 26°C produce cell surface associated curli fibers that are visible by transmission electron microscopy. Scale bar is 500nm. **B.** The uropathogenic *E. coli* strain UTI89 develops a complex rugose colony morphology that is dependent on curli.

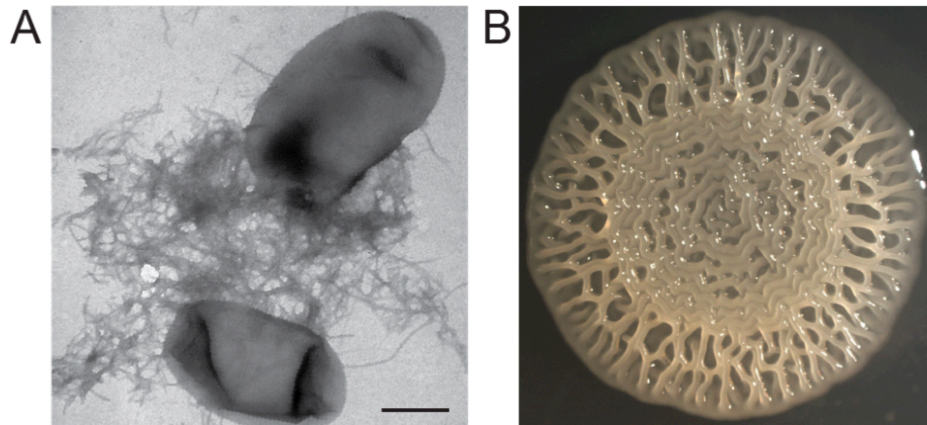


Figure 1.2. Model of curli biogenesis. Excluding CsgD, the master curli regulator, all Csg proteins have Sec-dependent signal sequences allowing their secretion into the periplasm. The lipoprotein CsgG forms a pore-like structure in the outer membrane. The major subunit protein CsgA and the nucleator CsgB are secreted to the cell surface in a CsgG- and CsgE-dependent manner. CsgF associates with the outer membrane and is required for cell association of the minor curli fiber subunit CsgB. Situated at the cell surface, CsgB nucleates soluble, unstructured CsgA into a highly ordered amyloid fiber. Curli production can be visualized by CR binding, which is absent in a *csgA* mutant, and by transmission electron microscopy (left inserts). Also shown are two CsgA subunits interacting in a cross- β conformation, with the R1–R5 interaction depicted (right inset).

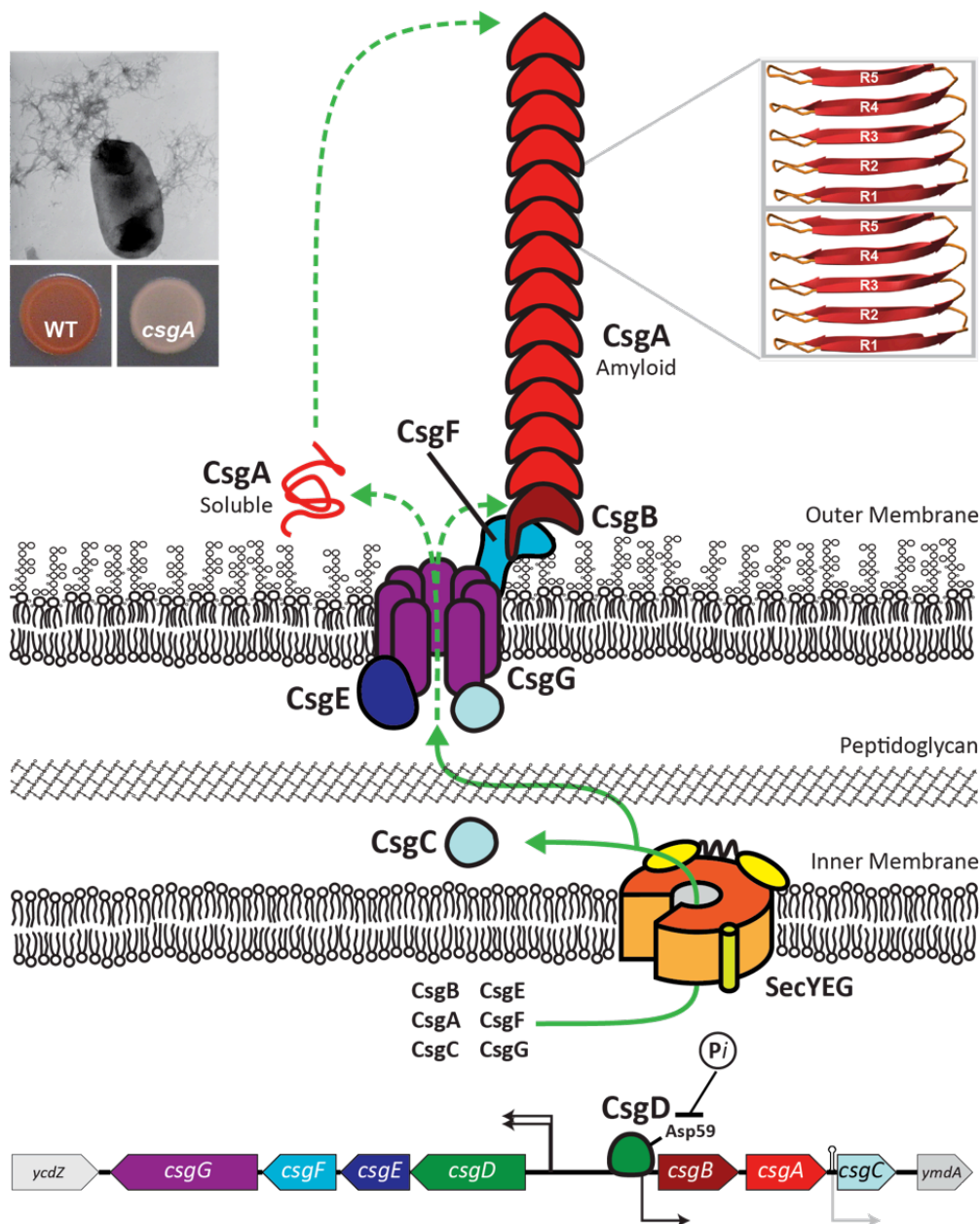


Figure 1.3. The curli biogenesis system possesses a unique outer membrane secretion apparatus. The CsgG pore is composed of nine subunits with a 2 nm wide central pore. Both CsgE and CsgF interact directly with the CsgG pore. CsgE is periplasmic and required for directing soluble CsgA to the CsgG pore for secretion while CsgF is surface exposed and contributes to the assembly of CsgB into a surface associated, amyloid-templating conformation. Once outside the cell, CsgA interacts with CsgB and assembles into an amyloid fiber.

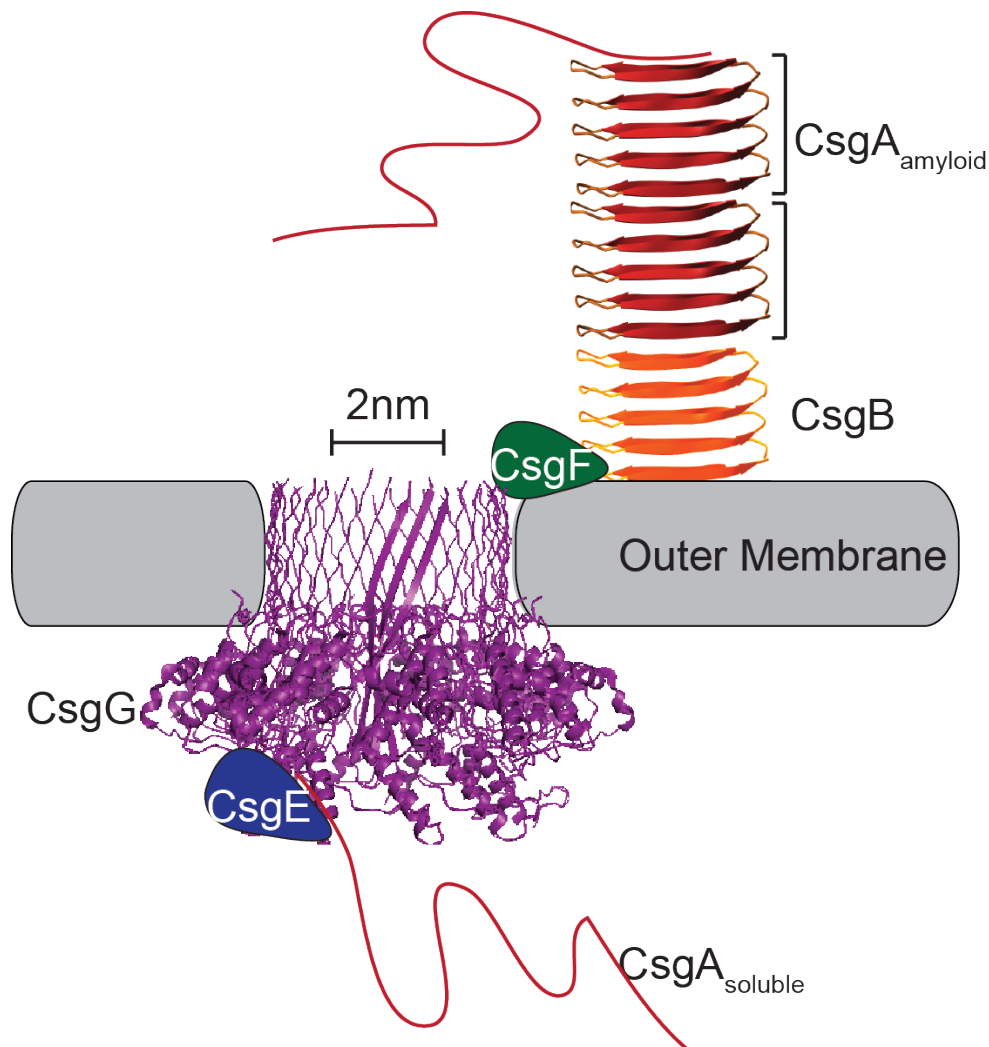
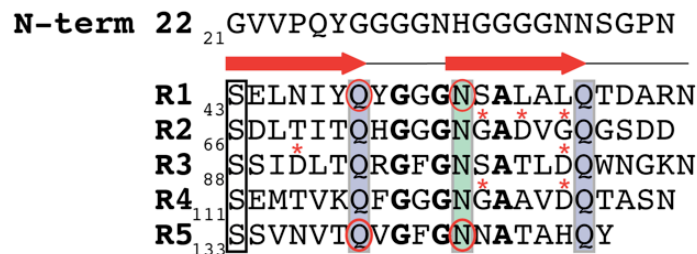
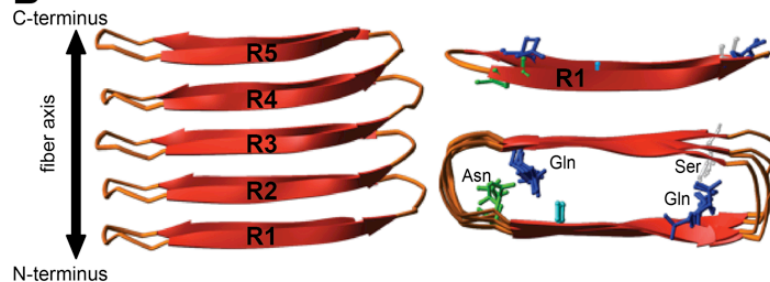


Figure 1.4. The molecular details of CsgA and CsgB. **A.** The mature CsgA protein is composed of an N-terminal 22 amino acids and 5 amyloid repeating units, each with a β -sheet-turn- β -sheet (indicated by the red arrows). Ser, Gln and Asn residues (boxes) in each repeating unit align in stacks that stabilize the amyloid conformation. The Gln residues at positions 49 and 139 and the Asn residues at positions 54 and 144 (circled) are essential for amyloid formation. Repeating units R2, R3 and R4 contain “gatekeeper” residues (*) that temper amyloid formation. The conserved glycine and alanine residues are indicated in bold font. **B.** A cartoon representation of the predicted structure of CsgA shows the five repeating units assemble into a β -helical, cross- β structure (side view, left). The Gln, Asn and Ser residues of R1 (upper right) are shown as sticks and the overhead view of CsgA (lower right) shows the alignment of these residues within the predicted structure. **C.** The mature CsgB protein is composed of an N-terminal 22 amino acids and 5 amyloid repeating units with similarly conserved Gln and Asn stacks (boxes). The conserved glycine and alanine residues in R1-R4 are indicated in bold font. Repeating unit 5 lacks one of the Asn repeats, but instead contains four charged residues (indicated by +) that may be important for tethering CsgB to the cell surface via R5.

A CsgA



B



C CsgB

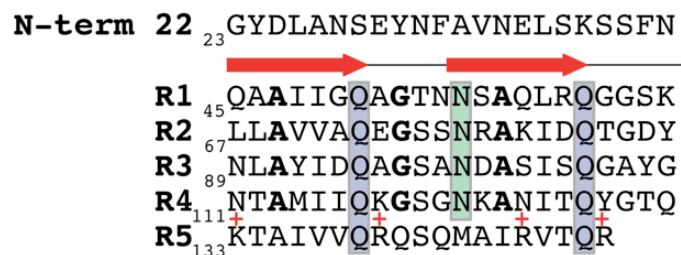
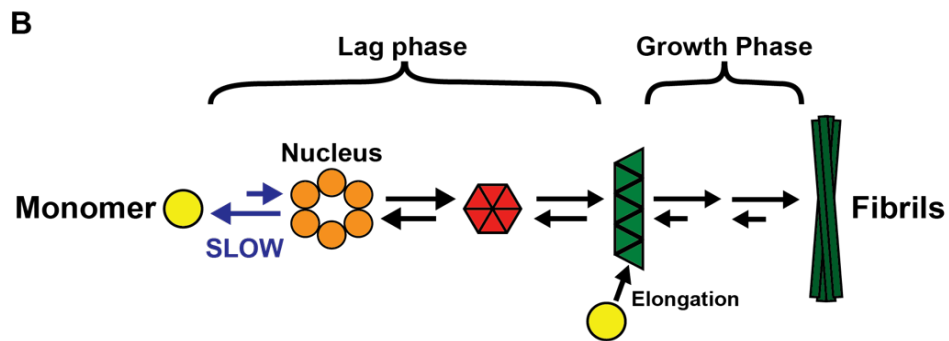
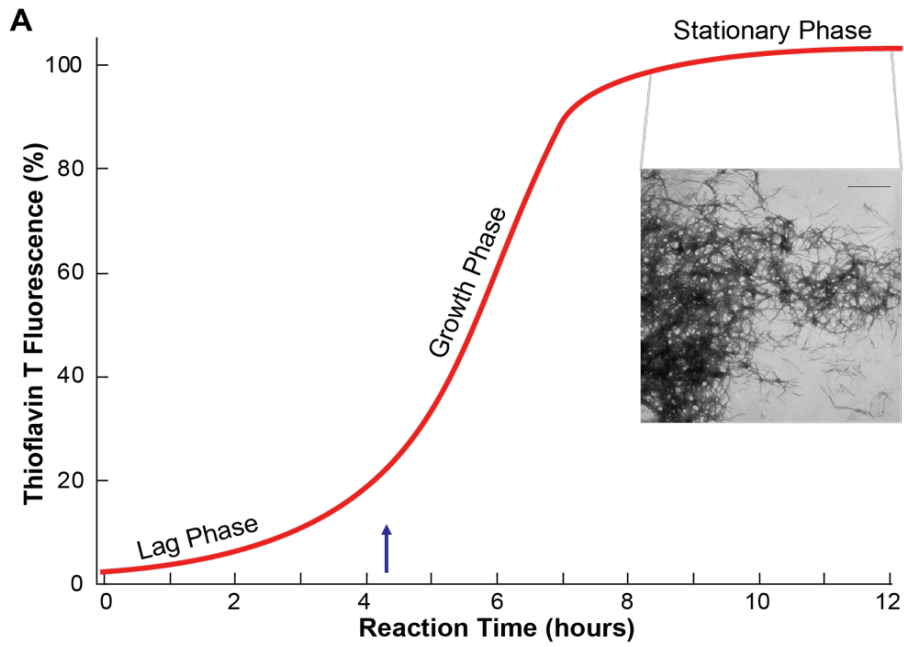


Figure 1.5. Schematic representation of amyloid polymerization. (a) Typical ThT fluorescence kinetics of soluble purified CsgA monomers polymerizing into curli [15]. The lag, growth and stationary phases are indicated. The blue arrow indicates the end of the lag phase. The insert shows a transmission electron micrograph of CsgA fibers formed when purified CsgA is allowed to polymerize in vitro as described by Wang et al. [8]. Scale bar, 500 nm. (b) The transition from soluble monomeric proteins to polymeric and insoluble amyloid fibers is characterized by distinguishable steps that result in loss- or gain-of-function properties for the protein. In the lag phase, soluble protein assembles into a common intermediate or nucleus that is proposed to be toxic to membranes [29,88]. The formation of the intermediate is proposed to be the rate-limiting step of amyloidogenesis. Once the nucleus is formed, monomers are templated into growing amyloid fibers causing an increase in ThT fluorescence. When the monomer population is depleted, elongation stops and enters the stationary phase. The green boxes below the schematic highlight properties of some of the functional amyloids, whereas the red boxes highlight some general properties of disease-associated amyloids.



MONOMERS	OLIGOMERIC INTERMEDIATES	MATURE AMYLOIDS
<ul style="list-style-type: none"> • Little sequence homology • Various cellular activities in normal form • Transition to the amyloid impacts peptide function 	<ul style="list-style-type: none"> • Found in functional and disease causing amyloids • Disrupt membranes • Usually toxic 	<ul style="list-style-type: none"> • Can be systemic or localised • Accumulation disrupts cellular trafficking • Many produce free radicals
	<ul style="list-style-type: none"> • Act as antimicrobials by disrupting membranes 	<ul style="list-style-type: none"> • Constituents of biofilm scaffolds • Enhance adherence and attachment • Change surface properties • Protect against innate immune responses • Protect from toxins and environmental insults • Increase adaptability through inheritance

Figure 1.6. Interbacterial complementation. Curli subunit sharing between adjacent cells, or interbacterial complementation, is made possible by the nucleation-precipitation mechanism of curli fiber assembly. A *csgB* mutant (or *csgA*⁺ donor strain) secretes soluble CsgA into the extracellular milieu. CsgA from a *csgB* mutant can polymerize on a *csgA* mutant (or *csgB*⁺ acceptor) that is presenting CsgB on the cell surface when grown in close proximity to one another on a plate. The left panel shows a *csgB* mutant (top) streaked near a *csgA* mutant (bottom), and on the edge of the CsgB-expressing streak there is a Congo red staining region.

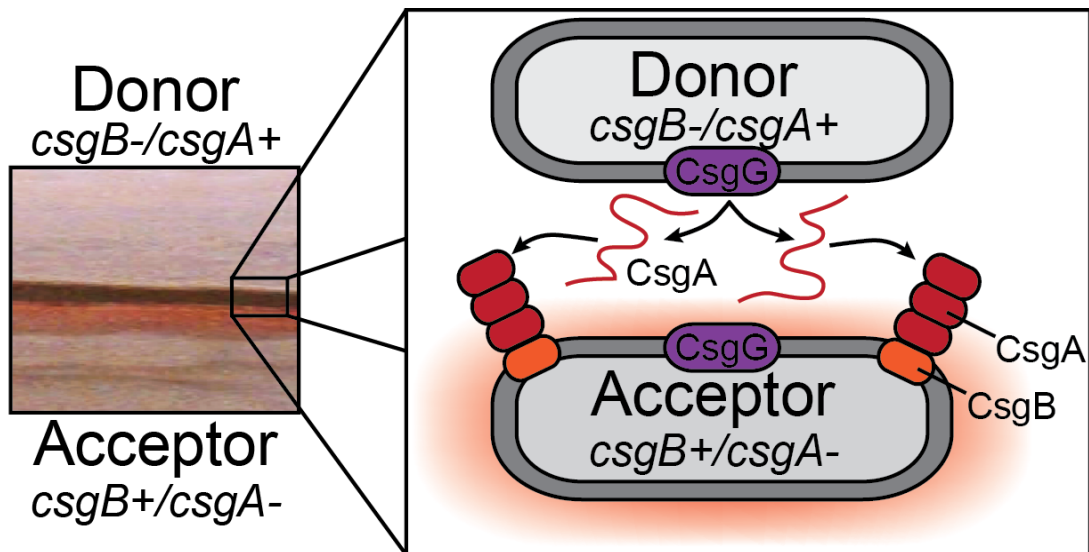


Table 1.1. Direct Regulators of the Curli Operons.

	Regulator	P _{csgBAC}	P _{csgDEFG}	Evidence	Reference(s)
Transcriptional Regulators	RpoS	+	+	Expression analysis, consensus binding site	(103, 104, 121, 181)
	Crl	+	+	Interacts with RpoS and stabilizes binding to <i>csg</i> promoters	(102, 104)
	CsgD	+	+	Expression analysis, consensus binding site	(82, 108)
	MlrA		+	Expression analysis, consensus binding site	(105, 106)
	Cra (FruR)		+	Expression analysis, consensus binding site	(112)
	Crp		+	Expression analysis	(114)
	RcdA		+	Expression analysis, consensus binding site	(113)
DNA Modifying Enzymes	IHF		+	Expression analysis, consensus binding site	(111, 120)
	H-NS		-/+ (<i>E. coli</i> / <i>S. typhimurium</i>)	Expression analysis, consensus binding site	(103, 111, 121)/(120)
Two-Component Systems	CpxA/R	-	-	Expression analysis, consensus binding site	(111, 115, 118)
	EnvZ/OmpR		+	Expression analysis, consensus binding site	(111, 117-120, 182)
	RcsA/B	-	-	Expression analysis	(116, 118, 183)
	RstB/A		-/+ (basic/acidic conditions)	Expression analysis, consensus binding site	(111, 184)
	ArcA/B		+	Expression analysis, consensus binding site	(185)
	BasS/R		+	Expression analysis, consensus binding site	(186)
Small Regulatory RNAs	OmrA/B		-	Antisense binding to 5'UTR	(122)
	McaS		-	Antisense binding to 5'UTR	(123, 125)
	GcvB		-	Antisense binding to 5'UTR	(123)
	RprA		-	Antisense binding to 5'UTR	(123, 124)
	ArcZ		+	Expression analysis post-transcriptional regulation	(126)
	SdsR		+	Expression analysis, transcriptional regulation	(126)

Regulators of the *csgBAC* and *csgDEFG* promoters. Positive and negative regulation of each promoter is indicated by “+” or “-”, respectively.

References

1. Sipe JD, Cohen AS (2000) Review: history of the amyloid fibril. *J Struct Biol* 130:88–98.
2. Chiti F, Dobson CM (2006) Protein misfolding, functional amyloid, and human disease. *Annu Rev Biochem* 75:333–366.
3. Breydo L, Wu JW, Uversky VN (2012) Alpha-synuclein misfolding and Parkinson's disease. *Biochim Biophys Acta* 1822:261–285.
4. Hardy J, Selkoe DJ (2002) The amyloid hypothesis of Alzheimer's disease: progress and problems on the road to therapeutics. *Science* 297:353–356.
5. Zuccato C, Valenza M, Cattaneo E (2010) Molecular mechanisms and potential therapeutical targets in Huntington's disease. *Physiol Rev* 90:905–981.
6. Blanco LP, Evans ML, Smith DR, Badtke MP, Chapman MR (2012) Diversity, biogenesis and function of microbial amyloids. *Trends Microbiol* 20:66–73.
7. Hufnagel DA, Tukul C, Chapman MR (2013) Disease to dirt: the biology of microbial amyloids. *PLoS Pathog* 9:e1003740.
8. Chapman MR, Robinson LS, Pinkner JS, Roth R, Heuser J, Hammar M, Normark S, Hultgren SJ (2002) Role of *Escherichia coli* curli operons in directing amyloid fiber formation. *Science* 295:851–855.
9. Fowler DM, Koulov AV, Alory-Jost C, Marks MS, Balch WE, Kelly JW (2006) Functional amyloid formation within mammalian tissue. *PLoS Biol* 4:e6.
10. Larsen P, Nielsen JL, Dueholm MS, Wetzel R, Otzen D, Nielsen PH (2007) Amyloid adhesins are abundant in natural biofilms. *Environ Microbiol* 9:3077–3090.
11. Romero D, Aguilar C, Losick R, Kolter R (2010) Amyloid fibers provide structural integrity to *Bacillus subtilis* biofilms. *Proc Natl Acad Sci U S A* 107:2230–2234.
12. Scheibel T, Kowal AS, Bloom JD, Lindquist SL (2001) Bidirectional amyloid fiber growth for a yeast prion determinant. *Curr Biol* 11:366–369.
13. Davey ME, O'toole GA (2000) Microbial biofilms: from ecology to molecular genetics. *Microbiol Mol Biol Rev* 64:847–867.
14. DePas WH, Hufnagel DA, Lee JS, Blanco LP, Bernstein HC, Fisher ST, James GA, Stewart PS, Chapman MR (2013) Iron induces bimodal population development by *Escherichia coli*. *Proc Natl Acad Sci U S A* 110:2629–2634.
15. White AP, Gibson DL, Kim W, Kay WW, Surette MG (2006) Thin aggregative fimbriae and cellulose enhance long-term survival and persistence of *Salmonella*. *J Bacteriol* 188:3219–3227.
16. McLaurin J, Yang D, Yip CM, Fraser PE (2000) Review: modulating factors in amyloid-beta fibril formation. *J Struct Biol* 130:259–270.
17. Romling U (2005) Characterization of the rdar morphotype, a multicellular behaviour in Enterobacteriaceae. *Cell Mol Life Sci* 62:1234–1246.
18. Zogaj X, Bokranz W, Nimtz M, Romling U (2003) Production of cellulose and curli fimbriae by members of the family Enterobacteriaceae isolated from the human gastrointestinal tract. *Infect Immun* 71:4151–4158.
19. McCrate OA, Zhou X, Reichhardt C, Cegelski L (2013) Sum of the Parts: Composition and Architecture of the Bacterial Extracellular Matrix. *J Mol Biol*
20. Barnhart MM, Chapman MR (2006) Curli biogenesis and function. *Annu Rev Microbiol* 60:131–147.

21. Castonguay MH, van der Schaaf S, Koester W, Krooneman J, van der Meer W, Harmsen H, Landini P (2006) Biofilm formation by *Escherichia coli* is stimulated by synergistic interactions and co-adhesion mechanisms with adherence-proficient bacteria. *Res Microbiol* 157:471–478.
22. Prigent-Combaret C, Brombacher E, Vidal O, Ambert A, Lejeune P, Landini P, Dorel C (2001) Complex regulatory network controls initial adhesion and biofilm formation in *Escherichia coli* via regulation of the *csgD* gene. *J Bacteriol* 183:7213–7223.
23. Uhlich GA, Cooke PH, Solomon EB (2006) Analyses of the red-dry-rough phenotype of an *Escherichia coli* O157:H7 strain and its role in biofilm formation and resistance to antibacterial agents. *Appl Environ Microbiol* 72:2564–2572.
24. Ryu JH, Kim H, Frank JF, Beuchat LR (2004) Attachment and biofilm formation on stainless steel by *Escherichia coli* O157:H7 as affected by curli production. *Lett Appl Microbiol* 39:359–362.
25. Barak JD, Gorski L, Naraghi-Arani P, Charkowski AO (2005) *Salmonella enterica* virulence genes are required for bacterial attachment to plant tissue. *Appl Environ Microbiol* 71:5685–5691.
26. Torres AG, Jeter C, Langley W, Matthyse AG (2005) Differential binding of *Escherichia coli* O157:H7 to alfalfa, human epithelial cells, and plastic is mediated by a variety of surface structures. *Appl Environ Microbiol* 71:8008–8015.
27. Cegelski L, Pinkner JS, Hammer ND, Cusumano CK, Hung CS, Chorell E, Aberg V, Walker JN, Seed PC, Almqvist F *et al.* (2009) Small-molecule inhibitors target *Escherichia coli* amyloid biogenesis and biofilm formation. *Nat Chem Biol* 5:913–919.
28. Larsen P, Nielsen JL, Otzen D, Nielsen PH (2008) Amyloid-like adhesins produced by floc-forming and filamentous bacteria in activated sludge. *Appl Environ Microbiol* 74:1517–1526.
29. Dueholm MS, Petersen SV, Sonderkaer M, Larsen P, Christiansen G, Hein KL, Enghild JJ, Nielsen JL, Nielsen KL, Nielsen PH *et al.* (2010) Functional amyloid in *Pseudomonas*. *Mol Microbiol*
30. Romero D, Vlamakis H, Losick R, Kolter R (2011) An accessory protein required for anchoring and assembly of amyloid fibres in *B. subtilis* biofilms. *Mol Microbiol* 80:1155–1168.
31. Alteri CJ, Xicohtencatl-Cortes J, Hess S, Caballero-Olin G, Giron JA, Friedman RL (2007) *Mycobacterium tuberculosis* produces pili during human infection. *Proc Natl Acad Sci U S A* 104:5145–5150.
32. Dahl JL (2005) Scanning electron microscopy analysis of aged *Mycobacterium tuberculosis* cells. *Can J Microbiol* 51:277–281.
33. Merkal RS, Rhoades KR, Gallagher JE, Ritchie AE (1973) Scanning electron microscopy of mycobacteria. *Am Rev Respir Dis* 108:381–387.
34. Frank AT, Ramsook CB, Otoo HN, Tan C, Soybelman G, Rauceo JM, Gaur NK, Klotz SA, Lipke PN (2010) Structure and function of glycosylated tandem repeats from *Candida albicans* Als adhesins. *Eukaryot Cell* 9:405–414.
35. Klotz SA, Gaur NK, De Armond R, Sheppard D, Khardori N, Edwards JEJ, Lipke PN, El-Azizi M (2007) *Candida albicans* Als proteins mediate aggregation with bacteria and yeasts. *Med Mycol* 45:363–370.

36. Otoo HN, Lee KG, Qiu W, Lipke PN (2008) *Candida albicans* Als adhesins have conserved amyloid-forming sequences. *Eukaryot Cell* 7:776–782.
37. Ramsook CB, Tan C, Garcia MC, Fung R, Soybelman G, Henry R, Litewka A, O'Meally S, Otoo HN, Khalaf RA *et al.* (2010) Yeast cell adhesion molecules have functional amyloid-forming sequences. *Eukaryot Cell* 9:393–404.
38. Dranginis AM, Rauceo JM, Coronado JE, Lipke PN (2007) A biochemical guide to yeast adhesins: glycoproteins for social and antisocial occasions. *Microbiol Mol Biol Rev* 71:282–294.
39. Rauceo JM, Gaur NK, Lee KG, Edwards JE, Klotz SA, Lipke PN (2004) Global cell surface conformational shift mediated by a *Candida albicans* adhesin. *Infect Immun* 72:4948–4955.
40. Almeida RS, Brunke S, Albrecht A, Thewes S, Laue M, Edwards JE, Filler SG, Hube B (2008) the hyphal-associated adhesin and invasin Als3 of *Candida albicans* mediates iron acquisition from host ferritin. *PLoS Pathog* 4:e1000217.
41. Elliot MA, Karoonuthaisiri N, Huang J, Bibb MJ, Cohen SN, Kao CM, Buttner MJ (2003) The chaplins: a family of hydrophobic cell-surface proteins involved in aerial mycelium formation in *Streptomyces coelicolor*. *Genes Dev* 17:1727–1740.
42. Claessen D, Rink R, de Jong W, Siebring J, de Vreugd P, Boersma FG, Dijkhuizen L, Wosten HA (2003) A novel class of secreted hydrophobic proteins is involved in aerial hyphae formation in *Streptomyces coelicolor* by forming amyloid-like fibrils. *Genes Dev* 17:1714–1726.
43. de Jong W, Wosten HA, Dijkhuizen L, Claessen D (2009) Attachment of *Streptomyces coelicolor* is mediated by amyloid fimbriae that are anchored to the cell surface via cellulose. *Mol Microbiol* 73:1128–1140.
44. Claessen D, Stokroos I, Deelstra HJ, Penninga NA, Bormann C, Salas JA, Dijkhuizen L, Wosten HA (2004) The formation of the rodlet layer of streptomycetes is the result of the interplay between rodlines and chaplins. *Mol Microbiol* 53:433–443.
45. Sawyer EB, Claessen D, Haas M, Hurgobin B, Gras SL (2011) The assembly of individual chaplin peptides from *Streptomyces coelicolor* into functional amyloid fibrils. *PLoS One* 6:e18839.
46. Hammer ND, Schmidt JC, Chapman MR (2007) The curli nucleator protein, CsgB, contains an amyloidogenic domain that directs CsgA polymerization. *Proc Natl Acad Sci U S A* 104:12494–12499.
47. Capstick DS, Jomaa A, Hanke C, Ortega J, Elliot MA (2011) Dual amyloid domains promote differential functioning of the chaplin proteins during *Streptomyces* aerial morphogenesis. *Proc Natl Acad Sci U S A* 108:9821–9826.
48. de Jong W, Wosten HA, Dijkhuizen L, Claessen D (2009) Attachment of *Streptomyces coelicolor* is mediated by amyloid fimbriae that are anchored to the cell surface via cellulose. *Mol Microbiol* 73:1128–1140.
49. Wosten HA, de Vocht ML (2000) Hydrophobins, the fungal coat unravelled. *Biochim Biophys Acta* 1469:79–86.
50. Amanianda V, Latge JP (2010) Fungal hydrophobins form a sheath preventing immune recognition of airborne conidia. *Virulence* 1:185–187.

51. Morris VK, Ren Q, Macindoe I, Kwan AH, Byrne N, Sunde M (2011) Recruitment of class I hydrophobins to the air:water interface initiates a multi-step process of functional amyloid formation. *J Biol Chem* 286:15955–15963.
52. Wessels J, De Vries O, Asgeirsdottir SA, Schuren F (1991) Hydrophobin Genes Involved in Formation of Aerial Hyphae and Fruit Bodies in *Schizophyllum*. *Plant Cell* 3:793–799.
53. de Vocht ML, Scholtmeijer K, van der Vegte EW, de Vries OM, Sonveaux N, Wosten HA, Ruyschaert JM, Hadziloannou G, Wessels JG, Robillard GT (1998) Structural characterization of the hydrophobin SC3, as a monomer and after self-assembly at hydrophobic/hydrophilic interfaces. *Biophys J* 74:2059–2068.
54. Teertstra WR, van der Velden GJ, de Jong JF, Kruijtz JA, Liskamp RM, Kroon-Batenburg LM, Muller WH, Gebbink MF, Wosten HA (2009) The filament-specific Rep1-1 repellent of the phytopathogen *Ustilago maydis* forms functional surface-active amyloid-like fibrils. *J Biol Chem* 284:9153–9159.
55. Teertstra WR, Krijgsheld P, Wosten HA (2011) Absence of repellents in *Ustilago maydis* induces genes encoding small secreted proteins. *Antonie Van Leeuwenhoek* 100:219–229.
56. Jang H, Arce FT, Mustata M, Ramachandran S, Capone R, Nussinov R, Lal R (2011) Antimicrobial protegrin-1 forms amyloid-like fibrils with rapid kinetics suggesting a functional link. *Biophys J* 100:1775–1783.
57. Lagos R, Wilkens M, Vergara C, Cecchi X, Monasterio O (1993) Microcin E492 forms ion channels in phospholipid bilayer membrane. *FEBS Lett* 321:145–148.
58. Duquesne S, Petit V, Peduzzi J, Rebuffat S (2007) Structural and functional diversity of microcins, gene-encoded antibacterial peptides from enterobacteria. *J Mol Microbiol Biotechnol* 13:200–209.
59. Destoumieux-Garzon D, Thomas X, Santamaria M, Goulard C, Barthelemy M, Boscher B, Bessin Y, Molle G, Pons AM, Letellier L *et al.* (2003) Microcin E492 antibacterial activity: evidence for a TonB-dependent inner membrane permeabilization on *Escherichia coli*. *Mol Microbiol* 49:1031–1041.
60. Bieler S, Estrada L, Lagos R, Baeza M, Castilla J, Soto C (2005) Amyloid formation modulates the biological activity of a bacterial protein. *J Biol Chem* 280:26880–26885.
61. Hetz C, Bono MR, Barros LF, Lagos R (2002) Microcin E492, a channel-forming bacteriocin from *Klebsiella pneumoniae*, induces apoptosis in some human cell lines. *Proc Natl Acad Sci U S A* 99:2696–2701.
62. Lagos R, Tello M, Mercado G, Garcia V, Monasterio O (2009) Antibacterial and antitumorigenic properties of microcin E492, a pore-forming bacteriocin. *Curr Pharm Biotechnol* 10:74–85.
63. Alfano JR, Kim HS, Delaney TP, Collmer A (1997) Evidence that the *Pseudomonas syringae* pv. *syringae* hrp-linked hrmA gene encodes an Avr-like protein that acts in an hrp-dependent manner within tobacco cells. *Mol Plant Microbe Interact* 10:580–588.
64. Ham JH, Cui Y, Alfano JR, Rodriguez-Palenzuela P, Rojas CM, Chatterjee AK, Collmer A (2004) Analysis of *Erwinia chrysanthemi* EC16 pelE::uidA, pelL::uidA, and hrpN::uidA mutants reveals strain-specific atypical regulation of the Hrp type III secretion system. *Mol Plant Microbe Interact* 17:184–194.

65. Oh J, Kim JG, Jeon E, Yoo CH, Moon JS, Rhee S, Hwang I (2007) Amyloidogenesis of type III-dependent harpins from plant pathogenic bacteria. *J Biol Chem* 282:13601–13609.
66. Wickner RB, Edskes HK, Shewmaker F, Nakayashiki T (2007) Prions of fungi: inherited structures and biological roles. *Nat Rev Microbiol* 5:611–618.
67. Ross CA, Poirier MA (2004) Protein aggregation and neurodegenerative disease. *Nat Med* 10 Suppl:S10–7.
68. Baxa U, Cassese T, Kajava AV, Steven AC (2006) Structure, function, and amyloidogenesis of fungal prions: filament polymorphism and prion variants. *Adv Protein Chem* 73:125–180.
69. Paushkin SV, Kushnirov VV, Smirnov VN, Ter-Avanesyan MD (1997) In vitro propagation of the prion-like state of yeast Sup35 protein. *Science* 277:381–383.
70. Wickner RB (1994) [URE3] as an altered URE2 protein: evidence for a prion analog in *Saccharomyces cerevisiae*. *Science* 264:566–569.
71. Vitrenko YA, Gracheva EO, Richmond JE, Liebman SW (2007) Visualization of aggregation of the Rnq1 prion domain and cross-seeding interactions with Sup35NM. *J Biol Chem* 282:1779–1787.
72. Vitrenko YA, Pavon ME, Stone SI, Liebman SW (2007) Propagation of the [PIN+] prion by fragments of Rnq1 fused to GFP. *Curr Genet* 51:309–319.
73. Coustou-Linares V, Maddelein ML, Begueret J, Saupe SJ (2001) In vivo aggregation of the HET-s prion protein of the fungus *Podospora anserina*. *Mol Microbiol* 42:1325–1335.
74. Crow ET, Du Z, Li L (2011) A small, glutamine-free domain propagates the [SWI(+)] prion in budding yeast. *Mol Cell Biol* 31:3436–3444.
75. Du Z, Crow ET, Kang HS, Li L (2010) Distinct subregions of Swi1 manifest striking differences in prion transmission and SWI/SNF function. *Mol Cell Biol* 30:4644–4655.
76. Dueholm MS, Albertsen M, Otzen D, Nielsen PH (2012) Curli functional amyloid systems are phylogenetically widespread and display large diversity in operon and protein structure. *PLoS One* 7:e51274.
77. Olsen A, Jonsson A, Normark S (1989) Fibronectin binding mediated by a novel class of surface organelles on *Escherichia coli*. *Nature* 338:652–655.
78. Zogaj X, Nimtz M, Rohde M, Bokranz W, Romling U (2001) The multicellular morphotypes of *Salmonella typhimurium* and *Escherichia coli* produce cellulose as the second component of the extracellular matrix. *Mol Microbiol* 39:1452–1463.
79. Bian Z, Brauner A, Li Y, Normark S (2000) Expression of and cytokine activation by *Escherichia coli* curli fibers in human sepsis. *J Infect Dis* 181:602–612.
80. Boyer RR, Sumner SS, Williams RC, Pierson MD, Popham DL, Kniel KE (2007) Influence of curli expression by *Escherichia coli* 0157:H7 on the cell's overall hydrophobicity, charge, and ability to attach to lettuce. *J Food Prot* 70:1339–1345.
81. Collinson SK, Doig PC, Doran JL, Clouthier S, Trust TJ, Kay WW (1993) Thin, aggregative fimbriae mediate binding of *Salmonella enteritidis* to fibronectin. *J Bacteriol* 175:12–18.
82. Hammar M, Arnqvist A, Bian Z, Olsen A, Normark S (1995) Expression of two csg operons is required for production of fibronectin- and congo red-binding curli polymers in *Escherichia coli* K-12. *Mol Microbiol* 18:661–670.

83. Kai-Larsen Y, Luthje P, Chromek M, Peters V, Wang X, Holm A, Kadas L, Hedlund KO, Johansson J, Chapman MR *et al.* (2010) Uropathogenic *Escherichia coli* modulates immune responses and its curli fimbriae interact with the antimicrobial peptide LL-37. *PLoS Pathog* 6:e1001010.
84. Olsen A, Wick MJ, Morgelin M, Bjorck L (1998) Curli, fibrous surface proteins of *Escherichia coli*, interact with major histocompatibility complex class I molecules. *Infect Immun* 66:944–949.
85. Pawar DM, Rossman ML, Chen J (2005) Role of curli fimbriae in mediating the cells of enterohaemorrhagic *Escherichia coli* to attach to abiotic surfaces. *J Appl Microbiol* 99:418–425.
86. Nilsson MR (2004) Techniques to study amyloid fibril formation in vitro. *Methods* 34:151–160.
87. Dueholm MS, Nielsen SB, Hein KL, Nissen P, Chapman M, Christiansen G, Nielsen PH, Otzen DE (2011) Fibrillation of the major curli subunit CsgA under a wide range of conditions implies a robust design of aggregation. *Biochemistry* 50:8281–8290.
88. Wang X, Smith DR, Jones JW, Chapman MR (2007) In vitro polymerization of a functional *Escherichia coli* amyloid protein. *J Biol Chem* 282:3713–3719.
89. Collinson SK, Parker JM, Hodges RS, Kay WW (1999) Structural predictions of AgfA, the insoluble fimbrial subunit of *Salmonella* thin aggregative fimbriae. *J Mol Biol* 290:741–756.
90. Nelson R, Sawaya MR, Balbirnie M, Madsen AO, Riek C, Grothe R, Eisenberg D (2005) Structure of the cross-beta spine of amyloid-like fibrils. *Nature* 435:773–778.
91. Shewmaker F, McGlinchey RP, Thurber KR, McPhie P, Dyda F, Tycko R, Wickner RB (2009) The functional curli amyloid is not based on in-register parallel beta-sheet structure. *J Biol Chem* 284:25065–25076.
92. Sivanathan V, Hochschild A (2012) Generating extracellular amyloid aggregates using *E. coli* cells. *Genes Dev* 26:2659–2667.
93. Epstein EA, Reizian MA, Chapman MR (2009) Spatial clustering of the curlin secretion lipoprotein requires curli fiber assembly. *J Bacteriol* 191:608–615.
94. Grantcharova N, Peters V, Monteiro C, Zakikhany K, Romling U (2010) Bistable expression of CsgD in biofilm development of *Salmonella enterica* serovar typhimurium. *J Bacteriol* 192:456–466.
95. Serra DO, Richter AM, Klauck G, Mika F, Hengge R (2013) Microanatomy at cellular resolution and spatial order of physiological differentiation in a bacterial biofilm. *MBio* 4:e00103–13.
96. Gerstel U, Romling U (2001) Oxygen tension and nutrient starvation are major signals that regulate agfD promoter activity and expression of the multicellular morphotype in *Salmonella typhimurium*. *Environ Microbiol* 3:638–648.
97. Olsen A, Arnqvist A, Hammar M, Normark S (1993) Environmental regulation of curli production in *Escherichia coli*. *Infect Agents Dis* 2:272–274.
98. Prigent-Combaret C, Vidal O, Dorel C, Lejeune P (1999) Abiotic surface sensing and biofilm-dependent regulation of gene expression in *Escherichia coli*. *J Bacteriol* 181:5993–6002.

99. Collinson SK, Clouthier SC, Doran JL, Banser PA, Kay WW (1997) Characterization of the agfBA fimbrial operon encoding thin aggregative fimbriae of *Salmonella enteritidis*. *Adv Exp Med Biol* 412:247–248.
100. Rudd KE (2000) EcoGene: a genome sequence database for *Escherichia coli* K-12. *Nucleic Acids Res* 28:60–64.
101. Ishihama A (2010) Prokaryotic genome regulation: multifactor promoters, multitarget regulators and hierarchic networks. *FEMS Microbiol Rev* 34:628–645.
102. Arnqvist A, Olsen A, Pfeifer J, Russell DG, Normark S (1992) The Crl protein activates cryptic genes for curli formation and fibronectin binding in *Escherichia coli* HB101. *Mol Microbiol* 6:2443–2452.
103. Arnqvist A, Olsen A, Normark S (1994) Sigma S-dependent growth-phase induction of the csgBA promoter in *Escherichia coli* can be achieved in vivo by sigma 70 in the absence of the nucleoid-associated protein H-NS. *Mol Microbiol* 13:1021–1032.
104. Bougdour A, Lelong C, Geiselmann J (2004) Crl, a low temperature-induced protein in *Escherichia coli* that binds directly to the stationary phase sigma subunit of RNA polymerase. *J Biol Chem* 279:19540–19550.
105. Brown PK, Dozois CM, Nickerson CA, Zuppardo A, Terlonge J, Curtiss Rr (2001) MlrA, a novel regulator of curli (AgF) and extracellular matrix synthesis by *Escherichia coli* and *Salmonella enterica* serovar Typhimurium. *Mol Microbiol* 41:349–363.
106. Ogasawara H, Yamamoto K, Ishihama A (2010) Regulatory role of MlrA in transcription activation of csgD, the master regulator of biofilm formation in *Escherichia coli*. *FEMS Microbiol Lett* 312:160–168.
107. Brombacher E, Dorel C, Zehnder AJ, Landini P (2003) The curli biosynthesis regulator CsgD co-ordinates the expression of both positive and negative determinants for biofilm formation in *Escherichia coli*. *Microbiology* 149:2847–2857.
108. Ogasawara H, Yamamoto K, Ishihama A (2011) Role of the biofilm master regulator CsgD in cross-regulation between biofilm formation and flagellar synthesis. *J Bacteriol* 193:2587–2597.
109. Romling U, Rohde M, Olsen A, Normark S, Reinkoster J (2000) AgfD, the checkpoint of multicellular and aggregative behaviour in *Salmonella typhimurium* regulates at least two independent pathways. *Mol Microbiol* 36:10–23.
110. Zakikhany K, Harrington CR, Nimtz M, Hinton JC, Romling U (2010) Unphosphorylated CsgD controls biofilm formation in *Salmonella enterica* serovar Typhimurium. *Mol Microbiol* 77:771–786.
111. Ogasawara H, Yamada K, Kori A, Yamamoto K, Ishihama A (2010) Regulation of the *Escherichia coli* csgD promoter: interplay between five transcription factors. *Microbiology* 156:2470–2483.
112. Reshamwala SM, Noronha SB (2011) Biofilm formation in *Escherichia coli* cra mutants is impaired due to down-regulation of curli biosynthesis. *Arch Microbiol* 193:711–722.
113. Shimada T, Katayama Y, Kawakita S, Ogasawara H, Nakano M, Yamamoto K, Ishihama A (2012) A novel regulator RcdA of the csgD gene encoding the master regulator of biofilm formation in *Escherichia coli*. *Microbiologyopen* 1:381–394.

114. Zheng D, Constantinidou C, Hobman JL, Minchin SD (2004) Identification of the CRP regulon using in vitro and in vivo transcriptional profiling. *Nucleic Acids Res* 32:5874–5893.
115. Dorel C, Vidal O, Prigent-Combaret C, Vallet I, Lejeune P (1999) Involvement of the Cpx signal transduction pathway of *E. coli* in biofilm formation. *FEMS Microbiol Lett* 178:169–175.
116. Ferrieres L, Clarke DJ (2003) The RcsC sensor kinase is required for normal biofilm formation in *Escherichia coli* K-12 and controls the expression of a regulon in response to growth on a solid surface. *Mol Microbiol* 50:1665–1682.
117. Gerstel U, Kolb A, Romling U (2006) Regulatory components at the csgD promoter—additional roles for OmpR and integration host factor and role of the 5' untranslated region. *FEMS Microbiol Lett* 261:109–117.
118. Jubelin G, Vianney A, Beloin C, Ghigo JM, Lazzaroni JC, Lejeune P, Dorel C (2005) CpxR/OmpR interplay regulates curli gene expression in response to osmolarity in *Escherichia coli*. *J Bacteriol* 187:2038–2049.
119. Romling U, Bian Z, Hammar M, Sierralta WD, Normark S (1998) Curli fibers are highly conserved between *Salmonella typhimurium* and *Escherichia coli* with respect to operon structure and regulation. *J Bacteriol* 180:722–731.
120. Gerstel U, Park C, Romling U (2003) Complex regulation of csgD promoter activity by global regulatory proteins. *Mol Microbiol* 49:639–654.
121. Olsen A, Arnqvist A, Hammar M, Sukupolvi S, Normark S (1993) The RpoS sigma factor relieves H-NS-mediated transcriptional repression of csgA, the subunit gene of fibronectin-binding curli in *Escherichia coli*. *Mol Microbiol* 7:523–536.
122. Holmqvist E, Reimegard J, Sterk M, Grantcharova N, Romling U, Wagner EG (2010) Two antisense RNAs target the transcriptional regulator CsgD to inhibit curli synthesis. *EMBO J* 29:1840–1850.
123. Jorgensen MG, Thomason MK, Havelund J, Valentin-Hansen P, Storz G (2012) Dual function of the McaS small RNA in controlling biofilm formation. *Genes Dev* 27:1132–1145.
124. Mika F, Busse S, Possling A, Berkholz J, Tschowri N, Sommerfeldt N, Pruteanu M, Hengge R (2012) Targeting of csgD by the small regulatory RNA RprA links stationary phase, biofilm formation and cell envelope stress in *Escherichia coli*. *Mol Microbiol* 84:51–65.
125. Thomason MK, Fontaine F, De Lay N, Storz G (2012) A small RNA that regulates motility and biofilm formation in response to changes in nutrient availability in *Escherichia coli*. *Mol Microbiol* 84:17–35.
126. Monteiro C, Papenfort K, Hentrich K, Ahmad I, Le Guyon S, Reimann R, Grantcharova N, Romling U (2012) Hfq and Hfq-dependent small RNAs are major contributors to multicellular development in *Salmonella enterica* serovar Typhimurium. *RNA Biol* 9:489–502.
127. Mika F, Hengge R (2013) Small Regulatory RNAs in the Control of Motility and Biofilm Formation in *E. coli* and *Salmonella*. *Int J Mol Sci* 14:4560–4579.
128. Collinson SK, Clouthier SC, Doran JL, Banser PA, Kay WW (1996) *Salmonella enteritidis* agfBAC operon encoding thin, aggregative fimbriae. *J Bacteriol* 178:662–667.

129. Gibson DL, White AP, Rajotte CM, Kay WW (2007) AgfC and AgfE facilitate extracellular thin aggregative fimbriae synthesis in *Salmonella enteritidis*. *Microbiology* 153:1131–1140.
130. Hammar M, Bian Z, Normark S (1996) Nucleator-dependent intercellular assembly of adhesive curli organelles in *Escherichia coli*. *Proc Natl Acad Sci U S A* 93:6562–6566.
131. Desvaux M, Hebraud M, Talon R, Henderson IR (2009) Secretion and subcellular localizations of bacterial proteins: a semantic awareness issue. *Trends Microbiol* 17:139–145.
132. Taylor JD, Zhou Y, Salgado PS, Patwardhan A, McGuffie M, Pape T, Grabe G, Ashman E, Constable SC, Simpson PJ *et al.* (2011) Atomic resolution insights into curli fiber biogenesis. *Structure* 19:1307–1316.
133. Goyal P, Krasteva PV, Van Gerven N, Gubellini F, Van den Broeck I, Troupiotis-Tsailaki A, Jonckheere W, Pehau-Arnaudet G, Pinkner JS, Chapman MR *et al.* (2014) Structural and mechanistic insights into the bacterial amyloid secretion channel CsgG. *Nature*
134. Nenninger AA, Robinson LS, Hultgren SJ (2009) Localized and efficient curli nucleation requires the chaperone-like amyloid assembly protein CsgF. *Proc Natl Acad Sci U S A* 106:900–905.
135. Nenninger AA, Robinson LS, Hammer ND, Epstein EA, Badtke MP, Hultgren SJ, Chapman MR (2011) CsgE is a curli secretion specificity factor that prevents amyloid fibre aggregation. *Mol Microbiol* 81:486–499.
136. Robinson LS, Ashman EM, Hultgren SJ, Chapman MR (2006) Secretion of curli fibre subunits is mediated by the outer membrane-localized CsgG protein. *Mol Microbiol* 59:870–881.
137. Cherny I, Rockah L, Levy-Nissenbaum O, Gophna U, Ron EZ, Gazit E (2005) The formation of *Escherichia coli* curli amyloid fibrils is mediated by prion-like peptide repeats. *J Mol Biol* 352:245–252.
138. Collinson SK, Emody L, Muller KH, Trust TJ, Kay WW (1991) Purification and characterization of thin, aggregative fimbriae from *Salmonella enteritidis*. *J Bacteriol* 173:4773–4781.
139. Wang X, Chapman MR (2008) Sequence determinants of bacterial amyloid formation. *J Mol Biol* 380:570–580.
140. Kayed R, Head E, Thompson JL, McIntire TM, Milton SC, Cotman CW, Glabe CG (2003) Common structure of soluble amyloid oligomers implies common mechanism of pathogenesis. *Science* 300:486–489.
141. Zhou Y, Smith D, Leong BJ, Brannstrom K, Almqvist F, Chapman MR (2012) Promiscuous cross-seeding between bacterial amyloids promotes interspecies biofilms. *J Biol Chem* 287:35092–35103.
142. Wang X, Zhou Y, Ren JJ, Hammer ND, Chapman MR (2010) Gatekeeper residues in the major curlin subunit modulate bacterial amyloid fiber biogenesis. *Proc Natl Acad Sci U S A* 107:163–168.
143. Wang X, Hammer ND, Chapman MR (2008) The molecular basis of functional bacterial amyloid polymerization and nucleation. *J Biol Chem* 283:21530–21539.
144. Hammer ND, McGuffie BA, Zhou Y, Badtke MP, Reinke AA, Brannstrom K, Gestwicki JE, Olofsson A, Almqvist F, Chapman MR (2012) The C-terminal

- repeating units of CsgB direct bacterial functional amyloid nucleation. *J Mol Biol* 422:376–389.
145. Bian Z, Normark S (1997) Nucleator function of CsgB for the assembly of adhesive surface organelles in *Escherichia coli*. *EMBO J* 16:5827–5836.
 146. Loferer H, Hammar M, Normark S (1997) Availability of the fibre subunit CsgA and the nucleator protein CsgB during assembly of fibronectin-binding curli is limited by the intracellular concentration of the novel lipoprotein CsgG. *Mol Microbiol* 26:11–23.
 147. White AP, Collinson SK, Baner PA, Gibson DL, Paetzel M, Strynadka NC, Kay WW (2001) Structure and characterization of AgfB from *Salmonella enteritidis* thin aggregative fimbriae. *J Mol Biol* 311:735–749.
 148. Bardy SL, Maddock JR (2007) Polar explorations Recent insights into the polarity of bacterial proteins. *Curr Opin Microbiol* 10:617–623.
 149. Ebersbach G, Jacobs-Wagner C (2007) Exploration into the spatial and temporal mechanisms of bacterial polarity. *Trends Microbiol* 15:101–108.
 150. Soto GE, Hultgren SJ (1999) Bacterial adhesins: common themes and variations in architecture and assembly. *J Bacteriol* 181:1059–1071.
 151. Evans ML, Schmidt JC, Ilbert M, Doyle SM, Quan S, Bardwell JC, Jakob U, Wickner S, Chapman MR (2011) *E. coli* chaperones DnaK, Hsp33 and Spy inhibit bacterial functional amyloid assembly. *Prion* 5:323–334.
 152. Andersson EK, Bengtsson C, Evans ML, Chorell E, Sellstedt M, Lindgren AEG, Hufnagel DA, Bhattacharya M, Tessier PM, Wittung-Stafshede P *et al.* (2013) Modulation of curli assembly and pellicle biofilm formation by chemical and protein chaperones. *Chemistry and Biology*
 153. Hardy GG, Allen RC, Toh E, Long M, Brown PJ, Cole-Tobian JL, Brun YV (2010) A localized multimeric anchor attaches the *Caulobacter* holdfast to the cell pole. *Mol Microbiol* 76:409–427.
 154. Cole JL, Hardy GG, Bodenmiller D, Toh E, Hinz A, Brun YV (2003) The HfaB and HfaD adhesion proteins of *Caulobacter crescentus* are localized in the stalk. *Mol Microbiol* 49:1671–1683.
 155. Sivanathan V, Hochschild A (2013) A bacterial export system for generating extracellular amyloid aggregates. *Nat Protoc* 8:1381–1390.
 156. Kaye R, Head E, Sarsoza F, Saing T, Cotman CW, Necula M, Margol L, Wu J, Breydo L, Thompson JL *et al.* (2007) Fibril specific, conformation dependent antibodies recognize a generic epitope common to amyloid fibrils and fibrillar oligomers that is absent in prefibrillar oligomers. *Mol Neurodegener* 2:18.
 157. O'Nuallain B, Wetzel R (2002) Conformational Abs recognizing a generic amyloid fibril epitope. *Proc Natl Acad Sci U S A* 99:1485–1490.
 158. Ladiwala AR, Bhattacharya M, Perchiacca JM, Cao P, Raleigh DP, Abedini A, Schmidt AM, Varkey J, Langen R, Tessier PM (2012) Rational design of potent domain antibody inhibitors of amyloid fibril assembly. *Proc Natl Acad Sci U S A* 109:19965–19970.
 159. Perchiacca JM, Ladiwala AR, Bhattacharya M, Tessier PM (2012) Structure-based design of conformation- and sequence-specific antibodies against amyloid beta. *Proc Natl Acad Sci U S A* 109:84–89.

160. Aberg V, Norman F, Chorell E, Westermark A, Olofsson A, Sauer-Eriksson AE, Almqvist F (2005) Microwave-assisted decarboxylation of bicyclic 2-pyridone scaffolds and identification of Abeta-peptide aggregation inhibitors. *Org Biomol Chem* 3:2817–2823.
161. Svensson A, Larsson A, Emtenas H, Hedenstrom M, Fex T, Hultgren SJ, Pinkner JS, Almqvist F, Kihlberg J (2001) Design and evaluation of pilicides: potential novel antibacterial agents directed against uropathogenic *Escherichia coli*. *Chembiochem* 2:915–918.
162. Horvath I, Weise CF, Andersson EK, Chorell E, Sellstedt M, Bengtsson C, Olofsson A, Hultgren SJ, Chapman M, Wolf-Watz M *et al.* (2012) Mechanisms of protein oligomerization: inhibitor of functional amyloids templates alpha-synuclein fibrillation. *J Am Chem Soc* 134:3439–3444.
163. Broadley SA, Hartl FU (2009) The role of molecular chaperones in human misfolding diseases. *FEBS Lett* 583:2647–2653.
164. Renkawek K, Bosman GJ, Gaestel M (1993) Increased expression of heat-shock protein 27 kDa in Alzheimer disease: a preliminary study. *Neuroreport* 5:14–16.
165. Renkawek K, Voorter CE, Bosman GJ, van Workum FP, de Jong WW (1994) Expression of alpha B-crystallin in Alzheimer's disease. *Acta Neuropathol* 87:155–160.
166. Renkawek K, Bosman GJ, de Jong WW (1994) Expression of small heat-shock protein hsp 27 in reactive gliosis in Alzheimer disease and other types of dementia. *Acta Neuropathol* 87:511–519.
167. Santos SD, Magalhaes J, Saraiva MJ (2008) Activation of the heat shock response in familial amyloidotic polyneuropathy. *J Neuropathol Exp Neurol* 67:449–455.
168. Wilhelmus MM, Otte-Holler I, Wesseling P, de Waal RM, Boelens WC, Verbeek MM (2006) Specific association of small heat shock proteins with the pathological hallmarks of Alzheimer's disease brains. *Neuropathol Appl Neurobiol* 32:119–130.
169. Shashidharan P, Good PF, Hsu A, Perl DP, Brin MF, Olanow CW (2000) TorsinA accumulation in Lewy bodies in sporadic Parkinson's disease. *Brain Res* 877:379–381.
170. McLean PJ, Kawamata H, Shariff S, Hewett J, Sharma N, Ueda K, Breakefield XO, Hyman BT (2002) TorsinA and heat shock proteins act as molecular chaperones: suppression of alpha-synuclein aggregation. *J Neurochem* 83:846–854.
171. Evans CG, Wisen S, Gestwicki JE (2006) Heat shock proteins 70 and 90 inhibit early stages of amyloid beta-(1-42) aggregation in vitro. *J Biol Chem* 281:33182–33191.
172. Luk KC, Mills IP, Trojanowski JQ, Lee VM (2008) Interactions between Hsp70 and the hydrophobic core of alpha-synuclein inhibit fibril assembly. *Biochemistry* 47:12614–12625.
173. Roodveldt C, Bertoncini CW, Andersson A, van der Goot AT, Hsu ST, Fernandez-Montesinos R, de Jong J, van Ham TJ, Nollen EA, Pozo D *et al.* (2009) Chaperone proteostasis in Parkinson's disease: stabilization of the Hsp70/alpha-synuclein complex by Hip. *EMBO J* 28:3758–3770.
174. Pemberton S, Madiona K, Pieri L, Kabani M, Bousset L, Melki R (2011) Hsc70 protein interaction with soluble and fibrillar alpha-synuclein. *J Biol Chem* 286:34690–34699.

175. Hoshino T, Murao N, Namba T, Takehara M, Adachi H, Katsuno M, Sobue G, Matsushima T, Suzuki T, Mizushima T (2011) Suppression of Alzheimer's disease-related phenotypes by expression of heat shock protein 70 in mice. *J Neurosci* 31:5225–5234.
176. Fonte V, Kapulkin WJ, Taft A, Fluet A, Friedman D, Link CD (2002) Interaction of intracellular beta amyloid peptide with chaperone proteins. *Proc Natl Acad Sci U S A* 99:9439–9444.
177. Balch WE, Morimoto RI, Dillin A, Kelly JW (2008) Adapting proteostasis for disease intervention. *Science* 319:916–919.
178. Lindquist SL, Kelly JW (2011) Chemical and biological approaches for adapting proteostasis to ameliorate protein misfolding and aggregation diseases: progress and prognosis. *Cold Spring Harb Perspect Biol* 3
179. Ryno LM, Wiseman RL, Kelly JW (2013) Targeting unfolded protein response signaling pathways to ameliorate protein misfolding diseases. *Curr Opin Chem Biol* 17:346–352.
180. Evans ML, Chapman MR (2014) Curli biogenesis: order out of disorder. *Biochim Biophys Acta* 1843:1551–1558.
181. Pratt LA, Silhavy TJ (1998) Crl stimulates RpoS activity during stationary phase. *Mol Microbiol* 29:1225–1236.
182. Vidal O, Longin R, Prigent-Combaret C, Dorel C, Hooreman M, Lejeune P (1998) Isolation of an *Escherichia coli* K-12 mutant strain able to form biofilms on inert surfaces: involvement of a new ompR allele that increases curli expression. *J Bacteriol* 180:2442–2449.
183. Vianney A, Jubelin G, Renault S, Dorel C, Lejeune P, Lazzaroni JC (2005) *Escherichia coli* tol and rcs genes participate in the complex network affecting curli synthesis. *Microbiology* 151:2487–2497.
184. Ogasawara H, Hasegawa A, Kanda E, Miki T, Yamamoto K, Ishihama A (2007) Genomic SELEX search for target promoters under the control of the PhoQP-RstBA signal relay cascade. *J Bacteriol* 189:4791–4799.
185. Liu X, De Wulf P (2004) Probing the ArcA-P modulon of *Escherichia coli* by whole genome transcriptional analysis and sequence recognition profiling. *J Biol Chem* 279:12588–12597.
186. Ogasawara H, Shinohara S, Yamamoto K, Ishihama A (2012) Novel regulation targets of the metal-response BasS-BasR two-component system of *Escherichia coli*. *Microbiology* 158:1482–1492.

Chapter 2

***Escherichia coli* Chaperones DnaK, Hsp33 and Spy Inhibit Bacterial Functional Amyloid Assembly²**

Abstract

Amyloid formation is an ordered aggregation process, where β -sheet rich polymers are assembled from unstructured or partially folded monomers. How two *Escherichia coli* cytosolic chaperones, DnaK and Hsp33, and a more recently characterized periplasmic chaperone, Spy, modulate the aggregation of a functional amyloid protein, CsgA is examined in this chapter. DnaK, the Hsp70 homologue in *E. coli*, and Hsp33, a redox-regulated holdase, potently inhibited CsgA amyloidogenesis. The Hsp33 anti-amyloidogenesis activity was oxidation dependent, as oxidized Hsp33 was significantly more efficient than reduced Hsp33 at preventing CsgA aggregation. When soluble CsgA was seeded with preformed amyloid fibers, neither Hsp33 nor DnaK were able to efficiently prevent soluble CsgA from adopting the amyloid conformation. Moreover, both DnaK and Hsp33 increased the time that CsgA was reactive with the amyloid oligomer conformation-specific A11 antibody. The ability of the periplasmic chaperone Spy to inhibit CsgA polymerization was also investigated. Like DnaK and Hsp33, Spy also inhibited CsgA polymerization *in vitro*. Overexpression of Spy resulted in increased chaperone activity in periplasmic extracts and in reduced curli biogenesis *in vivo*. We propose that DnaK, Hsp33 and Spy exert their effects during the nucleation stages of

² A modified version of this chapter was published in *Prion* (86). Jens Schmidt, Marianne Ilbert and Shannon Doyal conducted the DnaK and Hsp33 experiments (Figures 2.1, 2.2, 2.3AB and 2.4). Shu Quan, from James Bardwell's lab, and Ursula Jakob's lab generously donated Spy, DnaK and Hsp33 protein. Sue Wickner contributed the DnaK V436F mutant. I contributed the experiments in Figures 2.3C, 2.5 and 2.6.

CsgA fibrillation. Thus, both housekeeping and stress induced cytosolic and periplasmic chaperones may be involved in discouraging premature CsgA interactions during curli biogenesis.

Introduction

Amyloid formation is central to human ailments such as Alzheimer's disease, Parkinson's disease, Huntington's disease, transmissible spongiform encephalopathies, and type II diabetes (1, 2). Proteins and peptides of various primary sequence signatures can assemble into amyloids, which are biophysically distinguished as 4-12 nm wide, β -sheet rich fibers that are highly resistant to denaturation and bind to dyes such as thioflavin T (ThT) and Congo red (CR) (3). Amyloid subunits spontaneously polymerize into amyloid fibers *in vitro* after a defined lag phase, which is followed by rapid fiber growth (4-6). Although many proteins, if not all, can adopt the amyloid conformation *in vitro*, certain amino acid sequences or cellular environments significantly influence *in vivo* amyloidogenesis (1, 5, 7).

A new class of 'functional' amyloids has been linked to important physiological processes in cells. Unlike disease-associated amyloid formation *in vivo*, which is sporadic and difficult to predict, the formation of 'functional' amyloids is a tightly regulated cellular process (8, 9). Functional amyloids have been identified in nearly all walks of life, from bacteria (10-13) to fungi (14-16) to mammals (17, 18). Understanding how functional amyloids can form without apparent cellular toxicity will provide new insights into the processes that break down during disease-associated amyloid formation.

The first described functional amyloid was curli; extracellular organelles assembled by enteric bacteria such as *Escherichia coli* and *Salmonella* species (11). Curli fibers play an important role in biofilm formation (19-21), cell adhesion (22), cell invasion (23, 24), and induction of the host inflammatory response (25-27). Curli biogenesis is a highly regulated process and requires the products of two divergently transcribed operons (*csgBAC* and *csgDEFG*) (28). CsgD is a transcriptional activator of the *csgBAC* operon. (28, 29) CsgG forms an outer membrane lipoprotein required for the secretion of the major and minor curli subunits CsgA and CsgB, respectively (29, 30).

CsgA is secreted as a soluble, unstructured peptide and is nucleated into an extracellular amyloid fiber by the cell surface-associated CsgB (11, 31-33). CsgF assists in attachment of CsgA fibers to the cell surface and assists CsgB in its nucleation function (34). CsgE functions as a specificity factor in the periplasm for CsgG-mediated secretion of curli subunits and possesses chaperone activity *in vitro* (35). CsgC putatively collaborates with CsgG to regulate the passage of proteins and small molecules through CsgG (36, 37). Curli biogenesis must be a finely tuned system in order to prevent intracellular aggregation of CsgA.

The primary amino acid sequence of CsgA features five imperfect repeating units that are predicted to form a β -helix with an overall cross β -strand structure (38, 39). Repeating units one and five are highly amyloidogenic and contain conserved glutamine and asparagine residues that promote amyloid formation (40). Repeating units two, three and four contain gatekeeper residues, which reduce the propensity to form amyloids on their own (41). The separation of the amyloidogenic regions of CsgA is believed to help reduce the occurrence of premature amyloid formation within the cell. CsgA also contains a Sec-secretion signal sequence and an N-terminal 22 amino acid sequence on the mature protein that is required for CsgG-mediated translocation across the outer membrane (30, 35). Both CsgA and CsgB proteins are at undetectable levels by western blot in the absence of CsgG (29). Whether this is due to proteolytic degradation of CsgA and CsgB or transcriptional repression remains to be established.

During synthesis and export, CsgA may be exposed to the cytosolic and periplasmic chaperone machinery, which could modulate amyloidogenesis by preventing inappropriate amyloid fiber formation within the cell. How the cellular chaperone machinery engages amyloidogenic proteins, especially functional amyloids, is poorly understood. Recent studies have shown that the human chaperone Hsp70 partially prevents amyloid formation of the disease-associated proteins A β (1-42) and α -synuclein (42, 43). Hsp70 is an ATPase but can inhibit A β amyloidogenesis in the absence of ATP and its cochaperone Hsp40 (44). DnaK, the Hsp70 homologue in *E. coli* (45), has been shown to prevent protein aggregation and assist in the refolding of denatured proteins or remodeling of large protein aggregates (46, 47). DnaK is composed of two functional domains, the ATPase domain and the substrate-binding

domain (48). Substrate binding and release by DnaK is regulated by the nature of the nucleotide bound to the ATPase domain (49, 50). The ATP bound form of DnaK has a significantly lower substrate affinity than the ADP bound form (48). The ATPase cycle of DnaK is regulated by the co-chaperones DnaJ and GrpE (46). DnaJ stimulates the DnaK ATPase activity, while GrpE is a nucleotide exchange factor that stimulates the release of ADP from DnaK (51, 52). DnaJ, or a DnaJ homolog, and GrpE are essential for DnaK activity *in vivo* and in *in vitro* luciferase disaggregation assays (53).

Hsp33 is a “holdase” chaperone (54). Holdase chaperones are not thought to actively refold denatured substrates, but instead quench exposed hydrophobic regions of proteins during periods of transient cellular stress (54). Hsp33 expression is controlled by σ^{32} , the heat shock transcription initiation factor, and is induced at elevated temperatures and other conditions that trigger protein denaturation (55). Hsp33 is activated at the protein level by oxidizing and denaturing conditions (54). Four cysteine residues located in Hsp33’s C-terminal redox-switch domain coordinate Zn^{2+} under reducing conditions (56, 57). When oxidized, these cysteine residues form two disulfide bonds and the Zn^{2+} is released from the protein (58). A second region on the C-terminal domain of Hsp33 senses denaturing conditions (59). The combination of oxidizing and denaturing conditions triggers full activation and dimerization of Hsp33, which then acts as a holdase with broad specificity (54). Hsp33 efficiently protects the cell from protein aggregation in the cytoplasm under aggregation inducing conditions (60).

CsgA traverses the periplasmic space where it may be exposed to periplasmic proteostatic mediators that may play a role in maintaining CsgA in a soluble form prior to secretion across the outer membrane. The curli specific accessory protein CsgE exhibits chaperone activity towards CsgA *in vitro* by inhibiting polymerization.(35) Spy, a newly characterized periplasmic holdase (61), can prevent CsgA from polymerizing into an amyloid aggregate *in vitro*. Spy is under the regulation of the Cpx and Bae two-component systems, both of which are induced by stresses that promote protein misfolding and aggregation (62-65). Interestingly, both of the curli operons are negatively regulated by the Cpx system (64). Whether the Cpx stress response is induced during curli biogenesis has yet to be determined.

In this chapter Hsp33, DnaK and Spy are demonstrated to be potent inhibitors of CsgA fiber formation *in vitro*. Sub-stoichiometric amounts of DnaK transiently prevent CsgA polymerization in the absence of the co-chaperones DnaJ and GrpE, and without the addition of ATP. Hsp33 not only interfered with polymerization initiation, but also reduced the total amount of amyloid fibers formed. Spy, in addition to inhibiting CsgA polymerization *in vitro*, reduced curli biogenesis when overexpressed *in vivo*. The inhibition of CsgA fiber formation by DnaK, Hsp33 and Spy can be overcome by the addition of preformed CsgA fibers. Moreover, Hsp33 and DnaK did not prevent the formation of a structurally conserved transient CsgA intermediate that is also formed by disease-associated amyloids. These chaperones may be part of a control mechanism protecting the cell from inappropriate amyloid formation within the cell.

Results

DnaK inhibits CsgA amyloid formation.

The conversion of soluble amyloidogenic monomeric proteins to an ordered amyloid fiber *in vitro* can be measured using the amyloid specific dye thioflavin T (ThT). When freshly purified CsgA was mixed with ThT, fluorescence emission increased rapidly after an approximately 2-hour lag phase (Fig. 2.1A). The rapid growth phase of CsgA fibers was followed by a stationary phase, consistent with previous findings (Fig. 2.1A) (6). When comparing CsgA polymerization profiles in the presence or absence of chaperone proteins, two parameters were measured. The first kinetic parameter was calculated as the time period preceding rapid fiber growth, called lag phase. The second parameter, called the elongation phase, was calculated as the time period encompassing the fiber growth phase from initiation of rapid polymerization to its completion (6, 66).

To determine if DnaK affects CsgA amyloid formation *in vitro*, ThT fluorescence was measured in the presence or absence of DnaK. DnaK increased the lag phase 3 and 8 fold at molar ratios of 1:20 and 1:5 (DnaK:CsgA), respectively (Fig. 2.1A). However, once CsgA started to aggregate, neither the rate of fiber formation nor the maximal ThT fluorescence were affected by the presence of the chaperone (Fig. 2.1A). To determine if the ability of DnaK to inhibit CsgA polymerization was dependent on the

intact DnaK substrate-binding domain, the DnaK^{V436F} mutant was tested in the ThT assay. The DnaK^{V436F} mutant has reduced substrate affinity, but similar substrate specificity (67). When added to soluble CsgA, DnaK^{V436F} was significantly less efficient at inhibiting CsgA fiber formation compared to wild type DnaK (Fig. 2.1B). Wild type DnaK prevented CsgA polymerization for greater than 30 hours, while an equivalent concentration of DnaK^{V436F} only increased the lag phase from 2 hours to 7 hours (Fig. 2.1B).

To verify that the observed effect was due to the inhibition of CsgA polymerization, and not due to an indirect effect such as interference of the chaperone with ThT fluorescence CsgA solubility was measured in the presence and absence of DnaK. As an amyloid, curli are highly resistant to denaturation and require treatment with a harsh denaturant such as formic acid (FA) or hexafluoro-2-propanol (HFIP) to liberate the monomeric species (11). After 13 hours of incubation, polymerization reactions were centrifuged to separate the soluble and insoluble CsgA prior to analysis by SDS-PAGE. Duplicate samples were treated with 80% (w/w) FA to depolymerize CsgA aggregates (11, 68). CsgA was present only in the FA treated pellet samples after 13 hours of incubation in the absence of DnaK indicating that CsgA was entirely in the polymerized form (Fig. 2.1C lanes 1-4). After 13 hours in the presence of DnaK, however, CsgA was still detected in the non-FA treated supernatant samples suggesting that DnaK maintains CsgA in a soluble state (Fig. 2.1C lanes 5-8). These results were in agreement with transmission electron micrograph (TEM) images. CsgA formed unbranched fibers in the absence of DnaK; however, no such fibers were observed when CsgA was incubated in the presence of DnaK for 13 hours (Fig. 2.1D, 1E).

Oxidized Hsp33 inhibits CsgA polymerization in vitro.

Hsp33 is a homodimeric molecular chaperone which, when activated by oxidative stress, functions as a potent holdase. To determine if Hsp33 influences amyloid formation, CsgA fiber formation was monitored *in vitro* using ThT fluorescence (69, 70). Reduced, chaperone-inactive, Hsp33red, and oxidized, chaperone-active, Hsp33ox, were assayed for the ability to inhibit CsgA polymerization *in vitro*.(54) The presence of

Hsp33ox at a 1:80 (Hsp33ox dimer:CsgA) molar ratio increased the lag phase of CsgA fiber formation to 8 hours (Fig. 2.2A). The presence of Hsp33ox at a molar ratio of 1:20 increased the lag phase by 13 hours, while a molar ratio of 1:4 prevented CsgA polymerization for a time that was greater than the duration of the experiment (Fig. 2.2A). To verify that Hsp33 interfered with CsgA fiber formation and not with the ThT fluorescence, a CsgA solubility assay was conducted. All CsgA-containing samples had one band corresponding to CsgA in the pellet fraction treated with FA (Fig. 2.2B, lane 4). The majority of CsgA was present in the supernatant fraction of samples that contained Hsp33ox and CsgA at a 1:2 molar ratio signifying that CsgA was maintained in an SDS-soluble form (Fig. 2.2B, lanes 5-6). Fibers were observed by TEM in samples containing only CsgA, while no fibers were observed in samples containing both CsgA and Hsp33ox (Fig. 2.2C and 2D).

In contrast to Hsp33ox, Hsp33red had only marginal effects on CsgA polymerization *in vitro* (Fig. 2.2E). Consistent with the ThT results, CsgA was mostly present in the pellet fraction of samples containing Hsp33red and CsgA at a 1:2 molar ratio (Fig. 2.2F lane 8). Significantly smaller amounts of CsgA were present in the supernatant fraction along with large quantities of Hsp33red (Fig. 2.2F, lanes 5-6). CsgA polymerization was also monitored by TEM. Regular, unbranched fibers were observed when CsgA was incubated alone or with Hsp33red for 13 hours (Fig. 2.2G, 2H). Together, these results demonstrate that oxidized, but not reduced, Hsp33 maintains CsgA in a soluble state.

Hsp33ox and DnaK prolong the presence of a transient folding intermediate common to amyloids.

The conformation-specific antibody A11 recognizes a conserved, transient folding intermediate that is present during the polymerization of many functional and disease-associated amyloids (6, 71, 72). Although the exact molecular structure that A11 recognizes is unresolved, it is proposed to be an ordered intermediate that precedes the mature amyloid fiber (71). A11 transiently recognizes freshly purified CsgA during the first part of its transition to an amyloid fiber. However, once polymerization reaches stationary phase, no A11 reactive species can be observed (6). The A11 antibody was

therefore used to test if Hsp33ox and DnaK act on CsgA in a manner that impacts progression from an A11-reactive conformation to an amyloid conformation. Freshly purified CsgA monomers were incubated with substoichiometric concentrations of DnaK or Hsp33ox. Samples were removed at the indicated time points (Fig. 2.3A, arrows) and spotted onto a nitrocellulose membrane. An A11-reactive species was detectable up to approximately 8 hours when CsgA was incubated in the absence of chaperone (Fig. 2.3A, 3B). In the presence of DnaK, the lag phase is increased from 2 hours to 10 hours and the A11-reactive species was detectable for up to 15 hours (Fig. 2.3A, 3B). When CsgA was incubated with Hsp33ox the A11-reactive species did not disappear for more than 24 hours after the start of the reaction (Fig. 2.3B). The persistence of the A11 reactive species was not due to cross-reactivity with Hsp33ox, as the A11 antibody did not react with the above assayed concentration of purified Hsp33ox (Figure 2.3C). The small amount of cross-reactivity observed for the A11 antibody with DnaK (Fig. 2.3C) is consistent with previous findings that the A11 antibody reacts with Hsp70 and particularly with the substrate binding domain of Hsp70; however, Lotz *et al.* did not observe reactivity with full-length DnaK (44, 73).

The inhibitory effects of Hsp33 and DnaK are abolished by the addition of CsgA seed.

CsgA amyloid formation can be accelerated or 'seeded' by the addition of preformed CsgA fibers.(6) To determine whether DnaK and Hsp33ox alter CsgA seeding by preformed fibers, polymerization assays were carried out in the presence of different CsgA seed concentrations. CsgA seed concentrations as low as 3% (weight/weight relative to soluble monomer) eliminated the lag phase of CsgA amyloid formation as has been previously demonstrated (Fig. 2.4A) (6). The inhibitory effects of DnaK and Hsp33ox, as well as the lag phase of CsgA fiber formation, were reduced by the addition of 3% (w/w) CsgA seed, and abolished by 12% (w/w) CsgA seed for both chaperones (Fig. 2.4B, 4C; note the time scales are different in A from B and C). In the presence of 3% seed there was an initial burst of fluorescence signal, a phase of minimal fluorescence increase and a more rapid growth phase that concluded in a stationary phase (Fig. 2.4B, 4C). Hsp33 reduced the maximum ThT fluorescence by a similar amount in the presence and absence of CsgA seed (Fig. 2.4C). The observation

that the final ThT fluorescence remains reduced in the presence of Hsp33 and 12% CsgA seeds suggests that Hsp33 is sequestering a population of CsgA that cannot be incorporated into an amyloid (Fig. 2.4C compare solid and dotted lines).

Spy inhibits CsgA Polymerization in vitro.

Spy is a periplasmic chaperone that is regulated by the Cpx and Bae extracellular stress responses, both of which are induced by conditions that stress the proteome (62-65). Spy exists as a homodimer and is structurally homologous to CpxP, the adaptor protein of the Cpx two-component stress response system. CpxP has also been proposed to act as a chaperone (61, 74, 75). However, Spy has two hydrophobic patches in the concave surface of its structure that may be involved in substrate binding and chaperone activity; similar hydrophobic patches are less well defined in CpxP (61, 75). CsgA was tested as a substrate for Spy since CsgA passes through the periplasm and, as a functional amyloid, is prone to ordered aggregation. No amyloid aggregates have been detected in the periplasm, therefore, we hypothesized that chaperone proteins like Spy may help to keep CsgA soluble as it passes through the periplasm to the cell surface.

To test the ability of Spy to prevent CsgA aggregation, purified Spy was mixed with freshly purified, monomeric CsgA and monitored polymerization *in vitro* by ThT fluorescence. Spy inhibited CsgA polymerization in a concentration dependent manner (Fig. 2.5A). Like DnaK and Hsp33, inhibition by Spy could also be overcome by the addition of preformed fibers (Fig. 2.5B). Spy inhibited CsgA polymerization but the addition of comparable concentrations of CpxP to soluble CsgA had no effect on the polymerization of CsgA (data not shown). Comparison of these seemingly similar proteins will likely reveal their distinct functions in envelope stress responses.

Deletion of *spy* from the curli-expressing strain BW25113 had no effect on curli biogenesis (data not shown). It has been shown that some periplasmic chaperones are functionally redundant and can compensate for the loss of a single chaperone (76, 77). It is therefore not surprising that the *spy* deletion did not produce an observable phenotype. However, when Spy was overexpressed, cells exhibited reduced Congo red binding (Fig. 2.6A) consistent with reduced CsgA protein levels by western blot (Fig.

2.6B). One possible explanation for this result is that stabilization of unfolded CsgA by Spy in the periplasm allows for more efficient proteolytic degradation of CsgA and therefore less secretion and curli assembly. Alternatively, the excessive production and secretion of Spy may have titrated resources that are required for the production and secretion of curli subunits. CsgG levels are not as dramatically reduced as CsgA levels, suggesting that CsgA is more sensitive to Spy overexpression. Because CsgG levels remain similar to WT when Spy is overexpressed, it is unlikely that there was not competition for secretion or significant feedback repression of the curli operons (Fig. 2.6B).

Next, it was tested whether reduced curli assembly was due to an increased chaperone capacity in the periplasm. Periplasmic protein extracts (PEs) were harvested and added back to freshly purified CsgA monomers, polymerization was monitored by ThT fluorescence *in vitro* (Fig. 2.6C). Periplasmic proteins from WT BW25113 with empty vector (vector) or overexpressing Spy (pSpy) were harvested. PEs from cells with empty vector showed a minimal effect on CsgA polymerization (Fig. 2.6C, long dashes). However, PEs from cells overexpressing Spy inhibited CsgA polymerization (Fig. 2.6C, short dashes). After 20 hours, CsgA was found to be in an SDS-insoluble state after incubation with periplasmic extracts from WT cells with empty vector only but primarily in an SDS-soluble state after incubation with periplasmic extracts from cells overexpressing Spy (Fig. 2.6D). These results demonstrate that the periplasmic chaperone activity was likely due to an increase in Spy protein in the periplasm.

Discussion

Amyloidogenesis is an ordered aggregation process. Amyloidogenic proteins, such as CsgA, are unstructured prior to their assembly into highly ordered aggregates making them likely targets for chaperone proteins. Consistent with this idea, human Hsp70 influences amyloid fiber formation of A β (1-42) and α -synuclein (42, 43). Also, the small heat shock protein (sHsp) α B-crystallin and the sHsp-like clusterin have been shown to influence amyloid formation (78-80). Our results demonstrate that the endogenous bacterial chaperones DnaK, Hsp33 and Spy are potent inhibitors of CsgA fiber formation.

Like most amyloidogenic proteins, CsgA polymerizes by a nucleation-precipitation growth mechanism. Fiber growth is preceded by a lag phase, during which nuclei putatively form and subsequently drive fiber formation. Nucleation is the rate-limiting step of CsgA polymerization, resulting in an approximately 2-hour lag phase (Fig. 2.4A) during which “needlelike” protofibers have been observed by TEM (81, 82). The presence of DnaK and Hsp33 significantly increased the length of the lag phase of CsgA polymerization, apparently by maintaining CsgA in a soluble state. This data suggests that both chaperones interfere with CsgA amyloidogenesis. Spy also inhibited CsgA but required a 1:1 molar ratio (Spy dimer:CsgA monomer), suggesting either an alternative mechanism of inhibition or simply lower affinity for CsgA.

While DnaK increased the lag phase of CsgA polymerization, it does not appear to significantly affect fiber growth. The presence of DnaK did not appreciably change the time from the onset of fast polymerization to stationary phase, or the maximum ThT fluorescence. The ability of DnaK to inhibit CsgA polymerization required an intact DnaK substrate-binding site, as the DnaK V436F mutant, which shows reduced substrate affinity, was far less efficient in inhibiting CsgA fiber formation. Therefore, we suggest that DnaK most likely interacts transiently with CsgA, preventing an early step in fiber formation, while it does not interfere with polymerization after nucleation in the absence of ATP. This model is also supported by the observation that the same maximal ThT fluorescence is detected in the presence and absence of DnaK.

In contrast to DnaK, Hsp33 not only lengthened the lag phase of CsgA fiber formation but it also altered CsgA fiber elongation kinetics. Hsp33 decreased the rate of elongation and reduced the total amount of polymerized CsgA. Fiber formation is prevented entirely at an Hsp33 to CsgA molar ratio of 1 to 4. This observation is similar to the results of previous studies with the sHsp-like clusterin (78). The inhibitory effect of Hsp33 is dependent on its redox state. The reduced form shows little inhibitory activity, while the oxidized form is a very potent inhibitor. We propose that Hsp33, like DnaK, binds to a folding intermediate, preventing nucleus formation or maturation from the “needlelike” oligomers into a fiber-competent conformation. Two models can be proposed in order to explain why sub-stoichiometric amounts of Hsp33 are sufficient to prevent CsgA fiber formation. Hsp33 could tightly associate with an oligomeric folding

intermediate, arresting a large amount of CsgA in an elongation incompetent state, leading to a reduced CsgA monomer and amyloid fiber concentration. Such a reduced monomer concentration would explain the slower polymerization and overall reduced yield of amyloid fibers formed. Alternatively, a transient interaction could lead to the release of an altered CsgA molecule with modified amyloid forming potential. Similar models have been proposed to explain the inhibition of A β fiber formation by Hsp70/40 and Hsp90 (42).

Spy may inhibit CsgA polymerization at a step prior to oligomerization. Spy has a slight effect on CsgA polymerization at substoichiometric concentrations, but does not exhibit full inhibition unless at a 1:1 molar ratio of CsgA to Spy dimer (Fig. 2.5A). Seeding assays provide further evidence that Spy inhibits oligomerization given that the polymerization kinetics of a seeded reaction in the presence of Spy more closely resemble that of a seeded reaction in the absence of chaperone (Fig. 2.5B). These results suggest that Spy is stabilizing the soluble monomeric species of CsgA and are consistent with the findings of Quan *et al* demonstrating full aggregation inhibition of denatured MDH and aldolase at a 1:1 molar ratio (61).

It has been proposed that there are two nucleation pathways involved in amyloid fiber formation: 1) Fiber independent nucleation is involved in the initial formation of amyloid fibers during the lag phase, and 2) fiber dependent nucleation predominates after initial fiber formation and is the driving force of seeded polymerization reactions. The presence of both pathways has been demonstrated for amyloid formation by Islet Amyloid Polypeptide (83). When CsgA monomer is nucleated by preformed fibers, the presence of Hsp33, DnaK or Spy no longer prevented the seeding of CsgA into an amyloid fiber (Fig. 2.4, Fig. 2.5), suggesting that they interfere with fiber independent nucleation, and not with fiber dependent nucleation. The folding step that is inhibited by Hsp33, DnaK and Spy might not be necessary for CsgA to be competent for fiber dependent nucleation. This would explain the observation that preformed fibers circumvent the inhibitory effects of these chaperones. However, even in a seeded reaction, Hsp33 reduces the amount of CsgA fibers formed, although no effect on the lag phase is observed. This observation suggests again that Hsp33 arrests a fraction of CsgA in a state incompetent for fiber formation. DnaK and Spy, on the other hand,

appear to act at an earlier stage: possibly stabilizing soluble monomers of CsgA prior to oligomerization.

Disease associated amyloids such as A β and PrP form a transient oligomeric species, which is recognized by the A11 antibody (71). Freshly purified CsgA is recognized by the A11 antibody, while CsgA denatured with guanidine hydrochloride is not recognized (6). The CsgA species that is recognized by the A11-antibody has been shown to be either monomeric or dimeric, but may be an off-pathway step in amyloid fiber formation (6). DnaK and Hsp33 increase the time that the A11-recognized species is present during CsgA polymerization, suggesting that CsgA undergoes at least one rapid folding step into the A11-recognized species before the chaperones inhibit further folding and fiber elongation. Further experiments will have to be carried out to determine the relevance of the species recognized by the A11-antibody in the amyloid formation pathway of CsgA. Hsp33 may be a suitable tool for these experiments.

A role for DnaK, Hsp33 and Spy during curli biogenesis *in vivo* remains to be determined. Our data suggest that chaperones could provide a cellular control mechanism to protect the cell from premature amyloid formation prior to export of CsgA covering different physiological situations and in different subcellular compartments. They most likely interfere with fiber independent nucleation, which would be predominant in the cytosol after CsgA synthesis and during secretion across the periplasmic space. Curli assembly was reduced by increasing the chaperone capacity of the periplasm through the overexpression of Spy, suggesting that cells carefully balance curli subunit secretion with proteostatic mediators in the periplasm. Curli biogenesis is tightly controlled at the level of transcription, export and nucleation (reviewed in ref. (84)); chaperone mediated assembly of curli adds another dimension to the controlled nature this system.

Materials and Methods

CsgA Purification. CsgG and CsgA-6XHis were overexpressed in LSR12 (C600:: Δ csg) and CsgA-6XHis was purified from the growth media as previously described (6, 11). To remove the imidazole, eluates were run over a gel filtration column (Sephadex G-25 fine, Amersham Biosciences), into either 50 mM potassium phosphate buffer pH 7.2 (KPi), or

50 mM KPi pH 7.2 that was supplemented with 50 mM potassium chloride (KCl). CsgA-6XHis polymerizes into an amyloid fiber with similar kinetics to wild type CsgA *in vitro*, and will be referred to as 'CsgA' in this paper (11).

Hsp33 Purification. Hsp33 was purified as previously described (54). The reduction of Hsp33 was performed as previously described (58). To oxidize Hsp33, it was treated with 2 mM H₂O₂ at 43°C for 1 hour prior to buffer exchange into 40 mM KPi pH 7.5, as previously described (59).

DnaK purification. Wild type and mutant DnaK (V436F) was purified as previously described (85) with slight modifications. Mutant DnaK was created by site-directed mutagenesis using the QuikChange kit (Stratagene).

Spy Purification. Spy was purified as previously described (61).

Periplasmic Extract Preparation. WT BW25133 cells were made chemically competent and transformed with pCDFT (vector) or pCDFTrckanBamHI-spy (pSpy)(61) were grown in LB at 37°C overnight and then plated on YESCA plates supplemented with kanamycin and grown for 2 days at 26°C. It was unnecessary to induce Spy expression as increased Spy levels could be observed by coomassie stained SDS-PAGE (data not shown). Cells were harvested in 20 mM Tris (pH 8.0). Cells were collected by centrifugation at 8,000 rcf for 10 minutes followed by incubation in osmotic shock buffer (30 mM Tris, 40% sucrose 2 mM EDTA, pH 7.3) for 10 minutes. Cells were pelleted at room temperature and resuspended in 2 mM MgCl₂, incubated on ice for 3 minutes and pelleted again. The supernatant was kept as the periplasmic extract (PE).

ThT Fiber Formation Assay. Each experiment shown is a representative of at least three replicates. Freshly purified CsgA was mixed with 20 μM ThT and incubated in the presence of DnaK or Hsp33 in a black 96-well flat bottom plate (Corning Inc.), which was placed in a Spectramax M2 plate reader (Molecular Devices; Figures 1-4). The plate reader was maintained at 25°C for all experiments. 50 mM KPi pH 7.2 was used as reaction buffer for all experiments involving Hsp33. For experiments involving DnaK, 50 mM KPi 50 mM KCl pH 7.2 was used as reaction buffer. Unless stated differently the reaction volumes were 100 μl. Molar ratios are reported in terms of monomeric DnaK and dimeric Hsp33. Fluorescence was monitored in ten-minute intervals at 495 nm after excitation at 438 nm. The cut off of the plate reader was set to 475 nm. The plate was

shaken for 5 seconds prior to each read. CsgA polymerization in the presence of Spy and periplasmic extracts were conducted in 50 μ L reaction volumes in 50 mM KPi (pH 7.3) with 20 μ M ThT. ThT readings were taken in a Infinite 200 Pro NanoQuant plate reader (Tecan Group LTD; Figures 5 and 6) every 10 minutes after 2 seconds of shaking at 2.5 mm amplitude with an excitation wavelength of 438 nm and emission wavelength of 495 nm. Molar ratios are reported in terms of Spy dimer. At least three replicates of each assay were conducted.

CsgA Solubility Assay. 100 μ L CsgA samples supplemented with the respective chaperones were incubated in 96-well plates in a Spectramax M2 plate reader at 25 $^{\circ}$ C. Identical samples were supplemented with 20 μ M ThT to monitor amyloid formation. ThT fluorescence was monitored as described above. After 13 hours 30 μ L aliquots were taken from the CsgA samples and centrifuged at 70,000 x g for one hour at 4 $^{\circ}$ C in 1.5 ml polyallomer tubes (Beckman Instruments) using a TLA-55 rotor (Beckman Coulter) in an Optima TLX ultracentrifuge (Beckman Coulter). After centrifugation, the supernatant fractions (~30 μ L) were transferred into a fresh tube. Pellet fractions were treated with 50 μ L 95% (w/w) formic acid (Sigma-Aldrich, F0507), while 95% formic acid was added to the supernatant fraction yielding a final formic acid concentration of 76%. Immediately after addition of formic acid the samples were placed in a SPD111V SpeedVac (Thermo Fisher Scientific) and all solvent was removed. The formic acid treated samples were resuspended in 4xSDS sample buffer (125 mM Tris pH 6.8, 10% 2-Mercaptoethanol, 20% Glycerol, 6% sodium dodecyl sulfate, 0.02% bromophenol blue), sonicated for ten minutes in a Solidstate/Ultrasonic FS-14 bath sonicator (Fisher Scientific) before incubating at 95 $^{\circ}$ C for 10 minutes. Formic acid treated and untreated samples were then analyzed by SDS-PAGE and Coomassie staining. The solubility of CsgA after incubation with periplasmic extracts was determined similarly. Soluble and insoluble CsgA were separated by centrifugation in an Eppendorf 5415R centrifuge in duplicate. Pellets were treated with 40 μ L 4xSDS sample buffer or 50 μ L hexafluoro-2-propanol (HFIP; Sigma Aldrich) for 10 minutes and then dried in a SPD111V SpeedVac (Thermo Fisher Scientific) before resuspension in 40 μ L of 4xSDS sample buffer. Supernatants were treated with an equal volume of 4xSDS sample buffer or with a final concentration of 80% HFIP for 10 minutes, dried and then resuspended in 40 μ L

4xSDS sample buffer. Samples were boiled for 10 minutes prior to loading on a 15% SDS-PAGE gel and analyzed by Coomassie staining.

Dot-Blot Assay with A11. The blot assay was carried out as previously described.(6) CsgA samples were taken from fiber formation reactions in 96 well plates that were simultaneously monitored with ThT fluorescence in separate wells at 25°C, as described above.

Whole cell Western Blot. BW25113 with pCDFT (vector) or pCDFT_{rckanBamHI-spy} (pSpy) were grown overnight in LB supplemented with kanamycin at 37°C. Cultures were diluted to OD=1.0 in 50 mM KPi (pH 7.3) and 4 µL were spotted on a YESCA plate and grown for 48 hours at 26°C. Cells were harvested in 1 mL of 50 mM KPi (pH 7.3). Two 100µL samples were taken from a 1.0 OD suspension and pelleted at 16,000 rcf for 10 minutes. Samples were either treated with 40 µL of 2 x SDS loading buffer or 50µL of hexafluoro-2-propanol (Sigma-Aldrich, 52512), dried in a Thermo Savant SPD SpeedVac (Thermo Fisher Scientific) and then treated with 40 µL of 2x SDS loading buffer. 7 µL were loaded in a 15% SDS PAGE gel, transferred to 0.45 µm PVDF transfer membrane (Thermo Fisher Scientific), and blocked overnight in TBS-T 5% skim milk. Blots were probed with anti-CsgA (1:10,000) and anti-CsgG (1:70,000) polyclonal antibodies followed by goat-anti-rabbit (1:10,000; Sigma-Aldrich, A0545).

Electron Microscopy. Electron microscopy sample preparation and image acquisition was carried out as previously described (6).

Figures

Figure 2.1. *In vitro* CsgA fiber formation in the presence of DnaK. (A) Freshly purified 20 μM CsgA was incubated with 20 μM ThT alone or with various concentrations of DnaK. Fluorescence was measured in 10-minute intervals at 495 nm after excitation at 438 nm. Fluorescence is reported in arbitrary units (AU). (B) A mutation in the substrate-binding domain significantly reduces DnaK's inhibitory effect on CsgA fiber formation *in vitro*. Freshly purified 20 μM CsgA was incubated with 20 μM ThT alone or with either DnaK or DnaK^{V436F} at a 1:4 molar ratio (DnaK:CsgA). Fluorescence was measured as in (A). (A) and (B) are representative data of three replicates. (C) After 13 hours samples were taken from the CsgA alone or DnaK+CsgA (1:4 molar ratio, DnaK:CsgA) polymerization reactions shown in Fig. 2.1A and separated into soluble (S) and polymerized (P) fractions by centrifugation prior to treatment with FA. The fractions were run on a 13% SDS-PAGE gel and visualized by Coomassie brilliant blue staining. At the same timepoint 10 μL samples containing CsgA only (D) or CsgA and DnaK (E) were applied to formvar coated copper grids, stained with uranyl acetate and examined by TEM.

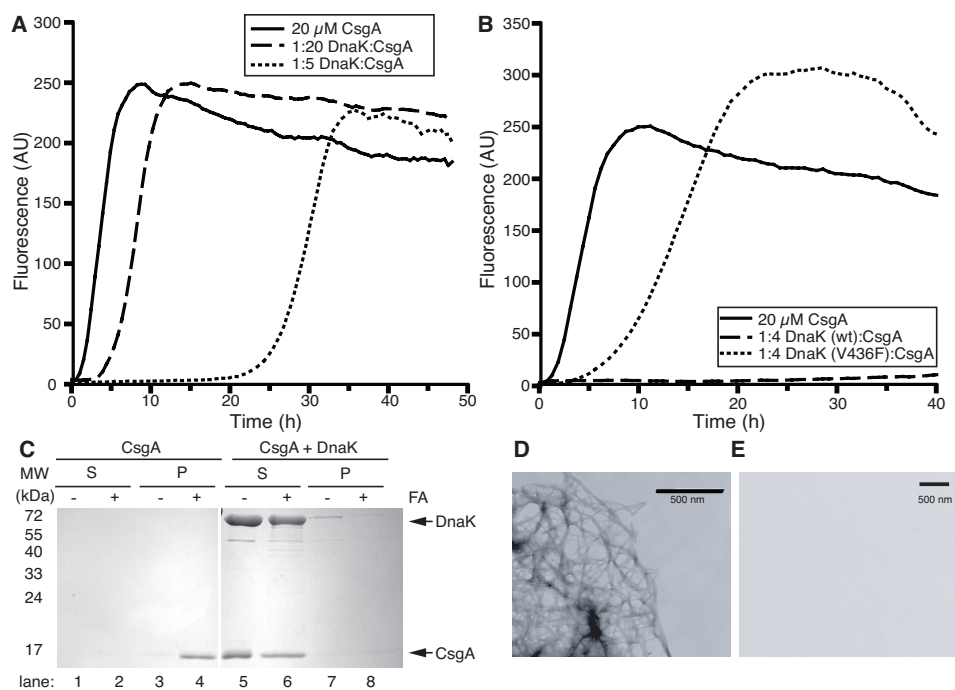


Figure 2.2. *In vitro* CsgA fiber formation in the presence of Hsp33. (A) Freshly purified 20 μ M CsgA was incubated with 20 μ M ThT both alone and with various concentrations of Hsp33ox. Fluorescence was measured as in Fig. 2.1A. Shown are representative data of three replicates. (B) After 13 hours samples were taken from the CsgA alone or Hsp33+CsgA at a 1:4 molar ratio (Hsp33:CsgA) polymerization reactions shown in (A,) separated into soluble (S) and polymerized (P) fractions and treated as described in Fig. 2.1C. At the same timepoint, 10 μ L samples containing CsgA only (C) or CsgA and Hsp33 (D) were applied to formvar coated copper grids, stained with uranyl acetate and examined by TEM. Hsp33red only minimally effects *in vitro* CsgA polymerization. (E) Freshly purified 20 μ M CsgA was incubated with 20 μ M ThT alone or with either Hsp33ox or Hsp33red, each at a 1:4 molar ratio (Hsp33:CsgA). Shown are representative data of three replicates. (F) After 13 hours samples were taken from the polymerization reactions (1:4Hsp33ox:CsgA and 1:2 Hsp33red:CsgA), separated into soluble (S) and polymerized (P) fractions and treated as described in Fig. 2.1C. Samples were also analyzed by negative stain TEM. CsgA only (G) or CsgA and Hsp33red (H) were applied to formvar coated copper grids, stained with uranyl acetate and examined by TEM.

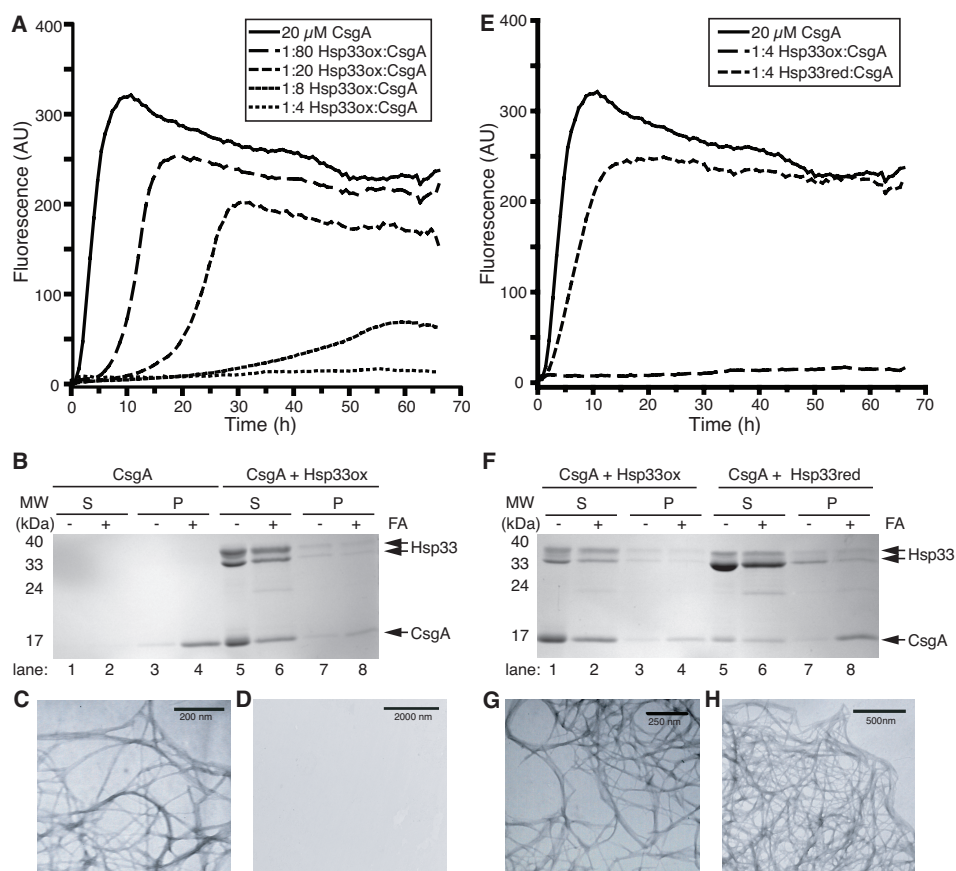


Figure 2.3. Hsp33ox and DnaK significantly prolong the presence of a CsgA intermediate that is recognized by the A11 antibody. (A) Freshly purified 40 μ M CsgA was incubated with 20 μ M ThT alone or with either DnaK or Hsp33ox. Fluorescence was measured as described in Fig. 2.1A. Shown are representative data of three replicates. (B) Samples (3 μ L) of identical polymerization reactions, containing no ThT, were spotted on a nitrocellulose membrane and were probed with the A11 antibody. Samples were taken at indicated intervals (arrows) over the course of 24 hours. (C) Freshly purified 40 μ M CsgA, 5 μ M DnaK and 5 μ M Hsp33ox, the same concentrations used in parts (A) and (B), were spotted on a nitrocellulose membrane and probed with the A11 antibody.

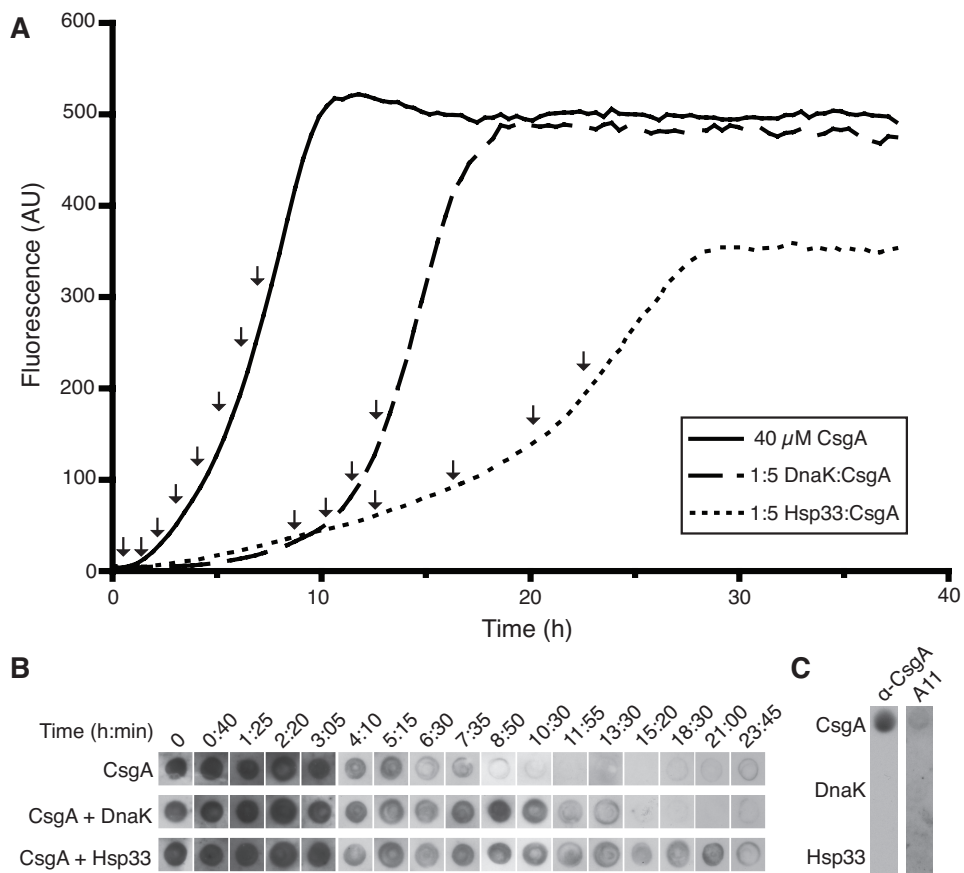


Figure 2.4. The addition of preformed fibers abolishes the inhibitory effects of Hsp33ox and DnaK on CsgA amyloid formation. (A) Freshly purified 20 μ M CsgA was incubated with 20 μ M ThT and DnaK (B) or Hsp33ox (C). In addition, 3% (w/w relative to CsgA monomer) or 12% sonicated, preformed CsgA fibers were added to the polymerization reactions as indicated. Fluorescence was measured as described in Fig. 2.1A. Shown are representative data sets of three replicates.

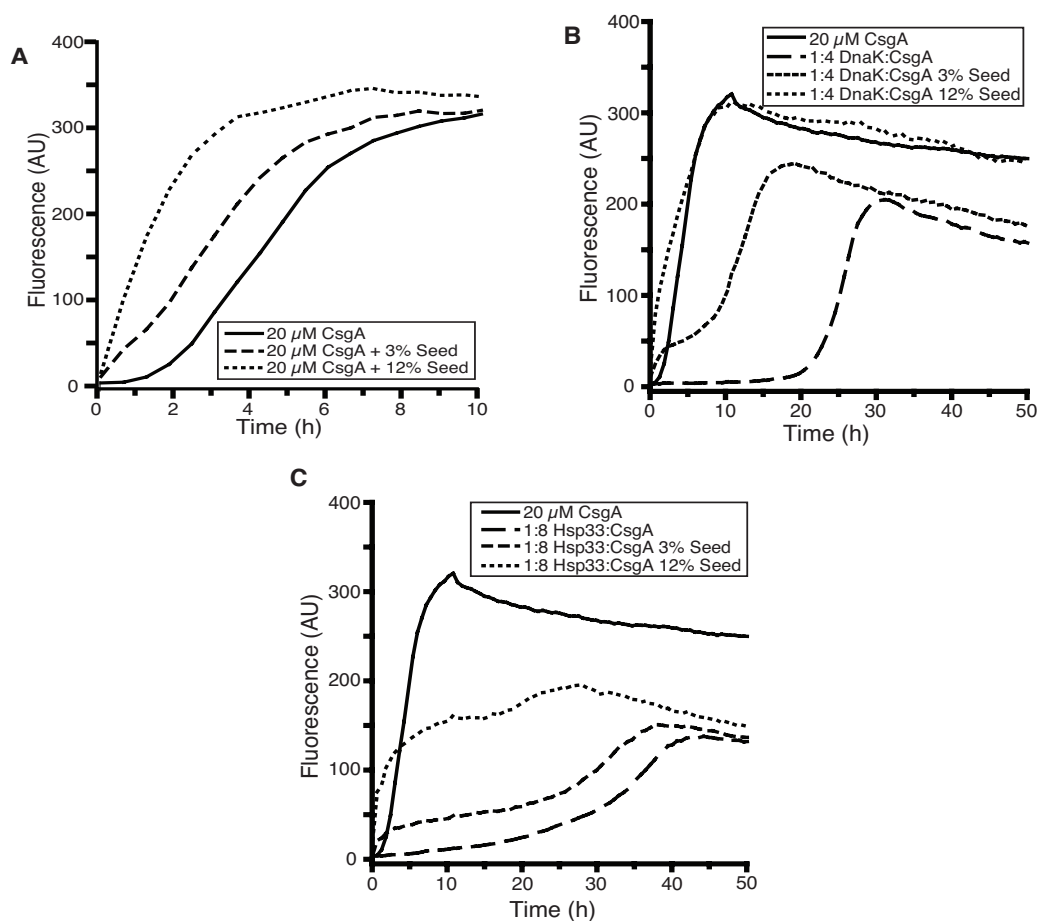


Figure 2.5. *In vitro* CsgA fiber formation in the presence of Spy. (A) 20 μ M freshly purified CsgA was incubated with 20 μ M ThT alone or in the presence of various molar ratios of Spy. Fluorescence was measured as described in Fig. 2.1A. (B) Freshly purified 20 μ M CsgA was incubated with 20 μ M ThT alone or in the presence of 20 μ M Spy with and without 2% (w/w relative to CsgA monomer) sonicated, preformed CsgA fibers. Fluorescence was measured as described in Fig. 2.1A. Shown are representative data sets of three replicates.

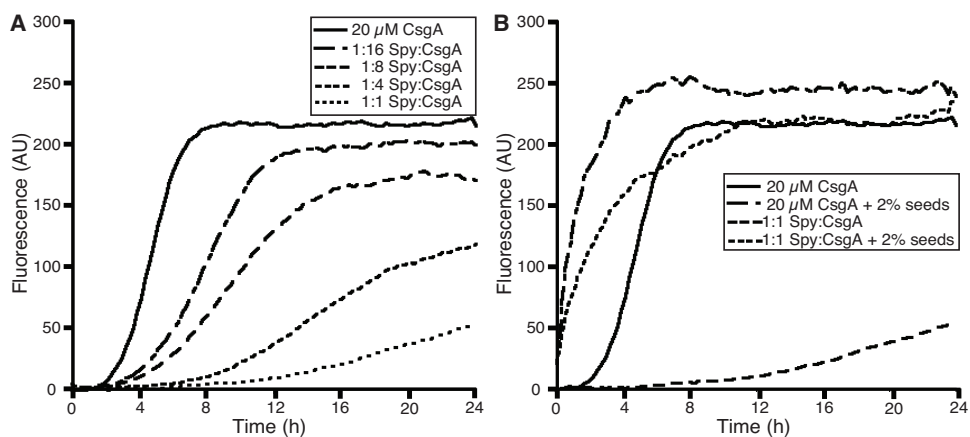
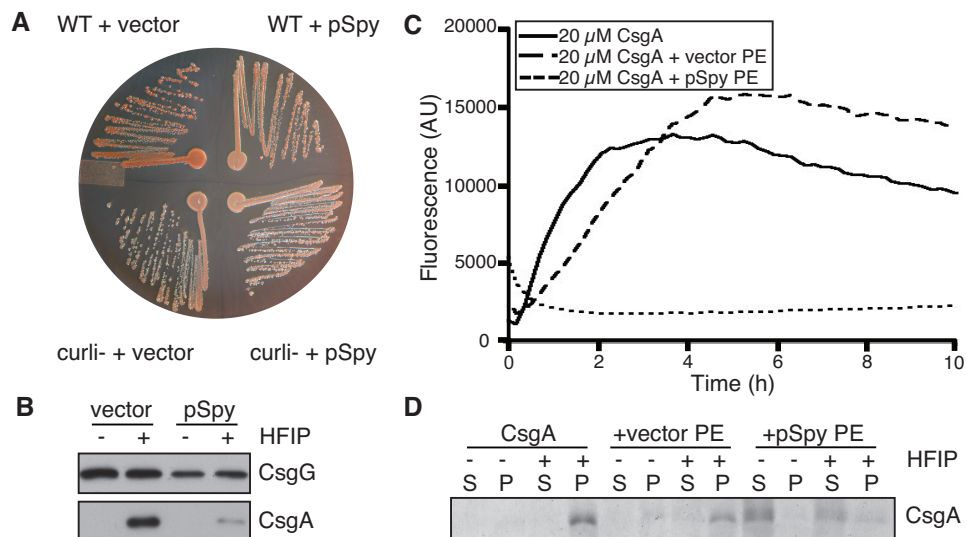


Figure 2.6. Overexpression of Spy reduces curli secretion and assembly. (A) WT BW25113 and *curli-* (*csgBAC-* *csgDEFG-*) were transformed with pCDFTrc (vector) or pCDFTrckanBamHI-spy (pSpy). Overnight cultures were washed with 50mM KPi (pH 7.3) and diluted to OD=1.0. 4 μ L of washed cells were spotted on a YESCA plate containing Congo red and grown for 2 days at 26°C. (B) WT BW25113 cells transformed with vector control or pSpy were grown on a Congo red containing YESCA plate for 2 days at 26°C. Cells were harvested, normalized by OD₆₀₀ and subjected to Western blot using polyclonal antibodies against CsgG (top) and CsgA (bottom) (C) 20 μ M CsgA polymerization was monitored by ThT fluorescence in the presence of periplasmic extracts (PEs) from BW25113+vector control or BW25113+pSpy. PEs were normalized to 100ug/mL. Fluorescence was measured as described in Fig. 2.1A. Shown are representative data of three replicates. (D) Soluble and insoluble CsgA were separated by centrifugation after incubation alone, with BW25113+vector control or with BW25113+pSpy periplasmic extracts. Samples were either treated with SDS loading buffer or first with HFIP, dried and then treated with SDS loading buffer. Samples were loaded on an 18% SDS PAGE gel and stained with Coomassie.



References

1. Chiti F, Dobson CM (2006) Protein misfolding, functional amyloid, and human disease. *Annu Rev Biochem* 75:333–366.
2. Westermark P (1972) Quantitative studies on amyloid in the islets of Langerhans. *Ups J Med Sci* 77:91–94.
3. Kitamoto T, Hikita K, Tashima T, Tateishi J, Sato Y (1986) Scrapie-associated fibrils (SAF) purification method yields amyloid proteins from systemic and cerebral amyloidosis. *Biosci Rep* 6:459–465.
4. Glover JR, Kowal AS, Schirmer EC, Patino MM, Liu JJ, Lindquist S (1997) Self-seeded fibers formed by Sup35, the protein determinant of [PSI⁺], a heritable prion-like factor of *S. cerevisiae*. *Cell* 89:811–819.
5. Guijarro JI, Sunde M, Jones JA, Campbell ID, Dobson CM (1998) Amyloid fibril formation by an SH3 domain. *Proc Natl Acad Sci U S A* 95:4224–4228.
6. Wang X, Smith DR, Jones JW, Chapman MR (2007) In vitro polymerization of a functional *Escherichia coli* amyloid protein. *J Biol Chem* 282:3713–3719.
7. Fandrich M, Fletcher MA, Dobson CM (2001) Amyloid fibrils from muscle myoglobin. *Nature* 410:165–166.
8. Epstein EA, Chapman MR (2008) Polymerizing the fibre between bacteria and host cells: the biogenesis of functional amyloid fibres. *Cell Microbiol* 10:1413–1420.
9. Hammer ND, Wang X, McGuffie BA, Chapman MR (2008) Amyloids: friend or foe? *J Alzheimers Dis* 13:407–419.
10. Bieler S, Estrada L, Lagos R, Baeza M, Castilla J, Soto C (2005) Amyloid formation modulates the biological activity of a bacterial protein. *J Biol Chem* 280:26880–26885.
11. Chapman MR, Robinson LS, Pinkner JS, Roth R, Heuser J, Hammar M, Normark S, Hultgren SJ (2002) Role of *Escherichia coli* curli operons in directing amyloid fiber formation. *Science* 295:851–855.
12. Elliot MA, Karoonuthaisiri N, Huang J, Bibb MJ, Cohen SN, Kao CM, Buttner MJ (2003) The chaplins: a family of hydrophobic cell-surface proteins involved in aerial mycelium formation in *Streptomyces coelicolor*. *Genes Dev* 17:1727–1740.
13. Claessen D, Rink R, de Jong W, Siebring J, de Vreugd P, Boersma FG, Dijkhuizen L, Wosten HA (2003) A novel class of secreted hydrophobic proteins is involved in aerial hyphae formation in *Streptomyces coelicolor* by forming amyloid-like fibrils. *Genes Dev* 17:1714–1726.
14. Wickner RB (1994) [URE3] as an altered URE2 protein: evidence for a prion analog in *Saccharomyces cerevisiae*. *Science* 264:566–569.
15. Coustou-Linares V, Maddelein ML, Begueret J, Saupe SJ (2001) In vivo aggregation of the HET-s prion protein of the fungus *Podospora anserina*. *Mol Microbiol* 42:1325–1335.
16. True HL, Lindquist SL (2000) A yeast prion provides a mechanism for genetic variation and phenotypic diversity. *Nature* 407:477–483.
17. Fowler DM, Koulov AV, Alory-Jost C, Marks MS, Balch WE, Kelly JW (2006) Functional amyloid formation within mammalian tissue. *PLoS Biol* 4:e6.
18. Maji SK, Perrin MH, Sawaya MR, Jessberger S, Vadodaria K, Rissman RA, Singru PS, Nilsson KP, Simon R, Schubert D *et al.* (2009) Functional amyloids as natural storage of peptide hormones in pituitary secretory granules. *Science* 325:328–332.

19. Austin JW, Sanders G, Kay WW, Collinson SK (1998) Thin aggregative fimbriae enhance *Salmonella enteritidis* biofilm formation. *FEMS Microbiol Lett* 162:295–301.
20. Zogaj X, Bokranz W, Nimtz M, Romling U (2003) Production of cellulose and curli fimbriae by members of the family Enterobacteriaceae isolated from the human gastrointestinal tract. *Infect Immun* 71:4151–4158.
21. Zogaj X, Nimtz M, Rohde M, Bokranz W, Romling U (2001) The multicellular morphotypes of *Salmonella typhimurium* and *Escherichia coli* produce cellulose as the second component of the extracellular matrix. *Mol Microbiol* 39:1452–1463.
22. Johansson C, Nilsson T, Olsen A, Wick MJ (2001) The influence of curli, a MHC-I-binding bacterial surface structure, on macrophage-T cell interactions. *FEMS Immunol Med Microbiol* 30:21–29.
23. Gophna U, Barlev M, Seiffers R, Oelschlaeger TA, Hacker J, Ron EZ (2001) Curli fibers mediate internalization of *Escherichia coli* by eukaryotic cells. *Infect Immun* 69:2659–2665.
24. Gophna U, Oelschlaeger TA, Hacker J, Ron EZ (2002) Role of fibronectin in curli-mediated internalization. *FEMS Microbiol Lett* 212:55–58.
25. Bian Z, Brauner A, Li Y, Normark S (2000) Expression of and cytokine activation by *Escherichia coli* curli fibers in human sepsis. *J Infect Dis* 181:602–612.
26. Bian Z, Yan ZQ, Hansson GK, Thoren P, Normark S (2001) Activation of inducible nitric oxide synthase/nitric oxide by curli fibers leads to a fall in blood pressure during systemic *Escherichia coli* infection in mice. *J Infect Dis* 183:612–619.
27. Tukul C, Raffatellu M, Humphries AD, Wilson RP, Andrews-Polymenis HL, Gull T, Figueiredo JF, Wong MH, Michelsen KS, Akcelik M *et al.* (2005) CsgA is a pathogen-associated molecular pattern of *Salmonella enterica* serotype Typhimurium that is recognized by Toll-like receptor 2. *Mol Microbiol* 58:289–304.
28. Hammar M, Arnqvist A, Bian Z, Olsen A, Normark S (1995) Expression of two csg operons is required for production of fibronectin- and congo red-binding curli polymers in *Escherichia coli* K-12. *Mol Microbiol* 18:661–670.
29. Loferer H, Hammar M, Normark S (1997) Availability of the fibre subunit CsgA and the nucleator protein CsgB during assembly of fibronectin-binding curli is limited by the intracellular concentration of the novel lipoprotein CsgG. *Mol Microbiol* 26:11–23.
30. Robinson LS, Ashman EM, Hultgren SJ, Chapman MR (2006) Secretion of curli fibre subunits is mediated by the outer membrane-localized CsgG protein. *Mol Microbiol* 59:870–881.
31. Bian Z, Normark S (1997) Nucleator function of CsgB for the assembly of adhesive surface organelles in *Escherichia coli*. *EMBO J* 16:5827–5836.
32. Hammar M, Bian Z, Normark S (1996) Nucleator-dependent intercellular assembly of adhesive curli organelles in *Escherichia coli*. *Proc Natl Acad Sci U S A* 93:6562–6566.
33. Hammer ND, Schmidt JC, Chapman MR (2007) The curli nucleator protein, CsgB, contains an amyloidogenic domain that directs CsgA polymerization. *Proc Natl Acad Sci U S A* 104:12494–12499.

34. Nenninger AA, Robinson LS, Hultgren SJ (2009) Localized and efficient curli nucleation requires the chaperone-like amyloid assembly protein CsgF. *Proc Natl Acad Sci U S A* 106:900–905.
35. Nenninger AA, Robinson LS, Hammer ND, Epstein EA, Badtke MP, Hultgren SJ, Chapman MR (2011) CsgE is a curli secretion specificity factor that prevents amyloid fibre aggregation. *Mol Microbiol* 81:486–499.
36. Gibson DL, White AP, Rajotte CM, Kay WW (2007) AgfC and AgfE facilitate extracellular thin aggregative fimbriae synthesis in *Salmonella enteritidis*. *Microbiology* 153:1131–1140.
37. Taylor JD, Zhou Y, Salgado PS, Patwardhan A, McGuffie M, Pape T, Grabe G, Ashman E, Constable SC, Simpson PJ *et al.* (2011) Atomic resolution insights into curli fiber biogenesis. *Structure* 19:1307–1316.
38. Shewmaker F, McGlinchey RP, Thurber KR, McPhie P, Dyda F, Tycko R, Wickner RB (2009) The functional curli amyloid is not based on in-register parallel beta-sheet structure. *J Biol Chem* 284:25065–25076.
39. Collinson SK, Parker JM, Hodges RS, Kay WW (1999) Structural predictions of AgfA, the insoluble fimbrial subunit of *Salmonella* thin aggregative fimbriae. *J Mol Biol* 290:741–756.
40. Wang X, Chapman MR (2008) Sequence determinants of bacterial amyloid formation. *J Mol Biol* 380:570–580.
41. Wang X, Zhou Y, Ren JJ, Hammer ND, Chapman MR (2010) Gatekeeper residues in the major curlin subunit modulate bacterial amyloid fiber biogenesis. *Proc Natl Acad Sci U S A* 107:163–168.
42. Evans CG, Wisen S, Gestwicki JE (2006) Heat shock proteins 70 and 90 inhibit early stages of amyloid beta-(1-42) aggregation in vitro. *J Biol Chem* 281:33182–33191.
43. Huang C, Cheng H, Hao S, Zhou H, Zhang X, Gao J, Sun QH, Hu H, Wang CC (2006) Heat shock protein 70 inhibits alpha-synuclein fibril formation via interactions with diverse intermediates. *J Mol Biol* 364:323–336.
44. Yoshiike Y, Minai R, Matsuo Y, Chen YR, Kimura T, Takashima A (2008) Amyloid oligomer conformation in a group of natively folded proteins. *PLoS One* 3:e3235.
45. Bardwell JC, Craig EA (1984) Major heat shock gene of *Drosophila* and the *Escherichia coli* heat-inducible dnaK gene are homologous. *Proc Natl Acad Sci U S A* 81:848–852.
46. Bukau B, Horwich AL (1998) The Hsp70 and Hsp60 chaperone machines. *Cell* 92:351–366.
47. Zolkiewski M (1999) ClpB cooperates with DnaK, DnaJ, and GrpE in suppressing protein aggregation. A novel multi-chaperone system from *Escherichia coli*. *J Biol Chem* 274:28083–28086.
48. Flaherty KM, Wilbanks SM, DeLuca-Flaherty C, McKay DB (1994) Structural basis of the 70-kilodalton heat shock cognate protein ATP hydrolytic activity. II. Structure of the active site with ADP or ATP bound to wild type and mutant ATPase fragment. *J Biol Chem* 269:12899–12907.
49. Schmid D, Baici A, Gehring H, Christen P (1994) Kinetics of molecular chaperone action. *Science* 263:971–973.

50. Szabo A, Langer T, Schroder H, Flanagan J, Bukau B, Hartl FU (1994) The ATP hydrolysis-dependent reaction cycle of the *Escherichia coli* Hsp70 system DnaK, DnaJ, and GrpE. *Proc Natl Acad Sci U S A* 91:10345–10349.
51. Packschies L, Theyssen H, Buchberger A, Bukau B, Goody RS, Reinstein J (1997) GrpE accelerates nucleotide exchange of the molecular chaperone DnaK with an associative displacement mechanism. *Biochemistry* 36:3417–3422.
52. Russell R, Wali Karzai A, Mehl AF, McMacken R (1999) DnaJ dramatically stimulates ATP hydrolysis by DnaK: insight into targeting of Hsp70 proteins to polypeptide substrates. *Biochemistry* 38:4165–4176.
53. Schroder H, Langer T, Hartl FU, Bukau B (1993) DnaK, DnaJ and GrpE form a cellular chaperone machinery capable of repairing heat-induced protein damage. *EMBO J* 12:4137–4144.
54. Jakob U, Muse W, Eser M, Bardwell JC (1999) Chaperone activity with a redox switch. *Cell* 96:341–352.
55. Chuang SE, Blattner FR (1993) Characterization of twenty-six new heat shock genes of *Escherichia coli*. *J Bacteriol* 175:5242–5252.
56. Janda I, Devedjiev Y, Derewenda U, Dauter Z, Bielnicki J, Cooper DR, Graf PC, Joachimiak A, Jakob U, Derewenda ZS (2004) The crystal structure of the reduced, Zn²⁺-bound form of the *B. subtilis* Hsp33 chaperone and its implications for the activation mechanism. *Structure* 12:1901–1907.
57. Won HS, Low LY, Guzman RD, Martinez-Yamout M, Jakob U, Dyson HJ (2004) The zinc-dependent redox switch domain of the chaperone Hsp33 has a novel fold. *J Mol Biol* 341:893–899.
58. Graumann J, Lilie H, Tang X, Tucker KA, Hoffmann JH, Vijayalakshmi J, Saper M, Bardwell JC, Jakob U (2001) Activation of the redox-regulated molecular chaperone Hsp33—a two-step mechanism. *Structure* 9:377–387.
59. Ilbert M, Horst J, Ahrens S, Winter J, Graf PC, Lilie H, Jakob U (2007) The redox-switch domain of Hsp33 functions as dual stress sensor. *Nat Struct Mol Biol* 14:556–563.
60. Winter J, Ilbert M, Graf PC, Ozcelik D, Jakob U (2008) Bleach activates a redox-regulated chaperone by oxidative protein unfolding. *Cell* 135:691–701.
61. Quan S, Koldewey P, Tapley T, Kirsch N, Ruane KM, Pfizenmaier J, Shi R, Hofmann S, Foit L, Ren G *et al.* (2011) Genetic selection designed to stabilize proteins uncovers a chaperone called Spy. *Nat Struct Mol Biol* 18:262–269.
62. Bury-Mone S, Nomane Y, Reymond N, Barbet R, Jacquet E, Imbeaud S, Jacq A, Bouloc P (2009) Global analysis of extracytoplasmic stress signaling in *Escherichia coli*. *PLoS Genet* 5:e1000651.
63. MacRitchie DM, Buelow DR, Price NL, Raivio TL (2008) Two-component signaling and gram negative envelope stress response systems. *Adv Exp Med Biol* 631:80–110.
64. Price NL, Raivio TL (2009) Characterization of the Cpx regulon in *Escherichia coli* strain MC4100. *J Bacteriol* 191:1798–1815.
65. Raffa RG, Raivio TL (2002) A third envelope stress signal transduction pathway in *Escherichia coli*. *Mol Microbiol* 45:1599–1611.

66. DePace AH, Santoso A, Hillner P, Weissman JS (1998) A critical role for amino-terminal glutamine/asparagine repeats in the formation and propagation of a yeast prion. *Cell* 93:1241–1252.
67. Rudiger S, Mayer MP, Schneider-Mergener J, Bukau B (2000) Modulation of substrate specificity of the DnaK chaperone by alteration of a hydrophobic arch. *J Mol Biol* 304:245–251.
68. Collinson SK, Emody L, Muller KH, Trust TJ, Kay WW (1991) Purification and characterization of thin, aggregative fimbriae from *Salmonella enteritidis*. *J Bacteriol* 173:4773–4781.
69. LeVine Hr (1993) Thioflavine T interaction with synthetic Alzheimer's disease beta-amyloid peptides: detection of amyloid aggregation in solution. *Protein Sci* 2:404–410.
70. LeVine Hr (1999) Quantification of beta-sheet amyloid fibril structures with thioflavin T. *Methods Enzymol* 309:274–284.
71. Kaye R, Head E, Thompson JL, McIntire TM, Milton SC, Cotman CW, Glabe CG (2003) Common structure of soluble amyloid oligomers implies common mechanism of pathogenesis. *Science* 300:486–489.
72. Shorter J, Lindquist S (2004) Hsp104 catalyzes formation and elimination of self-replicating Sup35 prion conformers. *Science* 304:1793–1797.
73. Lotz GP, Legleiter J, Aron R, Mitchell EJ, Huang SY, Ng C, Glabe C, Thompson LM, Muchowski PJ (2010) Hsp70 and Hsp40 functionally interact with soluble mutant huntingtin oligomers in a classic ATP-dependent reaction cycle. *J Biol Chem* 285:38183–38193.
74. DiGiuseppe PA, Silhavy TJ (2003) Signal detection and target gene induction by the CpxRA two-component system. *J Bacteriol* 185:2432–2440.
75. Thede GL, Arthur DC, Edwards RA, Buelow DR, Wong JL, Raivio TL, Glover JN (2011) Structure of the periplasmic stress response protein CpxP. *J Bacteriol* 193:2149–2157.
76. Rizzitello AE, Harper JR, Silhavy TJ (2001) Genetic evidence for parallel pathways of chaperone activity in the periplasm of *Escherichia coli*. *J Bacteriol* 183:6794–6800.
77. Sklar JG, Wu T, Kahne D, Silhavy TJ (2007) Defining the roles of the periplasmic chaperones SurA, Skp, and DegP in *Escherichia coli*. *Genes Dev* 21:2473–2484.
78. Kumita JR, Poon S, Caddy GL, Hagan CL, Dumoulin M, Yerbury JJ, Stewart EM, Robinson CV, Wilson MR, Dobson CM (2007) The extracellular chaperone clusterin potently inhibits human lysozyme amyloid formation by interacting with prefibrillar species. *J Mol Biol* 369:157–167.
79. Raman B, Ban T, Sakai M, Pasta SY, Ramakrishna T, Naiki H, Goto Y, Rao C (2005) AlphaB-crystallin, a small heat-shock protein, prevents the amyloid fibril growth of an amyloid beta-peptide and beta2-microglobulin. *Biochem J* 392:573–581.
80. Yerbury JJ, Poon S, Meehan S, Thompson B, Kumita JR, Dobson CM, Wilson MR (2007) The extracellular chaperone clusterin influences amyloid formation and toxicity by interacting with prefibrillar structures. *FASEB J* 21:2312–2322.
81. Dueholm MS, Nielsen SB, Hein KL, Nissen P, Chapman M, Christiansen G, Nielsen PH, Otzen DE (2011) Fibrillation of the major curli subunit CsgA under a

wide range of conditions implies a robust design of aggregation. *Biochemistry* 50:8281–8290.

82. Hardy J, Selkoe DJ (2002) The amyloid hypothesis of Alzheimer's disease: progress and problems on the road to therapeutics. *Science* 297:353–356.
83. Ruschak AM, Miranker AD (2007) Fiber-dependent amyloid formation as catalysis of an existing reaction pathway. *Proc Natl Acad Sci U S A* 104:12341–12346.
84. Barnhart MM, Chapman MR (2006) Curli biogenesis and function. *Annu Rev Microbiol* 60:131–147.
85. Skowyra D, Wickner S (1993) The interplay of the GrpE heat shock protein and Mg²⁺ in RepA monomerization by DnaJ and DnaK. *J Biol Chem* 268:25296–25301.
86. Evans ML, Schmidt JC, Ilbert M, Doyle SM, Quan S, Bardwell JC, Jakob U, Wickner S, Chapman MR (2011) *E. coli* chaperones DnaK, Hsp33 and Spy inhibit bacterial functional amyloid assembly. *Prion* 5:323–334.

Chapter 3

The Bacterial Curli System Possesses a Potent and Selective Inhibitor of Amyloid Formation³

Abstract

Curli are extracellular functional amyloids that are assembled by enteric bacteria during biofilm formation and host colonization. An efficient secretion system and chaperone network ensures that the major curli fiber subunit, CsgA, does not form intracellular amyloid aggregates. We discovered that the periplasmic protein CsgC was a highly effective inhibitor of CsgA amyloid formation. In the absence of CsgC, CsgA formed toxic intracellular aggregates. *In vitro*, CsgC inhibited CsgA amyloid formation at low substoichiometric concentrations and maintained CsgA in a non- β -sheet rich conformation. Interestingly, CsgC inhibited amyloid assembly of human α -synuclein, but not A β ₄₂, *in vitro*. A common D-Q- Φ -X_{0,1}-G-K-N- ζ motif was identified in CsgC client proteins that is not found in A β ₄₂. CsgC is therefore both an efficient and selective amyloid inhibitor. Dedicated functional amyloid inhibitors may be a key feature that distinguishes functional amyloids from disease-associated amyloids.

Introduction

Maintaining proper cellular proteostasis is essential for all life. Unfolded or misfolded

³This chapter has been accepted for publication in *Molecular Cell*. Erik Chorell in Fredrik Almqvist's lab at Umeå University conducted the α -synuclein experiments (Figure 3.9DE and 3.10G). Jonathan conducted the sequential NMR experiments (Figure 3.7CDE) and Marion Koch and Lea Sefer conducted the cytoplasmic coexpression experiments (Figure 3.6G). Fei Li, a former graduate student in the Chapman lab, initiated this entire project. Jörgen Åden and Anna Götheson provided the α -synuclein mutants. I conducted the experiments presented in Figures 3.1, 3.2, 3.3, 3.4, 3.5, 3.6A-F, 3.7ABFGH, 3.8, 3.9ABC, 3.10A-F. Daniel Smith, Michelle Barnhart and Yizhou Zhou constructed some of the strains and plasmids used in this work.

proteins are susceptible to aggregation and can assemble into amyloid fibers. Highly ordered, β -sheet rich amyloid fibers are 8-10 nm wide and can be assembled by a variety of both native and intrinsically disordered proteins (1, 2). The distinct biochemical properties of all amyloids, resistance to protease digestion and chemical denaturants, and tinctorial properties when incubated with the dyes Congo red (CR) and Thioflavin T (ThT) make identification and characterization of amyloids straightforward (3). Amyloid deposits are one of the pathological hallmarks of neurodegenerative diseases, including Alzheimer's, Parkinson's, Huntington's and Prion diseases (4).

Amyloid formation, however, is not always the result of protein misfolding. 'Functional' amyloids are assembled by dedicated biogenesis systems and amyloid polymers participate in various cellular functions ranging from mediating epigenetic inheritance, to sequestering toxins, to acting as structural components of biofilms (5, 6). Curli are an extracellular functional amyloid produced by enteric bacteria that aid in surface attachment and biofilm formation (6-11). Curli biogenesis is exquisitely controlled so that curli amyloid fibers are only assembled at the right time and in place (12, 13).

The *csg* (curli specific gene) operons encode the major structural and accessory proteins that are required for curli production (14). CsgD is a transcription factor that positively regulates the *csgBAC* operon (15, 16). The *csgBAC* operon encodes the major and minor curli fiber components, CsgA and CsgB, respectively (14). CsgA is secreted to the extracellular milieu as an unfolded protein and then forms amyloid polymers upon interacting with the CsgB nucleator (17, 18). Although CsgA amyloid formation *in vivo* is dependent on CsgB, CsgA can self-assemble into amyloid fibers in the absence of CsgB *in vitro* (19). The *csgDEFG* operon encodes accessory and secretion proteins. CsgG assembles into a nonameric outer membrane pore that is required for secretion of CsgA and CsgB (20, 21). CsgE and CsgF are chaperone-like accessory proteins (22, 23). CsgE is a small periplasmic protein that is required for directing CsgA to CsgG for secretion and CsgE can inhibit amyloid assembly of CsgA *in vitro* (23, 24). CsgF is a surface exposed protein that associates with both CsgG and CsgB to tether the curli fiber to the cell surface (22). The *csgBAC* operon also encodes

CsgC, a small β -sheet-rich periplasmic protein (14, 25-27). The role of CsgC during curli biogenesis has only been indirectly assessed and remains unknown (25, 27).

CsgA is secreted from the cell in an amyloid-competent, yet unpolymerized form *in vivo* (7, 25). Mutations to *csgG* that prevent secretion do not result in the accumulation of intracellular CsgA or CsgB, although *csgA* and *csgB* are still expressed (21). This suggests that periplasmic CsgA and CsgB are somehow eliminated thereby preventing intracellular amyloid formation. We therefore sought to identify periplasmic chaperones and/or proteases that may be involved in ridding the cell of mislocalized curli subunits. Two general cytoplasmic chaperones, DnaK and Hsp33, and one general periplasmic chaperone, Spy, were reported previously to inhibit CsgA amyloid assembly *in vitro* (Chapter 2) (28). Furthermore, CsgE can inhibit CsgA amyloid formation *in vitro* (23, 24). These findings implicate an important role for molecular chaperones in inhibiting premature CsgA amyloid assembly during transport within the cell. Here we report that CsgC inhibits CsgA amyloid formation at substoichiometric molar ratios and in the absence of a hydrolysable energy source. Furthermore, we show that this bacterial protein inhibits human α -synuclein from forming amyloid fibers *in vitro* while having no effect on human A β ₄₂ amyloid formation. Together, our results demonstrate that CsgC is both a highly efficient and selective inhibitor of amyloid formation.

Results

Secretion deficient mutants have periplasmic amyloid inhibitory activity.

CsgA is secreted across the outer membrane as a predominately unstructured protein (19, 25). Furthermore, CsgA is undetectable in the secretion deficient Δ *csgG* mutant (21). We therefore hypothesized that efficient proteostatic mediators exist within the periplasm that prevent CsgA from prematurely forming amyloid aggregates inside the cell. To identify amyloid inhibitory factors periplasmic extracts (PEs) from WT and curli (*csg*) mutant strains were analyzed for the ability to prevent purified CsgA from aggregating into an amyloid *in vitro*. The *csg* mutant strains were grown under curli-inducing conditions prior to harvesting crude PEs by osmotic shock (modified from (29)). PEs were normalized by total protein and added to 20 μ M purified, SDS-soluble CsgA. CsgA polymerization into amyloid was then monitored by ThT fluorescence for 24 hours

as previously described (19). When purified CsgA was incubated alone, ThT fluorescence rapidly increased after approximately 2 hours of incubation indicative of CsgA amyloid assembly (Fig. 3.1AB, closed squares). The addition of PEs from a $\Delta csgG$ mutant to purified CsgA inhibited ThT fluorescence (Fig. 3.1A, open symbols). The inhibitory effect of the $\Delta csgG$ PE was titratable: the addition of 100 $\mu\text{g}/\text{mL}$ periplasmic protein to CsgA prevented ThT fluorescence for the duration of the experiment (Fig. 3.1A, open squares), while the addition of 25 $\mu\text{g}/\text{mL}$ periplasmic proteins only delayed ThT fluorescence for approximately 8 hours (Fig. 3.1A, open triangles). In contrast, PEs from a complete curli deletion (Δcsg , deletion of both curli operons and the intergenic region) or PEs from a $\Delta csgD$ mutant had little to no effect on ThT fluorescence of CsgA (Fig. 3.1B and Fig. 3.2 open triangles). CsgE is important for CsgA secretion and that CsgE can inhibit CsgA amyloid formation *in vitro* (23, 24). To test whether the observed inhibitory activity in the $\Delta csgG$ PEs was due to CsgE, *csgE* was deleted in the $\Delta csgG$ mutant background. The $\Delta csgG\Delta csgE$ and $\Delta csgE$ PEs both strongly inhibited CsgA ThT fluorescence, demonstrating that CsgE was not responsible for the observed inhibitory activity (Fig. 3.2B).

Inhibition of ThT fluorescence in the CsgA aggregation assay could be due to amyloid inhibition, proteolytic degradation of CsgA or the direct inhibition of ThT fluorescence. To distinguish between these possibilities, the stability of CsgA was assessed in the presence and absence of $\Delta csgD$ (not inhibitory; or Δcsg , data not shown) or $\Delta csgG$ (inhibitory) PEs. After 24 hours the samples were separated into soluble and insoluble fractions by centrifugation and then analyzed by SDS-PAGE and Western blot with or without HFIP treatment to solubilize CsgA amyloid aggregates (Fig. 3.1C). When incubated alone or in the presence of the $\Delta csgD$ PE, CsgA was found predominantly in the pelleted, SDS-insoluble fraction (Fig. 3.1C lanes 4 and 8). In contrast, CsgA was still detected in the SDS soluble fractions after incubation with the inhibitory $\Delta csgG$ PE (Fig. 3.1C lanes 9 and 10). Therefore, inhibition of ThT fluorescence by the $\Delta csgG$ PE was the result of CsgA amyloid inhibition and not proteolytic degradation of CsgA or quenching of ThT fluorescence.

Amyloid inhibitory activity is regulated by CsgD

The observation that the $\Delta csgD$ PE did not exhibit an amyloid inhibitory activity suggested that CsgD may regulate expression of the factor responsible for the activity. The $\Delta csgD$ mutant was then complemented by expressing *csgD* from a plasmid. Expression of *csgD* was able to restore amyloid inhibitory activity to the $\Delta csgD$ PEs (Figs. 3.3A, 3.4A). CsgD positively regulates the *csgBAC* operon which encodes the known major and minor curli subunits, CsgA and CsgB, respectively (7, 14), as well as CsgC whose function is poorly understood (25, 27). To determine if the amyloid inhibition activity was dependent on *csgA*, *csgB* or *csgC*, PEs from various *csg* mutants were tested for inhibition of CsgA amyloid formation *in vitro*. PEs from $\Delta csgA$ or $\Delta csgB$ mutants inhibited CsgA amyloid formation (Figs. 3.3B, 3.4B). However, deletion of *csgC* alone or in the $\Delta csgA$ or $\Delta csgB\Delta csgA$ mutant backgrounds resulted in PEs that had less inhibitory activity (Fig. 3.3B). Furthermore, PEs from a $\Delta csgG\Delta csgC$ double mutant did not inhibit CsgA amyloid formation compared to PEs from a $\Delta csgG$ single mutant (Fig. 3.3C). Additionally, when size exclusion chromatography was used to fractionate the inhibitory $\Delta csgG$ PEs further, western blot analysis revealed that CsgC was present in fractions that retained amyloid inhibitory behavior (Fig. 3.4CD). Together, our genetic and biochemical analysis suggested that CsgC was responsible for the amyloid inhibition activity.

Cells lacking CsgG and CsgC accumulate intracellular CsgA.

Subunits that go off pathway or are unable to be secreted might be prone to forming amyloid-like aggregates. We hypothesized that CsgC could discourage CsgA aggregation in the periplasm. On CR-indicator plates, curliated cells stain red while curli mutants produce white colonies (14). The $\Delta csgG$ mutant forms white colonies on CR-indicator plates because CsgA and CsgB are not secreted to the cell surface and no curli are assembled (Fig. 3.3AB and Fig. 3.6B) (21). Interestingly, a $\Delta csgG\Delta csgC$ double mutant produced pink colonies (Fig. 3.3A) and could be restored to white by expressing *csgC* from a plasmid (Fig. 3.3A). Cells were harvested from YESCA plates and subject them to Western and dot blot analysis. Western blot analysis revealed that the $\Delta csgG\Delta csgC$ mutant accumulated SDS soluble and insoluble CsgA (Fig. 3.3B). CsgA was no longer detected in the $\Delta csgG\Delta csgC$ mutant when *csgC* was

complemented on a plasmid (Fig. 3.3B). Furthermore, CsgA produced by the $\Delta\text{csgG}\Delta\text{csgC}$ mutant was only detected by dot blot Western after cells were lysed (Fig. 3.3C), suggesting that the CsgA aggregates were intracellular. Similarly to the ΔcsgG mutant, and in contrast to WT and ΔcsgC mutant, no extracellular fibrillar aggregates were observed by TEM on the $\Delta\text{csgG}\Delta\text{csgC}$ mutant (Fig. 3.6A-D). Therefore, in the absence of CsgC, secretion deficient mutants accumulate intracellular CsgA aggregates.

CsgC protects the cell from the toxicity associated with intracellular CsgA accumulation.

Amyloid aggregation can be toxic to biological membranes (30, 31). We therefore asked whether the accumulation of intracellular CsgA impacted the cellular fitness of the $\Delta\text{csgG}\Delta\text{csgC}$ mutant. LIVE/DEAD staining with SYTO 9 and propidium iodide was used to assess the proportion of viable cells grown in curli-inducing conditions. The $\Delta\text{csgG}\Delta\text{csgC}$ colonies had a larger percentage of dead cells (13.4%) compared to the WT colonies (5.8%) (Fig. 3.6E). We also asked whether the Cpx stress response was induced in the $\Delta\text{csgG}\Delta\text{csgC}$ mutant. A *cpxP* promoter *lacZ* fusion was used to investigate induction of the Cpx response. There was 2-fold increase in Cpx induction in the $\Delta\text{csgG}\Delta\text{csgC}$ cells at 48 hours compared to the WT (Fig. 3.6F).

We also asked whether CsgC could protect against toxicity in the cytoplasm. When recombinant CsgA (CsgA₂₂₋₁₅₁ that lacks the Sec secretion signal sequence) was overexpressed, the growth of the culture was inhibited (Fig. 3.6G). Interestingly, coexpression of CsgA₂₂₋₁₅₁ with CsgC₉₋₁₁₀ (Sec minus) in the cytoplasm of BL21(DE3) cells improved growth (Fig. 3.6G, closed circles). Cells coexpressing CsgA and CsgC in the cytoplasm continued to divide, reaching stationary phase and remaining viable after overnight incubation (Fig. 3.6G, closed circles). Expression of CsgC in the periplasm did not rescue the CsgA₂₂₋₁₅₁-induced growth arrest (Fig. 3.6G, open circles). Collectively, these results demonstrated that CsgC prevented CsgA from forming toxic intracellular aggregates.

CsgC inhibits amyloid formation

Our genetic and *in vivo* analyses suggested that CsgC has anti-amyloid activity. Therefore, purified recombinant CsgC was tested its ability to prevent CsgA polymerization *in vitro*. Purified CsgC inhibited CsgA amyloid formation at molar ratios as low as 1:500 (CsgC:CsgA) *in vitro* as measured by ThT fluorescence (Fig. 3.7A). The same molar ratio of BSA:CsgA had little effect on CsgA polymerization (Fig. 3.8A). Another fluorescent dye, 8-anilino-1-naphthalenesulfonic acid (ANS), was used to test whether CsgC was directing CsgA into non-amyloid aggregates that did not bind ThT. Interestingly, CsgC also inhibited ANS fluorescence of CsgA suggesting that CsgC does not simply direct CsgA into non-amyloid aggregates (Fig. 3.8C). After 24 hours of incubation with CsgC, CsgA ran as a SDS-soluble protein on an SDS-PAGE gel (Fig. 3.8B); therefore, the inability of CsgA to adopt the SDS-resistant amyloid form in the presence of CsgC was again due to chaperone-like inhibition and not due to proteolytic degradation (Fig. 3.8B).

I then asked whether CsgC prevented CsgA from adopting the β -sheet rich structure common to all amyloids (32). CsgA transitions from an unstructured protein to a β -sheet rich amyloid fiber as measured by far-UV circular dichroism (CD) (19, 33). As seen in previous studies, CsgA was unstructured immediately after purification and by 24 hours adopted a largely β -sheet secondary structure (Fig. 3.7B, closed symbols). However, when substoichiometric amounts of CsgC (1:10) were added to freshly purified CsgA, the CD spectrum of CsgA remained mostly unchanged for 24 hrs (Fig. 3.7B, open symbols). CsgC is itself a β -sheet rich protein (Fig. 3.8D); therefore the minimal β -sheet contribution from CsgC was subtracted from the CsgA+CsgC reaction. Even at 48 hrs of incubation in the presence of CsgC, CsgA remained unfolded and non-amyloidogenic as measured by CD and ThT (Fig. 3.8EFG).

To better understand how CsgC affects the structural transitions of CsgA over time, the ^1H NMR spectrum of CsgA alone or CsgA with CsgC was collected. Immediately after purification the ^1H NMR spectrum of CsgA alone showed the limited peak dispersion indicative of a disordered protein (Fig. 3.7C). Over several hours the overall peak intensity gradually decreased as CsgA monomers became incorporated into aggregates and were lost from the NMR spectrum due to fast transverse relaxation (Fig.

3.7C) (33). After approximately 10 hours the CsgA ^1H NMR spectrum had essentially disappeared, which coincided with maximal fluorescence in the ThT assay (Fig. 3.7A, 3.8C). When CsgC was mixed with freshly purified CsgA at a molar ratio of 1:150, the ^1H NMR peaks of CsgA remained visible for over 24 hours (Fig. 3.7D). In the presence of CsgC the CsgA ^1H NMR peaks decreased at a similar rate to the CsgA alone peaks during the first three hours, but then was relatively stable between 3-24 hours (Fig. 3.7E).

Given the low molar ratio of CsgC:CsgA required to achieve amyloid inhibition, we hypothesized that CsgC may be acting on multimeric species of CsgA. CsgA polymerization can be accelerated *in vitro* by the addition of either sonicated CsgA or CsgB preformed fibers in a process called “seeding” (Fig. 3.7F) (18, 19, 34). To address the question of whether CsgC inhibits fiber elongation we asked whether CsgC could inhibit amyloid assembly of CsgA in the presence of exogenously added CsgA seeds *in vitro*. The addition of 2% CsgA seeds by weight to freshly purified CsgA resulted in accelerated CsgA polymerization (Fig. 3.7F, open versus closed squares) while the addition of CsgC to CsgA at a 1:10 or 1:100 molar ratio inhibited CsgA polymerization (Fig. 3.7F, closed circles and triangles, respectively). Interestingly, the addition of seeds to CsgA in the presence of a 1:10 molar ratio of CsgC:CsgA was unable to overcome CsgC-mediated amyloid inhibition (Fig. 3.7F, circles). CsgA seeding was still largely inhibited even in the presence of CsgC at a 1:100 molar ratio of CsgC:CsgA (Fig. 3.7F, triangles). We also asked if CsgC prolonged the transient, pre-amyloid state of CsgA that is recognized by the conformational-specific A11 antibody (30). CsgA incubated in the absence of CsgC was recognized by the A11 antibody immediately after purification, but not after 24 hours (Fig. 3.7G) (19). In contrast, the A11 antibody still recognized CsgA after 24 hours of incubation with CsgC (Fig. 3.7G). Together, these results suggest that CsgC acts by stabilizing an A11-reactive pre-amyloid intermediate of CsgA.

To determine whether CsgC forms a stable complex with CsgA, CsgA was analyzed in the absence and presence of CsgC by native gel electrophoresis. Freshly purified CsgA ran as a several discrete bands approximately 66kDa and smaller suggesting that CsgA begins to self-associate rapidly after purification (Fig. 3.7H, lane 1 and 2). CsgA that had been incubated at 25°C for 24 hours no longer migrated into the gel (Fig. 3.7H,

lanes 3). However, CsgA that had been incubated for 24 hours with a 3-fold substoichiometric concentration of CsgC had a similar banding pattern as CsgA immediately after purification (Fig. 3.7H, lanes 5). The migration of CsgA and CsgC proteins in native gels suggested 1) that CsgC stabilizes CsgA in a heterogeneous mixture of homo-oligomeric species, and 2) that CsgA and CsgC do not form a stable hetero complex.

Next, we sought to identify the domain(s) of CsgA through which CsgC acts. CsgA is comprised of five imperfect repeating units (R1-R5). R1, R3 and R5 are amyloidogenic while R2 and R4 contain gatekeeper residues that temper amyloid formation (19, 35, 36). Deletion of R1, R3 or R5 in CsgA does not significantly abrogate CsgA amyloid assembly and synthetic peptides corresponding to each of the amyloidogenic repeating units can self-assemble into amyloid fibers (19, 35). The ability of CsgC to inhibit amyloid assembly of the CsgA Δ R1, Δ R3 and Δ R5 mutants *in vitro* was tested. CsgC was still capable of inhibiting amyloid formation of each CsgA repeating unit deletion mutants at substoichiometric molar ratios (Fig. 3.10A-C). CsgC also inhibited amyloid assembly of synthetic peptides corresponding to CsgA R1 and R5 at substoichiometric molar ratios (Fig. 3.10DE). Together, our results suggest that CsgC can interact with multiple domains of CsgA to inhibit amyloid assembly.

CsgC displays client protein selectivity.

Finally, we next sought to explore the specificity of CsgC-mediated amyloid inhibition. *Salmonella enterica* and *Citrobacter koseri* both produce curli and CsgA from both bacteria share approximately 75% sequence identity with *E. coli* CsgA (34). *E. coli* CsgA can be cross-seeded *in vitro* and *in vivo* by *S. enterica* and *C. koseri* CsgA (34). *E. coli* CsgC was capable of inhibiting amyloid formation of CsgA molecules from *S. enterica*, *C. koseri* and *E. coli* at the same molar ratios (Fig. 3.9A and Fig. 3.10F). The minor curli subunit, CsgB, shares 30% sequence identity with CsgA and can also assemble into an amyloid-like aggregate *in vitro* (18, 37). Furthermore, CsgB can seed CsgA polymerization both *in vivo* and *in vitro* (18, 35, 37). we tested a truncated version of CsgB (CsgB_{trunc}, lacking the 5th repeating unit) as a client for CsgC *in vitro*. Although

CsgA and CsgB_{trunc} share a large degree of similarity, a higher molar ratio (1:10, CsgC:CsgB_{trunc}) was required to achieve CsgB amyloid inhibition (Fig. 3.9B).

I then asked if CsgC could act as a general amyloid inhibitor and inhibit human amyloid-forming proteins. The Alzheimer's disease-associated amyloid protein A β ₄₂ and the Parkinson's disease-associated protein α -synuclein were tested as potential CsgC clients. Even at a 1:1 molar ratio (CsgC: A β ₄₂), CsgC did not inhibit A β ₄₂ amyloid assembly (Fig. 3.9C). In contrast, CsgC inhibited α -synuclein amyloid formation at 1:3 and 1:10 ratios and, to a lesser degree, at a 1:100 molar ratio (Fig. 3.9D). Sequence alignments revealed a D-Q- Φ -X_{0,1}-G-K-N- ζ motif (Φ =W/L, ζ =S/E) in α -synuclein (residues 98-104) and CsgA (residues 104-112) (Fig. 3.9F). CsgC was able to inhibit amyloid formation by CsgA lacking residues 88-110 and synthetic peptides corresponding the N- and C-terminal repeats of CsgA that contain similarly spaced glutamine and asparagine residues (Fig. 3.10). However, the D-Q- Φ -X_{0,1}-G-K-N- ζ motif only exists once in α -synuclein (Fig. 3.9F). Residues 98-104 in α -synuclein were either mutated to alanine residues (α -synuclein_{6ala}) or a scrambled sequence (α -synuclein_{scram}) and asked whether CsgC could still inhibit amyloid assembly. Interestingly, CsgC only modestly affected the polymerization of α -synuclein variants that were missing the D-Q- Φ -X_{0,1}-G-K-N- ζ motif (Fig. 3.9E and 3.10G). Together, these results suggest a common CsgC interaction motif in CsgA and α -synuclein.

Discussion

Protein misfolding and amyloid aggregation are hallmarks of many degenerative human diseases (4). Modulating the protein folding environment as a means to ameliorate amyloid-associated diseases is an area of intense research focus (38-40). Molecular chaperones have been shown to be important for inhibiting disease-associated amyloid assembly and amyloid-related cytotoxicity *in vitro* and *in vivo* (41). The heat shock protein Hsp70 inhibits amyloid assembly of the Alzheimer's Disease-associated protein A β and the Parkinson's Disease-associated protein α -synuclein *in vitro* (42-44). Overexpression of Hsp70 has also been found to reduce disease pathology in a murine model of Alzheimer's Disease (45). Similarly, overexpression of

the small heat shock protein Hsp16.2 in a *Caenorhabditis elegans* model of Alzheimer's Diseases resulted in decreased amyloid deposits and toxicity (46).

Functional amyloids, while sharing all of the biophysical characteristics of disease-associated amyloids, are distinguished from disease-associated amyloids by their dedicated and controlled biogenesis (47). Curli functional amyloid biogenesis is highly coordinated to ensure that curli fibers are assembled exclusively on the bacterial cell surface (12). Secretion of soluble curli subunits is, in part, facilitated by specific secretion (CsgE and CsgG) and nucleation (CsgB and CsgF) factors as well as general cytoplasmic and periplasmic molecular chaperones (7, 17, 18, 20, 22, 23, 28, 37). We therefore asked whether the curli biogenesis system also encoded specific molecular inhibitors of intracellular CsgA amyloidogenesis.

Mislocalized curli subunits in the periplasm are unstable and degraded when outer membrane secretion is disrupted (21). We therefore hypothesized that periplasmic proteostatic mediators existed to efficiently inhibit mislocalized, intracellular CsgA from aggregating. Our *in vitro* analysis of periplasmic extracts from curli mutants revealed an amyloid inhibitory activity in the periplasm of several mutant strains with curli gene deletions (Figs. 3.1-3.4). The addition of WT PEs accelerated or seeded CsgA polymerization *in vitro* likely due to extracellular curli fibers that copurified with the crude periplasmic extracts (Fig. 3.2A and data not shown). Expression of *csgD* was required for the observed amyloid inhibitory activity (Fig. 3.3.2A). Further genetic analysis revealed that expression of *csgC* was required for CsgA amyloid inhibition in all of our inhibitory PEs (Figs. 3.1-3.4).

CsgC could also inhibit intracellular CsgA amyloid assembly. Deletion of *csgC* in the $\Delta csgG$ background results in the accumulation of intracellular CsgA aggregates (Fig. 3.3BC). The CsgA trapped in these intracellular aggregates migrated on an SDS PAGE gel with a size consistent with that of processed CsgA (lacking the Sec-secretion signal sequence), suggesting that the CsgA aggregates were in the periplasm. CsgC does not appear to possess proteolytic activity itself (Fig. 3.1C and Fig. 3.8B). It is likely that the CsgC maintains CsgA in a state that is competent for secretion or in a state that is sensitive to periplasmic proteases. In addition to CsgC, there may be other periplasmic proteins that can also discourage CsgA amyloid formation. Compared to a $\Delta csgG$

mutant, PEs from a $\Delta csgG\Delta csgC$ mutant exhibited greatly reduced amyloid inhibitory activity; however, the $\Delta csgG\Delta csgC$ PEs still slightly impaired CsgA polymerization (Fig. 3.3C). Interestingly, the Cpx stress response system, which positively regulates periplasmic chaperones and proteases, is induced approximately two fold in the $\Delta csgG\Delta csgC$ mutant compared to WT (Fig. 3.6F) (48, 49). The weak inhibitory activity of the $\Delta csgG\Delta csgC$ PEs may therefore be due to an increased abundance of Cpx regulated periplasmic chaperones, which include Spy, a chaperone-like protein that has previously been shown to inhibit CsgA amyloid formation (28, 50, 51).

When grown under curli-inducing conditions the $\Delta csgG\Delta csgC$ mutant formed mucoid colonies, while WT, $\Delta csgG$ or $\Delta csgC$ were non-mucoid (data not shown). Additionally, the $\Delta csgG\Delta csgC$ cells clumped together when scraped off the agar surface and required vigorous vortexing to resuspend (data not shown). As amyloid intermediates can be toxic to membranes (30, 31), we hypothesized that the increase viscosity of the $\Delta csgG\Delta csgC$ colonies was due to an increase in cell death. Indeed, the $\Delta csgG\Delta csgC$ mutant had an increased number of dead cells per colony relative to the WT (Fig. 3.6E). Although the growth defect of the $\Delta csgG\Delta csgC$ mutant was only modest, this was not unexpected. There are two distinct cell populations within curli-dependent biofilms: one encased in a protective matrix of curli fibers and another that is not (52, 53). Furthermore, only about 30% of the cells in a biofilm express and assemble curli fibers (54). It is therefore likely that Cpx induction occurs in a subpopulation of curli expressing cells, and only when secretion across the outer membrane fails. Furthermore, Cpx induction likely helps protect the cells by both down-regulating the curli operons and up-regulating periplasmic proteases and chaperones (49, 55). When a truncated allele of CsgA that remained in the cytoplasm was expressed growth arrest was induced that was apparently linked to CsgA aggregation (Fig. 3.6G). The CsgA-induced growth arrest was ameliorated when CsgC was coexpressed along with CsgA in the cytoplasm (Fig. 3.6G).

CsgA amyloid formation can be inhibited by both protein and chemical “chaperones” acting via distinct mechanisms (23, 24, 28, 33, 56). Protein chaperones that inhibit CsgA polymerization at molar ratios close to 1:1, such as Spy and CsgE, likely exert their inhibitory activity during early stages of aggregation by interacting with monomers

of CsgA (23, 28). DnaK and Hsp33, on the other hand, inhibit CsgA polymerization at substoichiometric molar ratios by interacting with early oligomers or inhibiting fiber elongation, respectively (28). Small, heterocyclic 2-pyridones designed as peptidomimetic compounds can inhibit CsgA amyloid assembly by diverting CsgA into “off-pathway” oligomers that are unable to assemble or nucleate amyloid formation (33).

CsgC is a unique proteinaceous inhibitor of CsgA amyloid formation because it discourages amyloid assembly at much lower molar ratios (1:500) than any other previously reported CsgA amyloid inhibitor (Fig. 3.7A) (23, 24, 28, 56). Our biophysical and biochemical evidence (CD, NMR, ThT, seeding analysis, conformation-specific antibody analysis, gel electrophoresis) demonstrate that CsgC prevents CsgA from adopting the β -sheet rich, SDS insoluble, fibrous polymers (Figs. 3.7, 3.8). In the presences of CsgC, CsgA remains in an unstructured conformation (Fig. 3.7B and Fig. 3.8F) which can be distinguished from the off-pathway oligomers formed when CsgA is incubated with amyloid-inhibiting 2-pyridones (33). The potency of CsgC inhibition at substoichiometric concentrations suggests that it does not form stable 1:1 complexes with individual CsgA monomers to block amyloid formation. Instead it appears that CsgC acts somewhere further along the pre-amyloid folding pathway to stabilize an A11-reactive, non-amyloid species and inhibit transition into a fibrillar species (Fig. 3.7FGH, Fig. 3.11). It is possible that CsgC binds dynamically to a soluble but oligomeric pool of CsgA, and prevents its escape from this ‘molten oligomer’ to form seeds for nucleation into an amyloid (Fig. 3.11). Alternatively, CsgC may induce a structural change within a sub-population of CsgA, which biases the whole population away from forming amyloid. Both explanations are consistent with our data.

Unlike previously reported general molecular chaperones that can inhibit CsgA amyloid formation, CsgC appears to have client protein selectivity (Figs. 3.9, 3.10A) (28). *E. coli* CsgC inhibited the aggregation of CsgA proteins from closely related bacterial species, *C. koseri* and *S. enterica*, each of which shares 75% sequence identity with *E. coli* CsgA (Fig. 3.9A, 3.10F). Furthermore, CsgC inhibited a truncation mutant of the *E. coli* minor curli subunit CsgB from assembling into an amyloid (Fig. 3.9B). Although CsgB is closely related to CsgA, sharing ~30% sequence identity with CsgA and β -sheet-rich secondary structure, a higher molar ratio of CsgC:CsgB was

required to achieve amyloid inhibition over 24 hours (Fig. 3.9B). This implies that while CsgC is able to recognize CsgB at some stage during amyloidogenesis, the sites where CsgB differs from CsgA allow it to escape the action of CsgC more easily.

CsgC also inhibited amyloid formation of the human Parkinson's disease-associated protein α -synuclein, but not the Alzheimer's disease-associated protein $A\beta_{42}$ (Fig. 3.9CD). Although $A\beta_{42}$ does not share recognizable sequence homology with CsgA, an alignment of α -synuclein with CsgA revealed a shared D-Q- Φ -X_{0,1}-G-K-N- ζ motif that maps to R3 of CsgA and residues 98-104 of α -synuclein (Fig. 3.9B). The D-Q- Φ -X_{0,1}-G-K-N- ζ motif is less well conserved in CsgB (Fig. 3.9F). Remarkably, mutagenesis of residues 98-104 of α -synuclein to alanine residues (6ala) reduced the ability of CsgC to inhibit α -synuclein amyloid assembly (Fig. 3.9EF). α -synuclein contains three domains: an N-terminal amphipathic domain, a hydrophobic "non-amyloid component of Alzheimer's Disease" (NAC) and a C-terminal domain sometimes referred to as the solubilizing domain (Fig. 3.10A) (57-60). Interestingly, the D-Q- Φ -X_{0,1}-G-K-N- ζ motif shared with CsgA R3 maps to the C-terminal/solubilizing domain of α -synuclein suggesting that CsgC may be modulating the solubilizing activity of the α -synuclein C-terminal domain. The presence of the D-Q- Φ -X_{0,1}-G-K-N- ζ motif in α -synuclein is important for CsgC-mediated amyloid inhibition; however, it appears that CsgA possess multiple domains through which CsgC can mediate amyloid inhibition (Fig. 3.9). CsgA is comprised of five imperfect repeating units that have distinct propensities to form amyloid. R1, R3, and R5 are highly amyloidogenic, while R2 and R4 are not (19, 35). R2 and R4 contain specific "gatekeeper" residues that temper amyloid formation and that are not present in repeating units R1, R3 or R5 (36). CsgC can inhibit amyloid assembly of CsgA R1, R3 and R5 deletion mutants as well as synthetic peptides corresponding to R1 and R5 (Fig. 3.10A-E). CsgB is similarly comprised of five imperfect repeating units with R1, R2 and R4 being the most amyloidogenic (37). While the exact sequence motif in CsgA R3 that is shared with α -synuclein is not found in the other repeating units of CsgA or CsgB, a second similar motif, Q-X-G-X_{1,2}-N-X₅-Q, can be found in all the CsgA and CsgB repeating units as well as in α -synuclein (Fig. 3.10H). The observation that there may be multiple CsgC recognition domains in CsgA explains why CsgC was able to inhibit the polymerization of CsgA R1, R3, and R5

deletion mutants in addition to synthetic peptides corresponding to R1 and R5 (Fig. 3.10A-E). Collectively, these data suggest that CsgC client protein selectivity is dictated by a short, 8-10 amino acid, sequence that is repeated several times in CsgA and CsgB but only once in α -synuclein (Figs. 3.9E, 3.10A).

Specific amyloid inhibition by proteins at substoichiometric molar ratios is not unprecedented. Grafted Amyloid Motif Antibodies (gammabodies) have been engineered to contain amyloid domains of various amyloid-forming proteins. Gammabodies specifically recognize the amyloid conformation of the target protein and can in some instances inhibit amyloid formation of the target protein at 10-fold substoichiometric molar ratios (61, 62). In another report, the monomeric form of transthyretin (M-TTR) has been shown to inhibit A β and HypF-N amyloid oligomer toxicity *in vitro* at molar ratios comparable to that of CsgC and CsgA (1:100 to 1:500) (63). Although not completely understood, the protein-protein interactions that prevent amyloid formation in the case the gammabodies are hypothesized to be mediated through intermolecular amyloid-like contacts (61, 62). CsgC is non-amyloidogenic under all of the conditions tested, but it is a beta-sheet rich protein that might mimic the amyloid form of CsgA, leaving open the possibility that CsgC interacts with CsgA via an amyloid-like interaction. Clarifying how these amyloid inhibitors interact with their client amyloid-forming proteins awaits high-resolution biophysical studies.

Materials and Methods

Bacterial Growth. All overnight cultures were grown in LB at 37°C with shaking at 220rpm. Cultures were normalized to OD₆₀₀=1.0, 4 μ L were spotted YESCA agar (yeast extract casamino acids) plates and grown for 48 hours at 26°C to induce curli production. For Congo red analysis YESCA plates were supplemented with 50 μ g/mL Congo red and 1 μ g/mL Brilliant Blue G250. When necessary, plates were supplemented with ampicillin or kanamycin at 5 μ g/mL.

Periplasmic Extract Preparation. Overnight cultures were plated as a lawn on a YESCA plate and grown for 48 hours at 26°C. Cells were scraped off the plate with 3 mL of 20 mM Tris (pH 8.0). 40 OD_{600 nm} units for each strain were harvested by centrifugation at 8,000xg, resuspended in 500 μ L of osmotic shock buffer (30 mM Tris

pH 7.2, 40% sucrose, 2 mM EDTA) and incubated at room temperature for 10 minutes. Cells were pelleted for 10 min at 16,000xg, resuspended in 500 μ L of cold 2 mM MgCl₂, incubated on ice for 3 minutes and pelleted at 16,000xg for 10 minutes at 4°C. The supernatant was kept as the periplasmic fraction. All experiments were performed in BW25113 and MC4100 backgrounds at least three times and yielded very similar results.

Strains and Plasmids.

Individual mutants in BW25113 obtained from the Keio collection (64). The Δ *csgG* mutant was constructed by expressing the FLP recombinase from pCP20 at 37°C to remove the *kan* cassette from the Keio collection *csgG::kan* mutant (65). Additional mutations in BW25113 were constructed using lambda red recombination as described previously (See Table 3.1 and 3.3) (66). Mutations in MC4100 were generated using P1 transduction from BW25113. P1 phage were propagated on BW25113 mutants in LB supplemented with 100 mM CaCl₂ until the culture cleared. Remaining cells were killed by the addition of chloroform. Suspensions were pelleted for 10 min at 3,000xg and the supernatant was removed as the P1 lysate. MC4100 was transduced with P1 phage in 10 mM MgSO₄ 5 mM CaCl₂ for 30 min at 30°C. LB supplemented with 100 mM sodium citrate was added to the reactions and the cells were allowed to recover shaking at 37°C for 1 hour. Cells were pelleted and plated on LB supplemented with kanamycin. Strains were verified by PCR with either outside flanking primers or with a flanking primer and primer k1 (66). Plasmid *pcsgD* (pD10) was constructed by amplifying *csgD* from the chromosome with primers MMB116 and MMB117 by PCR followed by digestion and ligation into the EcoRI/BamHI site of pTrc99A. Plasmid *pcsgC* was constructed by amplifying *csgC* with primers KpnI-*csgC* and *csgC*-XbaI by PCR followed by digestion and ligation into the KpnI/XbaI site of pCKR101. Plasmid pCpx1 was constructed by amplifying 249 nucleotides upstream of the *cpxP* start codon from the chromosome with primers MMB92 and MMB93 followed by PCR followed by digestion and ligation into the EcoRI/BamHI site of pRJ800.

Protein Purification. CsgA, CsgB and variants of CsgA were purified as described previously (34). CsgC was purified as described previously (26). His-tagged human α -synuclein was expressed from pt77/434HK in BL21(DE3)pLysS cells. The cells were

grown in 5X LB containing 40 mg/L ampicillin at 36 °C. Protein expression was induced at OD of 0.6 by addition of IPTG (100 mg/L culture) and incubated for three hours before harvest. The pelleted cells were lysed by re-suspension in 8 M Urea, 20 mM Tris pH 8.0, and 20 mM imidazole. The solution was sonicated on ice for repeated cycles of 5s sonication followed by 30s resting for a total of 5-10 min (until non-viscous). The mixture was centrifuged at 20,000 rpm for 20 min and the supernatant was collected. A Ni-NTA (20 mL) column was charged using three column volumes (CV) of 100 mM NiSO₄, followed by five column volumes of water before being equilibrated with two CV of 8 M urea, 20 mM Tris pH 8.0, and 20 mM imidazole. The bacterial lysate was loaded on the column and washed with 10 CV of 20 mM imidazole, 50 mM NaCl, 20 mM Tris pH 7.5, and 5% glycerol. The protein was eluted with five CV of 250 mM imidazole, 50 mM NaCl, 20 mM Tris pH 7.5, and 5% glycerol. β -mercaptoethanol was added to a concentration of 20 mM followed by Caspase-7 (1:100 w:w) to cleave off the His-tag and the solution was incubated over night at 4°C. The protein solution was diluted two times with water and loaded on two serially connected Q-sepharose columns. Washed with 10 CV of 20 mM Tris pH 8.0 and eluted using a gradient of from 0-1 M NaCl over 10 CV. Gel filtration (superdex 75) was used to remove aggregated protein or minor contaminants. Pure fractions were dialyzed against 50 mM ammonium carbonate buffer and lyophilized.

Peptide Preparation. CsgA R1 and R5 peptides (Proteintech Group Inc.) and A β ₄₂ (Biosource) was dissolved in 1:1 trifluoroacetic acid (TFA): 1,1,1,3,3,3-hexafluoro-2-propanol (HFIP) to a concentration of 1 mg/mL and sonicated for 10 minutes. The TFA/HFIP were removed using a SpeedVac. The pellets were dissolved a second time in HFIP and dried again. HFIP treated (A β ₄₂) was dissolved in 20 μ L dimethylsulfoxide and then quickly diluted to 25 μ M with cold KPi (pH 7.3) and sonicated for 30 seconds.

Amyloid Inhibition Assays. Monomeric CsgA, CsgA Δ R1, CsgA Δ R3, CsgA Δ R5, CsgB Δ R5, A β ₄₂ or α -synuclein were added to 10 μ L of 50 mM KPi (pH 7.3) 100 mM NaCl or CsgC in a black flat-bottom 96-well plate with 20 μ M thioflavin T (ThT). The samples were incubated either in a Molecular Devices SpectraMax M2 or a Tecan Infinite M200 microtitre plate reader at 25°C. The plate was shaken linearly for 3 seconds prior to taking fluorescence readings (excitation: 438nm, emission: 495nm,

cutoff: 475nm) every 10 or 20 minutes. α -synuclein polymerization assays were conducted at 37°C with constant agitation with a 2 nm glass bead in each well. Seeding experiments were conducted by adding 2% (by weight) CsgA fibers that had been sonicated with a probe sonicator 3x10sec to each reaction. Graphs are representative of at least 3 independent experiments. Values are reported as normalized ThT fluorescence: buffer or CsgC alone values were subtracted from sample values and were divided by the maximum ThT reading for each sample and smoothed in KaleidaGraph (Synergy Software).

Circular Dichroism. CsgA (20 μ M in 20 mM KPi pH 7.3) or CsgA with CsgC (2 μ M in KPi pH 7.3) were analyzed using a Jasco J-810 spectropolarimeter from 190 to 250nm at 25°C immediately after purification and every 24 hours. The buffer or 2 μ M CsgC spectra were subtracted from the samples.

Nuclear magnetic resonance spectroscopy. One-dimensional proton NMR experiments were performed on 10 μ M CsgA alone, or with CsgC in a 150:1 molar ratio, in a buffer containing 50 mM potassium phosphate pH 7.4, 5% (v/v) D₂O. Sequential spectra (800 scans each) were recorded every 30 minutes over a period of ~24 hours. Spectra were processed within BioSpin (Bruker) and plotted in ORIGIN.

Denaturing Gel Electrophoresis and Western Blot. Overnight cultures were diluted to OD₆₀₀=1.0 and 4 μ L were spotted on a YESCA plate and incubated at 26°C for 2 days. The cells were harvested and resuspended in 50 mM KPi pH 7.3. 0.1 OD_{600 nm} units for each strain were harvested in duplicate by centrifugation. One duplicate was resuspended in 2X SDS loading buffer while the other was treated with HFIP for 10 min at room temperature, dried in a SpeedVac and then resuspended in 2X SDS loading buffer. Samples were run on a 15% SDS PAGE gel and transferred to a PVDF membrane. Blots were probed with antibodies against CsgA (1:12,000), CsgG (1:50,000), CsgC (1:4,000), Sigma70 (1:5,000) or A11 (1:10,000).

Native Gel Electrophoresis. Samples were mixed with 3X Native loading buffer (15 mM Tris, 144 mM glycine, 30% glycerol, 1% bromophenol blue) and loaded on a 7.5% nondenaturing Tris-glycine gel at 150V at 4°C and then transferred to a PVDF membrane for western blot.

Live/Dead Staining. Live/Dead staining was conducted using a LIVE/DEAD BacLight Bacterial Viability Kit (Molecular Probes). Briefly, 100 μ L of overnight culture of were spread on a YESCA plate as a lawn and grown at 26°C for 48 hours. Cells were harvested with 5 mL 0.85% NaCl and normalized to $OD_{600\text{ nm}} = 0.06$. 100 μ L of SYTO9/Propidium Iodide (10 μ M/60 μ M) were added to 100 μ L of cell suspension and incubated in the dark for 15 minutes. Fluorescence was read in a Molecular Devices SpectraMax M2 microtitre plate reader with an excitation wavelength of 485 nm and emission wavelength of 530 nm and 630 nm. Experiments were performed on BW25113 and MC4100 three times and yielded similar results in each strain background.

β -galactosidase Assay. Cells were transformed with pRJ800 empty vector or pCpx1 (with the *cpxP* promoter cloned upstream of *lacZ* in pRJ800) and grown on YESCA plates at 26°C for 48 hours and harvested in cold 50 mM potassium phosphate buffer (pH 7.3). Cells were permeabilized by detergent and assayed for β -galactosidase activity as described previously (67). Experiments were performed on BW25113 and MC4100 three times and yielded similar results in each strain background.

Transmission Electron Microscopy. MC4100 cells were prepared as a 1.0 $OD_{600\text{ nm}}$ suspension in 50 mM KPi (pH 7.3) and mounted on formvar-coated grids. Grids were imaged using a Philips CM100 transmission electron microscope.

Figures and Tables

Figure 3.1. Secretion deficient mutants induce an amyloid inhibitory activity in the periplasm. Periplasmic extracts (PEs) were harvested from BW25113 $\Delta csgG$ (A) or complete curli deletion (Δcsg ; B) and incubated with soluble CsgA for 24 hours. CsgA amyloid formation was monitored by ThT fluorescence. C) Soluble and insoluble CsgA were separated by centrifugation after 24 hours of incubation alone or in the presence of periplasmic protein extracts from a $\Delta csgD$ or $\Delta csgG$ mutant. Samples were suspended in SDS loading buffer with or without HFIP pretreatment. Samples were separated on a 15% SDS PAGE gel and stained with Coomassie (top panel) or analyzed by western blot for CsgA (lower panel).

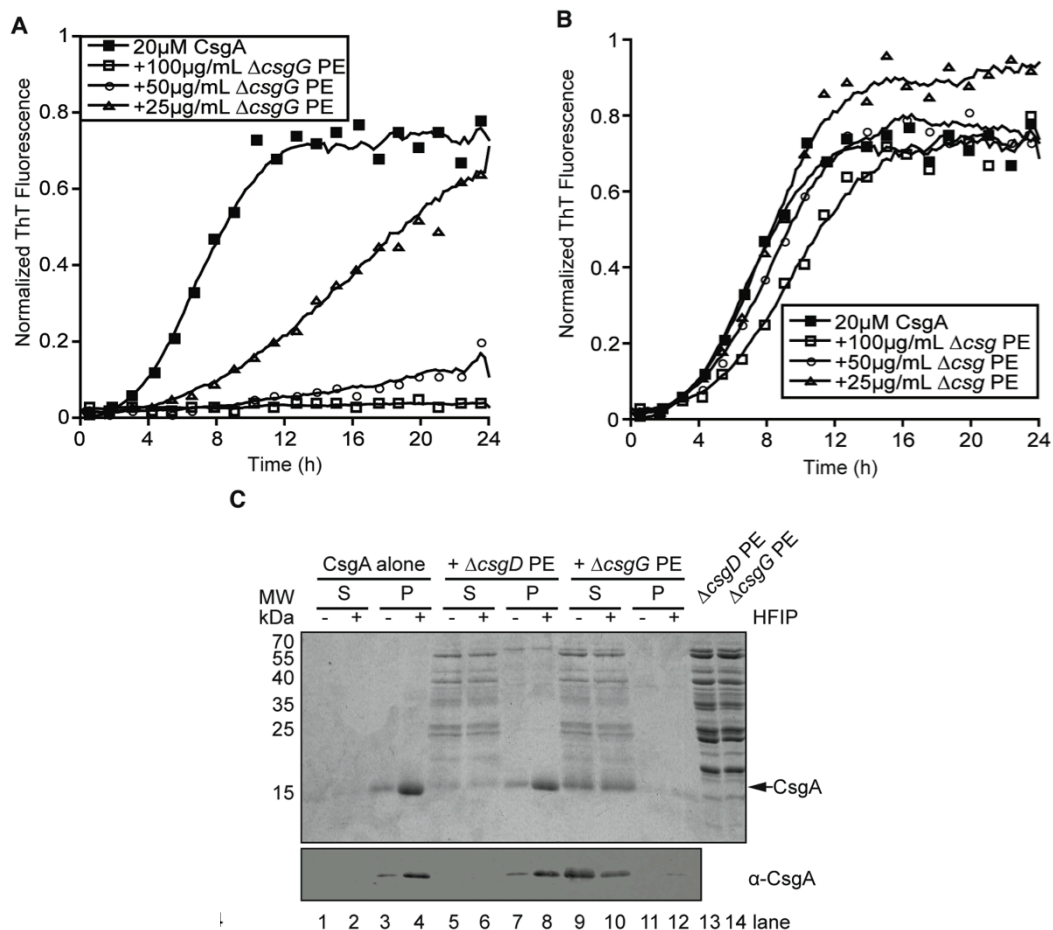


Figure 3.2. *csg* mutants exhibit varying degrees of amyloid inhibitory activity. PEs were harvested from WT BW25113 *E. coli* or various gene deletion mutants of curli biogenesis genes (A) or from a $\Delta csgG\Delta csgE$ double deletion strain (B) and assayed for CsgA amyloid inhibition *in vitro*. Polymerization of CsgA was monitored by ThT fluorescence. (C) Cells were analyzed by western blot and Congo red binding.

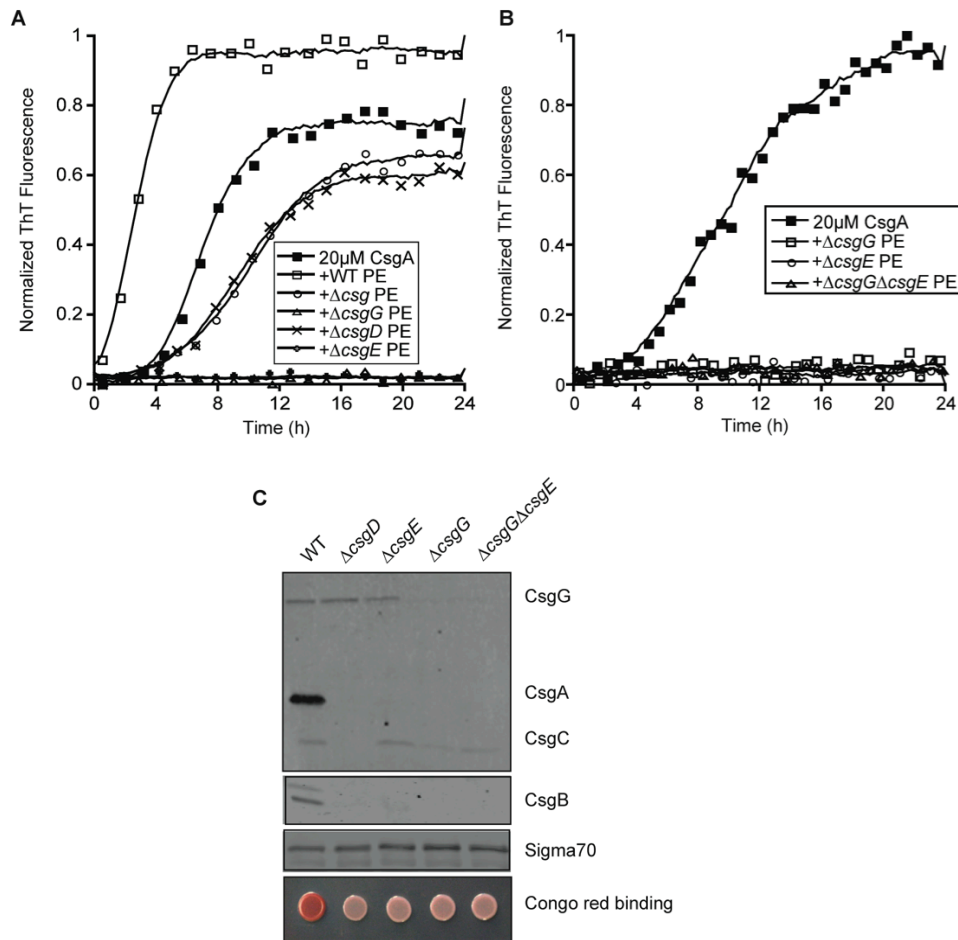


Figure 3.3. Amyloid inhibition requires expression of *csgC*. **A)** PEs from a BW25113 $\Delta csgD$ mutant with pTrc99A (vector) or pTrc99A-*csgD* (*pcsgD*) were assayed for CsgA amyloid inhibition *in vitro*. **BC)** PEs from BW25113 mutants ($\Delta csgA$, $\Delta csgB$, $\Delta csgC$) or BW25113 combination mutants ($\Delta csgB\Delta csgA$; $\Delta csgA\Delta csgC$; $\Delta csgB\Delta csgA\Delta csgC$) were assayed for CsgA amyloid inhibition. CsgA amyloid formation was monitored by ThT fluorescence.

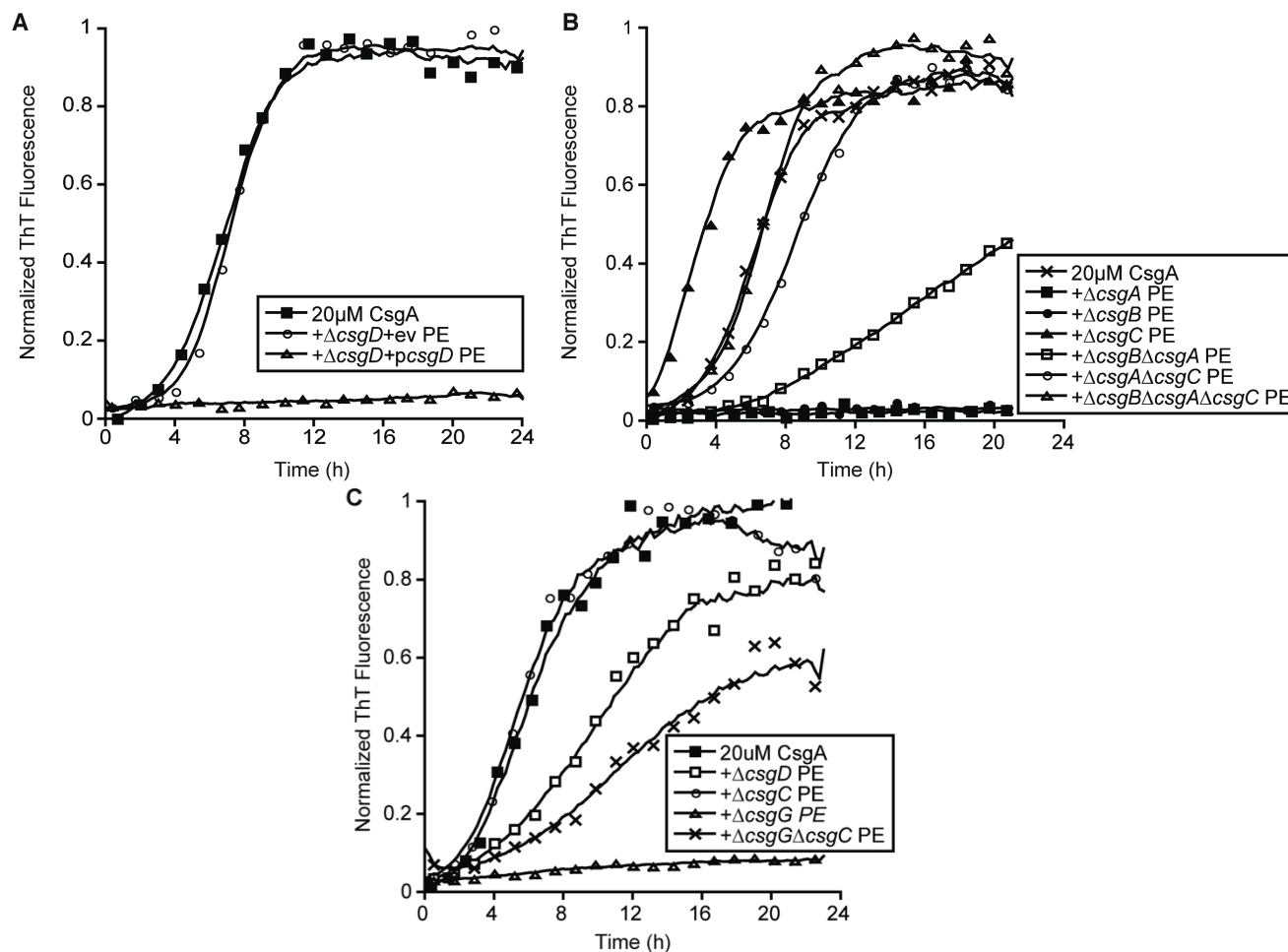


Figure 3.4. Amyloid inhibitory activity is regulated by CsgD and requires expression of *csgC*. **A)** BW25113 cells were spotted on YESCA-CR and grown for two days at 26°C to induce curli expression. WT cells were transformed with empty vector (pTrc99A, ev) and $\Delta csgD$ cells were transformed either with empty vector (ev) or pTrc99A-*csgD*. Whole cell extracts were analyzed by SDS-PAGE and Western blot with anti-CsgA and anti-CsgG antibodies with or without HFIP treatment. **B)** BW25113 deletion mutants in *csgA*, *csgB*, *csgC* or the indicated combination mutants were grown on YESCA-CR plates at 26°C for 2 days prior to analysis by SDS-PAGE, western blot and evaluation of Congo red binding. **C)** Size exclusion chromatography was used to fractionate PEs from a BW25113 $\Delta csgG$ mutant. Each fraction was assayed for CsgA amyloid inhibition *in vitro*. Polymerization of CsgA was monitored by ThT fluorescence. **D)** $\Delta csgG$ mutant PEs fractions were separated on a 15% SDS PAGE gel and analyzed by western blot with a CsgC antibody.

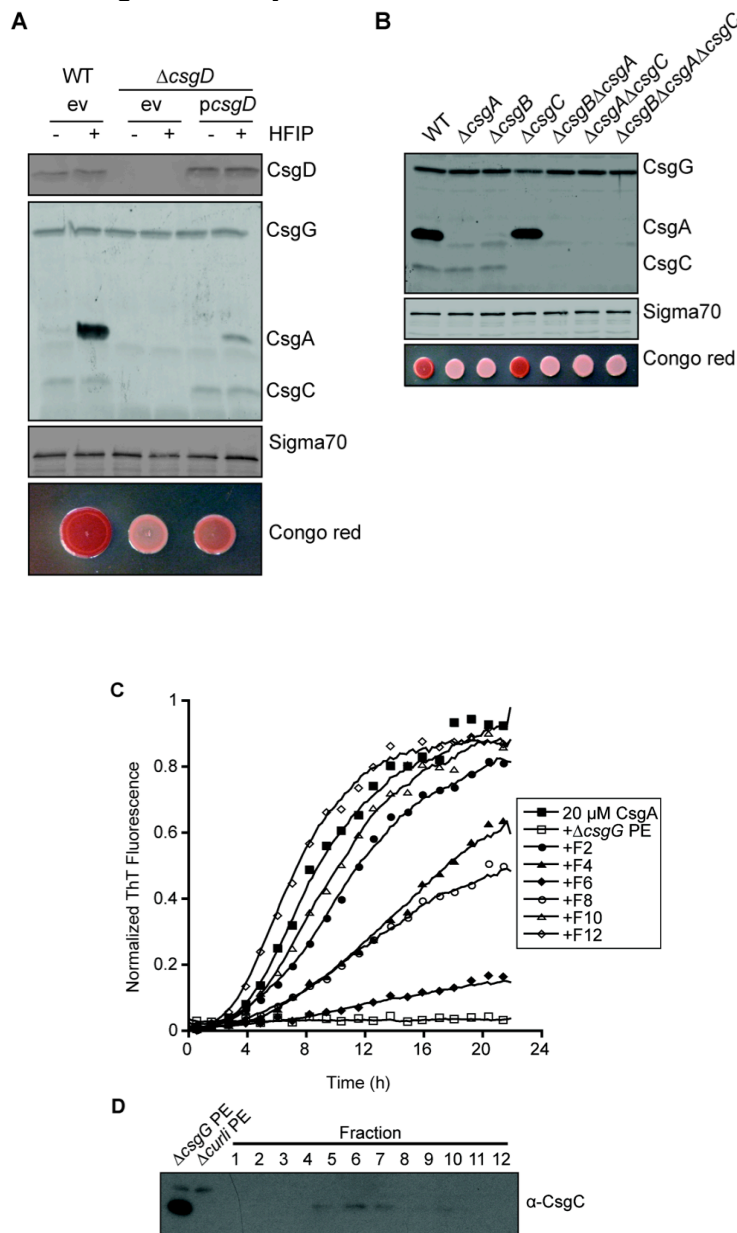


Figure 3.5. $\Delta csgG\Delta csgC$ mutants accumulate intracellular CsgA aggregates. A) BW25113 cells were grown on Congo red indicator plates at 26°C for 48 hrs to assess curli production *in vivo*. **B)** Cells grown under curli-inducing conditions were subject to western blot analysis with CsgG, CsgA, CsgC and Sigma70 antibodies. **C)** Intact or lysed cells were analyzed by dot blot western using CsgA antibodies.

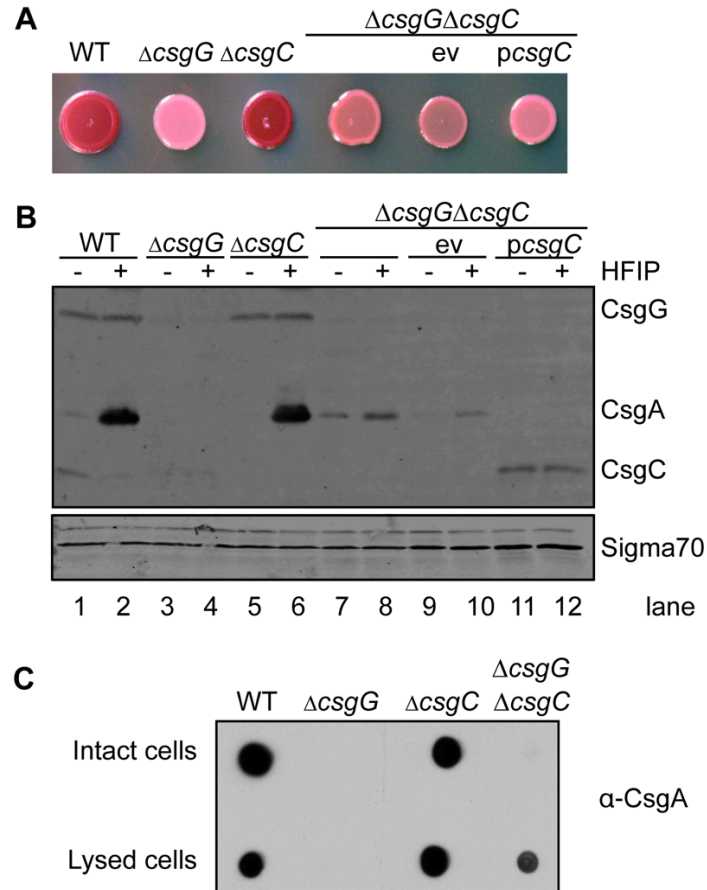


Figure 3.6. $\Delta csgG\Delta csgC$ cells do not produce extracellular curli fibers but exhibit a decrease in cellular fitness. A-D) MC4100 cells were grown for 2 days on YESCA plates at 26°C prior to being harvested, mounted on formvar coated grids, stained with uranyl acetate and imaged by transmission electron microscopy. E) Live-Dead stain of MC4100 cells grown on YESCA plates at 26°C. The percent dead cells was calculated relative to a WT standard curve. * $p < 0.001$, ** $p < 0.0002$. F) β -galactosidase activity was measured after MC4100 cells containing a *cpxP* promoter *lacZ* fusion construct were grown on YESCA plates at 26°C for 48 hours. * $p < 0.00008$. G) Overexpression of cytoplasmic CsgA (closed squares) alone causes growth arrest measured by $OD_{600\text{ nm}}$ over time. Coexpression of ev (pBAD33A, open squares) or periplasmic CsgC (open circles) failed to alleviate growth arrest. Coexpression of cytoplasmic CsgC (closed circles) improved cell growth and division.

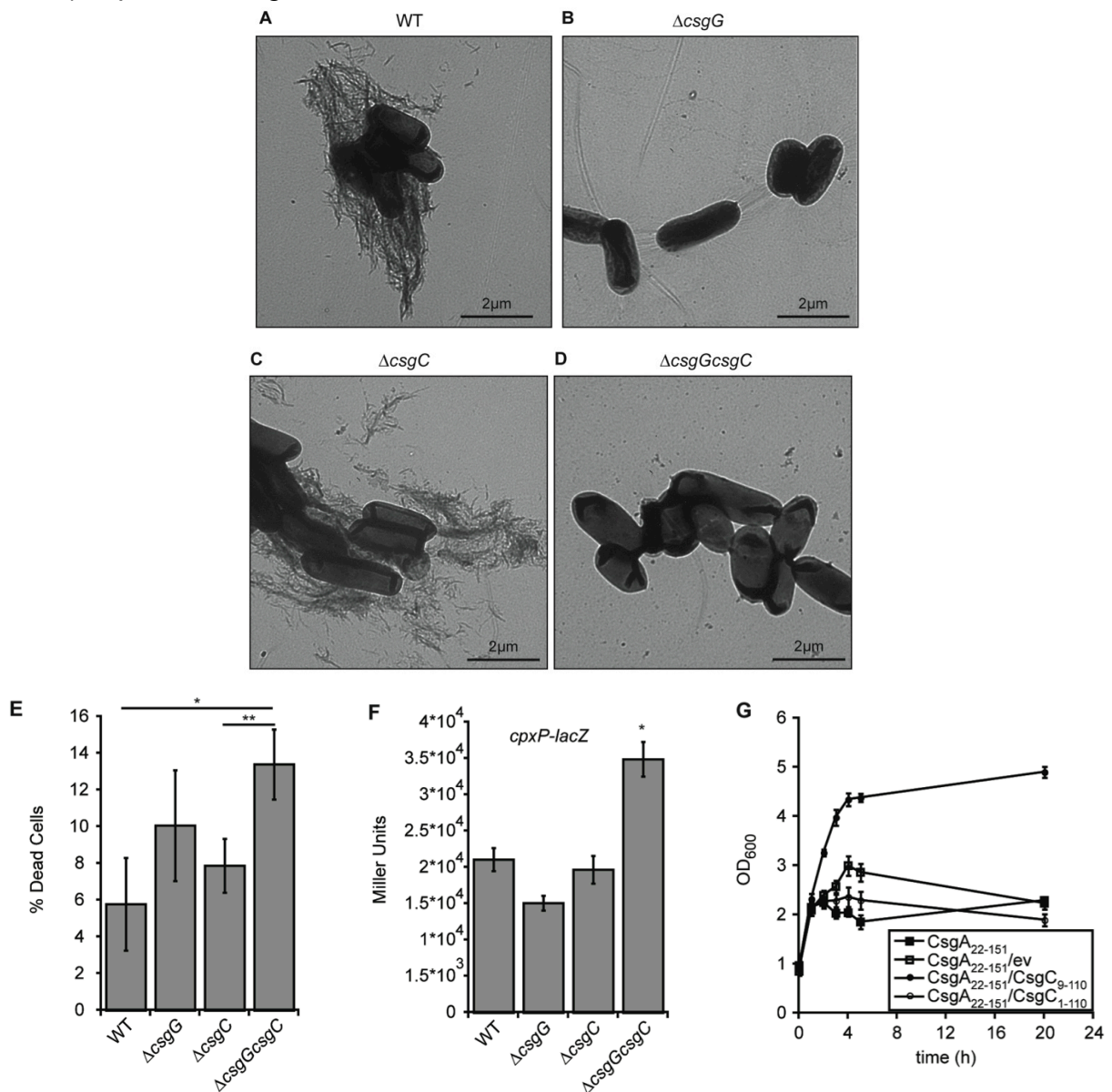


Figure 3.7. Purified CsgC inhibits CsgA amyloid formation at substoichiometric molar ratios. **A)** Polymerization of CsgA was monitored by ThT fluorescence over time in the presence or absence of purified CsgC. **B)** The secondary structure of CsgA was monitored by CD every 24 hours for 4 days in the absence (closed symbols) or presence (open symbols) of CsgC (1:10, CsgC:CsgA). Sequential ^1H NMR spectra of 10 μM CsgA alone (**C**) or in 150-fold molar excess over CsgC (**D**). The methyl proton spectral region is shown for clarity. **E)** The amplitude of the strongest methyl peak in the CsgA (C) and CsgA+CsgC (D) spectra (0.83 ppm) plotted over time. **F)** Polymerization of CsgA was seeded by the addition of 2% (by weight) CsgA seeds in the absence of CsgC (open squares) or the presence of CsgC (open circles and triangles). **G)** Dot blot analysis of CsgA alone, CsgC alone or CsgA+CsgC (1:3, CsgA:CsgC) immediately after purification (t=0h) or after 24 hours of incubation (t=24) with anti-CsgA, anti-CsgC and A11 antibodies. **H)** Native gel electrophoresis and Western blot of 20 μM soluble CsgA without and with 5 min of boiling, 20 μM CsgA that has been incubated at 25°C for 24h, 6.7 μM CsgC alone, or 20 μM CsgA that has been incubated with 2 μM CsgC for 24h.

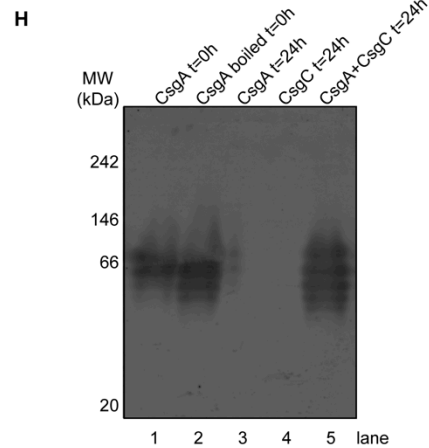
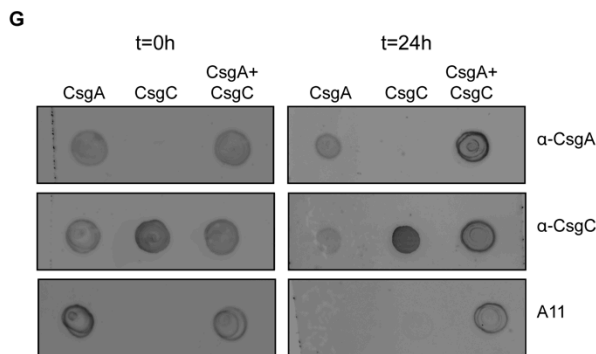
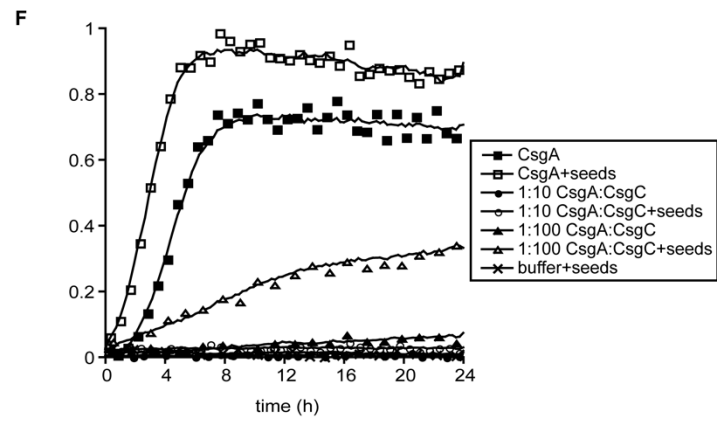
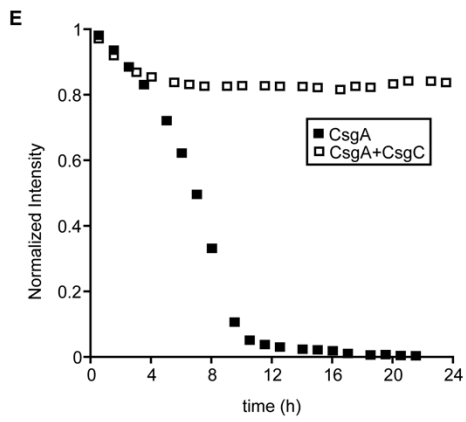
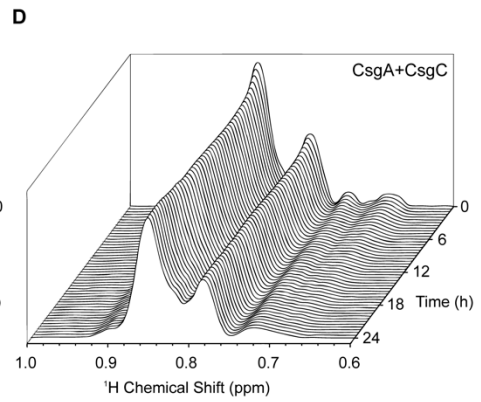
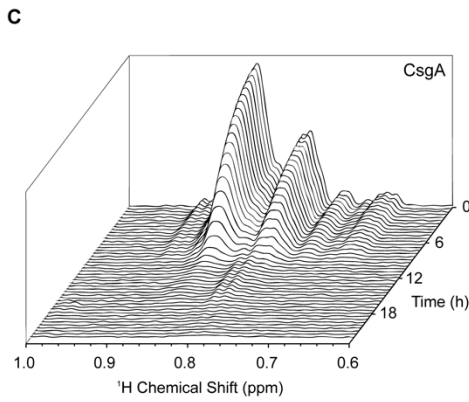
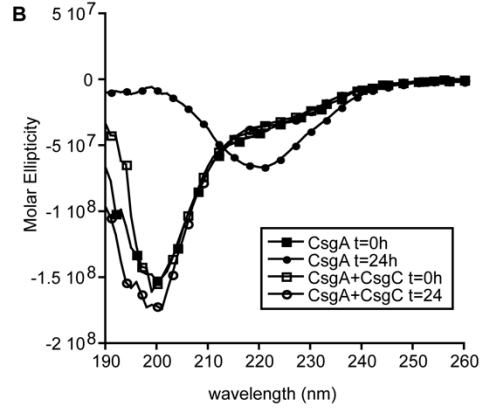
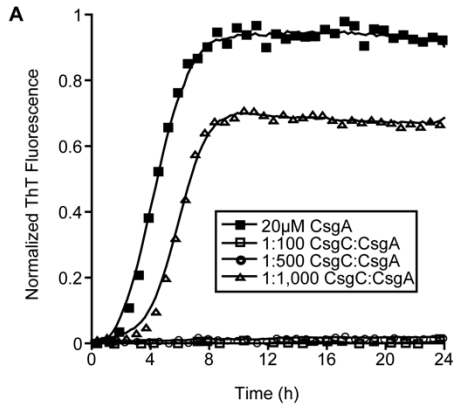


Figure 3.8. CsgA amyloid inhibition *in vitro*. **A)** CsgA was incubated with substoichiometric molar ratios of BSA for 24 hours. Polymerization of CsgA was monitored by ThT fluorescence. **B)** CsgA was separated into soluble and pelleted fractions by centrifugation after 24 hours of incubation alone or in the presence of CsgC (1:10, CsgC:CsgA). Samples were either treated with SDS loading buffer or pretreated with HFIP prior to being run on a 15% SDS PAGE gel and Western blot with anti-CsgA antibody. **C)** CsgA was incubated with CsgC at a 1:10 molar ratio and aggregation was monitored by ThT and ANS fluorescence over time. **D)** The CD spectrum of CsgC alone demonstrates that CsgC remains β -sheet rich over time. The secondary structure of CsgA alone (**E**) or in the presence of CsgC (**F**) at a 1:10 (CsgC:CsgA) molar ratio was monitored by CD every 24 hours for 4 days. ThT fluorescence of CsgA in the presence and absence of CsgC was monitored in parallel with CD (**G**).

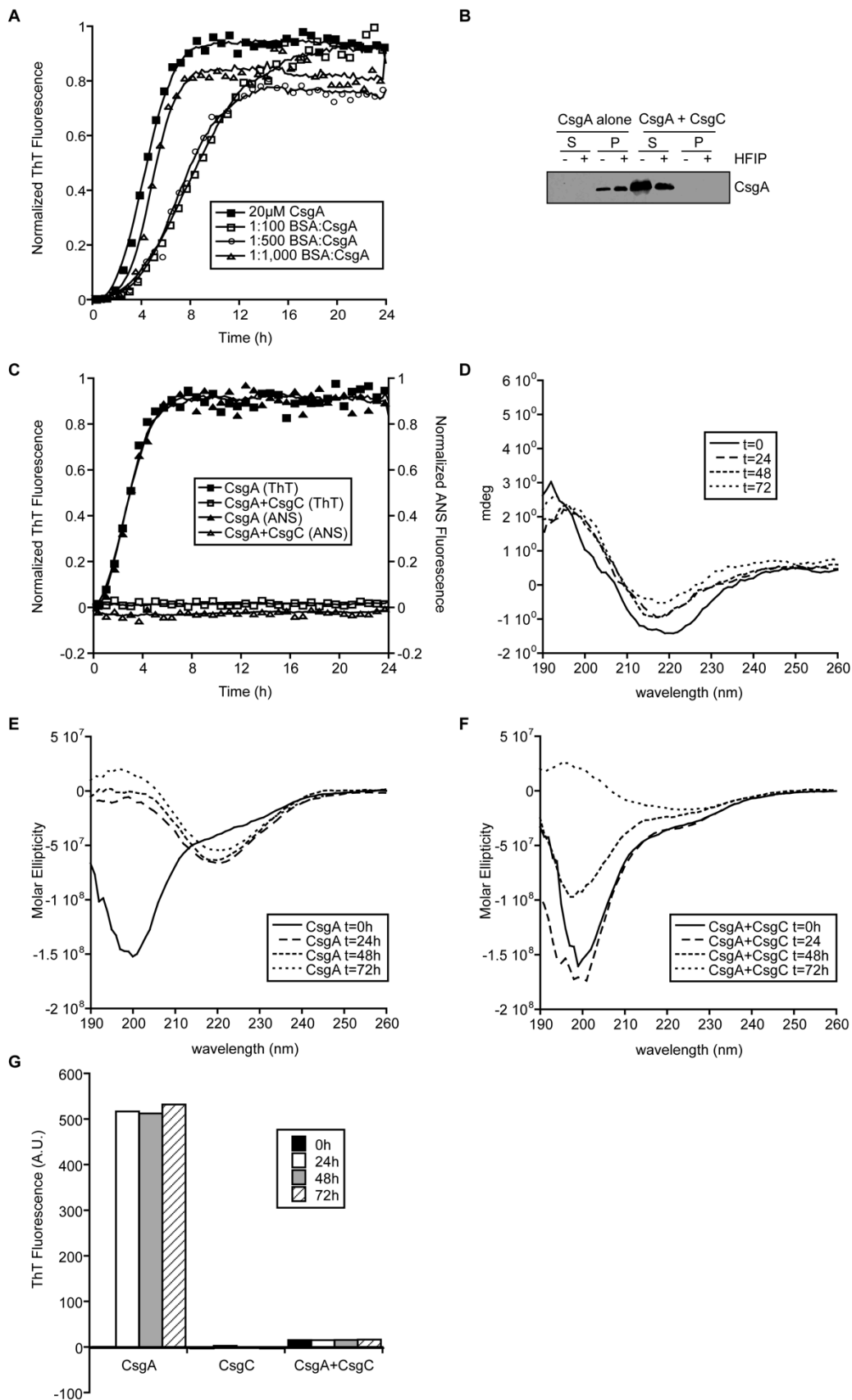


Figure 3.9. Amyloid inhibition by CsgC is specific. Using the ThT assay, *E. coli* CsgC was tested for amyloid inhibition against CsgA from *S. enterica* (A), *E. coli* CsgB (B), A β_{42} (C), α -synuclein (DE). F) Sequence alignment of *E. coli* CsgA, CsgB, human α -synuclein and the α -synuclein alanine variant used in panel E.

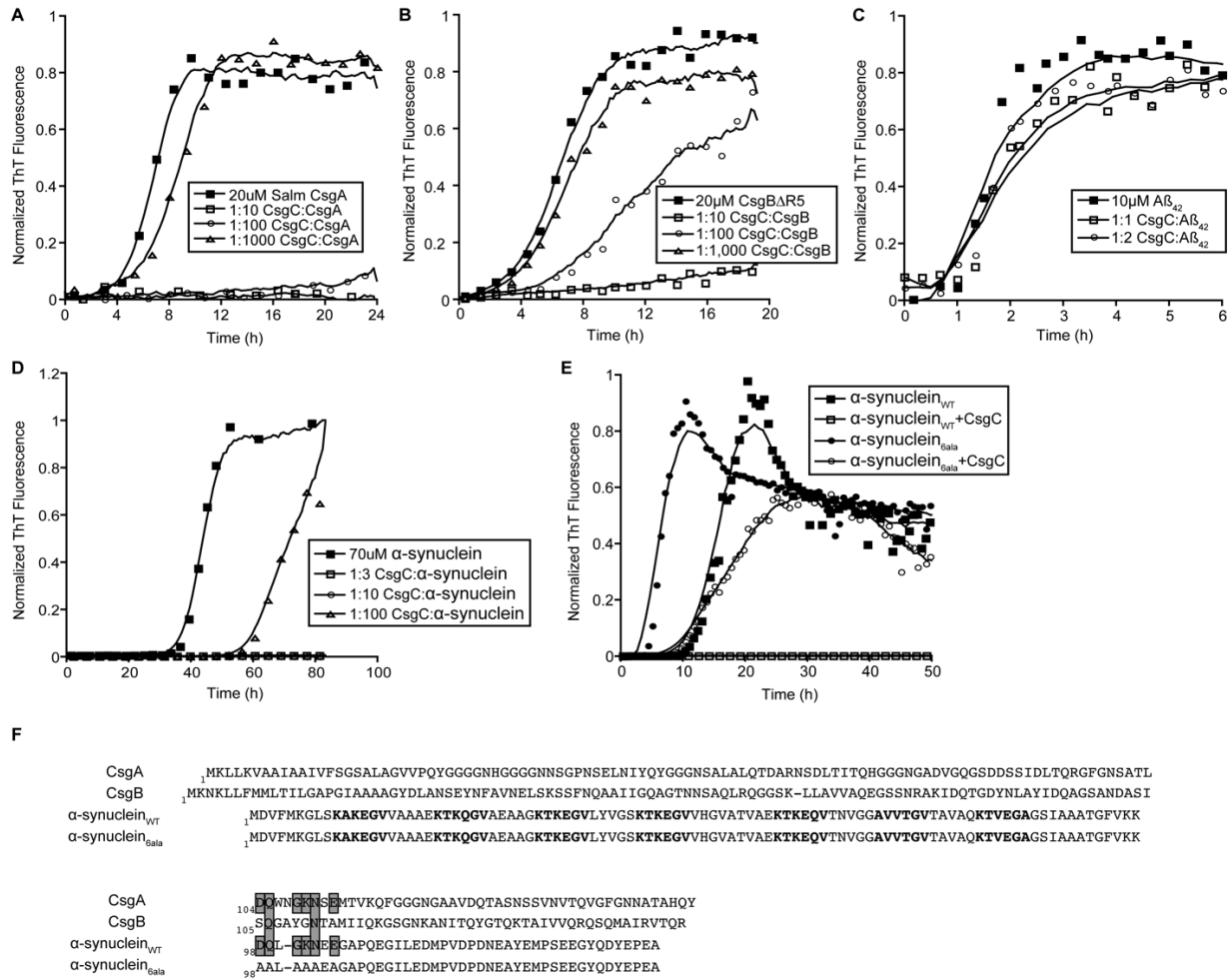


Figure 3.10. CsgC inhibits CsgA repeating unit deletion mutants and synthetic peptides. CsgC was tested for amyloid inhibition *in vitro* with purified repeating unit deletion mutants of CsgA (A) Δ R1, (B) Δ R3, (C) Δ R5 and synthetic peptides corresponding to R1 (D) and R5 (E). Polymerization was monitored by ThT fluorescence. (F) *C. koseri* CsgA was purified and allowed to polymerize in the presence or absence of *E. coli* CsgC. (G) Residues 98-104 or α -synuclein were scrambled (DQLGKNEE mutated to SQGAYGNTA). The purified α -synuclein_{scram} was purified and allowed to polymerize in the presence and absence of CsgC. Polymerization was monitored by ThT fluorescence. (H) Alignment of α -synuclein with CsgA.

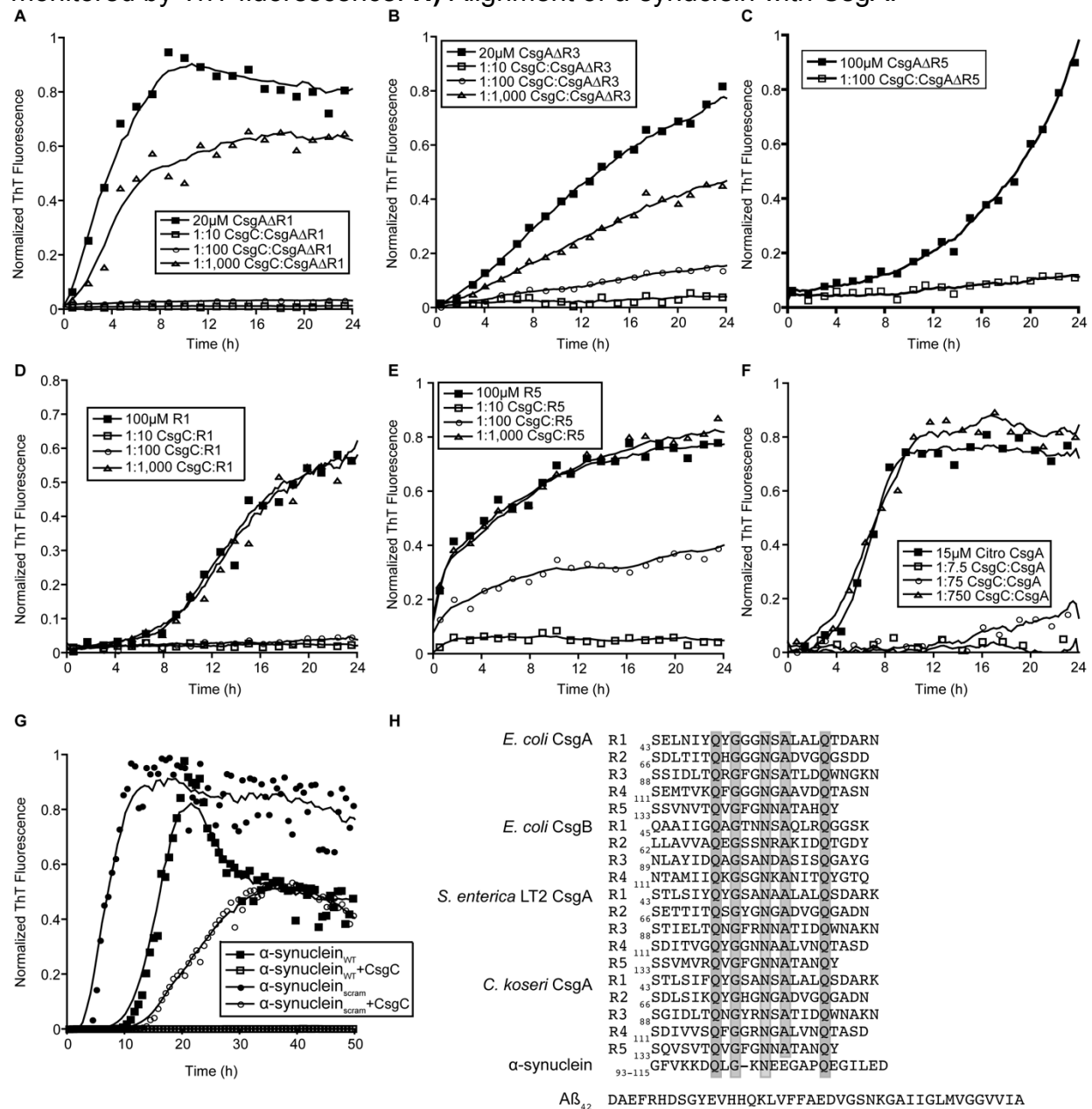


Figure 3.11. Model of CsgC-mediated amyloid inhibition. A predicted energy landscape of CsgA amyloidogenesis where CsgA forms dynamic, amorphous aggregates before assembling into amyloid-like, prefibrillar oligomers. Our data support a model where CsgC inhibits CsgA amyloid formation by transiently interacting with a prefibrillar CsgA species that results in keeping CsgA in an amorphous conformation.

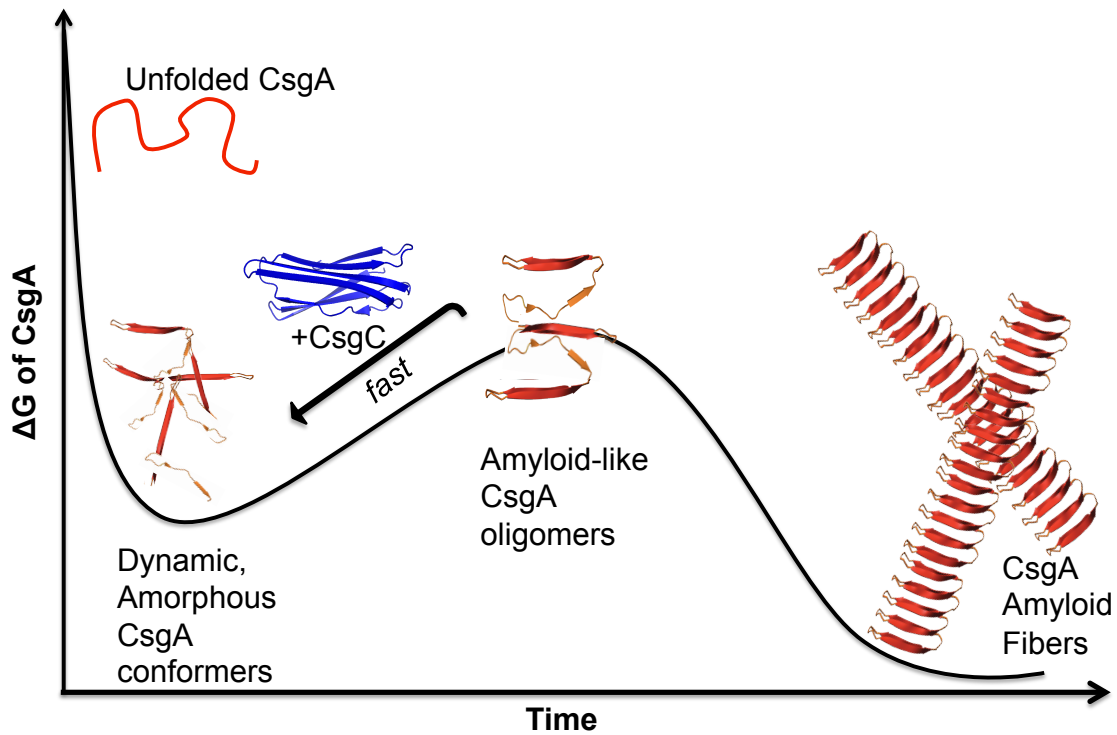


Table 3.1. Strains used in Chapter 3

Strains	Relevant Genotype	References
BW25113	F- $\Delta(araD-araB)567$, $\Delta lacZ4787(::rrnB-3)$, λ^- , <i>rph-1</i> , $\Delta(rhaD-rhaB)568$, <i>hsdR514</i>	(66)
Δcsg	BW25113 $\Delta csgDEFG... \Delta csgBAC$	This study
$\Delta csgA$	BW25113 <i>csgA::kan</i>	(64)
$\Delta csgB$	BW25113 <i>csgB::kan</i>	(64)
$\Delta csgC$	BW25113 <i>csgC::kan</i>	(64)
$\Delta csgD$	BW25113 <i>csgD::kan</i>	(64)
$\Delta csgE$	BW25113 <i>csgE::kan</i>	(64)
$\Delta csgG$	BW25113 $\Delta csgG$	This study
$\Delta csgBcsgA$	BW25113 <i>csgBcsgA::kan</i>	This study
$\Delta csgAcsgC$	BW25113 <i>csgAcsgC::kan</i>	This study
$\Delta csgBcsgAcsgC$	BW25113 <i>csgBcsgAcsgC::kan</i>	This study
$\Delta csgGcsgE$	BW25113 $\Delta csgG$ <i>csgE::kan</i>	This study
$\Delta csgGcsgC$	BW25113 $\Delta csgG$ <i>csgC::kan</i>	This study
MC4100	F- <i>araD139</i> $\Delta(argF-lac)$ U169 <i>rpsL150(strR)</i> <i>relA1</i> <i>fibB5301</i> <i>deoC1</i> <i>ptsF25</i> <i>rbsB</i>	(68)
$\Delta csgG$ (LSR1)	MC4100 <i>csgG::Tn105</i>	(14)
$\Delta csgC$	MC4100 <i>csgC::kan</i>	This study
$\Delta csgGcsgC$	MC4100 <i>csgG::Tn105</i> <i>csgC::kan</i>	This study
NEB3016	MiniF <i>lac^q</i> (Cam ^R) / <i>fhuA2</i> <i>lacZ::T7 gene1</i> [<i>lon</i>] <i>ompT</i> <i>gal</i> <i>sulA11</i> <i>R(mcr-73::miniTn10--Tet^S)2</i> [<i>dcm</i>] <i>R(zgb-210::Tn10--Tet^S)</i> <i>endA1</i> $\Delta(mcrC-mrr)114::IS10$	New England Biolabs
BL21(DE3)	F-, <i>ompT</i> , <i>hsdSB</i> (rB-, mB-), <i>dcm</i> , <i>gal</i> , λ (DE3)	New England Biolabs
BL21(DE3)pLysS	F-, <i>ompT</i> , <i>hsdSB</i> (rB-, mB-), <i>dcm</i> , <i>gal</i> , λ (DE3), pLysS, Cmr.	Promega

Table 3.2. Plasmids used in Chapter 3

Plasmids	Relevant Characteristics	References
pTrc99A	IPTG inducible expression vector	Pharmacia Biotech
p <i>csgD</i> (pD10)	<i>csgD</i> cloned into the EcoRI/BamHI site in pTrc99A	This study
pCKR101	IPTG inducible expression vector	(69)
p <i>csgC</i>	<i>csgC</i> cloned into KpnI/XbaI site in pCKR101	This study
pET11d	IPTG inducible expression vector	New England Biolabs
pNH11	C-terminal His ₆ tagged <i>E. coli csgA</i> cloned into NcoI/BamHI site in pET11d	(37)
pET11d-CsgAΔR1	C-terminal His ₆ tagged <i>E. coli csgA</i> ΔR1 was PCR amplified out of pΔR1 (35) and cloned into NcoI/BamHI site in pET11d	This study
pET11d-CsgAΔR3	C-terminal His ₆ tagged <i>E. coli csgA</i> ΔR3 was PCR amplified out of pΔR3 (35) and cloned into NcoI/BamHI site in pET11d	This study
pET11d-CsgAΔR5	C-terminal His ₆ tagged <i>E. coli csgA</i> ΔR5 was PCR amplified out of pΔR5 (35) and cloned into NcoI/BamHI site in pET11d	This study
pET11d-CsgA _{ST}	C-terminal His ₆ tagged <i>S. typhimurium csgA</i> cloned into NcoI/BamHI site in pET11d	(34)
pET11d-CsgA _{CK}	C-terminal His ₆ tagged <i>C. koseri csgA</i> cloned into NcoI/BamHI site in pET11d	(34)
pNH28	C-terminally His ₆ tagged <i>csgB</i> ΔR5 cloned into NcoI/BamHI site in pET11d	(37)
pET28a	IPTG inducible expression vector	New England Biolabs
pC3	C-terminal His ₆ tagged <i>csgC</i> cloned into pET28a	(26)
pCsgA ₂₂₋₁₅₁	C-terminal LEHHHHHH tagged <i>csgA</i> lacking the Sec-secretion signal sequence was cloned into NcoI/XhoI site in pET28a	This study
pBAD/Myc-his C	Arabinose inducible expression vector	Invitrogen
pCsgC ₁₋₁₁₀	C-terminal VEHHHHHH tagged <i>csgC</i> was cloned into the NcoI/SalI site of pBAD/Myc-his	This study
pCsgC ₉₋₁₁₀	C-terminal VEHHHHHH tagged <i>csgC</i> lacking the Sec-secretion signal sequence was cloned into the NcoI/SalI site of pBAD/Myc-his	This study
pt77/434HK	IPTG inducible expression of Caspase-7 cleavable His ₆ -tagged α-synuclein	AlexoTech AB (www.alexotech.com, Umeå, Sweden)
pRJ800	Promoterless <i>lacZ</i> construct	(70)
pCpx1	<i>cpxP</i> promoter cloned into the EcoRI/BamHI site	This study

	in pRJ800	
pCP20	Flp recombinase expressing vector	(65)

Table 3.3. Primers used in Chapter 3

Primer	Primer sequence	Constructs
CsgGH2P2	5'-CCGGATGATAATTCCGGCTTTTTTATCTGTCAGGATTC CGGTGGAACCGAGTGTAGGCTGGAGCTGCTTC-3'	Δ csg
CsgEH1P1	5'-CGCATTGCAGCCTCCGAACAATTTTTATTTAGAATTCA TCATGCGCCAACATATGAATATCCTCCTTAG-3'	Δ csgGcsgE
CsgEH2P2	5'-GACACAAGCGGTTTCCTGGGCAAACGATAACCTCAGG CGATAAAGCCATGGTGTAGGCTGGAGCTGCTTC-3'	Δ csgGcsgE
CsgCH1P1	5'-TATTACAGAAACAGGGCGCAAGCCCTGTTTTTTTTTCGG GAGAAGAATATGGTGTAGGCTGGAGCTGCTTC-3'	Δ csgGcsgC
CsgCH2P2	5'-ATTCATCTTATGCTCGATATTTCAACAAATTAAGACTTT TCTGAAGAGGGCATATGAATATCCTCCTTAG-3'	Δ csg Δ csgGcsgC Δ csgAcsG Δ csgBcsgA csgC
CsgBH1P1	5'-GAAATGATTTAATTTCTTAAATGTACGACCAGGTCCAG GGTGACAACATGGTGTAGGCTGGAGCTGCTT-3'	Δ csgBcsgA Δ csgBcsgA csgC
CsgAH1P1	5'-ACGTTAATTTCCATTCGACTTTTAAATCAATCCGATGG GGTTTTACATGGTGTAGGCTGGAGCTGCTTC-3'	Δ csgAcsG
CsgAH2P1	5'-CGCCCTGTTTCTGTAAATACAAATGATGTATTAGTACT GATGAGCGGTGCCCATATGAATATCCTCCTTAG	Δ csgBcsgA
MMB116	5'-CGGAATTCATGTTTAATGAAGTCCATAG-3'	pD10
MMB117	5'-CGGGATCCTTATCGCCTGAGGTTATCG-3'	pD10
KpnI-csgC	5'-GCGGGTACCATGAATACGTTATTACTC-3'	pcsgC
csgC-XbaI	5'-GCGAGATCTTTAAGACTTTTCTGAAGA-3'	pcsgC
MMB92	5'-CGGAATTCATCGTGGGCAAACAATCACG-3'	pCpx1
MMB93	5'-CGGGATCCTTGCTCCCAAATCTTTCTG-3'	pCpx1
NH55	5'-GCGTTTCCATGGGTGTTGTTCCCTCAGTACGGCGGC-3'	pET11d- CsgA Δ R1, pET11d- CsgA Δ R3, pET11d- CsgA Δ R5
NH56	5'-GTTTAAAGCTTGGATCCTTAGTGATGGTGATGGTGATG GTAAGTATGAGCGGTCGCGTTGTT-3'	pET11d- CsgA Δ R1, pET11d- CsgA Δ R3, pET11d- CsgA Δ R5
CsgA2F	5'-CGTTCCATGGGTGTTGTTCCCTCAGTACGG-3'	pCsgA ₂₂₋₁₅₁
CsgA2R	5'-TATTCTCGAGGTAAGTATGAGCGGTCGCGTTG-3'	pCsgA ₂₂₋₁₅₁
CsgCK12F	5'-TATTCCATGGGCACGTTATTACTCCTTGCGGC-3'	pCsgC ₁₋₁₁₀
CsgCcoli10 R	5'-TATTCTCGAGTTAAGACTTTTCTGAAGAGGGCGGC-3'	pCsgC ₁₋₁₁₀

CsgCcoli3F	5'-TCTTCCATGGGCTCCAGTCAGATAACCTTTAATACGACC- 3'	pCsgC ₉₋₁₁₀
CsgCcoli3R	5'-TATTCTCGAGAGACTTTTCTGAAGAGGGCGGCCATTG-3'	pCsgC ₉₋₁₁₀

References

1. Eichner T, Radford SE (2011) A diversity of assembly mechanisms of a generic amyloid fold. *Mol Cell* 43:8–18.
2. Shewmaker F, McGlinchey RP, Wickner RB (2011) Structural insights into functional and pathological amyloid. *J Biol Chem* 286:16533–16540.
3. Nilsson MR (2004) Techniques to study amyloid fibril formation in vitro. *Methods* 34:151–160.
4. Chiti F, Dobson CM (2006) Protein misfolding, functional amyloid, and human disease. *Annu Rev Biochem* 75:333–366.
5. Blanco LP, Evans ML, Smith DR, Badtke MP, Chapman MR (2012) Diversity, biogenesis and function of microbial amyloids. *Trends Microbiol* 20:66–73.
6. DePas WH, Chapman MR (2012) Microbial manipulation of the amyloid fold. *Res Microbiol* 163:592–606.
7. Chapman MR, Robinson LS, Pinkner JS, Roth R, Heuser J, Hammar M, Normark S, Hultgren SJ (2002) Role of *Escherichia coli* curli operons in directing amyloid fiber formation. *Science* 295:851–855.
8. Dueholm MS, Albertsen M, Otzen D, Nielsen PH (2012) Curli functional amyloid systems are phylogenetically widespread and display large diversity in operon and protein structure. *PLoS One* 7:e51274.
9. Hufnagel DA, Tukul C, Chapman MR (2013) Disease to dirt: the biology of microbial amyloids. *PLoS Pathog* 9:e1003740.
10. Olsen A, Jonsson A, Normark S (1989) Fibronectin binding mediated by a novel class of surface organelles on *Escherichia coli*. *Nature* 338:652–655.
11. Pawar DM, Rossman ML, Chen J (2005) Role of curli fimbriae in mediating the cells of enterohaemorrhagic *Escherichia coli* to attach to abiotic surfaces. *J Appl Microbiol* 99:418–425.
12. Evans ML, Chapman MR (2013) Curli biogenesis: Order out of disorder. *Biochim Biophys Acta*
13. Mika F, Hengge R (2013) Small Regulatory RNAs in the Control of Motility and Biofilm Formation in *E. coli* and *Salmonella*. *Int J Mol Sci* 14:4560–4579.
14. Hammar M, Arnqvist A, Bian Z, Olsen A, Normark S (1995) Expression of two csg operons is required for production of fibronectin- and congo red-binding curli polymers in *Escherichia coli* K-12. *Mol Microbiol* 18:661–670.
15. Zogaj X, Bokranz W, Nitz M, Romling U (2003) Production of cellulose and curli fimbriae by members of the family Enterobacteriaceae isolated from the human gastrointestinal tract. *Infect Immun* 71:4151–4158.
16. Dudin O, Geiselmann J, Ogasawara H, Ishihama A, Lacour S (2014) Repression of Flagellar Genes in Exponential Phase by CsgD and CpxR, Two Crucial Modulators of *Escherichia coli* Biofilm Formation. *J Bacteriol* 196:707–715.
17. Hammar M, Bian Z, Normark S (1996) Nucleator-dependent intercellular assembly of adhesive curli organelles in *Escherichia coli*. *Proc Natl Acad Sci U S A* 93:6562–6566.
18. Hammer ND, Schmidt JC, Chapman MR (2007) The curli nucleator protein, CsgB, contains an amyloidogenic domain that directs CsgA polymerization. *Proc Natl Acad Sci U S A* 104:12494–12499.

19. Wang X, Smith DR, Jones JW, Chapman MR (2007) In vitro polymerization of a functional *Escherichia coli* amyloid protein. *J Biol Chem* 282:3713–3719.
20. Goyal P, Krasteva PV, Van Gerven N, Gubellini F, Van den Broeck I, Troupiotis-Tsailaki A, Jonckheere W, Pehau-Arnaudet G, Pinkner JS, Chapman MR *et al.* (2014) Structural and mechanistic insights into the bacterial amyloid secretion channel CsgG. *Nature*
21. Loferer H, Hammar M, Normark S (1997) Availability of the fibre subunit CsgA and the nucleator protein CsgB during assembly of fibronectin-binding curli is limited by the intracellular concentration of the novel lipoprotein CsgG. *Mol Microbiol* 26:11–23.
22. Nenninger AA, Robinson LS, Hultgren SJ (2009) Localized and efficient curli nucleation requires the chaperone-like amyloid assembly protein CsgF. *Proc Natl Acad Sci U S A* 106:900–905.
23. Nenninger AA, Robinson LS, Hammer ND, Epstein EA, Badtke MP, Hultgren SJ, Chapman MR (2011) CsgE is a curli secretion specificity factor that prevents amyloid fibre aggregation. *Mol Microbiol* 81:486–499.
24. Andersson EK, Bengtsson C, Evans ML, Chorell E, Sellstedt M, Lindgren AE, Hufnagel DA, Bhattacharya M, Tessier PM, Wittung-Stafshede P *et al.* (2013) Modulation of curli assembly and pellicle biofilm formation by chemical and protein chaperones. *Chem Biol* 20:1245–1254.
25. Gibson DL, White AP, Rajotte CM, Kay WW (2007) AgfC and AgfE facilitate extracellular thin aggregative fimbriae synthesis in *Salmonella enteritidis*. *Microbiology* 153:1131–1140.
26. Salgado PS, Taylor JD, Cota E, Matthews SJ (2011) Extending the usability of the phasing power of diselenide bonds: SeCys SAD phasing of CsgC using a non-auxotrophic strain. *Acta Crystallogr D Biol Crystallogr* 67:8–13.
27. Taylor JD, Zhou Y, Salgado PS, Patwardhan A, McGuffie M, Pape T, Grabe G, Ashman E, Constable SC, Simpson PJ *et al.* (2011) Atomic resolution insights into curli fiber biogenesis. *Structure* 19:1307–1316.
28. Evans ML, Schmidt JC, Ilbert M, Doyle SM, Quan S, Bardwell JC, Jakob U, Wickner S, Chapman MR (2011) *E. coli* chaperones DnaK, Hsp33 and Spy inhibit bacterial functional amyloid assembly. *Prion* 5:323–334.
29. Quan S, Hiniker A, Collet JF, Bardwell JC (2013) Isolation of bacteria envelope proteins. *Methods Mol Biol* 966:359–366.
30. Kaye R, Head E, Thompson JL, McIntire TM, Milton SC, Cotman CW, Glabe CG (2003) Common structure of soluble amyloid oligomers implies common mechanism of pathogenesis. *Science* 300:486–489.
31. Kaye R, Sokolov Y, Edmonds B, McIntire TM, Milton SC, Hall JE, Glabe CG (2004) Permeabilization of lipid bilayers is a common conformation-dependent activity of soluble amyloid oligomers in protein misfolding diseases. *J Biol Chem* 279:46363–46366.
32. Tycko R, Wickner RB (2013) Molecular structures of amyloid and prion fibrils: consensus versus controversy. *Acc Chem Res* 46:1487–1496.
33. Horvath I, Weise CF, Andersson EK, Chorell E, Sellstedt M, Bengtsson C, Olofsson A, Hultgren SJ, Chapman M, Wolf-Watz M *et al.* (2012) Mechanisms of

- protein oligomerization: inhibitor of functional amyloids templates alpha-synuclein fibrillation. *J Am Chem Soc* 134:3439–3444.
34. Zhou Y, Smith D, Leong BJ, Brannstrom K, Almqvist F, Chapman MR (2012) Promiscuous cross-seeding between bacterial amyloids promotes interspecies biofilms. *J Biol Chem* 287:35092–35103.
 35. Wang X, Hammer ND, Chapman MR (2008) The molecular basis of functional bacterial amyloid polymerization and nucleation. *J Biol Chem* 283:21530–21539.
 36. Wang X, Zhou Y, Ren JJ, Hammer ND, Chapman MR (2010) Gatekeeper residues in the major curlin subunit modulate bacterial amyloid fiber biogenesis. *Proc Natl Acad Sci U S A* 107:163–168.
 37. Hammer ND, McGuffie BA, Zhou Y, Badtke MP, Reinke AA, Brannstrom K, Gestwicki JE, Olofsson A, Almqvist F, Chapman MR (2012) The C-terminal repeating units of CsgB direct bacterial functional amyloid nucleation. *J Mol Biol* 422:376–389.
 38. Balch WE, Morimoto RI, Dillin A, Kelly JW (2008) Adapting proteostasis for disease intervention. *Science* 319:916–919.
 39. Lindquist SL, Kelly JW (2011) Chemical and biological approaches for adapting proteostasis to ameliorate protein misfolding and aggregation diseases: progress and prognosis. *Cold Spring Harb Perspect Biol* 3
 40. Ryno LM, Wiseman RL, Kelly JW (2013) Targeting unfolded protein response signaling pathways to ameliorate protein misfolding diseases. *Curr Opin Chem Biol* 17:346–352.
 41. Broadley SA, Hartl FU (2009) The role of molecular chaperones in human misfolding diseases. *FEBS Lett* 583:2647–2653.
 42. Evans CG, Wisen S, Gestwicki JE (2006) Heat shock proteins 70 and 90 inhibit early stages of amyloid beta-(1-42) aggregation in vitro. *J Biol Chem* 281:33182–33191.
 43. Luk KC, Mills IP, Trojanowski JQ, Lee VM (2008) Interactions between Hsp70 and the hydrophobic core of alpha-synuclein inhibit fibril assembly. *Biochemistry* 47:12614–12625.
 44. Pemberton S, Madiona K, Pieri L, Kabani M, Bousset L, Melki R (2011) Hsc70 protein interaction with soluble and fibrillar alpha-synuclein. *J Biol Chem* 286:34690–34699.
 45. Hoshino T, Murao N, Namba T, Takehara M, Adachi H, Katsuno M, Sobue G, Matsushima T, Suzuki T, Mizushima T (2011) Suppression of Alzheimer's disease-related phenotypes by expression of heat shock protein 70 in mice. *J Neurosci* 31:5225–5234.
 46. Fonte V, Kipp DR, Yerg Jr, Merin D, Forrestal M, Wagner E, Roberts CM, Link CD (2008) Suppression of in vivo beta-amyloid peptide toxicity by overexpression of the HSP-16.2 small chaperone protein. *J Biol Chem* 283:784–791.
 47. Hammer ND, Wang X, McGuffie BA, Chapman MR (2008) Amyloids: friend or foe? *J Alzheimers Dis* 13:407–419.
 48. Danese PN, Snyder WB, Cosma CL, Davis LJ, Silhavy TJ (1995) The Cpx two-component signal transduction pathway of *Escherichia coli* regulates transcription of the gene specifying the stress-inducible periplasmic protease, DegP. *Genes Dev* 9:387–398.

49. Raivio TL, Silhavy TJ (2001) Periplasmic stress and ECF sigma factors. *Annu Rev Microbiol* 55:591–624.
50. Quan S, Koldewey P, Tapley T, Kirsch N, Ruane KM, Pfizenmaier J, Shi R, Hofmann S, Foit L, Ren G *et al.* (2011) Genetic selection designed to stabilize proteins uncovers a chaperone called Spy. *Nat Struct Mol Biol* 18:262–269.
51. Raffa RG, Raivio TL (2002) A third envelope stress signal transduction pathway in *Escherichia coli*. *Mol Microbiol* 45:1599–1611.
52. DePas WH, Hufnagel DA, Lee JS, Blanco LP, Bernstein HC, Fisher ST, James GA, Stewart PS, Chapman MR (2013) Iron induces bimodal population development by *Escherichia coli*. *Proc Natl Acad Sci U S A* 110:2629–2634.
53. Serra DO, Richter AM, Klauck G, Mika F, Hengge R (2013) Microanatomy at cellular resolution and spatial order of physiological differentiation in a bacterial biofilm. *MBio* 4:e00103–13.
54. Epstein EA, Reizian MA, Chapman MR (2009) Spatial clustering of the curlin secretion lipoprotein requires curli fiber assembly. *J Bacteriol* 191:608–615.
55. Jubelin G, Vianney A, Beloin C, Ghigo JM, Lazzaroni JC, Lejeune P, Dorel C (2005) CpxR/OmpR interplay regulates curli gene expression in response to osmolarity in *Escherichia coli*. *J Bacteriol* 187:2038–2049.
56. Cegelski L, Pinkner JS, Hammer ND, Cusumano CK, Hung CS, Chorell E, Aberg V, Walker JN, Seed PC, Almqvist F *et al.* (2009) Small-molecule inhibitors target *Escherichia coli* amyloid biogenesis and biofilm formation. *Nat Chem Biol* 5:913–919.
57. Bartels T, Ahlstrom LS, Leftin A, Kamp F, Haass C, Brown MF, Beyer K (2010) The N-terminus of the intrinsically disordered protein alpha-synuclein triggers membrane binding and helix folding. *Biophys J* 99:2116–2124.
58. Giasson BI, Murray IV, Trojanowski JQ, Lee VM (2001) A hydrophobic stretch of 12 amino acid residues in the middle of alpha-synuclein is essential for filament assembly. *J Biol Chem* 276:2380–2386.
59. Murray IV, Giasson BI, Quinn SM, Koppaka V, Axelsen PH, Ischiropoulos H, Trojanowski JQ, Lee VM (2003) Role of alpha-synuclein carboxy-terminus on fibril formation in vitro. *Biochemistry* 42:8530–8540.
60. Serpell LC, Berriman J, Jakes R, Goedert M, Crowther RA (2000) Fiber diffraction of synthetic alpha-synuclein filaments shows amyloid-like cross-beta conformation. *Proc Natl Acad Sci U S A* 97:4897–4902.
61. Ladiwala AR, Bhattacharya M, Perchiacca JM, Cao P, Raleigh DP, Abedini A, Schmidt AM, Varkey J, Langen R, Tessier PM (2012) Rational design of potent domain antibody inhibitors of amyloid fibril assembly. *Proc Natl Acad Sci U S A* 109:19965–19970.
62. Perchiacca JM, Ladiwala AR, Bhattacharya M, Tessier PM (2012) Structure-based design of conformation- and sequence-specific antibodies against amyloid beta. *Proc Natl Acad Sci U S A* 109:84–89.
63. Cascella R, Conti S, Mannini B, Li X, Buxbaum JN, Tiribilli B, Chiti F, Cecchi C (2013) Transthyretin suppresses the toxicity of oligomers formed by misfolded proteins in vitro. *Biochim Biophys Acta* 1832:2302–2314.

64. Baba T, Ara T, Hasegawa M, Takai Y, Okumura Y, Baba M, Datsenko KA, Tomita M, Wanner BL, Mori H (2006) Construction of *Escherichia coli* K-12 in-frame, single-gene knockout mutants: the Keio collection. *Mol Syst Biol* 2:2006.0008.
65. Cherepanov PP, Wackernagel W (1995) Gene disruption in *Escherichia coli*: TcR and KmR cassettes with the option of Flp-catalyzed excision of the antibiotic-resistance determinant. *Gene* 158:9–14.
66. Datsenko KA, Wanner BL (2000) One-step inactivation of chromosomal genes in *Escherichia coli* K-12 using PCR products. *Proc Natl Acad Sci U S A* 97:6640–6645.
67. Griffith KL, Wolf REJ (2002) Measuring beta-galactosidase activity in bacteria: cell growth, permeabilization, and enzyme assays in 96-well arrays. *Biochem Biophys Res Commun* 290:397–402.
68. Casadaban MJ (1976) Transposition and fusion of the lac genes to selected promoters in *Escherichia coli* using bacteriophage lambda and Mu. *J Mol Biol* 104:541–555.
69. Keyer K, Imlay JA (1996) Superoxide accelerates DNA damage by elevating free-iron levels. *Proc Natl Acad Sci U S A* 93:13635–13640.
70. Barnhart MM, Lynem J, Chapman MR (2006) GlcNAc-6P levels modulate the expression of Curli fibers by *Escherichia coli*. *J Bacteriol* 188:5212–5219.

Chapter 4

CsgE is Required for Efficient Translocation of Curli Subunits Across the Outer Membrane⁴

Abstract

Protein localization is essential for protein function. Enteric bacteria, including *Escherichia coli*, assemble curli, functional amyloid fibers on the cell surface that share structural and biochemical properties with disease-associated amyloids. The major curli subunit, CsgA, is secreted across the outer membrane as an unstructured protein. The outer membrane pore protein CsgG mediates secretion with the assistance of the accessory protein CsgE. CsgE is required for CsgA secretion and we have demonstrated that CsgE can inhibit CsgA amyloid assembly *in vitro*. In this chapter I report that CsgE directly interacts with *E. coli* CsgA and the minor curli subunit CsgB. CsgE can arrest actively polymerizing CsgA amyloid formation *in vitro*. Directed mutational analysis revealed several residues in CsgE that are important for proper function *in vivo*. Finally, the metalloprotease YfgC was identified in a mutagenesis screen for mutations that restore Congo red binding to a $\Delta csgE$ mutant. Deletion of *yfgC* in secretion mutants stabilized CsgC protein levels suggesting that CsgC may be a substrate of YfgC. Furthermore, cells deleted for *csgG*, *csgC* and *yfgC* accumulated increased levels of intracellular CsgA. Together, these findings suggest that YfgC may be involved in preventing the accumulation of intracellular amyloid assembly by CsgA.

⁴Portions of this chapter (Figure 4.1ABC, experiments that I conducted) are published in *Chemistry and Biology* (37). Sarah Kang cloned all of the CsgE mutants for the $\Delta csgE$ mutant complementation assays and erythromycin sensitivity assays. Sarah also conducted all the original $\Delta csgE$ complementation experiments (Figure 4.2) and contributed the erythromycin sensitivity data (Figure 4.3). Dr. Matt Badtke and Michael O'Conner conducted the Mariner transposon mutagenesis and first identified YfgC. I contributed the data presented in Figure 4.4.

Introduction

Protein localization is important for proper protein folding and function. There are two secretion mechanisms that facilitate proteins translocation across the inner membrane of Gram-negative bacteria: the Twin Arginine Translocation (Tat) and Sec pathways. The Tat secretion system secretes folded or partially folded substrates (1). On the other hand, the Sec translocation system secretes unfolding polypeptides (2). SecB is a chaperone-like protein that assists in maintaining peptides in an unfolded conformation and delivering them to the SecYEG pore for secretion across the inner membrane (3-6). Additional cytoplasmic proteins and chaperones, including the ribosome-associated protein Trigger Factor (TF) and the heat shock protein DnaK, assist in preventing inappropriate protein folding (6). Secreted proteins from Gram-negative bacteria present an additional protein folding challenge to the cell as these proteins must traverse two biological membranes. There are at least eight unique secretion systems in Gram-negative bacteria for delivering proteins outside the cell (7). One of the most intriguing secretion systems is the Type 8SS, better known as nucleation-precipitation, responsible for the assembly of the functional amyloid curli on the bacterial cell surface. Curli are extracellular fibers produced by *Escherichia coli* and *Salmonella* species that are important for adhesion to inert surfaces, adhesion to host cells during infection, during biofilm formation, and other community behaviors (8-11).

Secretion of the curli subunits presents additional challenges to the cell as curli rapidly assemble into amyloid fibers (12). Amyloid proteins are commonly associated with neurodegenerative disorders such as Alzheimer's, Huntington's, and Parkinson's diseases (13). Unrelated proteins of various size and primary amino acid sequences can assemble into amyloids that share the same biophysical properties (14): amyloids are 4–12 nm wide fibers, have a cross β -sheet structure, are highly resistant to denaturation, and bind amyloid-specific dyes such as Congo red and thioflavin T (ThT) (12, 15). A growing number of "functional" amyloids can be assembled by many cell types to fulfill normal physiological processes, including regulation of melanin synthesis, information transfer, or as structural materials (8, 16, 17).

Curli biogenesis is a highly regulated process and requires the products of two divergently transcribed operons (*csgBAC* and *csgDEFG*) (18). The major subunit

protein of curli is CsgA. CsgA is secreted to the cell surface as an unstructured protein and then templated into amyloid fibers by the minor curli subunit CsgB (19-23). The amyloid core of CsgA consists of five imperfect repeating units (R1–R5). R1 and R5 are highly amyloidogenic, whereas R2, R3, and R4 contain gatekeeper residues that reduce their ability to form amyloids (24-26). The secretion of CsgA and CsgB is dependent on CsgG, which forms an oligomeric pore in the outer membrane (27-29). CsgC is a periplasmic protein that specifically and efficiently inhibits amyloid formation of CsgA (Chapter 3 and (30, 31)). The chaperone-like CsgF assists the CsgB-CsgA interaction and aids the nucleation of CsgA polymerization *in vivo* (32). CsgE interacts with CsgG in a cap-like structure in the periplasm (29). CsgE is a putative chaperone of CsgA that also functions as a specificity factor in the periplasm to facilitate efficient curli subunit secretion (28, 32).

In this chapter, I report that CsgE directly interacts with CsgA and CsgB amyloid fibers and is capable of arresting polymerization of actively elongating fibers. I also report mutants in CsgE that influence CsgE function *in vivo*. Finally, YfgC was identified in a screen for mutation that restore Congo red binding to a Δ *csgE* mutant. YfgC is a periplasmic metalloprotease that may play a role in degrading curli subunits and accessory factors when secretion fails.

Results

CsgE interacts with CsgA to inhibit amyloid assembly in vitro

Molecular chaperones can inhibit CsgA amyloid formation (Chapter 2; (9)). CsgE is a putative periplasmic chaperone and has been shown to prevent CsgA self-assembly into amyloid fibers *in vitro* (Fig 4.1A) (32). To test whether the interaction between CsgE and CsgA fibers could prevent further CsgA fiber elongation, an order of addition experiment was conducted where CsgE was added at different times after the start of CsgA polymerization. CsgA was allowed to polymerize for 1, 2, 7, and 8 hr prior to the addition of CsgE. CsgE arrested CsgA polymerization at every time point tested (Fig 4.1A). These results are consistent with the idea that CsgE prevents fiber elongation, possibly by sequestering soluble CsgA.

Surface Plasmon Resonance (SPR) was then used to test whether CsgE directly

interacts with CsgA amyloid fibers. Purified CsgA was allowed to polymerize for 24 hr. Fibers were then sonicated and immobilized on a GE Sensor-Chip and CsgE was injected over the chip. A rapid increase in resonance units was observed upon addition of CsgE indicating a direct interaction between CsgE and CsgA fibers (Fig. 4.1B black line). Injection of a mock purification of CsgE to control for possible copurified proteins did not result in a large increase in resonance units (Fig 4.1B, gray line). CsgE also interacted with CsgB fibers immobilized on the SPR chip (Fig 4.1C). CsgE did not interact with the control protein BSA (Fig 4.1D). SPR experiments using mature CsgA fibers suggest that not only can CsgE stabilize CsgA monomers but can also interact with CsgA and CsgB fibers that may also inhibit monomer addition to fiber ends and nucleation.

Mutational analysis of CsgE in vivo

CsgE is required for curli biogenesis *in vivo* (12, 32). CsgE interact with CsgG and forms a cap-like structure on the periplasmic side of the CsgG pore (29). A *csgE* mutant can be complemented by expression of *csgE* from a plasmid or overexpression of *csgG* (32). The ability to complement the *csgE* mutant allowed us to investigate the effect of specific mutants on CsgE function *in vivo*. In collaboration with Dr. Christiane Ritter at the Helmholtz Centre for Infection Research in Braunschweig, Germany, and with the help of Sarah Kang, an undergraduate in the Chapman Lab, we have begun to investigate the molecular details of CsgE function.

The Ritter Lab has a preliminary solid-state NMR structure of CsgE (unpublished data) and has identified several residues that, when mutated, increase CsgE stability *in vitro*. We cloned three of the identified mutants (W49S, W52S and F68S) into an expression vector under control of the *csgBAC* promoter. The *csgE* mutant-containing plasmids were transformed into BW25113 Δ *csgE* and assayed for the ability to restore CR binding and CsgA protein levels. Expression of the W49S and W52S mutants fully restored CR binding to WT levels while expression of the F68S mutant only partially restored CR binding (Fig. 4.1A). Although CR binding was restored, WT CsgE protein was undetectable by western blot and complementation with either WT or the W49S mutant did not result in detectable levels of CsgE (Fig. 4.2B). Complementation with the

W52S and F68S mutants resulted in detectable levels of CsgE with the F68S mutant yielding the highest level of expression (Fig. 4.2B). The increased expression, and stability, of the F68S mutant is consistent with observations in the Ritter Lab that the F68S mutant has increase stability *in vitro*. CsgG protein levels remained unchanged when any of the mutants were used to complement the $\Delta csgE$ mutant (Fig. 4.2C). WT levels of CsgA were restored when WT, or the W49S and W52S mutants were used to complement the $\Delta csgE$ mutant (Fig. 4.2C). Consistent with the CR binding results, expression of the F68S mutant resulted in lower levels of CsgA protein by western blot (Fig. 4.2C).

CsgE gates CsgG

The observation that the CsgE F68S mutant was stably expressed but unable to complement the $\Delta csgE$ mutant suggested this variant of CsgE may still be capable of gating the CsgG pore. We therefore used an erythromycin sensitivity assay developed previously for investigating CsgG pore activity (32). Briefly, a complete curli deletion strain was grown in broth culture with empty vector (ev), expressing *csgG* alone or expressing both *csgG* and *csgE* from an IPTG-inducible promoter. After an hour, 30 $\mu\text{g}/\text{mL}$ erythromycin was added to the culture. Cells transformed with empty vector continued to grow whereas cells overexpressing *csgG* arrest growth (Fig. 4.3A-C, compare black squares with open squares) (32). Cells continued to grow in the presence of 30 $\mu\text{g}/\text{mL}$ erythromycin when both *csgG* and WT *csgE* are expressed (Fig. 4.3A-C, black circles). Overexpression of either the W49S or W52S mutant of CsgE did not block erythromycin sensitivity (Fig. 4.3A and B, respectively). On the other hand, overexpression of the F68S mutant of CsgE rescued growth to the same degree as WT CsgE (Fig. 4.3C).

Identification of a protease in the $\Delta csgE$ mutant

The fate of mislocalized CsgA and CsgB in the $\Delta csgE$ mutant is unknown. The curli genes are still expressed in the $\Delta csgE$ mutant (Elisabeth Ashman Epstein, unpublished results) and overexpression of *csgG* in a $\Delta csgE$ mutant restores CsgA secretion and CR binding. Together, these observations suggest that CsgA stability is

dependent on the ability of cells to secrete CsgA outside the cell before periplasmic proteases are able to degrade CsgA. To try to identify periplasmic proteases that may degrade CsgA and CsgB in a $\Delta csgE$ mutant, we conducted a transposon mutagenesis of $\Delta csgE$ and screened for mutants that restored CR binding. A post-doctoral researcher, Dr. Matthew Badtke, and an undergraduate researcher, Michael O'Conner in the Chapman Lab, conducted the initial mutagenesis and screening. The screen yielded *yfgC* (BepA), a metalloprotease involved in maintaining outer membrane integrity (33).

Deletion of *yfgC* in a $\Delta csgE$ mutant partially restored CR binding (Fig. 4.4A). However, increased CR binding relative to the $\Delta csgE$ mutant was not due to restored CsgA protein levels (Fig. 4.4B). To verify that this was not due to loss of a general periplasmic protease, the canonical periplasmic serine protease DegP was deleted. Unlike the $\Delta csgE\Delta yfgC$ mutant, deletion of *degP* in the $\Delta csgE$ mutant did not restore CR binding (Fig. 4.4A). CsgG protein levels were also investigated since YfgC is important for outer membrane protein (OMP) assembly and degradation (33). The absence of *yfgC* also does not influence CsgG protein levels (Fig. 4.4B). YfgC is important for maintaining outer membrane integrity; therefore, the observed rescue of CR binding in the $\Delta csgE\Delta yfgC$ mutant relative to the $\Delta csgE$ mutant may be due to loss of outer membrane integrity and an influx of CR into the periplasmic space.

To better investigate the possibility that CsgA is a substrate of YfgC, *yfgC* was deleted in a mutant background known to accumulate intracellular CsgA, the $\Delta csgG\Delta csgC$ mutant (Chapter 2). There was a very modest increase in CR binding of the $\Delta csgG\Delta csgC\Delta yfgC$ mutant compared to the $\Delta csgG\Delta csgC$ mutant (Fig. 4.4C). There was no apparent difference in CR binding of the $\Delta yfgC$ mutant compared to WT, the $\Delta csgG\Delta yfgC$ mutant compared to $\Delta csgG$ or the $\Delta csgC\Delta yfgC$ mutant compared to $\Delta csgC$ (Fig. 4.4C). However, unlike the $\Delta csgE\Delta yfgC$ mutant, the $\Delta csgG\Delta csgC\Delta yfgC$ mutant accumulated slightly more SDS insoluble CsgA compared to the $\Delta csgG\Delta csgC$ (Fig. 4.4D, lower panel). CsgC levels are reduced in a $\Delta csgG$ mutant (Chapter 3; Fig. 4.4E, lower panel). Interestingly, deletion of *yfgC* in the $\Delta csgG$ mutant restores CsgC back to WT levels suggesting that CsgC may be a substrate of YfgC (Fig. 4.4E, lower panel compare lane 6 to lane 2).

Discussion

Bacterial protein secretion is a controlled event. Most secreted proteins traverse the inner membrane of Gram-negative bacteria via the Sec translocon with SecB playing an important role inhibiting aggregation and directing peptides to the SecYEG inner membrane pore (2). In Gram-negative bacteria there are at least eight secretion systems for transporting proteins outside the cell (7). The curli system possesses a dedicated outer membrane secretion system (sometimes referred to as Type 8 secretion) (7). Secretion of the curli subunits presents additional challenges to the cell since curli rapidly assemble into amyloid fibers (12). Amyloid can be toxic to membranes; therefore, the curli secretion system must be both efficient and specific to avoid inappropriate intracellular amyloid aggregation (34).

The outer membrane curli secretion pore is composed of nine CsgG monomers arranged in a β -barrel imbedded in the membrane with a largely α -helical periplasmic domain. The inner diameter of the CsgG pore is approximately 2 nm wide, accommodating only largely unfolded polypeptides (28, 29, 35, 36). The diameter of the CsgG pore requires that periplasmic factors exist that keep CsgA from folding prior to secretion. CsgE interacts with CsgG and is required for CsgA secretion *in vivo* (12, 32). Expression of CsgE gates CsgG pore activity and client protein specificity *in vivo* (28, 32). CsgE also inhibits CsgA amyloid formation and interacts directly with CsgA and CsgB *in vitro* (Fig. 4.1ABC) (32, 37). I predict that CsgE maintains CsgA in a conformation that is presumably competent for secretion by inhibiting CsgA amyloid assembly (Fig. 4.4A; (32)). It is possible that CsgE plays a similar role during curli subunit secretion to that of SecB during secretion across the inner membrane. Both proteins appear to have dual functions: 1) inhibit protein aggregation and 2) to deliver client proteins to a dedicated secretion apparatus. Our observations support a SecB-like mechanism for CsgE during secretion and also suggest that CsgE can disrupt on-going fiber formation (Fig. 4.1A).

Dr. Christiane Ritter at the Helmholtz Centre for Infection Research has solved a preliminary structure of CsgE and has identified mutations within CsgE that improve CsgE stability *in vitro* (Fig. 4.2A). To gain a better understanding on the molecular details of CsgE function *in vivo* we expressed Dr. Ritter's CsgE mutants *in vivo* and

asked whether they could complement a $\Delta csgE$ mutant. The mutation that was most stabilizing *in vitro*, F68S, was also the mostly stably expressed mutant *in vivo* (Fig. 4.2C). However, the F68S mutant did not complement CR binding or CsgA protein levels when expressed in a $\Delta csgE$ mutant (Fig. 4.2BD). Interestingly, overexpression of the CsgE_{F68S} mutant with CsgG protected cells in the erythromycin sensitivity assay suggesting that the F68S mutant can still gate CsgG pore function (Fig. 4.3C). The two other mutations in CsgE, W49S and W52S, could complement CR binding and CsgA protein levels in a $\Delta csgE$ mutant but were erythromycin sensitive and therefore likely unable to gate CsgG in the erythromycin sensitivity assay (Fig. 4.2BCD and Fig. 4.3AB). Together, these results suggest that the F68 residue of CsgE may be more important for interaction with CsgA while the W49 and W52 residues may be more important for interacting with and gating CsgG.

In the absence of CsgE very little CsgA is secreted *in vivo*. CsgA also does not accumulate within the periplasm of $\Delta csgE$ cells (12, 32). Together with the observation that *csgA* expression is only modestly effected in a $\Delta csgE$ mutant (Elisabeth Ashman Epstein, unpublished results) suggests that CsgA is degraded in the periplasm if it cannot be secreted. A transposon screen for mutations that restored CR binding to a $\Delta csgE$ mutant was conducted to try to identify periplasmic proteases that may degrade CsgA. One protease that was identified was YfgC (Fig. 4.4A). YfgC is a periplasmic metalloprotease that plays a role in outer membrane β -barrel protein folding and insertion (33). *yfgC* is regulated by the Sigma^E alternative sigma factor and deletion of *yfgC* in a $\Delta surA$ or $\Delta degP$ backgrounds is lethal under some conditions (38, 39). SurA assists in folding and inserting a several outer membrane β -barrel proteins (35). If SurA and YfgC are functionally redundant then would not be unexpected to observe that the double deletion is a synthetic lethal mutant. The $\Delta surA$ mutant has decreased CR binding and decreased CsgG protein levels (Daniel Smith, unpublished data). The crystal structure of CsgG revealed the protein to be a β -barrel outer membrane protein (29). It is likely that CsgG is a client of SurA. CsgG levels are unchanged in a $\Delta yfgC$ mutant (Fig. 4.4BD).

The $\Delta yfgC \Delta degP$ mutant was also synthetic lethal at 37°C on SDS/EDTA suggesting a severe defect in outer membrane integrity (39). Interestingly, while loss of

yfgC in the $\Delta csgE$ mutant restored some CR binding, CsgA protein levels were not restored (Fig. 4.4AB). The restored CR binding when *yfgC* was deleted may have been due to CR leaking across the compromised outer membrane.

Finally, we asked whether YfgC could act on CsgA when CsgA was forced to accumulate in the periplasm. To do this *yfgC* was deleted from a $\Delta csgG\Delta csgC$ mutant that accumulates SDS-insoluble intracellular CsgA (Fig. 3.5). Deletion of *yfgC* in the $\Delta csgG\Delta csgC$ mutant slightly increased CR binding and CsgA protein levels (Fig. 4.4CD). The only modest increase in CsgA protein levels may be accounted for by the approximately 2-3-fold feedback repression of the *csgBAC* operon when *csgG* is deleted (Appendix A). Together, these results suggest that a small pool of CsgA may be degraded by YfgC in the periplasm. What is more interesting is the effect the *yfgC* deletion has on CsgC. CsgC protein levels are reduced in a $\Delta csgG$ mutant likely due to feedback repression of the *csgBAC* promoter (Appendix A). Deletion of *yfgC* in the $\Delta csgG$ mutant restored CsgC back to WT levels (Fig. 4.4E). YfgC has only been reported to degrade outer membrane β -barrel proteins (33). These findings suggest that CsgC, while not an outer membrane β -barrel protein, may also be a substrate of YfgC. Together, the data presented here represent the first molecular dissection of the multiple functions of CsgE and new insights into periplasmic proteostasis during curli biogenesis.

Materials and Methods

Bacterial Strains and Plasmids. BW25113 $\Delta dsbA$ (*dsbA::kan*) and $\Delta dsbB$ (*dsbB::kan*) obtained from the Keio collection (40). Additional mutations in BW25113 were constructed using lambda red recombination as described previously (41).

Soluble CsgA Purification. C-terminal His₆-tagged CsgA (12) was, with some modifications, purified as previously described (42). Briefly, NEB3016 *slyD::kan* pET11d-sec-csgA-6xhis cells were grown to OD₆₀₀ 0.9, induced with IPTG, and incubated at 37C for 1 hr. Cells were pelleted by centrifugation and stored at -80C. Cells were lysed by incubation with stirring in an 8 M guanidine hydrochloride, 50 mM potassium phosphate solution pH 7.3 for 24 hr at 4C. The insoluble portion of the lysate was removed by centrifugation and the remaining supernatant was incubated with

NiNTA resin (Sigma-Aldrich) for 1 hr at room temperature. The nickel affinity beads were washed with 50 mM potassium phosphate pH 7.3 and a 12.5 mM imidazole, 50 mM potassium phosphate solution. His₆-tagged CsgA was eluted with a 125 mM imidazole, 50 mM potassium phosphate solution. Protein concentration was determined by the BCA assay (Thermo Scientific).

CsgE Purification. CsgE-His was, with some modifications, expressed and purified as previously described (32). Briefly, CsgE-His was expressed from pNH27 (gene encoding cytoplasmic CsgE inserted into the NcoI-BamHI sites of pET11d) in strain NEB 3016 with 100 mg/ml ampicillin. Cells were grown to OD₆₀₀ 0.9 and induced for 1 hr with IPTG. Cells were pelleted by centrifugation and resuspended in lysis buffer. Cells were lysed using a French press and after centrifugation the supernatant was incubated with NiNTA resin (Sigma- Aldrich) at 4°C overnight. The nickel affinity beads were washed with lysis buffer, followed by a 12.5 mM Imidazole, 50 mM potassium phosphate solution pH 7.3. His-tagged CsgE was eluted with a 250 mM Imidazole, 50 mM potassium phosphate solution pH 7.3. The protein buffer was exchanged to 50 mM potassium phosphate, 200 mM sodium chloride pH 7.3 with 1 mM PMSF on a Zeba Desalt Spin Column (Thermo Scientific).

***In Vitro* CsgA Polymerization Inhibition.** Equimolar concentrations of CsgE and CsgA or equal volumes of compound and CsgA were mixed in a 96-well black plate (Corning). Control experiments were performed with 0.5% DMSO. Thioflavin T was added to a final concentration of 20 mM and fluorescence was measured at 480 nm (excitation 440 nm) for 18 hr at 20°C with agitation every 15 min on a Tecan Infinite 200i to monitor amyloid formation.

Surface Plasmon Resonance. Interaction studies between CsgA amyloid fibers and CsgE were conducted as previously described with some modification (43). 40 µL of 1 mM CsgE or an equivalent volume of a mock purification (NEB3013 with pET11d) was injected over the sensor chip at 20 mL/min. The injection was stopped at 120 s, and the flow of 50 mM potassium phosphate, 200 mM sodium chloride buffer was resumed. The response was recorded in resonance units.

Bacterial Growth. All overnight cultures were grown in LB at 37°C with shaking at 220rpm. Cultures were normalized to OD₆₀₀=1.0, 4 µL were spotted YESCA agar (yeast

extract casamino acids) plates and grown for 48 hours at 26°C to induce curli production. For Congo red analysis YESCA plates were supplemented with 50 µg/mL Congo red and 1 µg/mL Brilliant Blue G250. When necessary, plates were supplemented with ampicillin or kanamycin at 5 µg/mL.

Western Blot Analysis. Overnight cultures were diluted to $OD_{600}=1.0$ and 4 µL were spotted on a YESCA plate and incubated at 26°C for 2 days. The cells were harvested and resuspended in 50 mM KPi pH 7.3. 0.1 $OD_{600\text{ nm}}$ units for each strain were harvested in duplicate by centrifugation. One duplicate was resuspended in 2X SDS loading buffer while the other was treated with HFIP for 10 min at room temperature, dried in a SpeedVac and then resuspended in 2X SDS loading buffer. Samples were run on a 15% SDS PAGE gel and transferred to a PVDF membrane. Blots were probed with antibodies against CsgA (1:12,000), CsgG (1:50,000), CsgC (1:4,000) or YfgC (1:5000; the YfgC antibody was a generous gift from Dr. Jean Francoise Collet).

Erythromycin Sensitivity. An *E. coli* MC4100 complete curli deletion strain was transformed either with empty vector, pMC1 (expressing *csgG* only), pLR12 (expressing *csgG* and WT *csgE*), pSK1, pSK2 or pSK3 (expressing *csgG* and *csgE* W49S, W52S or F68S, respectively). Overnight cultures were diluted in duplicate 1:100 in LB supplemented with ampicillin and grown shaking for 30 min at 37°C in Klett flasks. IPTG was added to the cultures to a final concentration of 0.5mM and cultures were incubated again for 30 min at 37°C. Erythromycin was added to one of each duplicate to a concentration of 30 µg/mL, cultures were returned to the shaking incubator and grown at 37°C. Optical density was measured at t=0h and every 30 min during growth using a Klett Calorimeter.

Mariner Transposon Mutagenesis. Overnight cultures of *E. coli* BW1951 transformed with pFD1 (described previously (44)) and MC4100 Δ *csgE* (Strep^R) were mixed, rinsed once with YESCA media and grown for 2.5 hours at 37°C on a cellulose filter disc on a YESCA plate. The cells were then rinsed from the filter disc with 10 mL YESCA supplemented with streptomycin and IPTG and incubated for another 5 hours at 37°C to select again the donor strain and induce expression of the mariner transposase. Cells were pelleted and resuspended in 10mL YESCA supplemented with streptomycin and kanamycin and incubated for 1 hr at 37°C. Mutants were selected for on YESCA kan

plates and screened for CR binding at 26°C after 48 hr of growth. The location of the transposon in candidates with restored CR binding was determined with random-primer sequencing using primers 5'-GGCCACGCGTGCACTAGTACNNNNNNNNNTACNG-3' and 5'-ATCCATTTAATACTAGCGACGC-3' for the first round of PCR and primers 5'-GGCCACGCGTGCACTAGTAC-3' and 5'-GCCATCTATGTGTCAGACCGG-3' for the second round of PCR. Candidates that yielded a PCR product were sent for sequencing using primer 5'-GCCATCTATGTGTCAGACCGG-3'.

Figures and Tables

Figure 4.1. CsgE interacts with CsgA and CsgB. A) CsgE added to freshly purified CsgA or CsgA incubated for 1 hr inhibits CsgA polymerization. CsgE added to CsgA incubated for 7 hr or 8 hr efficiently inhibits further polymerization. B-D) Surface plasmon resonance sensograms of 1 mM purified CsgE (solid line) or a mock purification (dotted line) were injected over immobilized sonicated CsgA fibers (B), CsgB fibers (C) or BSA control (D) on a CM5 sensor chip. Flow of phosphate buffer was resumed after 120 s.

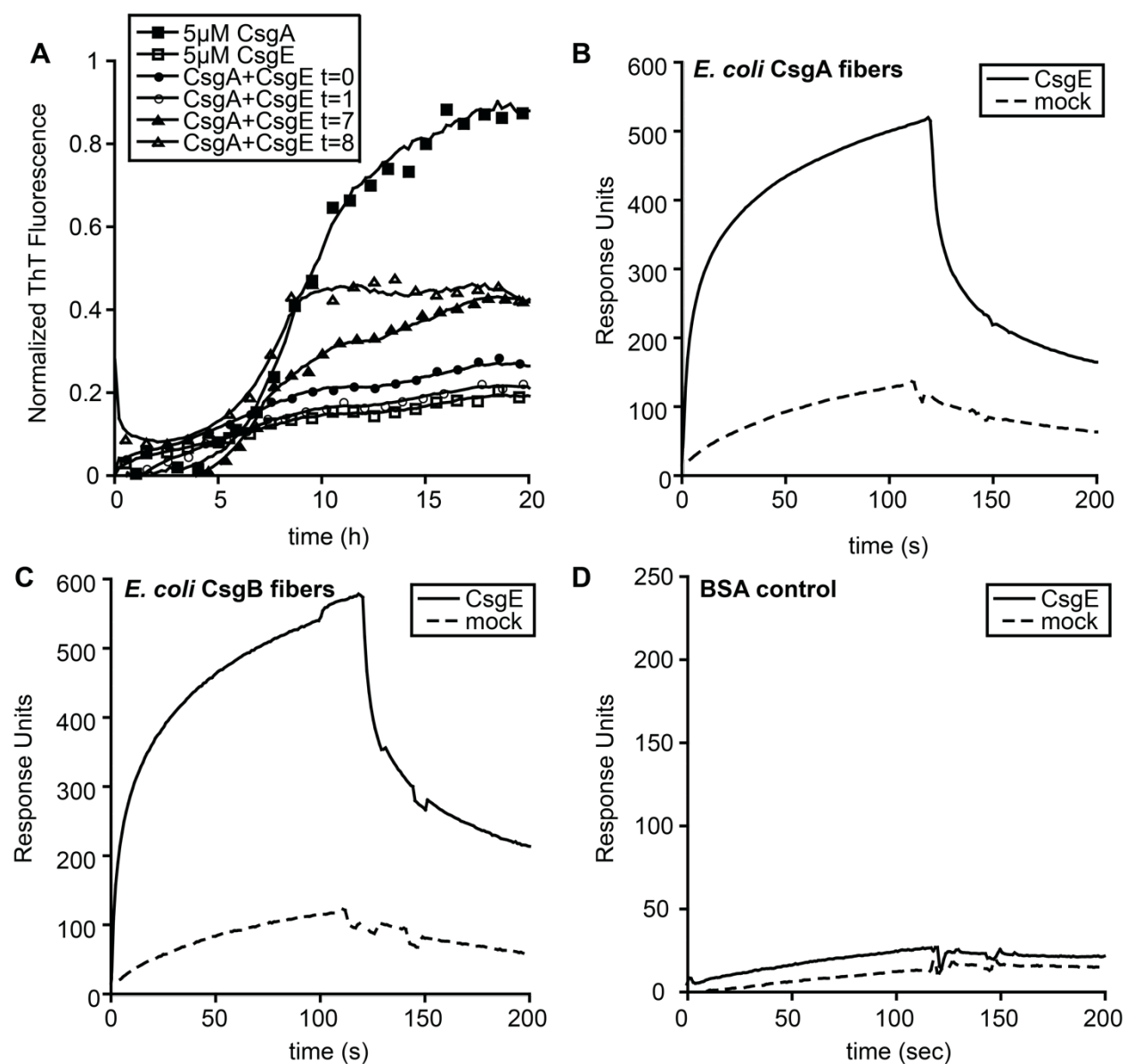


Figure 4.2. *csgE* mutants exhibit different curli biogenesis phenotypes *in vivo*. A) CR binding of $\Delta csgE$ complemented with WT or mutant versions of CsgE. B) Western blot analysis of CsgE levels in a $\Delta csgE$ mutant complemented with WT or mutant versions of CsgE. C) Western blot analysis of CsgG and CsgA levels in a $\Delta csgE$ mutant complemented with WT or mutant versions of CsgE.

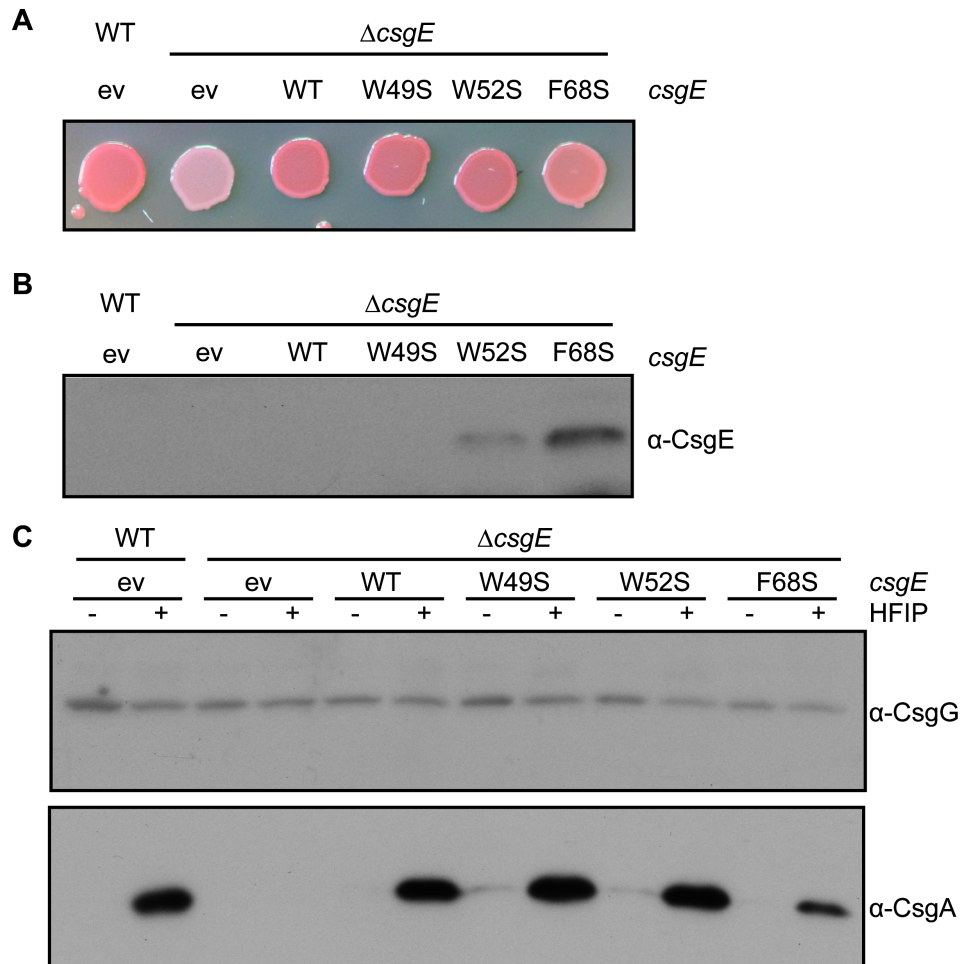


Figure 4.3. *csgE* mutants exhibit differential CsgG gating phenotypes *in vivo*. *E. coli* cells with empty vector (ev), overexpressing *csgG* alone (CsgG), *csgG* and WT *csgE* (CsgG+CsgE_{WT}) or *csgG* and the indicated *csgE* mutants. Expression was induced by the addition of IPTG at 0.5h and erythromycin was added at 1 h.

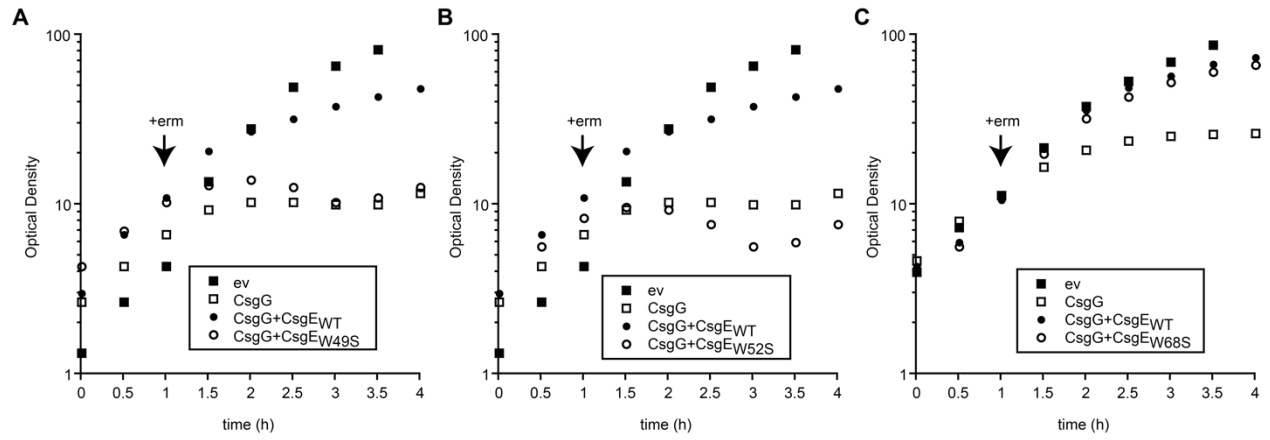


Figure 4.4. Analysis of *yfgC* function *in vivo*. A) CR binding of *E. coli* BW25113 showing partially restored CR binding of $\Delta csgE\Delta yfgC$ compared to $\Delta csgE$. B) Western blot analysis of CsgG and CsgA. C) CR binding of *E. coli* BW25113 and western blot analysis of CsgG, CsgA (D), YfgC and CsgC (E).

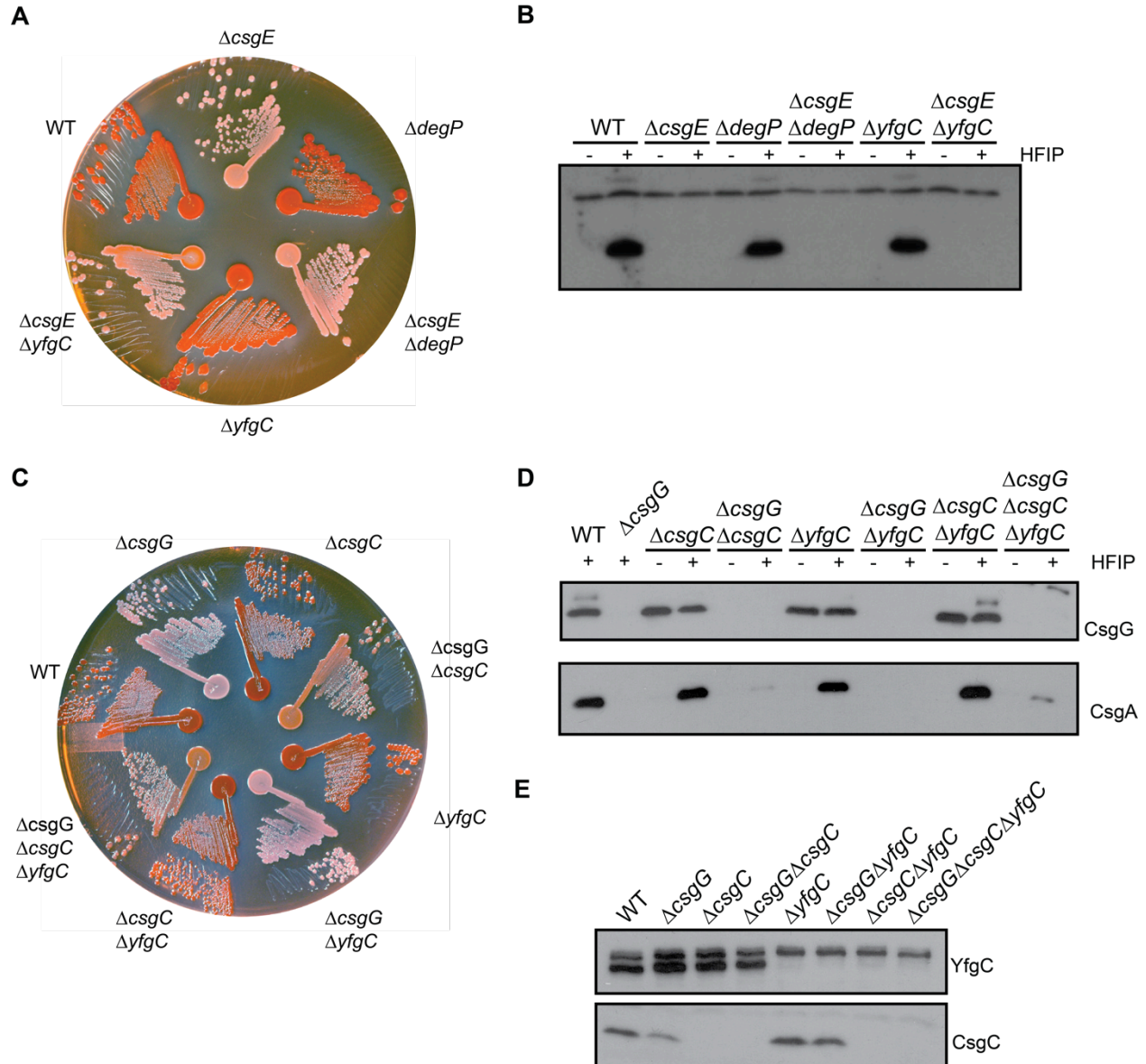


Table 4.1 Strains used in Chapter 4

Strains	Relevant Genotype	References
NEB3016	MiniF <i>lacI^q</i> (Cam ^R) / <i>fhuA2 lacZ::T7 gene1 [lon] ompT gal sulA11 R(mcr-73::miniTn10--Tet^S)2 [dcm] R(zgb-210::Tn10--Tet^S) endA1 Δ(mcrC-mrr)114::IS10</i>	New England Biolabs
BW25113	F ⁻ Δ(<i>araD-araB</i>)567, Δ <i>lacZ</i> 4787(::rrnB-3), λ ⁻ , <i>rph-1</i> , Δ(<i>rhaD-rhaB</i>)568, <i>hsdR514</i>	(41)
Δ <i>csgC</i>	BW25113 <i>csgC::kan</i>	(40)
Δ <i>csgE</i>	BW25113 <i>csgE::kan</i>	(40)
Δ <i>csgG</i>	BW25113 Δ <i>csgG</i>	Chapter 3
Δ <i>csgG</i> Δ <i>csgC</i>	BW25113 Δ <i>csgG csgC::kan</i>	Chapter 3
Δ <i>degP</i>	BW25113 <i>degP::kan</i>	(40)
Δ <i>yfgC</i>	BW25113 <i>yfgC::kan</i>	(40)
Δ <i>csgE</i> Δ <i>degP</i>	BW25113 Δ <i>csgE degP::cm</i>	This work
Δ <i>csgE</i> Δ <i>yfgC</i>	BW25113 Δ <i>csgE yfgC::cm</i>	This work
Δ <i>csgG</i> Δ <i>yfgC</i>	BW25113 Δ <i>csgG yfgC::cm</i>	This work
Δ <i>csgC</i> Δ <i>yfgC</i>	BW25113 Δ <i>csgC yfgC::cm</i>	This work
Δ <i>csgG</i> Δ <i>csgC</i> Δ <i>yfgC</i>	BW25113 Δ <i>csgGΔcsgC yfgC::cm</i>	This work
C600	F ⁻ <i>tonA21 thi-1 thr-1 leuB6 lacY1 glnV44 rfbC1 fhuA1 λ⁻</i>	(45)

Table 4.2 Plasmids used in Chapter 4

Plasmids	Relevant Characteristics	References
pTrc99A	IPTG inducible expression vector	Pharmacia Biotech
pNH11	C-terminal His ₆ tagged <i>E. coli csgA</i> cloned into NcoI/BamHI site in pET11d	(22)
pNH27	C-terminal His ₆ tagged <i>E. coli csgA</i> cloned into NcoI/BamHI site in pET11d	(32)
pLR1	The <i>csgBAC</i> promoter cloned into BamHI/PstI site in pACYC177	(28)
pLR70	WT <i>csgE</i> cloned into pLR1	(32)
pSK1	W49S <i>csgE</i> mutant cloned into pLR1	This work
pSK2	W52S <i>csgE</i> mutant cloned into pLR1	This work
pSK3	F68S <i>csgE</i> mutant cloned into pLR1	This work
pLR12	<i>csgG</i> and <i>csgE</i> cloned into pTrc99A	This work
pSK4	WT <i>csgE</i> replaced with W49S <i>csgE</i> mutant in pLR12	This work
pSK5	WT <i>csgE</i> replaced with W52S <i>csgE</i> mutant in pLR12	This work
pSK6	WT <i>csgE</i> replaced with F68S <i>csgE</i> mutant in pLR12	This work
pKD3	Cm resistance flanked by FRT sites	(41)

Table 4.3 Primers used in Chapter 4

Primer	Primer sequence	Constructs
csgE F Kpn-RBS-Nco	5'-GTTTGGTACCACACAGGAAACAGACC	pSK1, pSK2, pSK3
csgE R 3xS-Pst	5'-GTTTCTGCAGTTATTAGATCCTTAGAA	pSK1, pSK2, pSK3
csgE_W49S_f	5'-GGCCCAGTGCACGAAGCGGAAGCTG	pSK1, pSK4
csgE_W49S_r	5'-CGTTATAGTGATCCAGCTTCCGCTTC	pSK1, pSK4
csgE_W52S_f	5'-CCAGTGCACGATGGGGAAGCAGCAT	pSK2, pSK5
csgE_W52S_r	5'-GATTGACCGTTATAGTGATGCTGCTT	pSK2, pSK5
csgE_F68S_f	5'-GGACGTTATTTTCCAGACTTTTTTAAG	pSK3, pSK6
csgE_F68S_r	5'-CTCGAAGTCTCTTTTCAACGGGCTTA	pSK3, pSK6
DegPH1P1	5'-GAAGAACACAGCAATTTTGC GTTATCTGTTAAT CGAGACTGAAATACATG	$\Delta degP$
DegPH2P2	5'-TCCCGTTTTTCAGGAAGGGGTTGAGGGAGATTA CTGCATTAACAGGTAGAT	$\Delta degP$
YfgCH1P1	5'-CACAGTATCGGTCAAATGACTATCTCCAGAAA TACAGGATAGAGGTTATG	$\Delta yfgC$
YfgCH2P2	5'-TTTGGTCATTGTTCTTCCTTTAATGCGAATTAC ATCTTGGTATAAGGCTT	$\Delta yfgC$
degP fwd	5'-ATT ATA TCA GCG GTA	$\Delta degP$
degP rev	5'-CCA CGA TAT CCT GCG	$\Delta degP$
yfgC fwd	5'-TGA ACC TCA AGA GCG	$\Delta yfgC$
yfgC rev	5'-CAA TTC ACG GGC GCT	$\Delta yfgC$

References

1. Sargent F (2007) The twin-arginine transport system: moving folded proteins across membranes. *Biochem Soc Trans* 35:835–847.
2. Driessen AJ, Nouwen N (2008) Protein translocation across the bacterial cytoplasmic membrane. *Annu Rev Biochem* 77:643–667.
3. Collier DN, Bankaitis VA, Weiss JB, Bassford PJJ (1988) The antifolding activity of SecB promotes the export of the *E. coli* maltose-binding protein. *Cell* 53:273–283.
4. Hartl FU, Lecker S, Schiebel E, Hendrick JP, Wickner W (1990) The binding cascade of SecB to SecA to SecY/E mediates preprotein targeting to the *E. coli* plasma membrane. *Cell* 63:269–279.
5. Fekkes P, de Wit JG, van der Wolk JP, Kimsey HH, Kumamoto CA, Driessen AJ (1998) Preprotein transfer to the *Escherichia coli* translocase requires the co-operative binding of SecB and the signal sequence to SecA. *Mol Microbiol* 29:1179–1190.
6. Ullers RS, Luirink J, Harms N, Schwager F, Georgopoulos C, Genevaux P (2004) SecB is a bona fide generalized chaperone in *Escherichia coli*. *Proc Natl Acad Sci U S A* 101:7583–7588.
7. Desvaux M, Hebraud M, Talon R, Henderson IR (2009) Secretion and subcellular localizations of bacterial proteins: a semantic awareness issue. *Trends Microbiol* 17:139–145.
8. Blanco LP, Evans ML, Smith DR, Badtke MP, Chapman MR (2012) Diversity, biogenesis and function of microbial amyloids. *Trends Microbiol* 20:66–73.
9. Evans ML, Schmidt JC, Ilbert M, Doyle SM, Quan S, Bardwell JC, Jakob U, Wickner S, Chapman MR (2011) *E. coli* chaperones DnaK, Hsp33 and Spy inhibit bacterial functional amyloid assembly. *Prion* 5:323–334.
10. DePas WH, Syed AK, Sifuentes M, Lee JS, Warshaw D, Saggari V, Csankovszki G, Boles BR, Chapman MR (2014) Biofilm formation protects *Escherichia coli* against killing by *Caenorhabditis elegans* and *Myxococcus xanthus*. *Appl Environ Microbiol* 80:7079–7087.
11. Hufnagel DA, Tukul C, Chapman MR (2013) Disease to dirt: the biology of microbial amyloids. *PLoS Pathog* 9:e1003740.
12. Chapman MR, Robinson LS, Pinkner JS, Roth R, Heuser J, Hammar M, Normark S, Hultgren SJ (2002) Role of *Escherichia coli* curli operons in directing amyloid fiber formation. *Science* 295:851–855.
13. Chiti F, Dobson CM (2006) Protein misfolding, functional amyloid, and human disease. *Annu Rev Biochem* 75:333–366.
14. Goldschmidt L, Teng PK, Riek R, Eisenberg D (2010) Identifying the amyloids, proteins capable of forming amyloid-like fibrils. *Proc Natl Acad Sci U S A* 107:3487–3492.
15. Ban T, Hamada D, Hasegawa K, Naiki H, Goto Y (2003) Direct observation of amyloid fibril growth monitored by thioflavin T fluorescence. *J Biol Chem* 278:16462–16465.
16. Fowler DM, Koulov AV, Alory-Jost C, Marks MS, Balch WE, Kelly JW (2006) Functional amyloid formation within mammalian tissue. *PLoS Biol* 4:e6.
17. Hammer ND, Wang X, McGuffie BA, Chapman MR (2008) Amyloids: friend or foe? *J Alzheimers Dis* 13:407–419.

18. Hammar M, Arnqvist A, Bian Z, Olsen A, Normark S (1995) Expression of two csg operons is required for production of fibronectin- and congo red-binding curli polymers in *Escherichia coli* K-12. *Mol Microbiol* 18:661–670.
19. Bian Z, Normark S (1997) Nucleator function of CsgB for the assembly of adhesive surface organelles in *Escherichia coli*. *EMBO J* 16:5827–5836.
20. Hammar M, Bian Z, Normark S (1996) Nucleator-dependent intercellular assembly of adhesive curli organelles in *Escherichia coli*. *Proc Natl Acad Sci U S A* 93:6562–6566.
21. Hammer ND, Schmidt JC, Chapman MR (2007) The curli nucleator protein, CsgB, contains an amyloidogenic domain that directs CsgA polymerization. *Proc Natl Acad Sci U S A* 104:12494–12499.
22. Hammer ND, McGuffie BA, Zhou Y, Badtke MP, Reinke AA, Brannstrom K, Gestwicki JE, Olofsson A, Almqvist F, Chapman MR (2012) The C-terminal repeating units of CsgB direct bacterial functional amyloid nucleation. *J Mol Biol* 422:376–389.
23. Wang X, Hammer ND, Chapman MR (2008) The molecular basis of functional bacterial amyloid polymerization and nucleation. *J Biol Chem* 283:21530–21539.
24. Shewmaker F, McGlinchey RP, Thurber KR, McPhie P, Dyda F, Tycko R, Wickner RB (2009) The functional curli amyloid is not based on in-register parallel beta-sheet structure. *J Biol Chem* 284:25065–25076.
25. Wang X, Smith DR, Jones JW, Chapman MR (2007) In vitro polymerization of a functional *Escherichia coli* amyloid protein. *J Biol Chem* 282:3713–3719.
26. Wang X, Zhou Y, Ren JJ, Hammer ND, Chapman MR (2010) Gatekeeper residues in the major curlin subunit modulate bacterial amyloid fiber biogenesis. *Proc Natl Acad Sci U S A* 107:163–168.
27. Loferer H, Hammar M, Normark S (1997) Availability of the fibre subunit CsgA and the nucleator protein CsgB during assembly of fibronectin-binding curli is limited by the intracellular concentration of the novel lipoprotein CsgG. *Mol Microbiol* 26:11–23.
28. Robinson LS, Ashman EM, Hultgren SJ, Chapman MR (2006) Secretion of curli fibre subunits is mediated by the outer membrane-localized CsgG protein. *Mol Microbiol* 59:870–881.
29. Goyal P, Krasteva PV, Van Gerven N, Gubellini F, Van den Broeck I, Trounopoulos Tsailaki A, Jonckheere W, Pehau-Arnaudet G, Pinkner JS, Chapman MR *et al.* (2014) Structural and mechanistic insights into the bacterial amyloid secretion channel CsgG. *Nature*
30. Gibson DL, White AP, Rajotte CM, Kay WW (2007) AgfC and AgfE facilitate extracellular thin aggregative fimbriae synthesis in *Salmonella enteritidis*. *Microbiology* 153:1131–1140.
31. Taylor JD, Zhou Y, Salgado PS, Patwardhan A, McGuffie M, Pape T, Grabe G, Ashman E, Constable SC, Simpson PJ *et al.* (2011) Atomic resolution insights into curli fiber biogenesis. *Structure* 19:1307–1316.
32. Nenninger AA, Robinson LS, Hammer ND, Epstein EA, Badtke MP, Hultgren SJ, Chapman MR (2011) CsgE is a curli secretion specificity factor that prevents amyloid fibre aggregation. *Mol Microbiol* 81:486–499.

33. Narita S, Masui C, Suzuki T, Dohmae N, Akiyama Y (2013) Protease homolog BepA (YfgC) promotes assembly and degradation of beta-barrel membrane proteins in *Escherichia coli*. *Proc Natl Acad Sci U S A* 110:E3612–21.
34. Kaye R, Sokolov Y, Edmonds B, McIntire TM, Milton SC, Hall JE, Glabe CG (2004) Permeabilization of lipid bilayers is a common conformation-dependent activity of soluble amyloid oligomers in protein misfolding diseases. *J Biol Chem* 279:46363–46366.
35. Vertommen D, Ruiz N, Leverrier P, Silhavy TJ, Collet JF (2009) Characterization of the role of the *Escherichia coli* periplasmic chaperone SurA using differential proteomics. *Proteomics* 9:2432–2443.
36. Cao B, Zhao Y, Kou Y, Ni D, Zhang XC, Huang Y (2014) Structure of the nonameric bacterial amyloid secretion channel. *Proc Natl Acad Sci U S A*
37. Andersson EK, Bengtsson C, Evans ML, Chorell E, Sellstedt M, Lindgren AE, Hufnagel DA, Bhattacharya M, Tessier PM, Wittung-Stafshede P *et al.* (2013) Modulation of curli assembly and pellicle biofilm formation by chemical and protein chaperones. *Chem Biol* 20:1245–1254.
38. Rhodius VA, Suh WC, Nonaka G, West J, Gross CA (2006) Conserved and variable functions of the sigmaE stress response in related genomes. *PLoS Biol* 4:e2.
39. Weski J, Ehrmann M (2012) Genetic analysis of 15 protein folding factors and proteases of the *Escherichia coli* cell envelope. *J Bacteriol* 194:3225–3233.
40. Baba T, Ara T, Hasegawa M, Takai Y, Okumura Y, Baba M, Datsenko KA, Tomita M, Wanner BL, Mori H (2006) Construction of *Escherichia coli* K-12 in-frame, single-gene knockout mutants: the Keio collection. *Mol Syst Biol* 2:2006.0008.
41. Datsenko KA, Wanner BL (2000) One-step inactivation of chromosomal genes in *Escherichia coli* K-12 using PCR products. *Proc Natl Acad Sci U S A* 97:6640–6645.
42. Cegelski L, Pinkner JS, Hammer ND, Cusumano CK, Hung CS, Chorell E, Aberg V, Walker JN, Seed PC, Almqvist F *et al.* (2009) Small-molecule inhibitors target *Escherichia coli* amyloid biogenesis and biofilm formation. *Nat Chem Biol* 5:913–919.
43. Zhou Y, Smith D, Leong BJ, Brannstrom K, Almqvist F, Chapman MR (2012) Promiscuous cross-seeding between bacterial amyloids promotes interspecies biofilms. *J Biol Chem* 287:35092–35103.
44. Rubin EJ, Akerley BJ, Novik VN, Lampe DJ, Husson RN, Mekalanos JJ (1999) In vivo transposition of mariner-based elements in enteric bacteria and mycobacteria. *Proc Natl Acad Sci U S A* 96:1645–1650.
45. Appleyard RK (1954) Segregation of New Lysogenic Types during Growth of a Doubly Lysogenic Strain Derived from *Escherichia coli* K12. *Genetics* 39:440–452.

Chapter 5

Discussion and Future Directions

The classification of curli as an amyloid transformed the amyloid field by introducing a new class of what are now referred to as functional amyloids. Functional amyloids have now been discovered in all areas of life. The diversity of the functions performed by amyloids is staggering (1-3). Curli, and several other bacterial functional amyloids, serve as adhesive and structural components during biofilm formation (4-6). In mammalian cells, amyloid assembly by Pmel17 and peptide hormones serve as storage granules and are cytoprotective (7, 8). The translation termination factor Sup35 in *Saccharomyces cerevisiae* assembles into an amyloid and mediates epigenetic inheritance (9). Molecular chaperones are important modulators of amyloid formation and disaggregation of Sup35 amyloid aggregates (10, 11). In most cases, little is known about how inappropriate amyloid assembly is avoided. In this dissertation, I have demonstrated that controlled and directed secretion of curli subunits involves a multitude of factors, including general and dedicated molecular chaperones, amyloid inhibitors, secretion proteins, stress response induction and feedback repression of the curli genes. Together, these systems ensure proper localization and assembly of curli amyloid fibers.

Curli Biogenesis

Curli gene expression is subject to an extensive degree of transcriptional and post-transcriptional regulation (12). The curli operons, *csgBAC* and *csgDEFG*, encode the amyloid fiber subunits and the dedicated secretion and accessory factors required for assembly (13). At least 300 other genes are involved in curli biogenesis further supporting the claim that the curli system is one of the most extensively and precisely controlled systems in *E. coli* [(12) and Daniel Smith, unpublished findings]. CsgD is a major biofilm regulatory protein that positively regulates expression of the *csgBAC*

operon encoding the major and minor curli fiber subunits CsgA and CsgB, respectively (13). A third gene, *csgC*, is located downstream of *csgA* and encodes a potent and selective amyloid inhibitor (Chapter 3) (13-15). The *csgE*, *csgF* and *csgG* genes encode the necessary proteins required for curli secretion. With the exception of CsgD, the the curli proteins are secreted across the innermembrane via the Sec translocon.

The accessory periplasmic protein CsgE interact with both CsgA and CsgG and is required for CsgA secretion *in vivo* (4, 16, 17). CsgE also possesses chaperone-like activity and can inhibit the assembly of CsgA into an amyloid *in vitro* (Chapter 4) (17, 18). CsgF is an accessory protein that interacts with CsgG on the cell surface (19). CsgG assembles into a nonameric pore in the outer membrane and is required for secretion of CsgA and CsgB (16, 20, 21). The inner diameter of the CsgG pore is only 2 nm accommodating largely unfolding CsgA client proteins (14, 16). Once outside the cell the minor subunit, CsgB interacts with CsgF and assembles into a templating surface that nucleates the polymerization of CsgA into an amyloid on the cells surface (19, 22-24). CsgA can assemble into an amyloid in the absence of CsgB *in vitro*; however, CsgB is required for CsgA polymerization and surface localization *in vivo* (23, 25).

Reports that CsgA is secreted in a soluble, non-amyloid conformation across the outer membrane and yet CsgA does not accumulate within the cell when secretion is disrupted guided the major questions asked of my dissertation (14, 20). Namely, how bacterial cells ensure that CsgA only assembles into amyloid fibers on the cell surface? During secretion, the major amyloid fiber subunit CsgA and the minor templating subunits CsgB may encounter general chaperones and anti-aggregation factors. The ability of general aggregation inhibitors from both the cytoplasm and the periplasm to act on CsgA *in vitro* was therefore investigated in Chapter 2 of this dissertation. A second question that remained in the curli field prior to this dissertation was whether *E. coli* possesses dedicated and specific inhibitors of CsgA amyloid formation. A combined genetic and biochemical approach was used in Chapter 3 to identify the highly efficient and specific curli amyloid inhibitor CsgC. Finally, further investigations into the function and molecular details of CsgE-directed secretion of CsgA were conducted in Chapter 4. Together, the work presented in this dissertation has revealed important amyloid

inhibitory mechanisms in the *E. coli* curli biogenesis system and identified CsgC a new and unique inhibitor of amyloid formation.

General Protein Folding Factors Inhibit CsgA Amyloid Formation

Molecular chaperones are important for cellular proteostasis for several reasons. First, chaperones assist folding of newly synthesized polypeptides into their correct, functional conformation. In the event that a protein unfolds or misfolds chaperones redirect proteins back towards their native conformation and inhibit inappropriate intra- and intermolecular interactions that might lead to protein aggregation and potentially cytotoxic effects. Finally, chaperones deliver damaged or misfolded proteins to proteases to be degraded. Molecular chaperones that reside in both the bacterial cytoplasmic and periplasmic spaces were selected for analysis.

In Chapter 2 I report that the general cytoplasmic chaperones DnaK and Hsp33 inhibit CsgA amyloid formation at substoichiometric molar ratios (Chapter 2 and (26)). The addition of DnaK to CsgA only extended the lag phase of CsgA polymerization while the addition of Hsp33 extended the lag phase and decreased the final amount of ThT fluorescence (26). Furthermore, the addition of CsgA preformed fibers or seeds could more easily overcome CsgA amyloid inhibition by DnaK than Hsp33. Taken together, these findings support a model where DnaK acts primarily during early stages of CsgA polymerization while Hsp33 may also interact with CsgA protofibrils or oligomers to inhibit fiber elongation (26). Interestingly, DnaK inhibited CsgA polymerization in that absence of the cofactors DnaJ and GrpE and in the absence of ATP demonstrating that DnaK can function as a holdase or holding chaperone to inhibit CsgA amyloid assembly (26).

The periplasmic environment is distinct from the cytoplasmic environment in many ways; most notably, the periplasmic space is devoid of a hydrolysable energy source. Therefore, many periplasmic chaperones act as holdases. Spy is one such holdase that is regulated by the Cpx two-component and the Bae two-component systems (27-29). Spy can also inhibit CsgA amyloid formation *in vitro* but requires closer to a 1:1 molar ratio to achieve inhibition over a 24-hour experiment (Chapter 2) (26). The addition of CsgA seeds to a reaction with Spy and soluble CsgA could overcome

Spy-mediated inhibition (26). These results are again consistent with the model that Spy inhibits CsgA amyloid formation by interacting with soluble CsgA during early stages of polymerization. Furthermore, I found that overexpression of Spy in WT cells resulted in decreased detectable CsgA but not CsgG suggesting that when Spy is in large abundance in the periplasm it can retain CsgA in a protease-sensitive conformation (Chapter 2) (26).

Identification of CsgC as a Curli Amyloid Inhibitor

Curli are secreted by a dedicated secretion pore and assembled on a dedicated platform (12). I therefore hypothesize that there exist dedicated inhibitors to prevent intracellular amyloid formation (12). I used a combined biochemical and genetic approach to try to identify either curli-specific or curli-induced amyloid inhibitors in the periplasm of *E. coli*. These efforts ultimately revealed that CsgC is an extraordinarily efficient and selective CsgA amyloid inhibitor. In the experiments that lead to the discovery of CsgC as an amyloid inhibitor, periplasmic extracts (PEs) were harvested from various curli mutants that had been grown under curli-inducing conditions. PEs were added to newly purified CsgA and assays for inhibitory activity using the ThT assay. I found that mutants that were disrupted for secretion ($\Delta csgG$ or $\Delta csgE$) or localization ($\Delta csgB$, $\Delta csgF$, or $\Delta csgF\Delta csgB$) of CsgA exhibited an inducible chaperone-like activity. PEs from WT cells accelerated polymerization when added to newly purified CsgA likely due to seeding by co-purified CsgA fibers in the crude extracts. Loss of *csgA* or *csgB* in the $\Delta csgG$ mutant, loss of *csgA* in the $\Delta csgF\Delta csgB$ mutant or deletion of both *csgB* and *csgA* simultaneously relieved the CsgA amyloid inhibitory activity in PEs likely do to feedback repression of the *csgBAC* operon coupled with a polar effect on *csgC* expression in either *csgA* or *csgB* mutant (Fig. 3.2C and Fig. 3.4A). Size exclusion chromatography and western blotting combined with our observation that deletion of *csgC* in curli mutant backgrounds relieved the CsgA amyloid inhibitory activity in PEs lead us to conclude that the observed amyloid inhibitory activity was due to CsgC.

CsgC is a Potent and Selective Amyloid Inhibitor

CsgC inhibits CsgA amyloid formation at very low substoichiometric concentrations (1:500, CsgC:CsgA) and maintains the majority of CsgA in an unstructured conformation that can still be recognized by the oligomer-specific antibody A11 (Fig. 3.7). The remarkable ability of CsgC to prevent amyloid formation at very low substoichiometric levels (1:500; Fig. 3.7A), and in the absence of ATP hydrolysis, is unique among anti-amyloid, chaperone-like proteins. CsgC can still inhibit CsgA amyloid formation at substoichiometric concentrations even in the presence of CsgA seeds suggesting that CsgC functions during later stages of CsgA aggregation or directs CsgA into an off pathway species (Fig. 3.7F).

The molecular details of CsgC chaperone activity on CsgA are still not well understood and should be investigated in future biochemical and biophysical experiments. I found that purified CsgC interacts directly with CsgA in a by far Western dot blot analysis (Fig. 5.1). More detailed analysis of the direct interaction between CsgA and CsgC is needed. Surface Plasmon Resonance may be used to better investigate the dynamic of an interaction between CsgA and CsgC. Sequence and conformation specific CsgA gammabodies can be used to test whether CsgC is directing CsgA into a conformation that can be recognized by one of these conformation-specific antibodies. Given the observation that very low molar ratios of CsgC to CsgA can inhibit amyloid formation over several days, CsgC may be directing CsgA into a large, off-pathway oligomeric species. CD, size analysis, TEM and conformation-specific antibodies will enable further biochemical definition of the CsgA-CsgC complex. The characteristics of CsgA incubated with CsgC can further be probed by asking if CsgA incubated with CsgC is protease sensitive. CsgA incubated alone adopts a highly protease-resistant, SDS-insoluble form, typical of all amyloids (19, 25, 26). When CsgC is incubated with CsgA at substoichiometric concentrations, CsgA remains completely SDS soluble suggesting that CsgC maintains CsgA in a non-amyloid conformation. I predict that CsgA incubated with CsgC will also be sensitive to proteolysis.

The efficiency of CsgC-mediated amyloid inhibition is only one facet of what makes CsgC such a remarkable amyloid inhibitor. CsgC does not appear to act as a

general amyloid inhibitor but instead exhibits a high degree of client protein selectivity (Fig. 3.9 and 3.10). *E. coli* CsgA shares approximately 30% sequence identity with *E. coli* CsgB, and over 70% sequence identity with both *Salmonella enterica* and *Citrobacter koseri* CsgA (30). CsgC inhibited *S. enterica*, *C. koseri* and *E. coli* CsgA polymerization at the same molar ratios while inhibition of CsgB amyloid formation required a higher molar ratio compared to CsgA (1:10 CsgC:CsgB and 1:500 CsgC:CsgA; Fig. 3.7 and 3.9). Intriguingly, CsgC inhibited α -synuclein, but not A β ₄₂ amyloid formation. I identified an 8-9 amino acid motif (D-Q- Φ -X_{0,1}-G-K-N- ζ) that is present in the loop region between R3 and R4 of CsgA and in the solubilizing domain of α -synuclein. There is a high degree of sequence similarity shared by all of the CsgA repeating units. CsgC inhibited amyloid formation by Δ R1, Δ R3 and Δ R5 CsgA mutants as well as synthetic peptides corresponding to R1 and R5. CsgC likely has multiple interaction sites within CsgA, but only one in α -synuclein. CsgC was unable to inhibit amyloid formation by the α -synuclein motif mutants supporting my hypothesis that the D-Q- Φ -X_{0,1}-G-K-N- ζ motif is required for CsgC interaction (Fig. 3.9E and 3.10G).

There are still many questions to be asked about the client protein selectivity of CsgC and the importance of the D-Q- Φ -X_{0,1}-G-K-N- ζ motif in client proteins. Additional amyloid candidate client proteins that do not contain the motif should also be evaluated such as IAPP, Sup35, tau and TTR. It would also be of great interest to create A β ₄₂ peptides that have been amended with the D-Q- Φ -X_{0,1}-G-K-N- ζ motif and ask whether CsgC can now inhibit amyloid formation by these chimeric peptides. The possibility that CsgC can inhibit the aggregation of non-amyloidogenic proteins, such as citrate synthase (CS) and luciferase, should also be addressed. CS and luciferase are well-characterized general chaperone substrates. Chimeric versions of CS and luciferase with the D-Q- Φ -X_{0,1}-G-K-N- ζ motif can be used to ask whether CsgC can inhibit general aggregation if the motif is present on the client protein. Altogether, these additional experiments will definitively establish the substrate specificity of CsgC, and whether it is a general amyloid inhibitor, a general protein folding inhibitor or a specific inhibitor of CsgA and the importance of the D-Q- Φ -X_{0,1}-G-K-N- ζ motif in client proteins.

A Putative Substrate-Binding Domain in CsgC

When the crystal structure of CsgC was first reported it was predicted to act as a redox active protein in the periplasm. CsgC contains a conserved CxC motif and the structure of CsgC aligned very closely to the N-terminal domain of the oxidoreductase DsbD. CsgC was found to have a reduction potential similar to that of DsbC and DsbG. Under reducing conditions CsgC was less thermodynamically stable suggesting that disulfide bond formation of the CxC motif was important for protein stability (15). I found that disulfide bond formation is not important for the amyloid inhibitory activity of CsgC. Reduced CsgC has similar inhibitory activity against CsgA as oxidized CsgC and mutation of cysteine 29 to a serine yielded a CsgC protein that inhibited CsgA amyloid formation at molar ratios similar to that of WT CsgC (Fig. 5.2AB). I was unable to detect stable expression of the C29S mutant of CsgC *in vivo*; therefore, to evaluate the roll of disulfide bond formation of the CxC motif in CsgC *in vivo* genes encoding the disulfide bond catalyzing protein *dsbA* or *dsbB* were deleted and CsgC was detected by Western blot. Not unsurprisingly, CsgC protein levels were reduced in both the $\Delta dsbA$ and $\Delta dsbB$ mutants indicating that disulfide bond formation of the CxC motif in CsgC is important for protein stability both *in vitro* and *in vivo* (Fig. 5.2CDE).

Chaperones often work by presenting structurally disordered or aggregation prone regions. The substrate binding domains of molecular chaperones are typically hydrophobic, aggregation prone regions that become solvent-exposed under conditions that activate chaperone activity (31). Interestingly, a few molecular chaperones have substrate binding domains that have amyloid-like properties (32, 33). It is possible that CsgC might be functioning to inhibit CsgA amyloid formation by making amyloid-like interactions with the growing CsgA fiber. I identified a single region in CsgC that is predicted to be aggregative or amyloidogenic using the programs PASTA or TANGO and the ZipperDB, respectively (Fig. 5.3BCD) (34-37). The predicted aggregative/amyloidogenic region of CsgC is highlighted in red (Fig. 5.3E) Mutation analysis of residues within the predicted aggregative domain and in other domains of CsgC will be useful in determining the important regions or residues for client protein interaction. Dr Steve Matthews lab at the Imperial College of London has begun mutational analysis of CsgC. The Matthews lab has identified several mutations that

disrupt charged patches on the surface of CsgC and result in decreased CsgA amyloid inhibition activity but not CsgC protein folding or stability (unpublished results). Further characterization of mutations in CsgC that reduce amyloid inhibition or specificity are likely to yield important insights into how CsgC functions.

It is possible that amyloid inhibition by CsgC requires steric hindrance by the remainder of the CsgC protein. Inhibition of amyloid formation by gammabodies developed in Dr. Tessier's lab is mediated by homotypic interactions between similar amyloid domains in each protein. For example, gammabodies that contain grafted portions of A β specifically recognize and inhibit A β amyloid assembly at substoichiometric molar ratios (38, 39). Once domains of CsgC are identified that dictate the specificity or activity of CsgC these domains can be grafted into the gammabody scaffold. The gammabody may be able to recognize and inhibit CsgA amyloid assembly if the antibody portion can mimic the steric hindrance of CsgC. I hypothesize that a direct interaction between CsgA and CsgC grafted within the gammabody will inhibit CsgA amyloid formation.

CsgE is a Critical Curli Secretion Protein

Transporting proteins across membranes is a significant challenge to cells. The transport of aggregation-prone and amyloidogenic proteins presents an even greater challenge because inappropriate interactions between membranes and amyloids can compromise membrane function (7, 40-42). Our model for CsgA secretion posits that CsgE binds to CsgA in the periplasm and chaperones it to the CsgG secretion complex in the outer membrane. Consistent with this model, CsgE interacts with both CsgG and CsgA and is required for efficient CsgA secretion (16-18, 43). Furthermore CsgE can inhibit amyloid assembly of CsgA even after polymerization is initiated *in vitro* (Chapter 4) (17, 18). The domain in CsgA that CsgE recognizes is still unknown. Investigating whether CsgE can inhibit amyloid formation by CsgA repeating unit deletion mutants and repeating unit synthetic peptides will be the first step towards identifying the CsgE interaction domain(s) in CsgA. The N-terminal 22 amino acids of CsgA are not necessary for *in vitro* CsgA amyloid formation but are required for targeting peptides for

secretion through CsgG (44, 45). The N-terminal 22 amino acids of CsgA should also be evaluated as a potential CsgE interaction site.

The specificity of CsgE amyloid inhibition is unknown. The CsgA amyloid inhibitor protein CsgC exhibits a high degree of selectivity that is dictated by the presence of a D-Q-Φ-X_{0,1}-G-K-N-ζ motif in client protein. It is possible that CsgE can inhibit amyloid formation by other proteins. Future studies on CsgE chaperone activity should involve an investigation into a panel of proteins, as described above for CsgC. Dr. Pernilla Wittung-Stafshede and Dr. Fredrik Almqvist's labs already have evidence that CsgE can modulate α-synuclein amyloid formation (unpublished data). The ability of CsgC and CsgE to modulate CsgA and α-synuclein amyloid formation are reminiscent of strikingly different results obtained when the small peptidomimetic 2-pyridone molecule FN075 is incubated with CsgA compared to α-synuclein (46). FN075 inhibits CsgA amyloid formation and accelerates α-synuclein amyloid formation by directing both proteins into oligomers. Interestingly, the oligomers of CsgA that assemble in the presence of FN075 are “off-pathway” while the oligomers of α-synuclein that assemble in the presence of FN075 are “on-pathway” (46).

Understanding CsgE Function *in vivo*

CsgE is required for curli biogenesis *in vivo* but the molecular details of CsgE function are unknown (4, 17). The clear CsgE mutant phenotype *in vivo* and the chaperone activity of CsgE *in vitro* make mutation-function analysis relatively easy. In collaboration with Dr. Christiane Ritter we have begun to analyze mutations in CsgE that impact its several functions in distinct ways. The W49S and W52S mutations can complement a Δ*csgE* mutant *in vivo* but cannot gate CsgG pore activity (Fig. 4.2BD and Fig. 4.3AB). In contrast, the F68S mutant cannot complement a Δ*csgE* mutant but can still gate CsgG pore activity (Fig. 4.2BD and Fig. 4.3C). These results suggest that the W49 and W52 residues are located on a surface of CsgE that are important for interacting with CsgG and gating the pore but not necessarily important for interacting with CsgA or delivering CsgA to CsgG. On the other hand, the F68 residue is likely located on a surface of CsgE that is more important either for interacting with CsgA or for delivering CsgA to CsgG, not for gating CsgG. Alternatively, the F68S mutation

could alter the dynamics of the CsgE-CsgG interaction such that CsgG is always gated or occupied and is no longer accessible to CsgA. WT CsgE is associated with outer membrane fractions in a CsgG-dependent manner and coimmunoprecipitates with CsgG (21). It is possible that for CsgE and CsgG to function properly the interaction between CsgG and CsgE must be dynamic. The domains and specific residues of CsgE that are important for its multiple functions as a secretion and gating factor should be further investigated.

Amyloid Cytotoxicity and Designing Therapeutics

Oligomers formed early during amyloidogenesis are considered to be the toxic species (41, 47). Toxicity is not only associated with disease amyloids. Microcin E492 is a functional amyloid produced by *Klebsiella pneumoniae* that forms a soluble toxic oligomer as a defense against neighboring bacteria. Once Microcin E492 polymerizes into amyloid fibers it becomes inert (48, 49). The ability of CsgC and CsgE to modulate α -synuclein amyloid formation begets the question of whether CsgC and CsgE change the cytotoxicity associated with disease-associated amyloids like α -synuclein. Early oligomers and amyloids that are arrested at early stages of polymerization might be more cytotoxic to cultured cells whereas toxicity may be reduced if amyloid formation is accelerated. Future studies focusing on the mechanism and molecular details of amyloid modulation by proteins like CsgC and CsgE will help guide the rational design of amyloid therapeutics.

Concluding Remarks

Curli are a bacterial functional amyloid that serves as an excellent model for studying bacterial biofilm formation, protein secretion and amyloid biology. Curli gene expression and fiber assembly are beautifully coordinated and controlled events. Bacteria have evolved many mechanisms that work in concert in preventative measures and as fail-safe mechanisms to 1) ensure that curli subunits are secreted prior to amyloid assembly and 2) rapidly eliminate mislocalized and potentially dangerous subunits in the event that secretion fails. The multitiered mechanisms employed by *E.*

coli underscore the importance of controlled amyloidogenesis and hold the key to understanding both disease-associated and functional amyloid biology.

Materials and Methods

Strains and Plasmids.

BW25113 $\Delta dsbA$ (*dsbA::kan*) and $\Delta dsbB$ (*dsbB::kan*) obtained from the Keio collection (50).

Protein Purification. CsgA was purified as described previously (30). CsgC was purified as described previously (51). CsgC was reduced with by the addition of 10 mM dithiothreitol (DTT) at 37°C for 30 min.

CsgA Polymerization. CsgA was diluted to a final concentration of 20 μ M and incubated with CsgC and 20 μ M Thioflavin T (ThT). Readings were taken in either a Molecular Devices SpectraMax M2 or a Tecan Infinite M200 microtitre plate reader at 25°C. The plate was shaken linearly for 3 seconds prior to taking fluorescence readings (excitation: 438nm, emission: 495nm, cutoff: 475nm) every 10 or 20 minutes.

Western Blot. Cells were grown on YESCA agar plates at 26°C for either 24 or 48 hours. They were then scraped from the plate and normalized to OD₆₀₀=1.0 in 50mM potassium phosphate buffer (pH 7.3). 100 μ L of cell suspension were pelleted in duplicate. One duplicate was treated with 50 μ L 1,1,1,3,3,3-hexafluoro-2-propanol (HFIP) for 10 minutes, dried and then resuspended in 40 μ L SDS loading buffer while the other sample was only resuspended in SDS loading buffer. Samples were separated on a 15% acrylamide gel and transferred to PVDF with α -CsgA (1:15,000), α -CsgG (1:50,000) or α -CsgC (1:4000).

Far Western Blot. Freshly purified soluble CsgA (25 μ M), 25 μ M CsgA that had been allowed to polymerize into fibers for 24 hours, or fibers that had been sonicated 3 times 20 sec on ice were spotted as 4 μ L dots on 0.22 μ m nitrocellulose membrane and allowed to dry. Blots were blocked in 2% BSA in TBS-T. Blots were then either probed with α -CsgA (1:15,000), α -CsgC (1:4000) or incubated for 1 hour with 1 mg/mL purified CsgC protein prior to incubation with α -CsgC antibody (1:4000).

Figures

Figure 5.1 CsgC interacts directly with CsgA. Far western dot blot analysis was used to detect a direct interaction between CsgA and CsgC. CsgA monomers (mono), fibers or sonicated fibers (seeds) were spotted on a nitrocellulose membrane in triplicate and then blocked with 2% BSA. One blot was probed with an α -CsgA antibody, another blot was probed with an α -CsgC antibody and the last blot was incubated with CsgC protein at 1 mg/mL and then probed with an α -CsgC antibody.

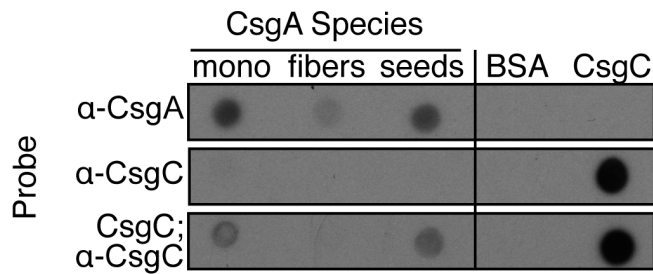


Figure 5.2 Intramolecular disulfide bond formation and CsgC stability.

A) The CxC disulfide bond in CsgC was reduced with 10 mM DTT for 30 minutes at 37°C and then assayed for CsgA amyloid inhibition in a ThT assay. B) WT CsgC and C29S mutant CsgC were purified and tested for CsgA amyloid inhibition in a ThT assay. C) Congo red binding of WT, $\Delta csgC$, $\Delta dsbA$ and $\Delta dsbB$ *E. coli*. D) Western blot analysis of CsgG and CsgA protein levels in WT, $\Delta csgC$, $\Delta dsbA$ and $\Delta dsbB$ cells. E) Western blot analysis of CsgC protein levels in WT, $\Delta csgC$, $\Delta dsbA$ and $\Delta dsbB$ cells.

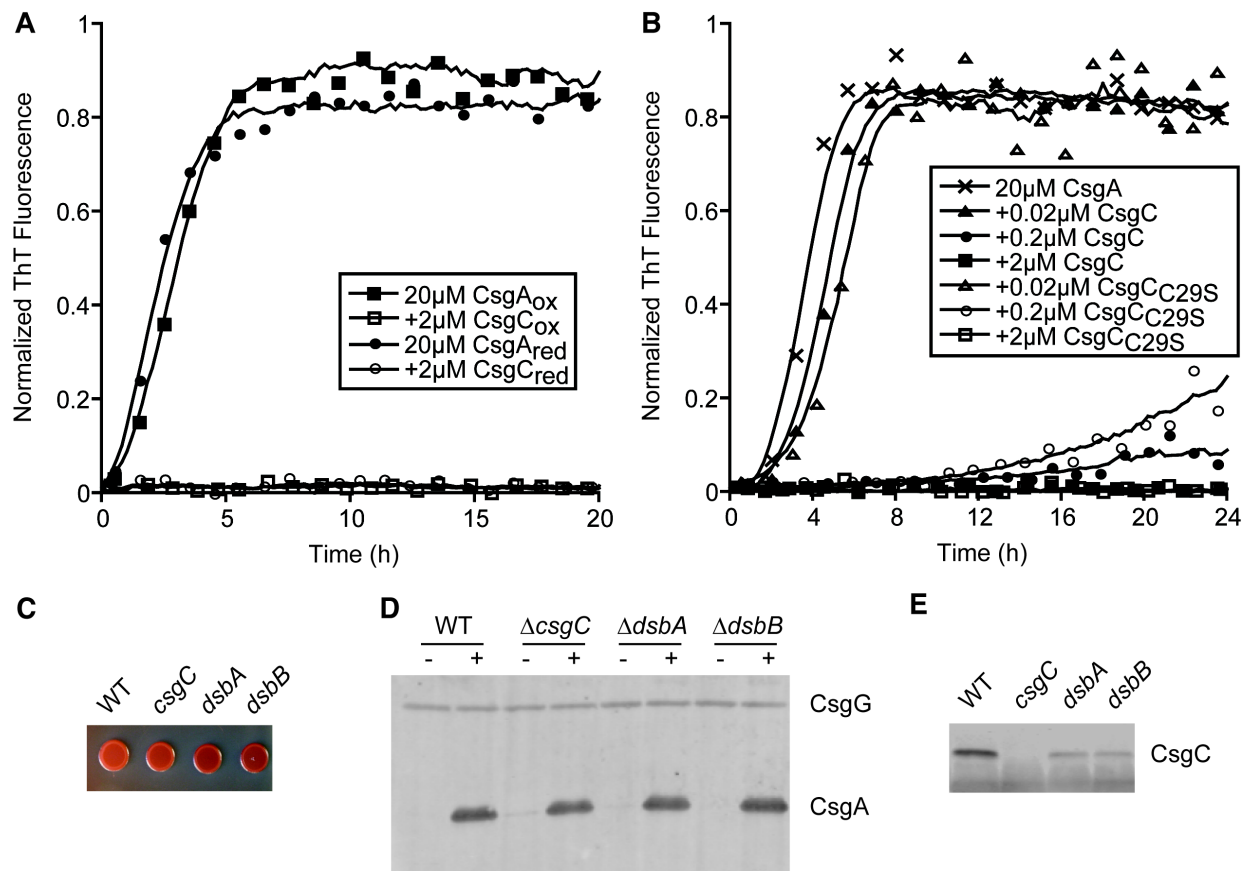
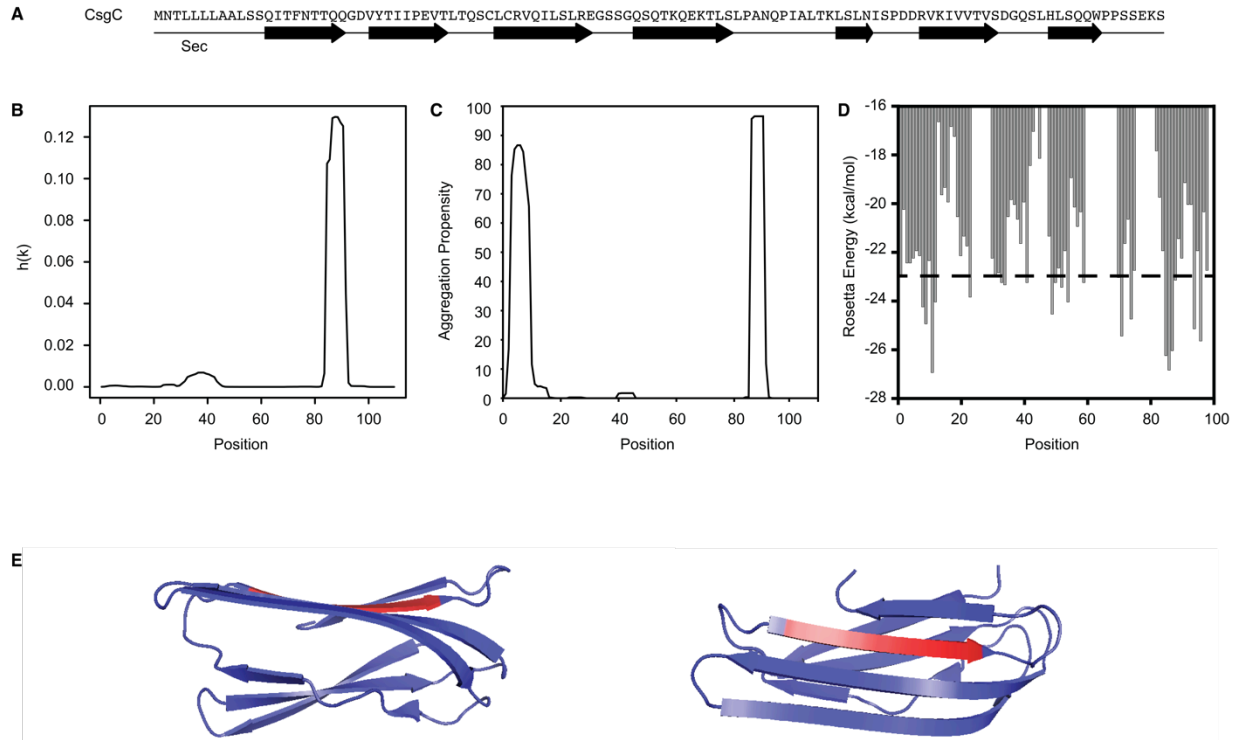


Figure 5.3 CsgC contains a predicted aggregative domain. A) CsgC sequence shown with the location of the β -sheets indicated. The primary sequence of CsgC was analyzed using the aggregation prediction algorithm PASTA (B), the amyloid prediction algorithm TANGO (C) or the ZipperDB (D). The predicted aggregative/amyloidogenic region of CsgC (residues 86-91) are highlighted in red (E).



References

1. Chiti F, Dobson CM (2006) Protein misfolding, functional amyloid, and human disease. *Annu Rev Biochem* 75:333–366.
2. Blanco LP, Evans ML, Smith DR, Badtke MP, Chapman MR (2012) Diversity, biogenesis and function of microbial amyloids. *Trends Microbiol* 20:66–73.
3. Hufnagel DA, Tukul C, Chapman MR (2013) Disease to dirt: the biology of microbial amyloids. *PLoS Pathog* 9:e1003740.
4. Chapman MR, Robinson LS, Pinkner JS, Roth R, Heuser J, Hammar M, Normark S, Hultgren SJ (2002) Role of *Escherichia coli* curli operons in directing amyloid fiber formation. *Science* 295:851–855.
5. Dueholm MS, Petersen SV, Sonderkaer M, Larsen P, Christiansen G, Hein KL, Enghild JJ, Nielsen JL, Nielsen KL, Nielsen PH *et al.* (2010) Functional amyloid in *Pseudomonas*. *Mol Microbiol*
6. Larsen P, Nielsen JL, Dueholm MS, Wetzel R, Otzen D, Nielsen PH (2007) Amyloid adhesins are abundant in natural biofilms. *Environ Microbiol* 9:3077–3090.
7. Fowler DM, Koulov AV, Alory-Jost C, Marks MS, Balch WE, Kelly JW (2006) Functional amyloid formation within mammalian tissue. *PLoS Biol* 4:e6.
8. Maji SK, Perrin MH, Sawaya MR, Jessberger S, Vadodaria K, Rissman RA, Singru PS, Nilsson KP, Simon R, Schubert D *et al.* (2009) Functional amyloids as natural storage of peptide hormones in pituitary secretory granules. *Science* 325:328–332.
9. King CY, Tittmann P, Gross H, Gebert R, Aebi M, Wuthrich K (1997) Prion-inducing domain 2-114 of yeast Sup35 protein transforms in vitro into amyloid-like filaments. *Proc Natl Acad Sci U S A* 94:6618–6622.
10. Kushnirov VV, Kryndushkin DS, Boguta M, Smirnov VN, Ter-Avanesyan MD (2000) Chaperones that cure yeast artificial [PSI⁺] and their prion-specific effects. *Curr Biol* 10:1443–1446.
11. Shorter J, Lindquist S (2004) Hsp104 catalyzes formation and elimination of self-replicating Sup35 prion conformers. *Science* 304:1793–1797.
12. Evans ML, Chapman MR (2014) Curli biogenesis: order out of disorder. *Biochim Biophys Acta* 1843:1551–1558.
13. Hammar M, Arnqvist A, Bian Z, Olsen A, Normark S (1995) Expression of two csg operons is required for production of fibronectin- and congo red-binding curli polymers in *Escherichia coli* K-12. *Mol Microbiol* 18:661–670.
14. Gibson DL, White AP, Rajotte CM, Kay WW (2007) AgfC and AgfE facilitate extracellular thin aggregative fimbriae synthesis in *Salmonella enteritidis*. *Microbiology* 153:1131–1140.
15. Taylor JD, Zhou Y, Salgado PS, Patwardhan A, McGuffie M, Pape T, Grabe G, Ashman E, Constable SC, Simpson PJ *et al.* (2011) Atomic resolution insights into curli fiber biogenesis. *Structure* 19:1307–1316.
16. Goyal P, Krasteva PV, Van Gerven N, Gubellini F, Van den Broeck I, Troupiotis-Tsailaki A, Jonckheere W, Pehau-Arnaudet G, Pinkner JS, Chapman MR *et al.* (2014) Structural and mechanistic insights into the bacterial amyloid secretion channel CsgG. *Nature*

17. Nenninger AA, Robinson LS, Hammer ND, Epstein EA, Badtke MP, Hultgren SJ, Chapman MR (2011) CsgE is a curli secretion specificity factor that prevents amyloid fibre aggregation. *Mol Microbiol* 81:486–499.
18. Andersson EK, Bengtsson C, Evans ML, Chorell E, Sellstedt M, Lindgren AE, Hufnagel DA, Bhattacharya M, Tessier PM, Wittung-Stafshede P *et al.* (2013) Modulation of curli assembly and pellicle biofilm formation by chemical and protein chaperones. *Chem Biol* 20:1245–1254.
19. Nenninger AA, Robinson LS, Hultgren SJ (2009) Localized and efficient curli nucleation requires the chaperone-like amyloid assembly protein CsgF. *Proc Natl Acad Sci U S A* 106:900–905.
20. Loferer H, Hammar M, Normark S (1997) Availability of the fibre subunit CsgA and the nucleator protein CsgB during assembly of fibronectin-binding curli is limited by the intracellular concentration of the novel lipoprotein CsgG. *Mol Microbiol* 26:11–23.
21. Robinson LS, Ashman EM, Hultgren SJ, Chapman MR (2006) Secretion of curli fibre subunits is mediated by the outer membrane-localized CsgG protein. *Mol Microbiol* 59:870–881.
22. Hammar M, Bian Z, Normark S (1996) Nucleator-dependent intercellular assembly of adhesive curli organelles in *Escherichia coli*. *Proc Natl Acad Sci U S A* 93:6562–6566.
23. Hammer ND, Schmidt JC, Chapman MR (2007) The curli nucleator protein, CsgB, contains an amyloidogenic domain that directs CsgA polymerization. *Proc Natl Acad Sci U S A* 104:12494–12499.
24. Hammer ND, McGuffie BA, Zhou Y, Badtke MP, Reinke AA, Brannstrom K, Gestwicki JE, Olofsson A, Almqvist F, Chapman MR (2012) The C-terminal repeating units of CsgB direct bacterial functional amyloid nucleation. *J Mol Biol* 422:376–389.
25. Wang X, Smith DR, Jones JW, Chapman MR (2007) In vitro polymerization of a functional *Escherichia coli* amyloid protein. *J Biol Chem* 282:3713–3719.
26. Evans ML, Schmidt JC, Ilbert M, Doyle SM, Quan S, Bardwell JC, Jakob U, Wickner S, Chapman MR (2011) *E. coli* chaperones DnaK, Hsp33 and Spy inhibit bacterial functional amyloid assembly. *Prion* 5:323–334.
27. Raffa RG, Raivio TL (2002) A third envelope stress signal transduction pathway in *Escherichia coli*. *Mol Microbiol* 45:1599–1611.
28. Leblanc SK, Oates CW, Raivio TL (2011) Characterization of the induction and cellular role of the BaeSR two-component envelope stress response of *Escherichia coli*. *J Bacteriol* 193:3367–3375.
29. Quan S, Koldewey P, Tapley T, Kirsch N, Ruane KM, Pfizenmaier J, Shi R, Hofmann S, Foit L, Ren G *et al.* (2011) Genetic selection designed to stabilize proteins uncovers a chaperone called Spy. *Nat Struct Mol Biol* 18:262–269.
30. Zhou Y, Smith D, Leong BJ, Brannstrom K, Almqvist F, Chapman MR (2012) Promiscuous cross-seeding between bacterial amyloids promotes interspecies biofilms. *J Biol Chem* 287:35092–35103.
31. Tompa P, Csermely P (2004) The role of structural disorder in the function of RNA and protein chaperones. *FASEB J* 18:1169–1175.

32. Yoshiike Y, Akagi T, Takashima A (2007) Surface structure of amyloid-beta fibrils contributes to cytotoxicity. *Biochemistry* 46:9805–9812.
33. Yoshiike Y, Minai R, Matsuo Y, Chen YR, Kimura T, Takashima A (2008) Amyloid oligomer conformation in a group of natively folded proteins. *PLoS One* 3:e3235.
34. Fernandez-Escamilla AM, Rousseau F, Schymkowitz J, Serrano L (2004) Prediction of sequence-dependent and mutational effects on the aggregation of peptides and proteins. *Nat Biotechnol* 22:1302–1306.
35. Goldschmidt L, Teng PK, Riek R, Eisenberg D (2010) Identifying the amyloids, proteins capable of forming amyloid-like fibrils. *Proc Natl Acad Sci U S A* 107:3487–3492.
36. Trovato A, Chiti F, Maritan A, Seno F (2006) Insight into the structure of amyloid fibrils from the analysis of globular proteins. *PLoS Comput Biol* 2:e170.
37. Trovato A, Seno F, Tosatto SC (2007) The PASTA server for protein aggregation prediction. *Protein Eng Des Sel* 20:521–523.
38. Ladiwala AR, Bhattacharya M, Perchiacca JM, Cao P, Raleigh DP, Abedini A, Schmidt AM, Varkey J, Langen R, Tessier PM (2012) Rational design of potent domain antibody inhibitors of amyloid fibril assembly. *Proc Natl Acad Sci U S A* 109:19965–19970.
39. Perchiacca JM, Ladiwala AR, Bhattacharya M, Tessier PM (2012) Structure-based design of conformation- and sequence-specific antibodies against amyloid beta. *Proc Natl Acad Sci U S A* 109:84–89.
40. Demuro A, Mina E, Kaye R, Milton SC, Parker I, Glabe CG (2005) Calcium dysregulation and membrane disruption as a ubiquitous neurotoxic mechanism of soluble amyloid oligomers. *J Biol Chem* 280:17294–17300.
41. Kaye R, Sokolov Y, Edmonds B, McIntire TM, Milton SC, Hall JE, Glabe CG (2004) Permeabilization of lipid bilayers is a common conformation-dependent activity of soluble amyloid oligomers in protein misfolding diseases. *J Biol Chem* 279:46363–46366.
42. Lashuel HA, Lansbury PTJ (2006) Are amyloid diseases caused by protein aggregates that mimic bacterial pore-forming toxins? *Q Rev Biophys* 39:167–201.
43. Epstein EA, Reizian MA, Chapman MR (2009) Spatial clustering of the curli secretion lipoprotein requires curli fiber assembly. *J Bacteriol* 191:608–615.
44. Sivanathan V, Hochschild A (2012) Generating extracellular amyloid aggregates using *E. coli* cells. *Genes Dev* 26:2659–2667.
45. Van Gerven N, Goyal P, Vandebussche G, De Kerpel M, Jonckheere W, De Greve H, Remaut H (2014) Secretion and functional display of fusion proteins through the curli biogenesis pathway. *Mol Microbiol* 91:1022–1035.
46. Horvath I, Weise CF, Andersson EK, Chorell E, Sellstedt M, Bengtsson C, Olofsson A, Hultgren SJ, Chapman M, Wolf-Watz M *et al.* (2012) Mechanisms of protein oligomerization: inhibitor of functional amyloids templates alpha-synuclein fibrillation. *J Am Chem Soc* 134:3439–3444.
47. Kaye R, Head E, Thompson JL, McIntire TM, Milton SC, Cotman CW, Glabe CG (2003) Common structure of soluble amyloid oligomers implies common mechanism of pathogenesis. *Science* 300:486–489.

48. Bieler S, Estrada L, Lagos R, Baeza M, Castilla J, Soto C (2005) Amyloid formation modulates the biological activity of a bacterial protein. *J Biol Chem* 280:26880–26885.
49. Shahnawaz M, Soto C (2012) Microcin amyloid fibrils A are reservoir of toxic oligomeric species. *J Biol Chem* 287:11665–11676.
50. Baba T, Ara T, Hasegawa M, Takai Y, Okumura Y, Baba M, Datsenko KA, Tomita M, Wanner BL, Mori H (2006) Construction of *Escherichia coli* K-12 in-frame, single-gene knockout mutants: the Keio collection. *Mol Syst Biol* 2:2006.0008.
51. Salgado PS, Taylor JD, Cota E, Matthews SJ (2011) Extending the usability of the phasing power of diselenide bonds: SeCys SAD phasing of CsgC using a non-auxotrophic strain. *Acta Crystallogr D Biol Crystallogr* 67:8–13.

Appendices

Appendix A: Investigating Feedback Repression of the Curli Operons

Loferer and colleagues (1997) reported that CsgA and CsgB protein levels are below the level of detection by Western blot in a $\Delta csgG$ mutant; however, they showed that *csgA* and *csgB* were both still expressed using translational fusion to each gene. I attempted to repeat these results using a *lacZ* transcriptional reporter under control of the *csgDEFG* or *csgBAC* promoter and qRT-PCR with either *csgD* or *csgB* primers. In contrast to the Loferer *et al.* (1997) result, I found that there is approximately a 3-fold decrease in expression from the *csgBAC* promoter while the *csgDEFG* promoter activity was unchanged in a $\Delta csgG$ mutant (Fig. A.1AB). The qRT-PCR results showed a similarly modest repression of *csgB* (Fig. A.1C). The CpxAR two-component system is one of the negative regulators of curli expression. I therefore asked whether CpxR was responsible for the observed feedback repression in the $\Delta csgG$ mutant by examining expression of the *csgDEFG-lacZ* and *csgBAC-lacZ* fusion constructs in a $\Delta csgG\Delta cpxR$ mutant. Expression of *csgDEFG-lacZ* increased approximately 2-fold when *cpxR* was deleted while expression of *cpxR* alone, but not in the $\Delta csgG$ mutant resulted in a dramatic increase in *csgBAC-lacZ* expression. Together, these results demonstrate that there is feedback repression of the *csgBAC* promoter in a $\Delta csgG$ mutant but that the repression is not mediated by the Cpx two-component system.

Materials and Methods

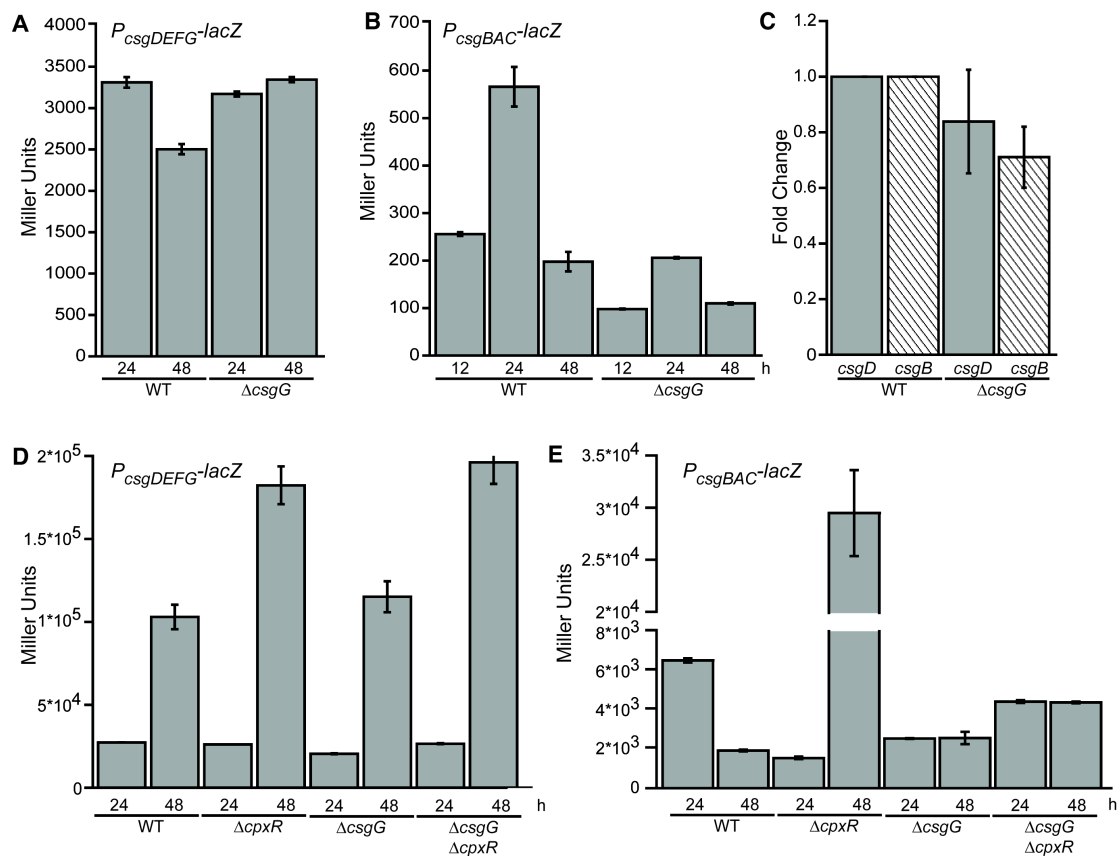
Bacterial Strains. Described in Chapter 3.

β -galactosidase Assay. Described in Chapter 3.

qRT-PCR. Cells were grown on YESCA plates for 24h at 26C. Cells were harvested with YESCA media containing RNase Protect (QIAGEN) and incubated for 5 min. Cells were pelleted at 5,000xg for 10 min and resuspended in Tris-EDTA containing 1 mg/mL lysozyme and incubated for 5 min before RLT (QIAGEN) was added. The cells were pelleted and the supernatant removed to a new tube with Molecular Biology Grade ethanol and inverted several times to mix. The RNA solution was transferred to a QIAGEN spin column and centrifuged for 15 sec. The column was washed RW1 buffer, RDD buffer containing DNase, and RPE buffer twice before eluting with 31 μ L of DNase free water. cDNA was synthesized using ImPromptII reverse transcriptase. SYBR Green

qPCR MasterMix was used for the quantitative PCR using primers 5'-GGTGCAAGCGTTAATCGGAA-3' and 5'-CTTCCGTGGATGTCAAGACC-3' for 16S, 5'-GCGGCGAATGCTACTTTACG-3' and 5'-CGCTGATGAACAACGAACGA-3' for *csgD* and 5'-TAGCAACCGGGCAAAGATTG-3' and 5'-CGTTGTGTCACGCGAATAGC-3' for *csgB*. Values are reported as $\Delta\Delta C_t$ and normalized to 16S.

Figure A.1. Transcription analysis of curli operons



Appendix B: One and Two Dimensional Gel Analysis of Periplasmic Extracts to Identify Amyloid Inhibitory Factors.

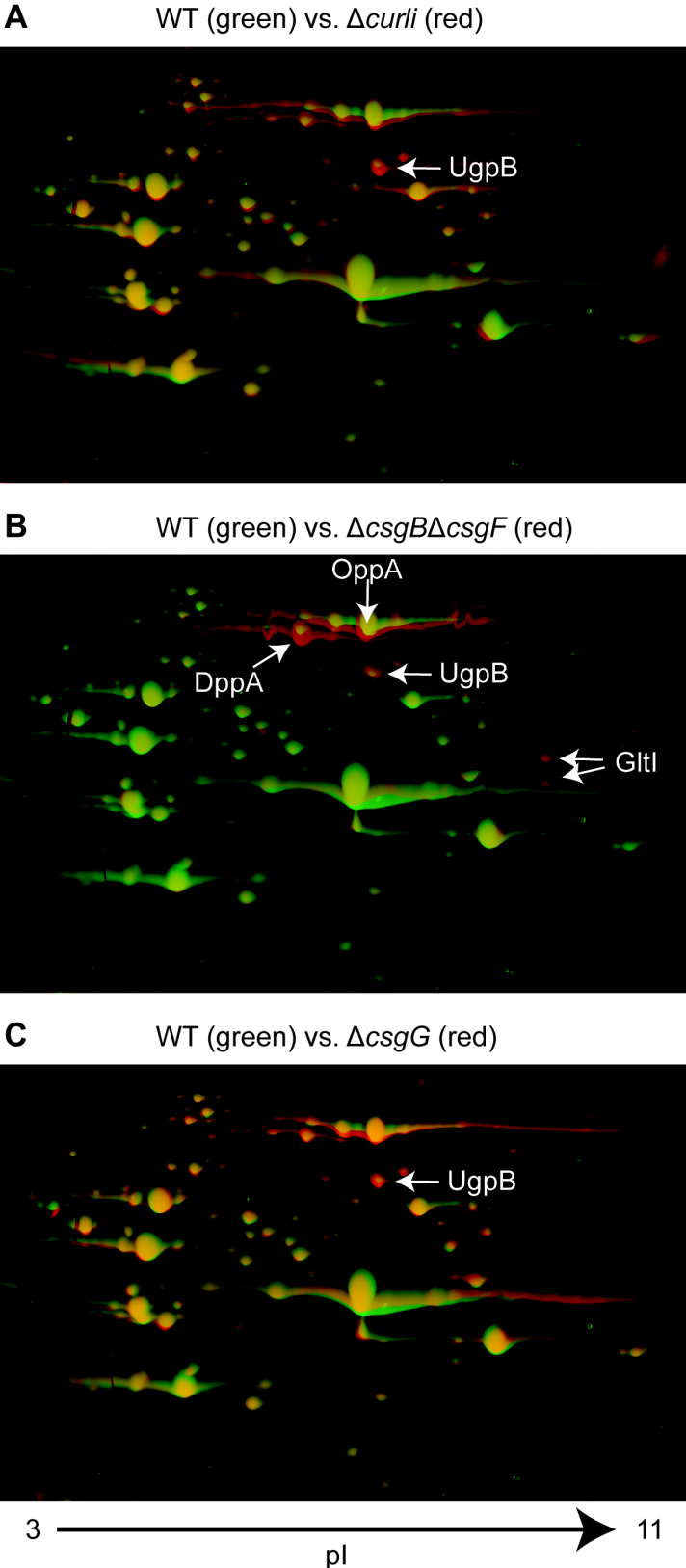
Mass spectrometry analysis of one and two dimensional gel electrophoresis of PEs from *E. coli* k-12 MC4100 revealed upregulation at 48 hours of growth of the substrate binding subunit of two ABC transporters: OppA and DppA. The Opp and Dpp systems are involved in recycling oligo- and dipeptides, respectively, back into the cell. OppA and DppA have both been reported to have general chaperone activity *in vitro* (Richarme and Caldas, 1997). However, deletion of both *oppA* and *dppA* in backgrounds that exhibited amyloid inhibitory PEs did not relieve the inhibitory activity. Consistently, neither OppA nor DppA were induced in isogenic curli mutants of *E. coli* k-12 BW25113, however, the inhibitory activities associated with the specific curli mutant PEs were the same as in MC4100. Why OppA and DppA are induced in some curli mutants in MC4100 but not BW25113 is unclear. Therefore, to simplify our investigation we selected BW25113 for the remainder of our studies.

Materials and Methods

Two-Dimensional Gel Electrophoresis.

Periplasmic extracts were collected as described in Chapter 3. Proteins were precipitated with 10% trifluoroacetic acid on ice for 30 min. The precipitated protein was centrifuged for 30 min at 16,000rpm at 4°C and the supernatant removed. Proteins were separated by isoelectric point using a 24 cm GE Healthcare Immobiline dry strip. The Immobiline strip was then placed at the top of a 13% acrylamide gel pH 8.6 and then stained with colloidal coomassie stain. Gels were analyzed using Delta 2D software and all spot intensities were normalized by the sum of the intensities for a given gel. Spots with intensities greater than 3-fold over WT were excised and set to the University of Michigan Proteomics Core for MS/MS analysis.

Figure B.1. Two-dimensional gel electrophoresis of periplasmic extracts



Appendix C: The Effect of Polyphosphate on Curli *in vivo* and *in vitro*.

Michael Gray, a post-doc in Ursula Jakob's lab, was studying the effect of polyphosphate on protein folding and approached me about investigating a potential role for polyphosphate during curli biogenesis and CsgA amyloid assembly. I found that deletion of the polyphosphate kinase, *ppk*, resulted in delayed CR binding of MG1655 relative to WT (24 h) while loss of the exopolyphosphatase, *ppx*, bound WT amounts of CR (Fig. D1A, left panel). All strains bound the same amount of CR after 48 h of growth (Fig. D1A, right panel). Interestingly, Western blot analysis revealed that the Δppk mutant produced similar amounts of total CsgA protein compared the WT; however, a larger proportion of the CsgA protein was SDS soluble in the Δppk mutant at 24 and 48h of growth (Fig. D1B). I then asked whether the Δppk or Δppx mutants had a curli-dependent biofilm phenotype. To do this I chose to use the uropathogenic *E. coli* isolate UTI89. UTI89 makes curli-dependent wrinkled or rugose colonies on YESCA agar plates and curli-dependent pellicle biofilms. Will DePas in the Chapman lab had constructed the Δppk mutant in UTI89 in a candidate approach to identify mutants with increased biofilm. Figure D1C is a photograph taken by Will DePas. Will observed that the Δppk mutant had a slightly larger colony diameter and appear to wrinkle less than the WT (Fig. D1C). When the Δppk mutant was grown in a pellicle biofilm the mutant formed a smooth pellicle compared to the wrinkled pellicle produced by the WT (Fig. D1D).

Next, I asked whether polyphosphate directly effected CsgA amyloid formation. I purified CsgA and diluted it to 10 μ M in the presence of 10 mM, 1 mM or 0.1 mM polyphosphate and monitored polymerization by ThT fluorescence. Polyphosphate alone did not result in ThT fluorescence. The addition of any concentration of polyphosphate to CsgA accelerated CsgA amyloid formation: decreasing the lag phase from approximately 4 hours to 20 minutes (Fig. D2). Together, these results suggest that *ppk* plays a role in the timing of curli biogenesis and the development of curli-dependent biofilms.

Figure C.1. Polyphosphate production curli biogenesis and curli-dependent biofilm formation *in vivo*.

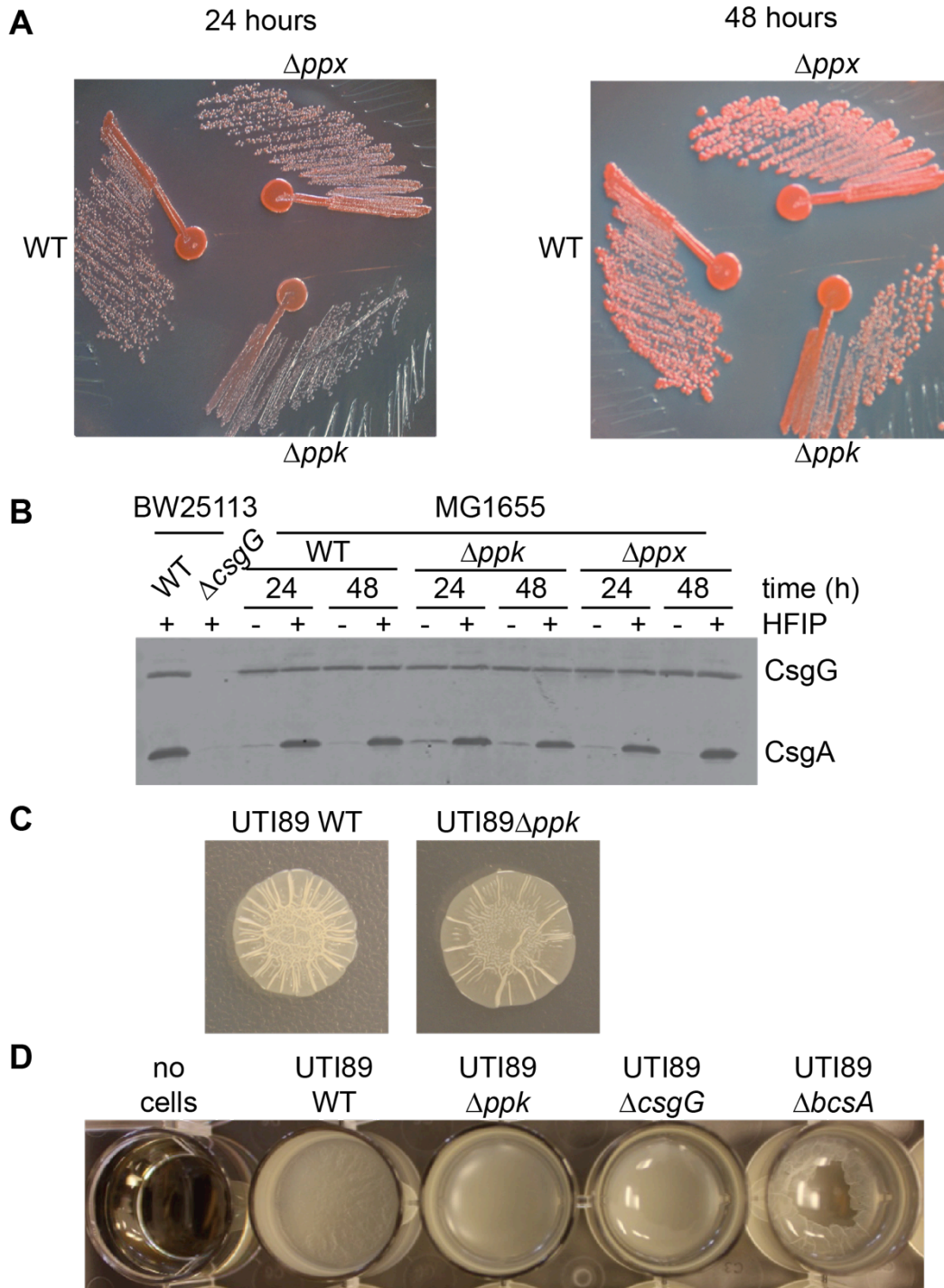


Figure C.2. Polyphosphate accelerates CsgA amyloid formation *in vitro*.

